Table of Contents

Table of Contents (Continued)

List of Figures

List of Figures (Continued)

List of Tables

List of Tables (Continued)

3.0 STRUCTURAL EVALUATION

This chapter describes the design and analysis of the principal structural components of the Universal Storage System under normal operating conditions. It demonstrates that the Universal Storage System meets the structural requirements for confinement of contents, criticality control, radiological shielding, and contents retrievability required by 10 CFR 72 [1] for the design basis normal operating conditions. Off-normal and accident conditions are evaluated in Chapter 11.0.

3.1 Structural Design

The Universal Storage System includes five configurations to accommodate three classes of PWR and two classes of BWR fuel assemblies. The five classes of fuel are determined primarily by the overall length of the fuel assembly. The allocation of a fuel design to a UMS class is shown in Tables 2.1.1-1 and 2.1.2-1 for PWR and BWR fuel, respectively.

The three major components of the Universal Storage System are the vertical concrete cask; the transportable storage canister (canister), and the transfer cask (see Figure 3.1-1). These components are provided in five different lengths corresponding to the five classes of fuel. They also have different weights, as shown in Table 3.2-1 for the PWR configurations, and in Table 3.2-2 for the BWR configurations. The weight differences reflect the differences in length of components and fuel, and differences in basket design between the PWR and BWR configurations.

The principal structural members of the vertical concrete cask are the reinforced concrete shell and steel liner. The principal structural members of the canister are the structural lid, shell, bottom plate, the welds joining these components, and the fuel basket assembly. For the transfer cask, the trunnions, the inner and outer steel walls, the bottom shield doors, and the shield door support rails, are the principal structural components.

The evaluations presented in this chapter are based on the bounding or limiting configuration of the UMS System for the condition being evaluated. In most cases, the bounding condition evaluates the heaviest configuration of the five classes. For each evaluated condition, the bounding configuration applied is identified. Margins of safety greater than ten are generally stated in the analyses as "+Large." Numerical values are shown for Margins of safety that are less than ten.

3.1.1 Discussion

The transportable storage canister is designed to be transported in the Universal Transport Cask (USNRC Docket Number 71-9270 [2]. Consequently, the canister diameter is same for each of the five configurations. The outside diameter of the vertical concrete cask is established by the shielding requirement for the design basis fuel used for the shielding evaluation. The shielding required for the design basis fuel is conservatively applied to the five concrete cask configurations.

Vertical Concrete Cask

The vertical concrete cask is a reinforced concrete cylinder with an outside diameter of 136 in. and an overall height (including the lid) ranging from 210.68 in. to 227.38 in., depending upon the configuration. The internal cavity of the concrete cask is lined by a 2.5-inch thick carbon steel inner shell having an inside diameter of 74.5 in. The support ring for the concrete cask shield plug at the top of the inner shell limits the available contents diameter to less than 69.5 in. The inner shell thickness is primarily determined by radiation shielding requirements, but is also related to the need to establish a practical limit for the diameter of the concrete shell. The concrete shell is constructed using Type II Portland Cement and has a nominal density of 140 lb/ft^3 and a nominal compressive strength of 4000 psi. The inner and outer rebar assemblies are formed by vertical hook bars and horizontal hoop bars.

A ventilation air-flow path is formed by inlets at the bottom of the cask, the annular space between the cask inner shell and the canister, and outlets near the top of the cask. The passive ventilation system operates by natural convection as cool air enters the bottom inlets, is heated by the canister, and exits from the top outlets.

A 5.375-in. thick shield plug that consists of a 1-in. thick layer of NS-4-FR neutron shield material enclosed by carbon steel, is installed in the concrete cask cavity above the canister. The plug is supported by a support ring welded to the inner shell. The 1.5-in. thick carbon steel lid provides a cover to protect the canister from adverse environmental conditions and postulated tornado driven missiles. The shield plug and lid provide shielding to reduce the skyshine radiation. When the lid is bolted in place, the shield plug is secured between the lid and the shield plug support ring.

Transportable Storage Canister

The transportable storage canister consists of a cylindrical shell assembly closed at its top end by an inner shield lid and an outer structural lid. The canister forms the confinement boundary for the basket assembly that contains the PWR or BWR spent fuel. The canister is designed in five lengths to accommodate the classes of spent fuel presented in Tables 2.1.1-1 and 2.1.2-1. The canister is fabricated from Type 304L stainless steel. SA-182 Type 304 stainless steel may be substituted for the SA-240 Type 304 stainless steel used in the shield lid provided that the SA-182 material has equal or higher yield and ultimate strengths are equal to or greater than those of the SA-240 material. Similarly, SA-182 Type 304L stainless steel may be substituted for the SA-240 Type 304L stainless steel used in the structural lid provided that the SA-182 material has equal or higher yield and ultimate strengths are equal to or greater than those of the SA-240 material. The canister shield lid is 7-in. thick, SA-240 Type 304 stainless steel, and the structural lid is 3.0-in. thick SA-240, Type 304L stainless steel. Both lids are welded to the canister shell to close the canister. The shield lid is supported by a support ring. The structural lid is supported, prior to welding, by the shield lid. A groove is machined into the structural lid circumference to accept a backing ring. The backing ring facilitates welding of the structural lid to the canister shell. The bottom of the canister is a 1.75-in. thick SA-240, Type 304L stainless steel plate that is welded to the canister shell. The canister is also described in Section 1.2.1.1.

The fuel basket assembly is provided in two configurations — one for up to 24 PWR fuel assemblies and one for up to 56 BWR fuel assemblies. The PWR basket is comprised of Type 17-4 PH stainless steel support disks, Type 6061-T651 aluminum alloy heat transfer disks, and Type 304 stainless steel fuel tubes equipped with aluminum-boron carbide (BORAL) neutron absorber and stainless steel cover. The remaining structural components are Type 304 stainless steel. The BWR basket is comprised of SA-533 carbon steel support disks coated with electroless nickel, Type 6061-T651 aluminum alloy heat transfer disks, and fuel tubes constructed of the same materials as the PWR tubes. The remaining structural components of the BWR basket are Type 304 stainless steel. The basket assemblies are more fully described in Section 1.2.1.2.

The fuel basket support disks, heat transfer disks, and fuel tubes, together with the top and bottom weldments, are positioned by tie rods (with spacers and washers) that extend the length of the basket and hold the assembly together. The support disks provide structural support for the fuel tubes. They also help to remove heat from the fuel tubes. The heat transfer disks provide the primary heat removal capability and are not considered to be structural components. The heat

transfer disks are sized so that differential thermal expansion does not result in disk contact with the canister shell. The number of heat transfer disks and support disks varies depending upon the length of the fuel to be confined in the basket. The fuel tubes house the spent fuel assemblies. The top and bottom weldments provide longitudinal support for the fuel tubes. The fuel tubes are fabricated from Type 304 stainless steel. No structural credit is taken for the presence of the fuel tubes in the basket assembly analysis. The walls of each PWR fuel tube support a sheet of BORAL neutron poison material that is covered by stainless steel. No structural credit is taken in the basket assembly analysis for the BORAL sheet or its stainless steel cover. The PWR assembly fuel tubes have a nominal inside dimension of 8.8 in. square and a composite wall thickness of 0.14 in. The BWR assembly fuel tubes have a nominal inside dimension of 5.9 in. square and a composite wall thickness of 0.20 in. Depending upon its location in the basket assembly, an individual BWR fuel tube may support BORAL neutron poison material on one or two sides. Certain fuel tubes located on the outer edge of the basket do not have neutron poison material. The fuel tubes have been evaluated to ensure that the BORAL neutron poison material remains in place under normal conditions and design basis off-normal and accident events.

Four over-sized fuel storage positions are located on the periphery of the BWR basket to provide additional space for BWR fuel assemblies with channels that have been reused, since reused channels are expected to have increased bowing or bulging. Normal BWR fuel assemblies may also be stored in these locations.

As mentioned above, five transportable storage canisters are designed for the storage of identified classes of PWR and BWR spent fuel. The analysis in this report is based on the identification of bounding conditions, and the application of those conditions to determine the maximum stresses that exist in the worst case.

The canister is designed to be transported in the Universal Transport Cask. Transport conditions establish the design basis loading, except for lifting, because the hypothetical accident transport conditions produce higher stresses in the canister and basket than do the design basis storage conditions. Consequently, the canister and basket design is conservative with respect to storage conditions. The evaluation of the canister and basket assembly for transport conditions is documented in the Safety Analysis Report for the Universal Transport Cask [2].

Transfer Cask

The transfer cask, with its lifting yoke, is primarily a lifting device used to move the canister. It provides biological shielding when it contains a loaded canister. The transfer cask is used for the vertical transfer of the canister between work stations and the concrete cask, or transport cask. Five transfer casks of different lengths are designed to handle five canisters of different lengths containing one of three classes of PWR or two classes of BWR fuel assemblies. The transfer cask is a heavy lifting device. Accordingly, it is designed, fabricated, and load-tested to the requirements of NUREG-0612 [8] and ANSI N14.6 [9].

The transfer cask incorporates a multiwall (steel/lead//NS-4-FR/steel) design, which limits the contact radiation dose rate. The transfer cask design incorporates a top retaining ring, which is bolted in place that prevents a loaded canister from being inadvertently removed through the top of the transfer cask. The transfer cask has retractable bottom shield doors. During loading operations, the doors are closed and secured by pins so they cannot inadvertently open. During unloading, the doors are retracted using hydraulic cylinders to allow the canister to be lowered into the storage or transport cask. The principal design parameters of the transfer cask are shown in Table 1.2-6.

Component Evaluation

The following components are evaluated in this chapter:

- canister lifting devices,
- canister shell, bottom, and structural lid,
- canister shield lid support ring,
- fuel basket assembly,
- transfer cask trunnions, shells, retaining ring, bottom doors, and support rails,
- vertical concrete cask body, and
- concrete cask steel components (reinforcement, inner shell, lid, bottom plate, bottom, etc.).

Other Universal Storage System components shown on the drawings in Section 1.6 are included as loads in the evaluation of the components listed above, as appropriate.

The structural evaluations in this chapter demonstrate that the Universal Storage System components meet their structural design criteria and are capable of safely storing the design basis PWR or BWR spent fuel.

3.1.2 Design Criteria

The Universal Storage System structural design criteria are described in Section 2.2. Load combinations for normal, off-normal, and accident loads are evaluated in accordance with ANSI 57.9 [3] and ACI-349 [4] for the concrete cask (see Table 2.2-1), and in accordance with the 1995 edition of the ASME Code, Section III, Division I, Subsection NB [5] for Class 1 components of the canister (see Table 2.2-2). The basket is evaluated in accordance with ASME Code, Section III, Subsection NG [6], and NUREG-6322 [7]. The transfer cask and the lifting yoke are lifting devices that are designed to NUREG-0612 [8] and ANSI N14.6 [9].

Figure 3.1-1 Principal Components of the Universal Storage System

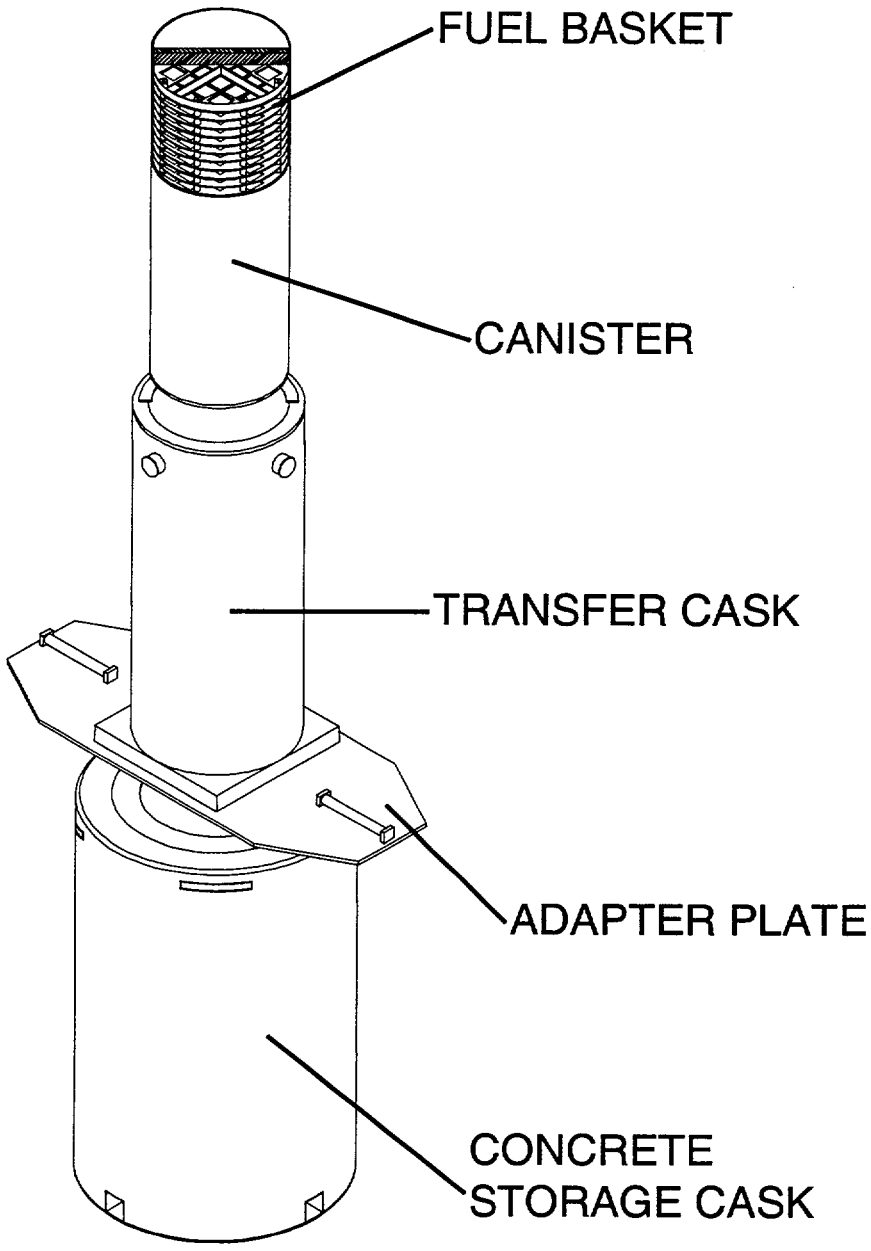

THIS PAGE INTENTIONALLY LEFT BLANK

3.2 Weights and Centers of Gravity

The weights and centers of gravity (CGs) for the Universal Storage System PWR configuration and components are summarized in Table 3.2-1. Those for the BWR configuration are summarized in Table 3.2-2. The weights and CGs presented in this section are calculated on the basis of nominal design dimensions.

Table 3.2-1 Universal Storage System Weights and CGs – PWR Configuration

Description	Class 1		Class 2		Class 3	
	Calculated Weight (lb)	Center of Gravity[1]	Calculated Weight (lb)	Center of Gravity[1]	Calculated Weight (lb)	Center of Gravity[1]
Fuel Contents (Including inserts)	37,608	—	38,448	—	35,520	—
Poison Rods (Inserts)	1,320	—	1,368	—	--	—
Concrete Cask Lid	2,449	—	2,449	—	2,449	—
Concrete Cask Shield Plug	4,845	—	4,845	—	4,845	—
Canister Structural Lid	2,927	—	2,927	—	2,927	—
Canister Shield Lid	6,825	—	6,825	—	6,825	—
Transfer Adapter Plate	11,912	—	11,912	—	11,912	—
Transfer Cask Lifting Yoke	5,816	—	5,816	—	5,816	—
Water in Canister	12,893	—	14,668	—	15,637	—
Canister (with basket; without fuel or lids)	23,345	—	24,727	—	25,511	—
Canister (with fuel, and shield and structural lids)	70,705	—	72,927	—	70,783	—
Concrete Cask (empty, with shield plug and lid)	221,696	—	230,390	—	237,649	—
Concrete Cask (with loaded Canister and lids)[2]	292,401	107.4	303,317	111.7	308,432	115.7
Transfer Cask (empty)	110,821	—	115,800	—	120,010	—
Transfer Cask and Canister, basket (empty, without lids)[3]	134,166	87.4	140,527	90.4	145,521	94.5
Transfer Cask and Canister (with fuel, water and shield lid)[3]	191,492	91.6	200,468	92.2	203,503	96.2
Transfer Cask and Canister (with fuel, dry with lids)[3]	181,526	93.0	188,727	93.9	190,793	98.0

[1] Weights and CGs are calculated from nominal design dimensions.

[2] Center of gravity is measured from the bottom of the concrete cask.

[3] Center of gravity is measured from the bottom of the canister.

Table 3.2-2 Universal Storage System Weights and CGs – BWR Configuration

Item Description	Class 4		Class 5	
	Calculated Weight (lb)	Center of Gravity[1]	Calculated Weight (lb)	Center of Gravity[1]
Fuel Contents (Including channels)	38,976	—	38,976	—
Concrete Cask Lid	2,449	—	2,449	—
Concrete Cask Shield Plug	4,845	—	4,845	—
Canister Structural Lid	2,927	—	2,927	—
Canister Shield Lid	6,825	—	6,825	—
Transfer Adapter Plate	11,912	—	11,912	—
Transfer Cask Lifting Yoke	5,816	—	5,816	—
Water in Canister	15,038	—	15,407	—
Canister (with basket, without fuel or lids)	26,631	—	27,168	—
Canister (with fuel, and shield and structural lids)	75,359	—	75,896	—
Concrete Cask (empty, with shield plug and lid)	231,728	—	236,314	—
Concrete Cask (with loaded Canister and lids)[2]	307,087	112.3	312,210	114.9
Transfer Cask (empty)	116,603	—	119,240	—
Transfer Cask and Canister (empty, without lids)[3]	143,234	91.0	146,408	93.5
Transfer Cask and Canister (with fuel, water and shield lid)[3]	204,073	92.6	207,616	95.3
Transfer Cask and Canister (with fuel, dry with lids)[3]	191,962	94.3	195,136	97.1

[1] Weights and CGs are calculated from nominal design dimensions.

[2] Center of gravity is measured from the bottom of the concrete cask.

[3] Center of gravity is measured from the bottom of the canister.

Table 3.2-3 Calculated Under-Hook Weights

Configuration	PWR Class 1	PWR Class 2	PWR Class 3	BWR Class 4	BWR Class 5
Transfer Cask, empty canister, and yoke	139,982	146,343	151,337	149,050	152,224
Transfer cask; wet, loaded canister (fuel, water, and shield lid); and yoke	197,308	206,284	209,319	209,889	213,432
Transfer cask; dry, loaded canister; and yoke	187,342	194,543	196,609	197,778	200,952

THIS PAGE INTENTIONALLY LEFT BLANK

3.3 Mechanical Properties of Materials

The mechanical properties of steels used in the fabrication of the Universal Storage System components are presented in Tables 3.3-1 through 3.3-10. The primary steels, Type 304 and Type 304L stainless steel, were selected because of their high strength, ductility, resistance to corrosion and brittle fracture, and metallurgical stability for long-term storage.

3.3.1 Primary Component Materials

The steels and aluminum alloy used in the fabrication of the canister and basket are:

Canister shell	ASME SA-240, Type 304L stainless steel
Canister bottom plate	ASME SA-240, Type 304L stainless steel
Canister shield lid	ASME SA-240, Type 304 stainless steel
Canister structural lid	ASME SA-240, Type 304L stainless steel
Support disks	
PWR basket	ASME SA-693, Type 630, 17-4 PH stainless steel
BWR basket	ASME SA-533, Type B class 2 carbon steel
Heat transfer disks	ASME SB-209, Type 6061-T651 aluminum alloy
Spacer nuts	ASME SA-479, Type 304 stainless steel
Tie rods	ASME SA-479, Type 304 stainless steel
Basket end weldments	ASME SA-240, Type 304 stainless steel
Fuel tubes	ASTM A240, Type 304 stainless steel

SA-182 Type 304 stainless steel may be substituted for SA-240 Type 304 stainless steel for the shield lid provided that the SA-182 material has yield and ultimate strengths greater than or equal to those of the SA-240 material. SA-182 Type 304L stainless steel may be substituted for SA-240 Type 304L stainless steel for the structural lid provided that the SA-182 material has yield and ultimate strengths greater than or equal to those of the SA-240 material.

Steels used in the fabrication of the vertical concrete cask are:

Inner shell	ASTM A36 carbon steel
Pedestal and base	ASTM A36 carbon steel
Reinforcing bar	ASTM A615, Grade 60 carbon steel

The steels used in the fabrication of the transfer cask are:

Inner shell	ASTM A588 low alloy steel
Outer shell	ASTM A588 low alloy steel
Bottom plate	ASTM A588 low alloy steel
Top plate	ASTM A588 low alloy steel
Retaining ring	ASTM A588 low alloy steel
Trunnions	ASTM A350, LF2 low alloy steel
Shield doors and rails	ASTM A350, LF2 low alloy steel
Retaining ring bolts	ASTM A193, Grade B6 high alloy steel

The mechanical properties of the 6061-T651 aluminum heat transfer disks in the fuel basket are shown in Table 3.3-11. The mechanical properties of the concrete are listed in Table 3.3-12.

Table 3.3-1 Mechanical Properties of SA-240 and A-240 Type 304 Stainless Steel

Property*	**Value**							
Temperature (°F)	-40	-20	70	200	300	400	500	750
Ultimate strength,[10] S_u (ksi)	75.0	75.0	75.0	71.0	66.0	64.4	63.5	63.1
Yield strength,[10] S_y (ksi)	30.0	30.0	30.0	25.0	22.5	20.7	19.4	17.3
Design Stress Intensity,[10] S_m (ksi)	20.0	20.0	20.0	20.0	20.0	18.7	17.5	15.6
Modulus of Elasticity,[10] E ($\times 10^3$ ksi)	28.7	28.7	28.3	27.6	27.0	26.5	25.8	24.4
Alternating Stress [11] @ 10 cycles (ksi)	718.0	718.0	708.0	690.5	675.5	663.0	645.5	610.4
Alternating Stress [11] @ 10^6 cycles (ksi)	28.7	28.7	28.3	27.6	27.0	26.5	25.8	24.4
Coefficient of Thermal Expansion,[10] α ($\times 10^{-6}$ in/in/°F)	8.13	8.19	8.46	8.79	9.00	9.19	9.37	9.76
Poisson's Ratio[10]	0.31							
Density[10]	503 lbm/ft^3 (0.291 lbm/in^3)							

* SA-182, Type 304 stainless steel may be substituted for SA-240 Type 304 stainless steel provided that the SA-182 material yield and ultimate strengths are equal to or greater than those of the SA-240 material. The SA-182 forging material and the SA-240 plate material are both Type 304 austenitic stainless steels. Austenitic stainless steels do not experience a ductile-to-brittle transition for the range of temperatures considered in this Safety Analysis Report. Therefore, fracture toughness is not a concern.

10 ASME Code, Section II, Part D.

11 ASME Code, Appendix I.

Table 3.3-2 Mechanical Properties of SA-479, Type 304 Stainless Steel

Property	Value							
Temperature (°F)	-40	-20	+70	+200	+300	+400	+500	+750
Ultimate strength, S_u, (ksi) *	—	75.0	75.0	71.0	66.0	64.4	63.5	63.1
Yield strength, S_y, (ksi) *	—	30.0	30.0	25.0	22.5	20.7	19.4	17.3
Design Stress Intensity,[10] S_m,(ksi)	20.0	20.0	20.0	20.0	20.0	18.7	17.5	15.6
Modulus of Elasticity[10] ($\times 10^3$ ksi)	28.8	28.7	28.3	27.6	27.0	26.5	25.8	24.4
Alternating Stress[11] @ 10 cycles (ksi)	720	718	708	683	675	663	645	610
Alternating Stress[11] @ 10^6 cycles (ksi)	28.8	28.7	28.3	27.6	27.0	26.5	25.8	24.4
Coefficient of Thermal Expansion,[10] α ($\times 10^{-6}$ in/in/°F)	—		8.46	8.79	9.00	9.19	9.37	9.76
Poisson's Ratio[10]	0.31							
Density[10]	503 lbm/ft^3 (0.291 lbm/in^3)							

[10] ASME Code, Section II, Part D.

[11] ASME Code, Appendix I.

* Calculated based on Design Stress Intensity:

$$\left(\frac{S_{m-temp}}{S_{m\,70^\circ}}\right) S_{u70} = S_{u-temp}$$

Table 3.3-3 Mechanical Properties of SA-240, Type 304L Stainless Steel

Property*	**Value**							
Temperature (°F)	-40	-20	70	200	300	400	500	750
Ultimate strength,[10] S_u, (ksi)	70.0	70.0	70.0	66.2	60.9	58.5	57.8	55.9
Yield strength,[10] S_y, (ksi)	25.0	25.0	25.0	21.4	19.2	17.5	16.4	14.7
Design Stress Intensity,[10] S_m,(ksi)	16.7	16.7	16.7	16.7	16.7	15.8	14.8	13.3
Modulus of Elasticity[10] ($\times 10^3$ ksi)	28.7	28.7	28.3	27.6	27.0	26.5	25.8	24.4
Alternating Stress[11] @ 10 cycles (ksi)	718.0	718.0	708.0	690.5	675.5	663.0	645.5	610.4
Alternating Stress[11] @ 10^6 cycles (ksi)	28.7	28.7	28.3	27.6	27.0	26.5	25.8	24.4
Coefficient of Thermal Expansion,[10] α ($\times 10^{-6}$ in/in/°F)	8.13	8.19	8.46	8.79	9.00	9.19	9.37	9.76
Poisson's Ratio[10]	0.31							
Density[10]	503 lbm/ft^3(0.291 lbm/in^3)							

* SA-182, Type 304 stainless steel may be substituted for SA-240 Type 304 stainless steel provided that the SA-182 material yield and ultimate strengths are equal to or greater than those of the SA-240 material. The SA-182 forging material and the SA-240 plate material are both Type 304 austenitic stainless steels. Austenitic stainless steels do not experience a ductile-to-brittle transition for the range of temperatures considered in this Safety Analysis Report. Therefore, fracture toughness is not a concern.

10 ASME Code, Section II, Part D.

11 ASME Code, Appendix I.

Table 3.3-4 Mechanical Properties of SA-564 and SA-693, Type 630, 17-4 PH Stainless Steel

Property	**Value**								
Temperature (°F)	-40	-20	70	200	300	400	500	650	800
Ultimate strength,[10] S_u, (ksi)	135.0	135.0	135.0	135.0	135.0	131.4	128.5	125.7	105.3[15]
Yield strength,[10] S_y, (ksi)	105.0	105.0	105.0	97.1	93.0	89.8	87.0	83.6	77.7[15]
Design Stress Intensity,[10] S_m,(ksi)	45.0	45.0	45.0	45.0	45.0	43.8	42.8	41.9	35.1
Modulus of Elasticity[10] ($\times 10^3$ ksi)	28.7	28.7	28.3	27.6	27.0	26.5	25.8	25.1	24.1
Alternating Stress[11] @ 10 cycles (ksi)	401.8	401.8	396.2	386.4	378.0	371.0	361.2	341.6	--
Alternating Stress[11] @ 10^6 cycles (ksi)	19.1	19.1	18.9	18.4	18.0	17.7	17.2	16.3	--
Coefficient of Thermal Expansion,[10] α ($\times 10^{-6}$ in/in/°F)	—		5.89	5.90	5.90	5.91	5.91	5.93	5.96
Poisson's Ratio[10]	0.31								
Density[10]	503 lbm/ft^3 (0.291 lbm/in^3)								

[10] ASME Code, Section II, Part D.

[11] ASME Code, Appendix I.

[15] MIL-HDBK-5G.

Table 3.3-5 Mechanical Properties of A-36 Carbon Steel

Property	**Value**							
Temperature (°F)	100	200	300	400	500	600	650	700
Ultimate strength, S_u, (ksi)[13]	58.0	58.0	58.0	58.0	—	—	—	—
Yield strength,[10] S_y, (ksi)	36.0	32.8	31.9	30.8	29.1	26.6	26.1	25.9
Design Stress Intensity,[10] S_m,(ksi)	19.3	19.3	19.3	19.3	19.3	17.7	17.4	17.3
Modulus of Elasticity, E ($\times 10^3$ ksi)[10]	29.0	28.8	28.3	27.7	27.3	26.7	26.1	25.5
Coefficient of Thermal Expansion, α ($\times 10^{-6}$ in/in/°F)[10]	5.53	5.89	6.26	6.61	6.91	7.17	7.30	7.41
Poisson's Ratio[10]	0.31							
Density[12]	0.284 lbm/in^3							

[10] ASME Code, Section II, Part D.

[12] Metallic Materials Specification Handbook.

[13] ASME Code Case, Nuclear Components, N-71-17.

Table 3.3-6 Mechanical Properties of A-615, Grade 60, Reinforcing Steel

Property	**Value**
Ultimate Strength [14] (ksi)	90.0
Yield Strength [14] (ksi)	60.0
Coefficient of Thermal Expansion, [12] α (in/in/°F)	6.1×10^{-6}
Density [12]	0.284 lbm/in^3

[12] Metallic Materials Specification Handbook.

[14] Annual Book of ASTM Standards.

Table 3.3-7 Mechanical Properties of SA-533, Type B, Class 2 Carbon Steel

Property	Value						
Temperature (°F)	-20	70	200	300	400	500	750
Ultimate strength [10] S_u, (ksi)	90.0	90.0	90.0	90.0	90.0	90.0	87.2
Yield strength, [10] S_y, (ksi)	70.0	70.0	65.5	64.5	63.2	62.3	59.3
Design Stress Intensity, [10] S_m,(ksi)	30.0	30.0	30.0	30.0	30.0	30.0	—
Modulus of Elasticity [10] E, ($\times 10^3$ ksi)	29.9	29.2	28.5	28.0	27.4	27.0	24.6
Alternating Stress [11] @ 10 cycles (ksi)	465.0	465.0	453.8	435.0	436.3	429.9	391.7
Alternating Stress [11] @ 10^6 cycles (ksi)	15.8	15.8	15.4	15.2	14.8	14.6	13.3
Coefficient of Thermal Expansion, [10] α ($\times 10^{-6}$ in/in/°F)	—	7.02	7.25	7.43	7.58	7.70	8.00
Poisson's Ratio [10]	0.31						
Density [10]	503 lbm/ft^3(0.291 lbm/in^3)						

[10] ASME Code, Section II, Part D.

[11] ASME Code, Section III, Appendix I.

Table 3.3-8 Mechanical Properties of A-588, Type A or B Low Alloy Steel

Property	**Value**							
Temperature (°F)	100	200	300	400	500	600	650	700
Ultimate strength, [13] S_u, (ksi)	70.0	70.0	70.0	70.0	70.0	70.0	70.0	70.0
Yield strength, [13] S_y, (ksi)	50.0	47.5	45.6	43.0	41.8	39.9	38.9	37.9
Design Stress Intensity, [13] S_m, (ksi)	23.3	23.3	23.3	23.3	23.3	23.3	23.3	23.3
Modulus of Elasticity [10] E, ($\times 10^3$ ksi)	29.0	28.8	28.3	27.7	27.3	26.7	26.1	25.5
Coefficient of Thermal Expansion, [10] α ($\times 10^{-6}$ in/in/°F)	5.53	5.89	6.26	6.61	6.91	7.17	7.30	7.41
Poisson's Ratio [10]	0.31							
Density [12]	0.284 lbm/in^3							

[10] ASME Code, Section II, Part D.

[12] Metallic Materials Specification Handbook.

[13] ASME Code Cases, Nuclear Components, NC-71-17, Tables 1, 2, 3, 4, and 5 for material thickness ≤ 4 in.

Table 3.3-9 Mechanical Properties of SA-350/A-350, Grade LF 2, Class 1 Low Alloy Steel

Property	**Value**					
Temperature (°F)	70	200	300	400	500	700
Ultimate strength, [10] S_u, (ksi)	70.0	70.0	70.0	70.0	70.0	70.0
Yield strength, [10] S_y (ksi)	36.0	32.8	31.9	30.8	29.1	25.9
Design Stress Intensity, [10] S_m (ksi)	23.3	21.9	21.3	20.6	19.4	17.3
Modulus of Elasticity, [10] E, ($\times 10^3$ ksi)	29.2	28.5	28.0	27.4	27.0	25.3
Coefficient of Thermal Expansion[10] α ($\times 10^{-6}$ in/in/°F)	—	5.89	6.26	6.61	6.91	7.41
Alternating Stress [11] at 10^6 cycles (ksi)	12.5	12.2	11.9	11.7	11.5	10.8
Alternating Stress [11] at 10 cycles (ksi)	580.0	566.0	556.1	544.2	536.3	502.5
Poisson's Ratio [10]	0.31					
Density [10]	0.279 lbm/in^3					

[10] ASME Code, Section II, Part D.

[11] ASME Code, Appendix I.

Table 3.3-10 Mechanical Properties of SA-193, Grade B6, High Alloy Steel Bolting Material

Property	Value							
Temperature (°F)	-40	-20	70	200	300	400	500	600
Ultimate Stress, S_u (ksi) * [10]	No Value Given	110.0	110.0	104.9	101.5	98.3	95.6	92.9
Yield Stress, S_y (ksi) * [10]	No Value Given	85.0	85.0	81.1	78.1	76.0	73.9	71.8
Design Stress Intensity, S_m (ksi) [10]	28.3	28.3	28.3	27.0	26.1	25.3	24.6	23.9
Modulus of Elasticity, E (ksi) [10]	30.1E+ 03	30.1E+ 03	29.2E+ 03	28.5E+ 03	27.9E+ 03	27.3E+ 03	26.7E+ 03	26.1E+03
Alternating Stress @ 10 cycles (ksi) [11]	1104.4	1100.0	1085.0	1058.0	1035.0	1015.0	989.0	935.3
Alternating Stress @ 10^6 cycles (ksi) [11]	13.0	12.9	12.7	12.4	12.2	11.9	11.6	11.0
Coefficient of Thermal Expansion, α (in/in/°F) [10]	5.73E-06	5.76E-06	5.92E-06	6.15E-06	6.30E-06	6.40E-06	6.48E-06	6.53E-06
Poisson's Ratio [10]	← 0.31 →							
Density [10]	← 503 lbm/ft^3(0.291 lbm/in^3) →							

[10] ASME Code, Section II, Part D.

[11] ASME Code, Appendix I.

* Calculated based on Design Stress Intensity:

$$\left(\frac{S_{m-temp}}{S_{m\,70^\circ}}\right)S_{u70} = S_{u-temp}$$

Table 3.3-11 Mechanical Properties of 6061-T651 Aluminum Alloy

Property	**Value**							
Temperature (°F)	70	100	200	300	400	500	600	700
Ultimate strength [15], S_u (ksi)	42.0	40.7	38.2	31.5	17.2	6.7	3.4	2.1
Yield strength, [15] Sy (ksi)	35.0	33.9	32.2	26.9	14.0	5.3	2.5	1.4
Design Stress Intensity [10] S_m (ksi)	10.5	10.5	10.5	8.4	4.4	--	--	--
Modulus of Elasticity, [10] E ($\times 10^3$ ksi)	10.0	9.9	9.6	9.2	8.7	8.1	7.0	--
Coefficient of Thermal Expansion, [10] α ($\times 10^{-6}$ in/in/°F)	—	12.6	12.91	13.22	13.52	13.7	14.3	--
Poisson's Ratio [10]	0.33							
Density [10]	0.098 lbm/in^3							

[10] ASME Code, Section II, Part D.

[15] Military Handbook MIL-HDBK-5G.

Table 3.3-12 Mechanical Properties of Concrete

Property	**Value**					
Temperature (°F)	70	100	200	300	400	500
Compressive Strength (psi) [16]	4000	4000	4000	3800	3600	3400
Modulus of Elasticity, [16] ($\times 10^3$ ksi)	—	3.64	3.38	3.09	3.73	3.43
Coefficient of Thermal Expansion, [16] α ($\times 10^{-6}$ in/in/°F)	5.5					
Density [16]	140 lbm/ft^3					

[16] Handbook of Concrete Engineering.

Table 3.3-13 Mechanical Properties of NS-4-FR

Property	**Value**			
Temperature (°F)	86	158	212	302
Compressive Modulus, [17] E_c (ksi)	561	561	561	561
Coefficient of Thermal Expansion, [17] α ($\times 10^{-5}$ in/in/°F)	5.19	5.77	5.72	5.9
Density [17], (lbm/in^3)	0.0607	0.0607	0.0607	0.0607

[17] GESC Product Data.

3.3.2 Fracture Toughness Considerations

The primary structural materials of the NAC-UMS® Transportable Storage Canister and basket are a series of stainless steels. These stainless steel materials do not undergo a ductile-to-brittle transition in the temperature range of interest for the NAC-UMS® System. Therefore, fracture toughness is not a concern for these materials.

The optional lift anchors for the NAC-UMS® Vertical Concrete Cask are fabricated from A 537, Class 2, and A 615, Grade 60 ferritic steels. Since there are eight rebars (A 615, Grade 60) for each lift anchor, the rebars are not considered fracture-critical components because multiple, redundant load paths exist, in the same manner that bolted systems are considered in Section 5 of NUREG/CR-1815. Therefore, brittle fracture evaluation of the rebar material is not required. The lifting lug and base plate of the lift anchors are designed as 2-inch thick, A 537 Class 2, steel plates in accordance with ANSI N14.6. Applying the fracture toughness requirements of ASME Code Section III, Subsection NF-2311(b)13 and Figure NF-2311(b)-1, the minimum allowable design metal temperature is –5°F (Curve D, 2-inch nominal thickness). The VCC lift anchors are restricted to be used only when the surrounding air temperatures are greater than, or equal to, 0°F (Section 12(B 3.4)(9)), so impact testing of the material is not required.

The NAC-UMS® BWR basket support disks are 0.625-inch thick, SA 533, Type B, Class 2, ferritic steel plate. Per ASME Code Section III, Subsection NG-2311(a)(1), impact testing of material with a nominal section thickness of 5/8 inch (16 mm) and less is not required. To provide added assurance of the fracture toughness of the BWR support disk material, Charpy V-notch (C_v) impact testing is specified on Drawing No. 790-573 for each plate of material in the heat treated condition in accordance with ASME Code Section III, Subsection NG-2320. Acceptance values shall be per ASTM A-370, Section 26.1, with a minimum average value of 20 Mils lateral expansion at a Lowest Service Temperature of - 40°F.

3.4 General Standards

3.4.1 Chemical and Galvanic Reactions

The materials used in the fabrication and operation of the Universal Storage System are evaluated to determine whether chemical, galvanic or other reactions among the materials, contents, and environments can occur. All phases of operation — loading, unloading, handling, and storage — are considered for the environments that may be encountered under normal, off-normal, or accident conditions. Based on the evaluation, no potential reactions that could adversely affect the overall integrity of the vertical concrete cask, the fuel basket, the transportable storage canister or the structural integrity and retrievability of the fuel from the canister have been identified. The evaluation conforms to the guidelines of NRC Bulletin 96-04 [18].

3.4.1.1 Component Operating Environment

Most of the component materials of the Universal Storage System are exposed to two typical operating environments: 1) an open canister containing fuel pool water or borated water with a pH of 4.5 and spent fuel or other radioactive material; or 2) a sealed canister containing helium, but with external environments that include air, rain water/snow/ice, and marine (salty) water/air. Each category of canister component materials is evaluated for potential reactions in each of the operating environments to which those materials are exposed. These environments may occur during fuel loading or unloading, handling or storage, and include normal, off-normal, and accident conditions.

The long-term environment to which the canister's internal components are exposed is dry helium. Both moisture and oxygen are removed prior to sealing the canister. The helium displaces the oxygen in the canister, effectively precluding chemical corrosion. Galvanic corrosion between dissimilar metals in electrical contact is also inhibited by the dry environment inside the sealed canister. NAC's operating procedures provide two helium backfill cycles in series separated by a vacuum-drying cycle during the preparation of the canister for storage. Therefore, the sealed canister cavity is effectively dry and galvanic corrosion is precluded.

3.4.1.2 Component Material Categories

The component materials are categorized in this section for their chemical and galvanic corrosion potential on the basis of similarity of physical and chemical properties and component functions.

The categories are stainless steels, nonferrous metals, carbon steel, coatings, concrete, and criticality control materials. The evaluation is based on the environment to which these categories could be exposed during operation or use of the canister.

The canister component materials are not reactive among themselves, with the canister's contents, nor with the canister's operating environments during any phase of normal, off-normal, or accident condition, loading, unloading, handling, or storage operations. Since no reactions will occur, no gases or other corrosion by-products will be generated.

3.4.1.2.1 Stainless Steels

No reaction of the canister component stainless steels is expected in any environment except for the marine environment, where chloride-containing salt spray could potentially initiate pitting of the steels if the chlorides are allowed to concentrate and stay wet for extended periods of time (weeks). Only the external canister surface could be so exposed. The corrosion rate will, however, be so low that no detectable corrosion products or gases will be generated. The Universal Storage System has smooth external surfaces to minimize the collection of such materials as salts.

Galvanic corrosion between the various types of stainless steels does not occur because there is no effective electrochemical potential difference between these metals. No coatings are applied to the stainless steels. An electrochemical potential difference does exist between austenitic (300 series) stainless steel and aluminum. However, the stainless steel becomes relatively cathodic and is protected by the aluminum.

The canister confinement boundary uses Type 304L stainless steel for all components, except the shield lid, which is made of Type 304 stainless steel. Type 304L resists chromium-carbide precipitation at the grain boundaries during welding and assures that degradation from intergranular stress corrosion will not be a concern over the life of the canister. Fabrication specifications control the maximum interpass temperature for austenitic steel welds to less than 350°F. The material will not be heated to a temperature above 800°F, other than by welding thermal cutting. Minor sensitization of Type 304 stainless steel that may occur during welding will not affect the material performance over the design life because the storage environment is relatively mild.

Based on the foregoing discussion, no potential reactions associated with the stainless steel canister or basket components are expected to occur.

3.4.1.2.2 Nonferrous Metals

Aluminum is used as a heat transfer component in the Universal Storage System spent fuel basket, and aluminum components in electrical contact with austenitic stainless steel could experience corrosion driven by electrochemical EMF when immersed in water. The conductivity of the water is the dominant factor. BWR fuel pool water is demineralized and is not sufficiently conductive to promote detectable corrosion for these metal couples. PWR pool water, however, does provide a conductive medium. The only aluminum components that will be in contact with stainless steel and exposed to the pool water are the alloy 6061-T651 heat transfer disks in the fuel basket.

Aluminum produces a thin surface film of oxidation that effectively inhibits further oxidation of the aluminum surface. This oxide layer adheres tightly to the base metal and does not react readily with the materials or environments to which the fuel basket will be exposed. The volume of the aluminum oxide does not increase significantly over time. Thus, binding due to corrosion product build-up during future removal of spent fuel assemblies is not a concern. The borated water in a PWR fuel pool is an oxidizing-type acid with a pH on the order of 4.5. However, aluminum is generally passive in pH ranges down to about 4 [19]. Data provided by the Aluminum Association [20] shows that aluminum alloys are resistant to aqueous solutions (1-15 %) of boric acid (at 140 °F). Based on these considerations and the very short exposure of the aluminum in the fuel basket to the borated water, oxidation of the aluminum is not likely to occur beyond the formation of a thin surface film. No observable degradation of aluminum components is expected as a result of exposure to BWR or PWR pool water at temperatures up to 200°F, which is higher than the permissible fuel pool water temperature.

Aluminum is high on the electromotive potential table, and it becomes anodic when in electrical contact with stainless or carbon steel in the presence of water. BWR pool water is demineralized and is not sufficiently conductive to promote detectable corrosion for these metal couples. PWR pool water is sufficiently conductive to allow galvanic activity to begin. However, exposure time of the aluminum components to the PWR pool environment is short. The long-term storage environment is sufficiently dry to inhibit galvanic corrosion.

From the foregoing discussion, it is concluded that the initial surface oxidation of the aluminum component surfaces effectively inhibits any potential galvanic reactions.

Heat transfer disks fabricated from 6061-T651 aluminum alloy are used in the NAC-UMS® Universal Storage System PWR and BWR fuel baskets to augment heat transfer from the spent fuel through the basket structure to the canister exterior. Vendor and Nuclear Regulatory Commission safety evaluations of the NUHOMS Dry Spent Fuel Storage System (Docket No. 72-1004) have concluded that combustible gases, primarily hydrogen, may be produced by a chemical reaction and/or radiolysis when aluminum or aluminum flame-sprayed components are immersed in spent fuel pool water. The evaluations further concluded that it is possible, at higher temperatures (above 150 - 160°F), for the aluminum/water reaction to produce a hydrogen concentration in the canister that approaches or exceeds the Lower Flammability Limit (LFL) for hydrogen of 4 percent. The NRC Inspection Reports No. 50-266/96005 and 50-301/96005 dated July 01, 1996, for the Point Beach Nuclear Plant concluded that hydrogen generation by radiolysis was insignificant relative to other sources.

Thus, it is reasonable to conclude that small amounts of combustible gases, primarily hydrogen, may be produced during UMS Storage System canister loading or unloading operations as a result of a chemical reaction between the 6061-T6 aluminum heat transfer disks in the fuel basket and the spent fuel pool water. The generation of combustible gases stops when the water is removed from the cask or canister and the aluminum surfaces are dry.

A galvanic reaction may occur at the contact surfaces between the aluminum disks and the stainless steel tie rods and spacers in the presence of an electrolyte, like the pool water. The galvanic reaction ceases when the electrolyte is removed. Each metal has some tendency to ionize, or release electrons. An Electromotive Force (EMF) associated with this release of electrons is generated between two dissimilar metals in an electrolytic solution. The EMF between aluminum and stainless steel is small and the amount of corrosion is directly proportional to the EMF. Loading operations generally take less than 24 hours, a large portion of which has the canister immersed in and open to the pool water after which the electrolyte (water) is drained and the cask or canister is dried and back-filled with helium, effectively halting any galvanic reaction.

The potential chemical or galvanic reactions do not have a significant detrimental effect on the ability of the aluminum heat transfer disks to perform their function for all normal and accident conditions associated with dry storage.

Loading Operations

After the canister is removed from the pool and during canister closure operations, an air space is created inside the canister beneath the shield lid by the drain-down of 50 gallons of water so that the shield-lid-to-canister-shell weld can be performed. The resulting air space is approximately 66 inches in diameter and 3 inches deep. As there is some clearance between the inside diameter of the canister shell and the outside diameter of the shield lid, it is possible that gases released from a chemical reaction inside the canister could accumulate beneath the shield lid. A bare aluminum surface oxidizes when exposed to air, reacts chemically in an aqueous solution, and may react galvanically when in contact with stainless steel in the presence of an aqueous solution.

The reaction of aluminum in water, which results in hydrogen generation, proceeds as:

$$2\ Al + 3\ H_20 \Rightarrow Al_2O_3 + 3\ H_2$$

The aluminum oxide (Al_2O_3) produces the dull, light gray film that is present on the surface of bare aluminum when it reacts with the oxygen in air or water. The formation of the thin oxide film is a self limiting reaction as the film isolates the aluminum metal from the oxygen source acting as a barrier to further oxidation. The oxide film is stable in pH neutral (passive) solutions, but is soluble in borated PWR spent fuel pool water. The oxide film dissolves at a rate dependent upon the pH of the water, the exposure time of the aluminum in the water, and the temperatures of the aluminum and water.

PWR spent fuel pool water is a boric acid and demineralized water solution. BWR spent fuel pool water does not contain boron and typically has a neutral pH (approximately 7.0). The pH, water chemistry, and water temperature vary from pool to pool. Since the reaction rate is largely dependent upon these variables, it may vary considerably from pool to pool. Thus, the generation rate of combustible gas (hydrogen) that could be considered representative of spent fuel pools in general is very difficult to accurately calculate, but the reaction rate would be less in the neutral pH BWR pool.

The BWR basket configuration incorporates carbon steel support plates that are coated with electroless nickel. The coating protects the carbon steel during the comparatively short time that the canister is immersed in, or contains, water. The coating is described in Section 3.8.3. The

coating is non-reactive with the BWR pool water and does not off-gas or generate gases as a result of contact with the pool water. Consequently, there are no flammable gases that are generated by the coating. A coating is not used in PWR basket configurations.

To ensure safe loading and/or unloading of the UMS transportable storage canister, the loading and unloading procedures defined in Chapter 8 are revised to provide for the monitoring of hydrogen gas before and during the welding operations joining the shield lid to the canister shell, and joining the vent and drain port covers to the shield lid. The monitoring system shall be capable of detecting hydrogen at 60% of the lower flammability limit for hydrogen (i.e. 0.6 x 4.0 = 2.4%). The hydrogen detector shall be mounted so as to detect hydrogen prior to initiation of the weld, and continuously during the welding operation. Detection of hydrogen in a concentration exceeding 2.4% shall be cause for the welding operation to stop. If hydrogen gas is detected at concentrations above 2.4% at any time, the hydrogen gas shall be removed by flushing ambient air into the region below the shield lid or port cover. To remove hydrogen from below the shield lid, the vacuum pump is attached to the vent port and operated for a sufficient period of time to remove at least five times the air volume of the space below the lid by drawing ambient air through the gap between the shield lid and the canister shell, thus removing or diluting any combustible gas concentrations.

The vacuum pump shall exhaust to a system or area where hydrogen flammability is not an issue. If hydrogen gas is detected at the port covers, the cover is removed and service air is used to flush combustible gases from the port. Once the root pass weld is completed there is no further likelihood of a combustible gas burn because the ignition source is isolated from the combustible gas. Once welding of the shield lid has been completed, the canister is drained, vacuum dried and back-filled with helium.

No hydrogen is expected to be detected prior to, or during, the welding operations. The vent port in the shield lid remains open from the time that the loaded canister is removed from the spent fuel pool until the time that the vent port cover is ready to be welded to the shield lid. Since the postulated combustible gases are very light, the open vent port provides an escape path for any gases that are generated prior to the time that the canister is vacuum dried. Once the canister is dry, no combustible gases form within the canister. The mating surfaces of the support ring and inner lid are machined to provide a good level fitup, but are not machined to provide a metal to metal seal. Consequently, additional exit paths for the combustible gases exist at the circumference of the shield lid.

Unloading Operations

It is not expected that the canister will contain a measurable quantity of combustible gases during the time period of storage. The canister is vacuum dried and backfilled with helium immediately prior to being welded closed. There are only minor mechanisms by which hydrogen is generated after the canister is dried and sealed.

As shown in Section 8.3, the principal steps in opening the canister are the removal of the structural lid, the removal of the vent and drain port covers, and the removal of the shield lid. These steps are expected to be performed by cutting or grinding. The design of the canister precludes monitoring for the presence of combustible gases prior to the removal of the structural lid and the vent or drain port covers. Following removal of the vent port cover, a vent line is connected to the vent port quick disconnect. The vent line incorporates a hydrogen gas detector which is capable of detecting hydrogen at a concentration of 2.4% (60% of its lower flammability limit of 4%). The pressurized gases (expected to be greater than 96% helium) in the canister are expected to carry combustible gases out of the vent port. If the exiting gases in the vent line contain no hydrogen at concentrations above 2.4%, the drain port cover weld is cut and the cover removed. If levels of hydrogen gas above 2.4% concentration are detected in the vent line, then the vacuum system is used to remove all residual gas prior to removal of the drain port cover. During the removal of the drain port cover, the hydrogen gas detector is attached to the vent port to ensure that the hydrogen gas concentration remains below 2.4%. Following removal of the drain port cover, the canister is filled with water using the vent and drain ports. Prior to cutting the shield lid weld, 50 gallons of water are removed from the canister to permit the removal of the shield lid. Monitoring for hydrogen would then proceed as described for the loading operations.

3.4.1.2.3 Carbon Steel

Carbon steel support disks are used in the BWR basket configuration. There is a small electrochemical potential difference between carbon steel (SA-533) and aluminum and stainless steel. When in contact in water, these materials exhibit limited electrochemically-driven corrosion. BWR pool water is demineralized and is not sufficiently conductive to promote detectable corrosion for these metal couples. In addition, the carbon steel support disks are coated with electroless nickel to protect the carbon steel surface during exposure to air or to spent fuel pool water, further reducing the possibility of corrosion. Once the canister is loaded, the water is drained from the cavity, the air is evacuated, and the canister is backfilled with helium and sealed. Removal of the water and the moisture eliminates the catalyst for galvanic corrosion.

The canister operating procedures (see Chapter 8) provide two backfill cycles in series separated by a vacuum drying cycle during closing of the canister. The displacement of oxygen by helium effectively inhibits corrosion.

The transfer cask structural components are fabricated primarily from ASTM A588 and A36 carbon steel. The exposed carbon steel components are coated with either Keeler & Long E-Series Epoxy Enamel or Carboline 890 to protect the components during in-pool use and to provide a smooth surface to facilitate decontamination.

The concrete shell of the vertical concrete cask contains an ASTM A36 carbon steel liner, as well as other carbon steel components. The exposed surfaces of the base of the concrete cask and the liner are coated with either Keeler & Long E-Series Epoxy Enamel, or Carboline 890, to provide protection from weather related moisture.

No potential reactions associated with the BWR basket carbon steel disks, the transfer cask components or vertical concrete cask components are expected to occur.

3.4.1.2.4 Coatings

The exposed carbon steel surfaces of the transfer cask, the transfer cask adaptor plate and the vertical concrete cask are coated with either Keeler & Long E-Series Epoxy Enamel or Carboline 890. These coatings are approved for Nuclear Service Level 2 use. Load bearing surfaces (i.e., the bottom surface of the trunnions and the contact surfaces of the transfer cask doors and rails) are not painted, but are coated with an appropriate nuclear grade lubricant, such as Neolube®. The technical specifications for these coatings are provided in Sections 3.8.1 and 3.8.2, respectively.

Carbon steel support disks used in the BWR canister basket are coated with electroless nickel. The coating is applied in accordance with ASTM B733-SC3, Type V, Class 1[37]. As described in Section 3.8.3, the electroless nickel coating process uses a chemical reducing agent in a hot aqueous solution to deposit nickel on a catalytic surface. The deposited nickel coating is a hard alloy of uniform thickness of 25 μm (0.001 inch), containing from 4% to 12% phosphorus. Following its application, the nickel coating combines with oxygen in the air to form a passive oxide layer that effectively eliminates free electrons on the surface that would be available to cathodically react with water to produce hydrogen gas. Consequently, the production of hydrogen gas in sufficient quantities to facilitate combustion is highly unlikely.

3.4.1.2.5 Concrete

The vertical concrete storage cask is fabricated of 4000 psi, Type 2 Portland cement that is reinforced with vertical and circumferential carbon steel rebar. Quality control of the proportioning, mixing, and placing of the concrete, in accordance with the NAC fabrication specification, will make the concrete highly resistant to water. The concrete shell is not expected to experience corrosion, or significant degradation from the storage environment through the life of the cask.

3.4.1.2.6 Criticality Control Material

The criticality control material is boron carbide mixed in an aluminum alloy matrix. Sheets of this material are affixed to one or more sides of the designated fuel tubes and completely enclosed by a welded stainless steel cover. The material resists corrosion similar to aluminum, and is protected by an oxide layer that forms shortly after fabrication and inhibits further interaction with the stainless steel. Consequently, no potential reactions associated with the aluminum-based criticality control material are expected.

3.4.1.2.7 Neutron Shielding Material

The neutron shielding material is a hydrogenated polymer, NS-4-FR, consisting primarily of aluminum, carbon, oxygen and hydrogen, to which boron carbide (B_4C) is added to improve shielding effectiveness. It is used in the transfer cask and in the shield plug of the vertical concrete storage cask to provide radiation shielding. The acceptable performance of the material has been demonstrated by use and testing. The material has been used in two licensed storage casks in the United States for up to 10 years and in more than 50 licensed casks in Japan, Spain and the United Kingdom. There are no reports that the shielding effectiveness of NS-4-FR material has degraded in these applications, demonstrating the long-term reliability for the purpose of shielding neutrons from personnel and the environment. There are no potential reactions associated with the polymer structure of the material and the stainless steel or carbon steel in which it is encapsulated during use.

The chemistry of the material (e.g., the way the elements are bonded to one another) contributes significantly to the fire retardant capability of the NS-4-FR. Even though the material contains hydrogen, the ingredients were selected so that the NS-4-FR resists fire. Approximately 90% of the off-gassing that does occur consists of water vapor.

The thermal performance of the NS-4-FR has been demonstrated by long-term functional stability tests of the material at temperatures from -40°F to 338°F. These tests included specimens open to the atmosphere and enclosed in a cavity at both constant and cyclic thermal loads. The tests evaluated material loss though off-gassing and material degradation. The results of the tests demonstrate that, in the temperature range of interest, the NS-4-FR does not exhibit loss of material by off-gassing, does not generate any significant gases, and does not suffer degradation or embrittlement. Further, the tests demonstrated that encased material, as it is used in the NAC-UMS®, performed significantly better than exposed material. Consequently, the formation of flammable gases is not a concern.

Radiation exposure testing of NS-4-FR in reactor pool water demonstrated no physical deterioration of the material and no significant loss of hydrogen (less than 1%). The tests also demonstrated that the NS-4-FR retains its neutron shield capability over the cask's 50-year design life with substantial margin. The radiation testing has shown that detrimental embrittlement and loss of hydrogen from the material do not occur at dose rates (9×10^{14} n/cm^2) that exceed those that would occur assuming the continuous storage of design basis fuel for a 50-year life (estimated to be 1.7×10^{12} cm^2/yr). Consequently, detrimental deterioration or embrittlement due to radiation flux does not occur.

Since the NS-4-FR in the NAC-UMS® transfer cask is sandwiched between the shell and the lead shield and enclosed within a welded steel shell where the shell seams are welded to top and bottom plates with full penetration or fillet welds, it will maintain its form over the expected lifetime of the transfer cask's radiation exposure. The material's placement between the lead shield and the outer shell does not allow the material to redistribute within the annulus.

The NS-4-FR shield material is similarly enclosed in the storage cask shield plug, since a disk of NS-4-FR is captured in an annulus formed by a carbon steel ring and two carbon steel plates. This material cannot redistribute within this volume.

3.4.1.3 General Effects of Identified Reactions

No potential chemical, galvanic, or other reactions have been identified for the Universal Storage System. Therefore, no adverse conditions, such as the generation of flammable or explosive quantities of combustible gases or an increase in neutron multiplication in the fuel (criticality)

because of boron precipitation, can result during any phase of canister operations for normal, off-normal, or accident conditions.

3.4.1.4 Adequacy of the Canister Operating Procedures

Based on this evaluation, which results in no identified reactions, it is concluded that the Universal Storage System operating controls and procedures presented in Chapter 8.0 are adequate to minimize the occurrence of hazardous conditions.

3.4.1.5 Effects of Reaction Products

No potential chemical, galvanic, or other reactions have been identified for the Universal Storage System. Therefore, the overall integrity of the canister and the structural integrity and retrievability of the spent fuel are not adversely affected for any operations throughout the design basis life of the canister. Based on the evaluation, no change in the canister or fuel cladding thermal properties is expected, and no corrosion of mechanical surfaces is anticipated. No change in basket clearances or degradation of any safety components, either directly or indirectly, is likely to occur since no potential reactions have been identified.

THIS PAGE INTENTIONALLY LEFT BLANK

3.4.2 Positive Closure

The Universal Storage System employs a positive closure system composed of multi-pass welds to join the canister shield lid and the canister structural lid to the shell. The penetrations to the canister cavity through the shield lid are sealed by welded port covers. The welded canister closure system (see Figure 3.4.2-1) precludes the possibility of inadvertent opening of the canister.

The top of the vertical concrete cask is closed by a bolted lid that weighs approximately 2,500 lbs. The weight of the lid, its inaccessibility, and the presence of the bolts effectively preclude inadvertent opening of the lid. In addition, a security seal is provided between two of the lid bolts to detect tampering with the closure lid.

Figure 3.4.2-1 Universal Storage System Welded Canister Closure

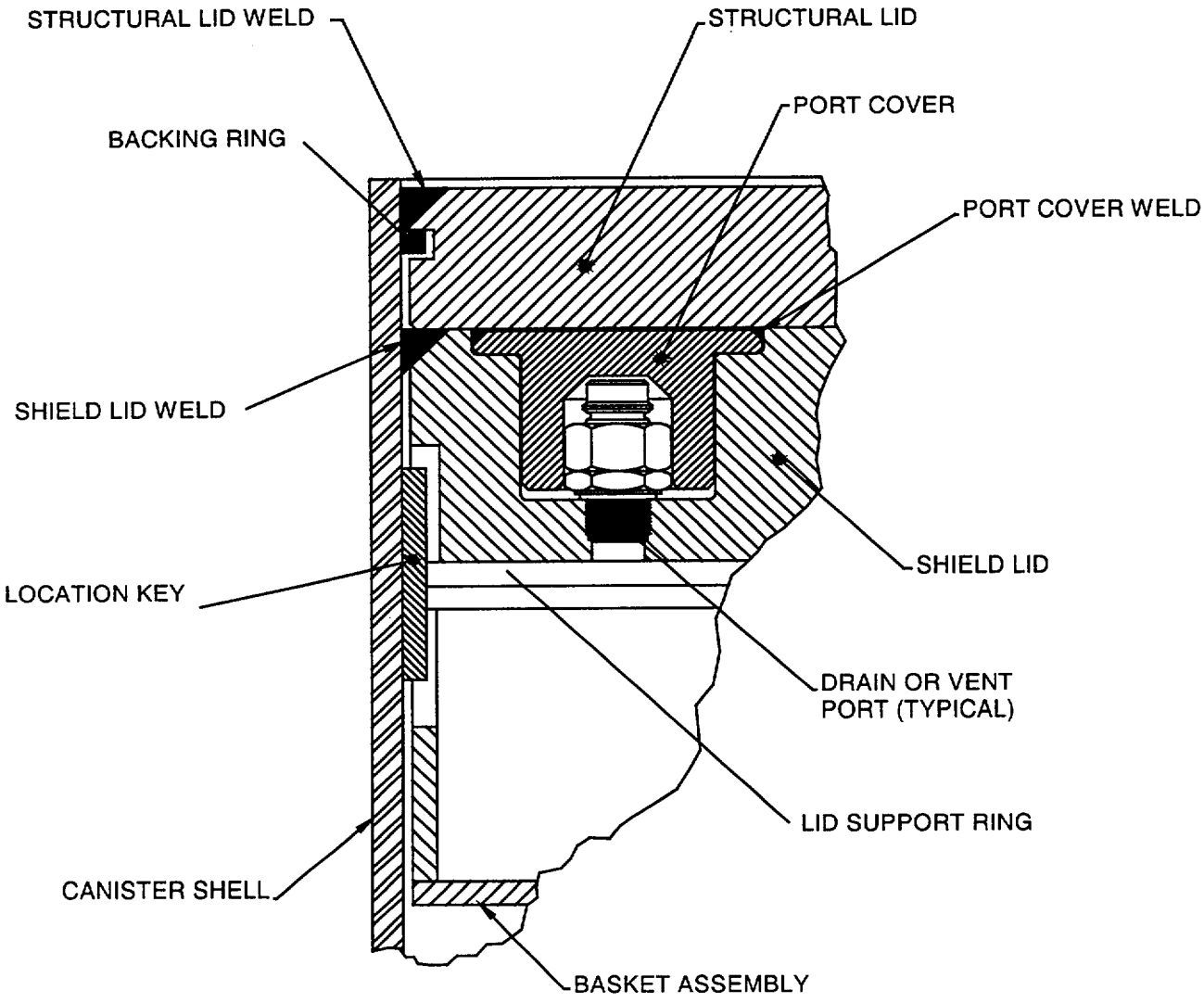

3.4.3 Lifting Devices

To provide more efficient handling of the Universal Storage System, different methods of lifting are designed for each of the components. The transfer cask, the transportable storage canister, and the concrete cask, are handled using trunnions, hoist rings, and a system of jacks and air pads, respectively.

The designs of the UMS® Universal Storage System and Universal Transport System components address the concerns identified in U.S. NRC Bulletin 96-02, "Movement of Heavy Loads Over Spent Fuel, Over Fuel in the Reactor Core, or Over Safety-Related Equipment" (April 11, 1996) as follows:

(1) The UMS® lifting and handling components satisfy the requirements of NUREG-0612 and ANSI N14.6 for safety factors on redundant or nonredundant load paths as described in this chapter.

(2) Transfer or transport cask lifting in the spent fuel pool or cask loading pit or transfer or transport cask lifting and movement above the spent fuel pool operating floor will be addressed on a plant-specific basis.

The transfer cask is lifted by two trunnions located near the top of the cask. The 10-in. diameter trunnions protrude 5 in. through the cask shell. The trunnions are attached by full-penetration welds to both the inner and the outer shells (Figure 3.4.3-1). The transfer cask is designed as a heavy-lifting device that satisfies the requirements of NUREG-0612 and ANSI N14.6 for lifting the fully loaded canister of fuel and water, together with the shield lid, which is the maximum weight for the transfer cask during a lifting operation with a given configuration.

The transportable storage canister remains within the transfer cask during all preparation, loading, canister closure, and transfer operations. The canister is equipped with six hoist rings threaded into the structural lid to lift the loaded canister and to lower it into the concrete cask after the shield doors are opened. The hoist rings, shown in Figure 3.4.3-2, are also used for any subsequent lifting of the loaded dry canister.

The vertical concrete cask is moved by means of a system of air pads. The cask is raised approximately 3 in. by four lifting jacks placed at the jacking pads located near the end of each

air inlet. A system consisting of 4 air pads is then inserted under the concrete cask. The cask is lowered onto the uninflated air pads, the jacks are removed, and the air pads are inflated to lift the concrete cask and position it as required on the storage pad or transport vehicle. When positioning is complete, the jacks are used to support the cask as the air pads are removed.

As an option, the loaded concrete cask may also be lifted and moved using lifting lugs at the top of the cask. The top lifting lugs are described in Section 3.4.3.1.3.

The structural evaluations in this section consider the bounding conditions for each aspect of the analysis. Generally, the bounding condition for lifting devices is represented by the heaviest component, or combination of components, of each configuration. The bounding conditions used in this section are:

Section	Evaluation	Bounding Condition	Configuration
3.4.3.1	Concrete Cask Lifting Jacks	Heaviest loaded Concrete Cask + 10% dynamic load factor	BWR Class 5
	Pedestal Loading	Heaviest loaded Canister + 10% dynamic load factor	BWR Class 5
	Concrete Cask Air Pads (Lifting)	Heaviest loaded Concrete Cask	BWR Class 5
	Concrete Cask Top Lifting Lugs (Lifting)	Heaviest loaded Concrete Cask + 10% dynamic load factor	BWR Class 5
3.4.3.2	Canister Lift	Heaviest loaded Canister + 10% dynamic load factor	BWR Class 5
3.4.3.3	Transfer Cask Lift	Heaviest loaded Transfer Cask + 10% dynamic load factor	BWR Class 5
3.4.3.3.3	Transfer Cask Shield Doors and Rails	Heaviest loaded Canister + water, shield doors and 10% dynamic load factor	BWR Class 5

Figure 3.4.3-1 Transfer Cask Lifting Trunnion

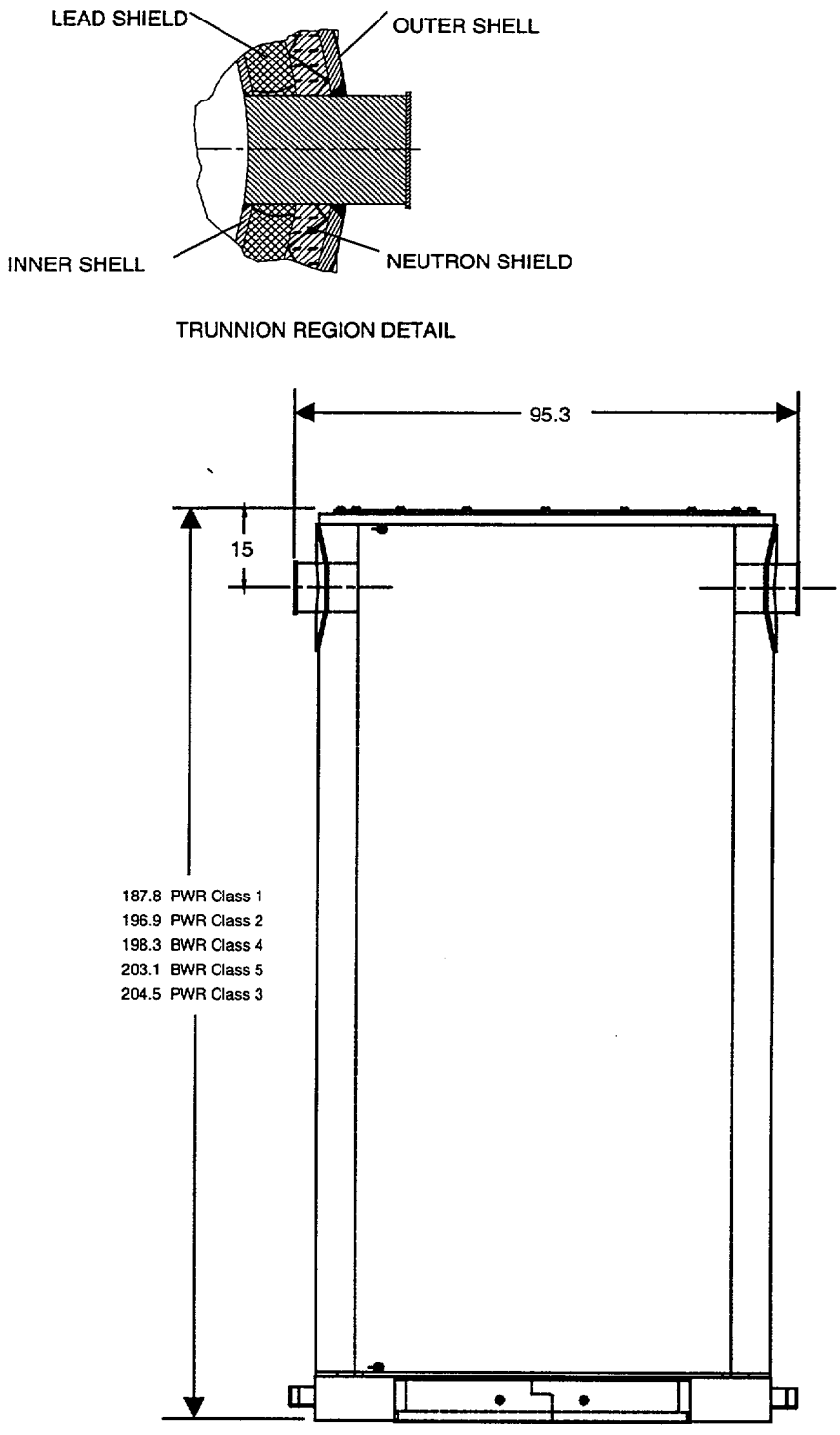

Dimensions in inches

Figure 3.4.3-2 Canister Hoist Ring Design

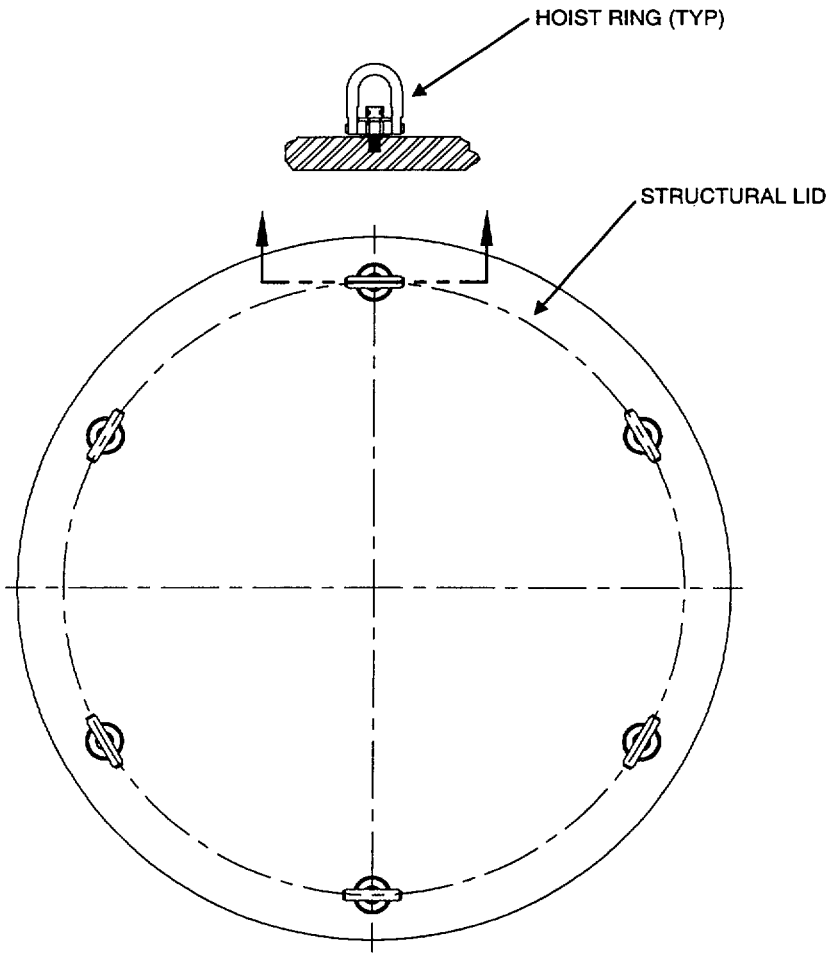

3.4.3.1 Vertical Concrete Cask Lift Evaluation

The vertical concrete cask may be lifted and moved using an air pad system under the base of the cask or four lifting lugs provided at the top of the cask.

Lifting jacks installed at jacking points in the air inlet channels are used to raise the cask so that the air pads can be inserted under the cask. The lifting jacks use a synchronous lifting system to equally distribute the hydraulic pressure among four hydraulic jack cylinders. The calculated weight of the heaviest, loaded concrete cask to be lifted by the jacking system, the BWR Class 5 configuration, is 312,210 pounds.

The lifting lugs are analyzed in accordance with ANSI N14.6 and ACI-349.

3.4.3.1.1 Bottom Lift By Hydraulic Jack

To ensure that the concrete bearing stress at the jack locations due to lifting the cask does not exceed the allowable stress, the area of the surface needed to adequately spread the load is determined in this section. The allowable bearing capacity of the concrete at each jack location is:

$$U_b = \phi f_c' A = \frac{(0.7)(4{,}000)\pi d^2}{4} = 2{,}199.1\ d^2,$$

where:

ϕ = 0.7 strength reduction factor for bearing,
f_c' = 4,000 psi concrete compressive strength,
$A = \frac{\pi d^2}{4}$, concrete bearing area (d = bearing area diameter).

The concrete bearing strength must be greater than the cask weight multiplied by a load reduction factor, $L_f = 1.4$.

$$2{,}199.1\,d^2 > \frac{L_f \times W}{n} = \frac{1.4(330{,}000\text{ lb})}{4} \Rightarrow d > 7.25\text{ in.},$$

where:

n = the number of jacks, 4
W = the weight of the vertical concrete cask, 330,000 lb.
L_f = the load factor, 1.4

The diameter obtained in the above equation corresponds to the minimum permissible area over which the load must be distributed. The force exerted by the jack is applied through the 2.25-in. - thick steel air inlet top plate. This increases the effective diameter of the load acting on the concrete surface from a 4.13-in. diameter jack cylinder to about 8.63 in., assuming a 45° angle for the cone of influence.

The bearing stress at each jack location with a bearing area of $\frac{\pi \times 8.63\text{in}^2}{4} \approx 58.5\text{in}^2$ is:

$$\sigma = \frac{P}{A} = \frac{(1.4)(330{,}000\text{ lb})}{4(58.5\text{ in}^2)} = 1{,}974\text{ psi}$$

The allowable bearing stress is:

$\sigma = \phi f_c = (0.7)(4{,}000\text{ psi}) = 2{,}800\text{ psi}$

The Margin of Safety is:

$$MS = \frac{2{,}800.0}{1{,}976.8} - 1 = +0.42$$

Bottom Plate Flexure

During a bottom lift of the concrete cask, the weight of the loaded canister, the pedestal, and the air inlet system are transferred to the bottom plate. As the load is applied, the bottom plate flexes, tending to separate from the concrete. Nelson studs are used to tie the concrete to the bottom plate and prevent separation.

Thirty-two 3/4 in. diameter × 6 3/16-in. long Nelson studs are used in the concrete cask. The shear capacity of each stud is about 23.9 kips [21]. The total load capacity of the studs is:

Capacity = 32 studs × 23.86 kips/stud = 763.5 kips.

The allowable load, P_u, with a load factor of 2.0, as specified in the manufacturer's design data [21], is:

$$P_u = \frac{763.5 \text{ kips}}{2.0} = 381.8 \text{ kips}$$

The total calculated load applied to the concrete cask bottom plate is 84,354 lb. A conservative weight of 84,400 lb, plus a 10% dynamic load factor is used in the following calculation.

84,400 lb × 1.1 = 92,840 lb

The margin of safety is:

$$MS = \frac{381.8 \text{ kips}}{92.8 \text{ kips}} - 1 = +3.1$$

Base Plate

The weight of the canister is uniformly distributed over the 2-in. thick circular base plate. The unit load is calculated using a weight that bounds the heaviest, loaded canister plus the weight of the cover plate, the base plate, and a 10% dynamic load factor:

$$q = \frac{W}{A} = \frac{(77{,}371 \text{ lb} + 2{,}033 \text{ lb})(1.1)}{\pi \times (33.75 \text{ in})^2} = 24.4 \text{ psi}$$

where:

W = total load on the base plate,
A = the base plate area, and
1.1= dynamic load factor.

The stress, assuming a simply supported plate, is [22]

$$\sigma_r = \frac{99q}{80}\left(\frac{r}{t}\right)^2 = \frac{99 \times 24.4\text{psi}}{80}\left(\frac{25\text{in.}}{2\text{in.}}\right)^2 = 4{,}718\text{ psi.}$$

The allowable stress for flexural members, per the Manual of Steel Construction [23], is: $F_{allowable} = 0.66\ F_y = 23{,}760$ psi. The margin of safety is:

$$MS = \frac{23{,}760\text{ psi}}{4{,}718\text{ psi}} - 1 = 4.0$$

The base plate is supported by the base plate stand at four welded locations, each with an arc length of 16.85 in. The bending moment at the cross section of the base plate at the support locations is:

$$M = (L_f)(q)(A)(P_c) = (1.1)(24.4\text{ psi})\left(\frac{\pi\left((33.75\text{ in})^2 - (25\text{ in})^2\right)}{4}\right)(4.375\text{ in.}) \approx 47{,}410\text{ in} \cdot \text{lb}$$

where:

A = area of the base plate stand from the plate support to the edge of the circular plate,
$P_c = 4.25$ in., the location of the resultant force, and
$L_f = 1.1$, a load factor to account for 10% dynamic loading.

The bending stress is:

$$f_b = \frac{6M}{bt^2} = \frac{(6)(47{,}410\text{ in} \cdot \text{lb})}{(16.85\text{ in.})(2\text{ in})^2} \approx 4{,}220\text{ psi}$$

where:

b = circumferential length of the base plate stand in contact with the base plate, and
t = the thickness of the base plate stand.

The base plate is made of ASTM A-36 carbon steel with a yield strength, F_y, of 36,000 psi. The allowable stress for flexural members, per the Manual of Steel Construction [23], is:

$F_b = 0.66\ F_y = 23{,}760$ psi.

The resulting margin of safety is:

$$MS = \frac{23{,}760\ psi}{4{,}220\ psi} - 1 = +4.60$$

The maximum shear stress at the support location is:

$$f_v = \frac{W}{L} = \frac{(77{,}371\,lb + 2{,}033\,lb)(1.1)}{4 \times (16.85\,in.)(2.0\,in.)} \approx 648\,psi$$

The allowable shear stress is 14,400 psi ($0.4 \times F_y = 0.4 \times 36{,}000$ psi), and the margin of safety is:

$$MS = \frac{14{,}400\ psi}{648\ psi} - 1 = 21.2$$

Base Plate Stand (Vertical Plate)

The cylindrical base plate stand is subjected to an axial compressive force and bending moments of the pedestal base plate due to the canister weight and the weight of the base plate stand, itself. The maximum compressive stress, f_a, at the critical cross-section (2 in. × 1.5 in., 8 locations) is:

$$f_a = \frac{(77{,}371\ lb + 2{,}033\ \ lb + 230\ lb)(1.1)}{8(1.5\ \ in.)(2\ \ in.)} = 3{,}650\ psi.$$

Using Part 5, Chapter E and Numerical Values Tables 3–5, Section 5, of the Manual of Steel Construction [23], for A-36 material (F_y = 36,000 psi), the allowable stress, F_a, for compression is:

$F_a = C_a F_y$ (from Table 3 [23]),

when

$Kl/r \leq C_c$.

In this case,

K = 0.65, effective-length factor for the end conditions (rotation and translation fixed),

l = 6.0 in., height of pedestal ring (unbraced member),

r = $\frac{1.5}{\sqrt{12}} = 0.433$, radius of gyration, and

C_c = 126.1, the slenderness ratio from Table 4 [23], and

$$\frac{Kl}{r} = \frac{0.65 \times 6}{0.433} = 9, \text{ which is} < C_c.$$

From Table 3 [23], for $\frac{Kl/r}{C_c} = \frac{9}{126.1} = 0.07$,

$C_a = 0.589$, and the allowable stress is

$F_a = (0.589)\ (36{,}000 \text{ psi}) = 21{,}200 \text{ psi}.$

The bending stress at the same cross-section is conservatively calculated as:

P_t = one-fourth of the total load = (77,371 + 2,033) / 4 = 19,851 lb.

The pedestal is represented as a combination of beams with a total length of 37.7 in. to describe the load path.

P_1 = 19,851 lb × (15.35 / 37.7)
= 8,083 lb, use 8100 lb.

P_2 = 19,851 lb × (22.35 / 37.7)
= 11,768.4 lb, use 11,800 lb.

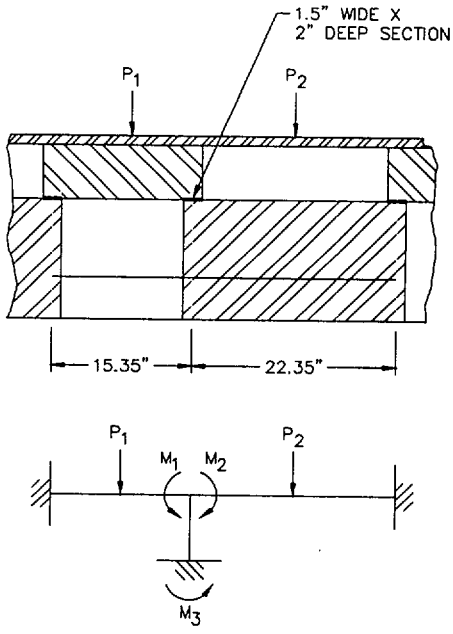

M_1 and M_2 are conservatively considered to be the fixed-end moments of beams with a concentrated load at mid-span (plus a 10% dynamic load factor). L_1 (15.35 in.) and L_2 (22.35 in.) are the lengths of the beams. M_3 (the moment at the 2 in. × 1.5 in. cross-section) is considered to be the difference between M_1 and M_2.

$$M_2 = \frac{1.1\,(P_2 L_2)}{8} = \frac{(1.1)(11{,}800\ \text{lb})(22.35\text{in.})}{8} = 36{,}263\ \text{in.·lb.}$$

$M_3 = M_2 - M_1 = 19{,}167$ in.·lb.

The maximum bending stress f_b is computed as

$$f_b = \frac{6M_3}{bt^2} = \frac{(6)(19{,}167\,\text{in}\cdot\text{lb})}{(1.5\text{in.})(2\text{in.})^2} = 19{,}167\ \text{psi}$$

The allowable stress for bending (F_b) is 23,760 psi ($0.66 \times F_y$). Since f_a / F_a is less than 0.15, Equation (H1-3) in the Manual of Steel Construction, Chapter H, is used to evaluate combined stress:

$$\frac{f_a}{F_a} + \frac{f_b}{F_b} = \frac{3{,}650}{21{,}200} + \frac{19167}{23{,}760} = 0.98 < 1.0$$

Therefore, the pedestal is structurally adequate to support the weight of the heaviest loaded canister.

3.4.3.1.2 Bottom Support by Air Pads

The concrete cask is supported by air pads in each of 4 quadrants during transport. The layout of the air pads (four 60 in. × 60 in. square pads) are designed to clear the air inlet locations by approximately 3 in. to allow for hydraulic jack access.

The air pad system maximum height is 6.0 in. (3-in. maximum lift, plus 3.0-in. overall height when deflated). The air pad system has a rated lift capacity of 560,000 lb. The air pads must supply sufficient force to overcome the weight of the concrete cask under full load plus a lift load factor of 1.1. The weight of the heaviest storage configuration, the BWR class 5 system, is about 320,000 lb. The air pad evaluation uses a conservative weight of 330,000 lb. The required lift load is 1.1 × (330,000 lb) = 363,000 lb. Since the available lift force is greater than the load, the air pads are adequate to lift the concrete cask. The lifting force margin of safety is:

MS = (560,000 / 363,000) -1 = + 0.54.

3.4.3.1.3 Top Lift By Lifting Lugs

A set of four lifting lugs is provided at the top of the vertical concrete cask so that the cask, with a loaded transportable storage canister, may be lifted from the top end. Similar to the bottom lift, the BWR Class 5 configuration maximum weight is used in the analysis of the lifting lugs.

The steel components of the lifting lugs are analyzed in accordance with ANSI N14.6. The allowable stress for the load-bearing members is the lesser of $S_y/3$ or $S_u/5$. The development length of the rebar embedded in the concrete is analyzed in accordance with ACI-349.

Lifting Lug Axial Load

The maximum loaded concrete cask weight is 312,210 pounds. Assuming a 10% dynamic load factor, the load (P) on each lug is:

$$P = \frac{312{,}210(1.1)}{4} = 85{,}858 \text{ lb}$$

For the analysis, P is taken as 86,000 lb. The lugs are evaluated for adequate strength under a uniform axial load in accordance with the method described in Section 9.3 of AFFDL-TR-69-42 [32].

The bearing stresses and loads for lug failure involving bearing, shear-tearout, and hoop tension are determined using an allowable load coefficient (K). Actual lug failures may involve more than one failure mode, but such interaction effects are accounted for in the value of K.

The allowable lug yield bearing stress (F_{bryL}) is:

$$F_{bryL} = K\frac{a}{D}\left(F_{ty}\right) \quad \text{(for e/D < 1.5)}$$

$$= 1.61\left(\frac{1.78}{4.063}\right)(60 \text{ ksi}) = 42.32 \text{ ksi}$$

where:

K = 1.61
a = 1.78 in.

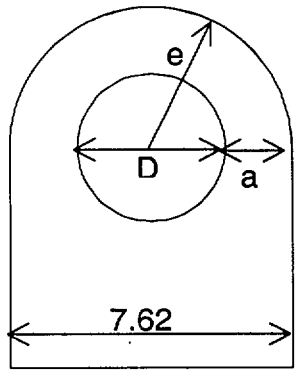

Lifting lug

$e = 3.81$ in.

$D = 4.063$ in.

$e/D = 3.81/4.063 = 0.94 < 1.5$

F_{ty} = yield strength = 60.0 ksi for ASME SA537, Class 2 carbon steel

The allowable ultimate bearing load (P_{bruL}) for lug failure in bearing, shear-out, or hoop tension is:

$$P_{bruL} = 1.304 \times F_{bryL} \times D \times t \quad (\text{if } F_{tu} > 1.304\, F_{ty})$$
$$= 1.304(42.32\text{ksi})(4.063\text{ in.})(2.0\text{ in.})$$
$$= 448.44 \text{ kips}$$

where:

$$\frac{F_{tu}}{F_{ty}} = \frac{80 \text{ ksi}}{60 \text{ ksi}} = 1.33 > 1.304$$

$t = 2.0$ in. (lug thickness)

F_{tu} = ultimate tensile strength = 80.0 ksi for SA537, Class 2 carbon steel

The lug ultimate load capacity (448.44 kips) divided by the lug maximum load (86 kips) is:

$$FS_u = \frac{448.44}{86.0} = 5.2 > 5$$

Therefore, the design criterion of a minimum factor of safety (FS) of 5 on the basis of material ultimate strength is met.

$$P_{bryL} = (42.32 \text{ ksi})(4.063 \text{ in.})(2.0 \text{ in.}) = 346.33 \text{ kips}$$

The lug yield load capacity (346.33 kips) divided by the lug maximum load (86 kips) is:

$$FS_y = \frac{346.33}{86.0} = 4.03 > 3$$

Therefore, the design criterion of a minimum factor of safety (FS) of 3 on the basis of material yield strength is met.

The tensile stress (σ) in the net cross-sectional area is:

$$\sigma = \frac{P}{A} = \frac{86 \text{ kips}}{7.12 \text{ in.}^2} = 12.1 \text{ ksi}$$

where:

P = the load on each lug
A = the net cross sectional area ($2 \times a \times t = 7.12 \text{ in.}^2$)

The factor of safety based on material yield strength $(FS_y)_t$ is:

$$(FS_y)_t = \frac{S_y}{\sigma} = \frac{60 \text{ ksi}}{12.1 \text{ ksi}} = 4.96 > 3$$

Therefore, the design criterion of a minimum factor of safety (FS) of 3 on the basis of material yield strength is met.

The factor of safety based on material ultimate strength $(FS_u)_t$ is:

$$(FS_u)_t = \frac{S_u}{\sigma} = \frac{80 \text{ ksi}}{12.1 \text{ ksi}} = 6.61 > 5$$

Therefore, the design criterion of a minimum factor of safety (FS) of 5 on the basis of material ultimate strength is met.

Embedded Plate

The load path from the lugs through the embedded plate and to the embedded reinforcing steel is symmetrical, with the edges of the lifting lugs being very near the axial center line of the reinforcing steel. Therefore, no significant bending moments are introduced into the embedded plate. The embedded plate cross-sectional area is more than double that of the lugs; therefore, the tensile strength of the plate is adequate by inspection.

Reinforcing Steel

Each embedded plate has two lifting lugs, therefore, the load (P_{pl}) on each embedded plate is 2 × 86,000 lb or

$$P_{pl} = 172{,}000 \text{ lb.}$$

The required cross-sectional area of reinforcing steel (A_s) is:

$$A = \frac{P_{pl}}{S_y} = \frac{172{,}000 \text{ lb}}{60{,}000 \text{ psi}} = 2.87 \text{ in.}^2$$

Eight #10 reinforcing steel deformed bars are selected to anchor the embedded plate to the concrete cask concrete shell.

The cross-sectional area (A_b) for each #10 bar is 1.27 in.^{2} [33]. Therefore, the total area (A_t) resisting the tensile load is:

$$A_t = 8 \times 1.27 \text{ in.}^2 = 10.16 \text{ in.}^2$$

The reinforcing steel actual cross-sectional area (10.16 in.^{2}) divided by the required cross-sectional area (2.87 in.^{2}) is:

$$FS = \frac{10.16}{2.87} = 3.54 > 3.$$

Therefore, the design criterion of a minimum factor of safety (FS) of 3 on the basis of material yield strength is met.

The development length (l_d) is the length of embedded reinforcing steel required to develop the design strength of the reinforcing steel at a critical section.

The required reinforcing steel development length (l_d) in accordance with ACI-349–90 Section 12.2.2 [34] is:

$$l_d = 0.04A_b\left(\frac{F_y}{\sqrt{f_c'}}\right), \text{but not less than } l_d = (0.0004)(d_b)(F_y)$$

$$l_d = 0.04A_b\left(\frac{F_y}{\sqrt{f_c'}}\right) = 0.04(1.27)\left(\frac{60{,}000}{\sqrt{4{,}000}}\right) = 48.2 \text{ in.}$$

$$l_d = (0.0004)(d_b)(F_y) = 0.0004(1.27)(60{,}000) = 30.5 \text{ in.}$$

where:

F_y = 60,000 psi (the reinforcing steel yield strength, A615, Grade 60 steel)

f_c' = 4,000 psi (concrete design strength)

The actual length of the reinforcing steel is 187.5 in.

$$FS = \frac{\text{Actual length}}{\text{Required length}} = \frac{187.5}{48.2} = 3.89 > 3$$

Therefore, the design criterion of a minimum factor of safety (FS) of 3 on the basis of material yield strength is met.

Welds

The lifting lugs are welded to the embedded plate with full penetration welds developing the full strength of the attached lugs.

The reinforcing steel is welded to the embedded plate with full penetration welds developing the full strength of the reinforcing steel, which has the same tensile yield strength as the embedded plate.

Therefore, all welds are adequate by inspection.

Nelson Studs

During a top end lift, the weight of the canister and pedestal applies a tensile load to the Nelson studs. Using the BWR Class 5 configuration, 75,896 pound canister weight (77,000 pounds used in analysis), an ANSYS finite element model is used to obtain the maximum load on the Nelson studs. The model, shown below, represents an eighth of the pedestal. The weight of the canister is applied as a pressure load to the top of the 2-inch base plate. The load is reacted through the Nelson studs and gap elements between the pedestal and the concrete. Using a 10% dynamic load factor, the maximum load on a Nelson stud is 13,467 pounds.

In accordance with ACI 349-90 [34], the design pullout strength of the concrete (P_d) for any embedment is based on a uniform tensile stress acting on an effective stress area which is defined by the projected area of stress cones radiating toward the attachment from the bearing edge of the anchor heads. The effective area shall be limited by overlapping stress cones, by the intersection of the cones with concrete surfaces, by the bearing area of anchor heads, and by the overall thickness of the concrete. A 45°-inclination angle is used for the stress cones.

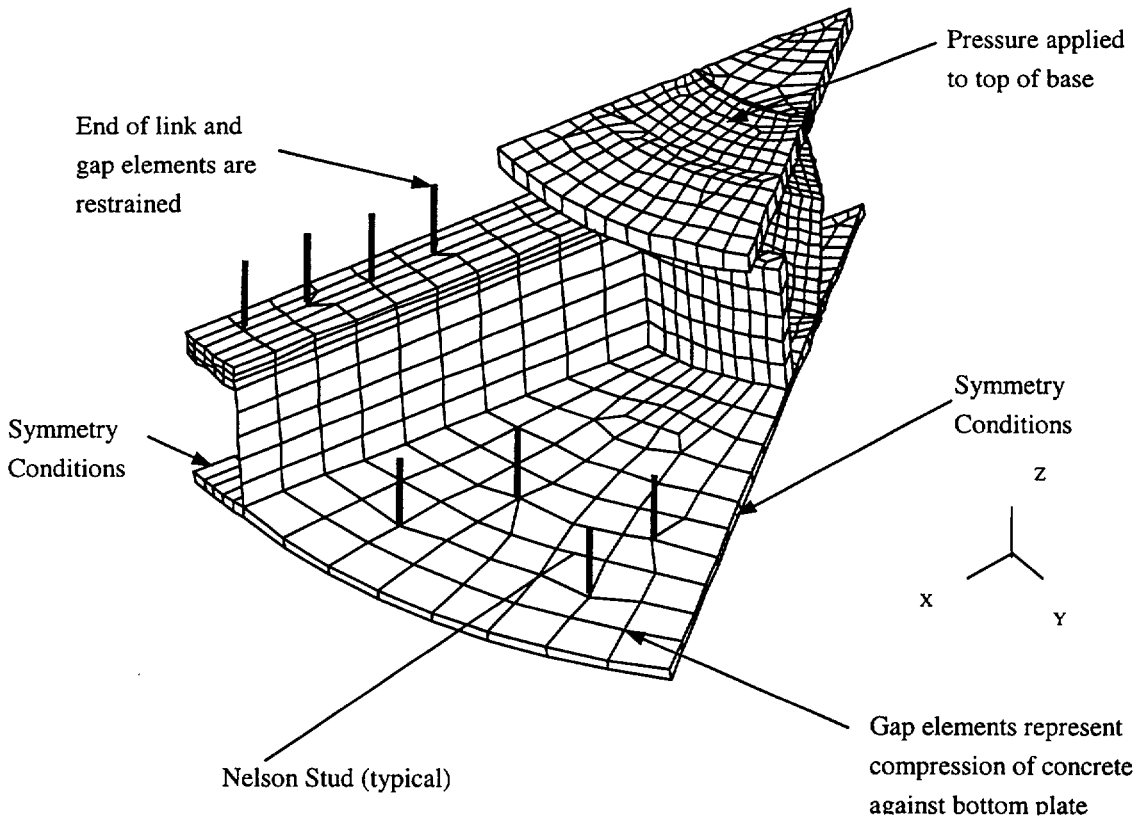

Pedestal Finite Element Model

The maximum pullout strength of the concrete (P_d) is defined by the equation

$$P_d = 4 \times \phi \times \sqrt{f_c'} \times A_{cd}$$

where:

ϕ - strength reduction factor = 0.85

f_c' - concrete compression strength = 4,000 psi

A_{cp} - projected surface area of stress cones for Nelson studs

The maximum load occurs in the eight Nelson studs located on the top of the air inlet. A_{cp} for the eight Nelson studs equals 471.62 inch^2. Therefore, P_d equals:

$$P_d = 4 \times 0.85 \times \sqrt{4000} \times 471.62 = 101{,}415 \text{ lb.}$$

The total load on the eight Nelson studs is 27,378 pounds.

The margin of safety for the concrete is:

$$MS = \frac{101,415}{27,378} - 1 = +2.70$$

For a single stress cone, the maximum load is 13,467 pounds. The corresponding pull-out strength is 117.8 inch^2.

$$P_d = 4 \times 0.85 \times 117.8 \times \sqrt{4,000} = 25,331 \text{ lbs.}$$

where the projected surface area for a single stress cone (Acp) of a single Nelson stud is 117.8.

The margin of safety for a single Nelson stud is:

$$MS = \frac{25,331}{13,467} - 1 = +0.88$$

Vertical Concrete Cask Pedestal

Using the same ANSYS Finite Element Model that was used for the Nelson Stud analysis, an analysis of the pedestal was performed. The maximum nodal stress intensity for the pedestal is 5,785 psi. From Tables 4.1-4 and 4.1-5, the maximum canister temperature is 376°F. For A36 steel, the allowable stress (S_m) is 19,300 psi. The margin of safety is, conservatively:

$$MS = \frac{19,300}{5,785} - 1 = 2.34$$

3.4.3.2 Canister Lift

The adequacy of the canister lifting devices is demonstrated by evaluating the hoist rings, the canister structural lid, and the weld that joins the structural lid to the canister shell against the criteria in NUREG-0612 [8] and ANSI N14.6 [9]. The lifting configuration for the PWR and BWR canisters consists of six hoist rings threaded into the structural lid at equally spaced angular intervals. The hoist rings are analyzed as a redundant system with two three-legged lifting slings. For redundant lifting systems, ANSI N14.6 requires that load-bearing members be capable of lifting three times the load without exceeding the tensile yield strength of the material and five times the load without exceeding the ultimate tensile strength of the material. The canister lid is evaluated for lift conditions as a redundant system that demonstrates a factor of safety greater than three based on yield strength and a factor of safety greater than five based on ultimate strength. The canister lift analysis is based on a load of 76,000 lb, which bounds the weight of the heaviest loaded canister configuration, plus a dynamic load factor of 10 %.

The canister lifting configuration is shown in the figure below, where: x is the distance from the canister centerline to the hoist ring center line (29.5 inches); F_y is the vertical component of force on the hoist ring; F_x is the horizontal component of force on the hoist ring; R is the sling length; and, F_R is the maximum allowable force on the hoist ring (30,000 lbs.). The angle θ is the angle from vertical to the sling. The vertical load, F_y, assuming a 10% dynamic load factor, is:

$$F_y = \frac{76{,}000 \text{ lbs x } 1.1}{3 \text{ lift points}} = 27{,}867 \text{ lbs}$$

The hoist rings are American Drill Bushing Company, Model 23200 Safety Engineered Hoist Rings, rated at 30,000 lbs., (or comparable ring from an alternative manufacture) with a safety factor of 5 on ultimate strength.

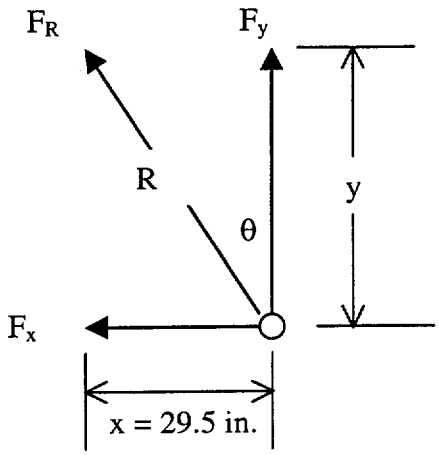

Calculating the maximum angle, θ, that will limit F_R to 30,000 lb:

$$\theta = \cos^{-1}\left(\frac{F_y}{F_R}\right) = \cos^{-1}\left(\frac{27{,}867}{30{,}000}\right) = 21.7 \text{ deg}$$

The minimum sling length, R, is

$$R = \frac{x}{\sin\theta} = \frac{29.5}{\sin 21.7^\circ} = 79.8 \text{ in.}$$

An 80-in. sling places the master link about 75 in. above the top of the canister (y = R cos θ = 80 cos 21.7° = 74.3 inches).

A minimum distance of 75 inches between the master link and the top of the canister is specified in Sections 8.1.2 and 8.2.

From the Machinery's Handbook [24], The shear area, A_n, in the structural lid bolt hole threads is calculated as

$$A_n = 3.1416\, n\, L_e\, D_s\text{min}\left[\frac{1}{2n} + 0.57735\left(D_s\text{min} - E_n\text{max}\right)\right]$$

$$= 3.1416(4.5)(2.0 \text{ in.})(1.9751 \text{ in.})\left[\frac{1}{2(4.5)} + 0.57735(1.9751 \text{ in.} - 1.8681 \text{ in.})\right]$$

$$= 9.654 \text{ in}^2$$

where:

n	=	4.5 threads per in,
L_e	=	2.0-in. bolt thread engagement length
$D_s$min	=	1.9751 in., minimum major diameter of class 2A bolt threads
$E_n$max	=	1.8681 in., maximum pitch diameter of class 2B lid threads

The shear stress, τ, in the structural lid bolt hole threads is calculated as:

$$\tau = \frac{F_y}{A_n} = \frac{27{,}867 \text{ lb}}{9.654 \text{ in}^2} = 2{,}887 \text{ psi}$$

The canister structural lid is constructed of SA240, Type 304L stainless steel. Using shear allowables of 0.6 S_y and 0.5 S_u at a temperature of 300°F, the shear stress of 2,887 psi results in factors of safety of:

$$(F.S.)_y = \frac{0.6 \times 19{,}200 \text{ psi}}{2{,}887 \text{psi}} = 4.0 > 3$$

$$(F.S.)_u = \frac{0.5 \times 60{,}900 \text{ psi}}{2{,}887 \text{psi}} = 10.5 > 5$$

The criteria of NUREG-0612 and ANSI N14.6 for a redundant systems are met. Therefore, the 2.0-inch length of thread engagement is adequate.

The total weight of the heaviest loaded transfer cask (Class 5 BWR) is approximately 208,000 lbs. Three (3) times the design weight of the loaded canister is (3 x 76,000) 228,000 lbs, which is greater than the weight of the heaviest loaded transfer cask. Consequently, the preceding analysis bounds the inadvertently lifting of the transfer cask by the canister, since the canister lid and the hoist rings do not yield.

The structural adequacy of the canister structural lid and weld is evaluated using a finite element model of the upper portion of the canister. As shown in Figure 3.4.3.2-1, the model represents one-half of the upper section of the canister, including the structural and shield lids. The model uses gap/spring elements to simulate contact between adjacent components. Specifically, contact between the canister structural and shield lids is modeled using COMBIN40 combination elements in the axial (UY) degree of freedom. Simulation of the backing ring is accomplished using a ring of COMBIN40 gap/spring elements connecting the shield lid and the canister in the axial direction at the lid lower outside radius. CONTAC52 elements are used to model the interaction between the structural lid and canister shell and the shield lid and canister shell just below the respective lid weld joints. The size of the CONTAC52 gaps was determined from nominal dimensions of contacting components. The COMBIN40 elements used between the structural and shield lids, and for the backing ring, were assigned small gap sizes of 1×10^{-8} in. All gap/spring elements are assigned a stiffness of 1×10^{8} lb/in.

Boundary conditions were applied to enforce symmetry at the cut boundary of the model (in the x-y plane). All nodes on the x-y symmetry plane were restrained perpendicular to the symmetry plane (UZ). In addition, the nodes in the x-z plane at the bottom of the model were restrained in the axial direction (UY).

The lifting configuration for the canister consists of six hoist rings bolted to the structural lid at equally spaced angular intervals. To simulate the lifting of the canister, point loads equal to one-sixth of the total loaded canister weight plus a dynamic loading factor of 10% were applied to the model as forces at the lift locations while restraining the model at its base in the axial direction. Because of the symmetry conditions of the model, the forces applied to nodes on the symmetry plane were one-half of that applied at the other locations. The nodal point forces applied to the model as depicted in Figure 3.4.3.2-1 are calculated (including a dynamic load factor of 10%) as

$$W/6 = (76{,}000 \text{ lb} \times 1.1)/6 = 13{,}934 \text{ lb}$$

$$W/12 = (76{,}000 \text{ lb} \times 1.1)/12 = 6{,}967 \text{ lb}$$

The results of the finite element analysis of the canister for lift conditions are presented graphically in Figure 3.4.3.2-2. The maximum nodal stress intensity experienced by the various canister components during lift conditions are:

Component Description	Nodal Stress (psi)
Canister shell (inner surface of shell below structural weld at lifting location)	3,002
Structural Lid	2,825
Shield Lid	1,157
Structural Lid Weld	1,510
Shield Lid Weld	1,381

The canister shell and structural lid are constructed of SA240, Type 304L stainless. At a temperature of 300°F, the yield strength = 19,200 psi and the ultimate strength = 60,900 psi. The strength of the weld joint is taken as the same as the strength of the base material. Thus, when compared to the yield and ultimate strengths, the maximum nodal stress intensity of 3,002 psi produces the following factors of safety:

$$(F.S.)_{yield} = \frac{\text{yield strength}}{\text{maximum nodal stress intensity}} = \frac{19{,}200 \text{ psi}}{3{,}002 \text{ psi}} = 6.4 \quad (> 6)$$

$$(F.S.)_{ultimate} = \frac{\text{ultimate strength}}{\text{maximum nodal stress intensity}} = \frac{60{,}900 \text{ psi}}{3{,}002 \text{ psi}} = 20.3 \quad (> 10).$$

The criteria of NUREG-0612 and ANSI N14.6 for nonredundant systems are met. Thus, the canister shell and structural lid are adequate.

Figure 3.4.3.2-1 Canister Lift Finite Element Model

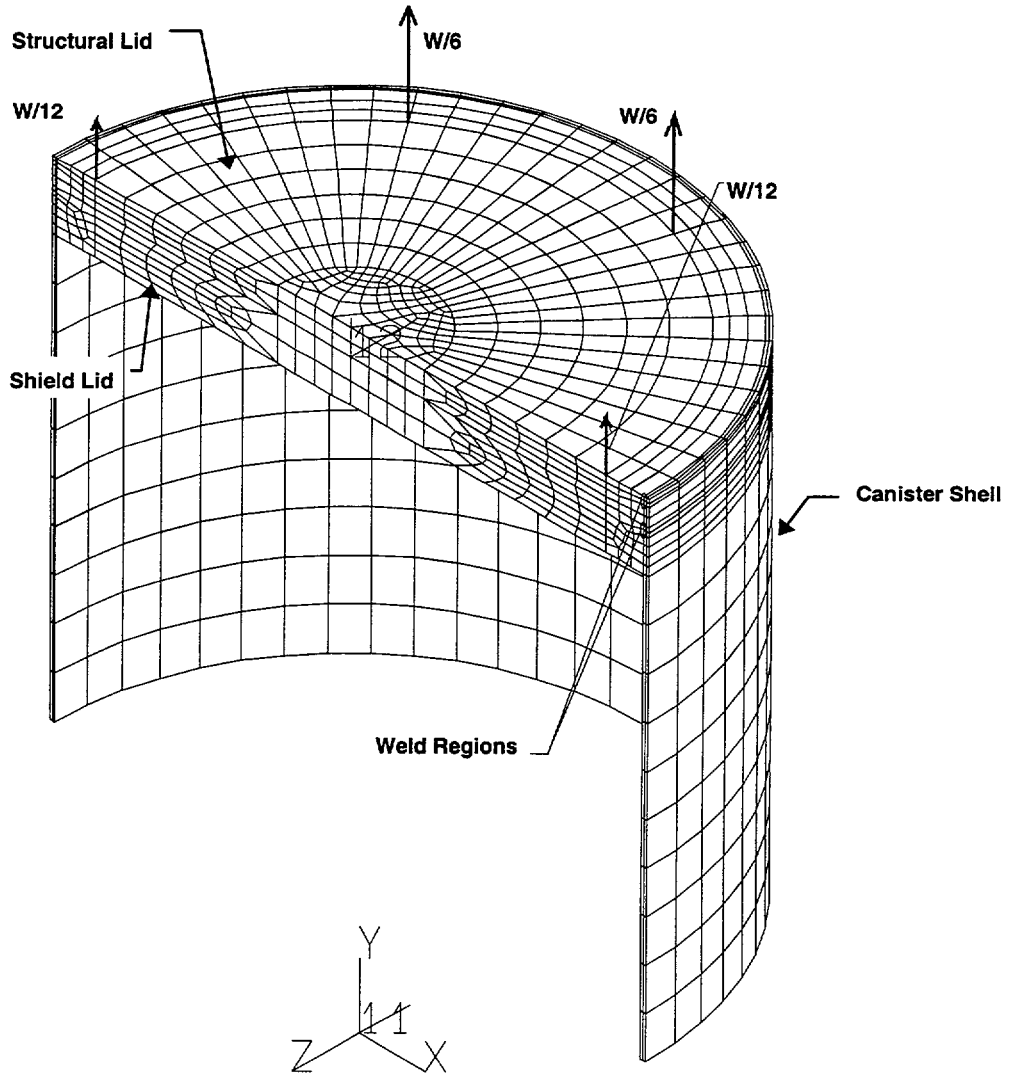

Figure 3.4.3.2-2 Canister Lift Model Stress Intensity Contours (psi)

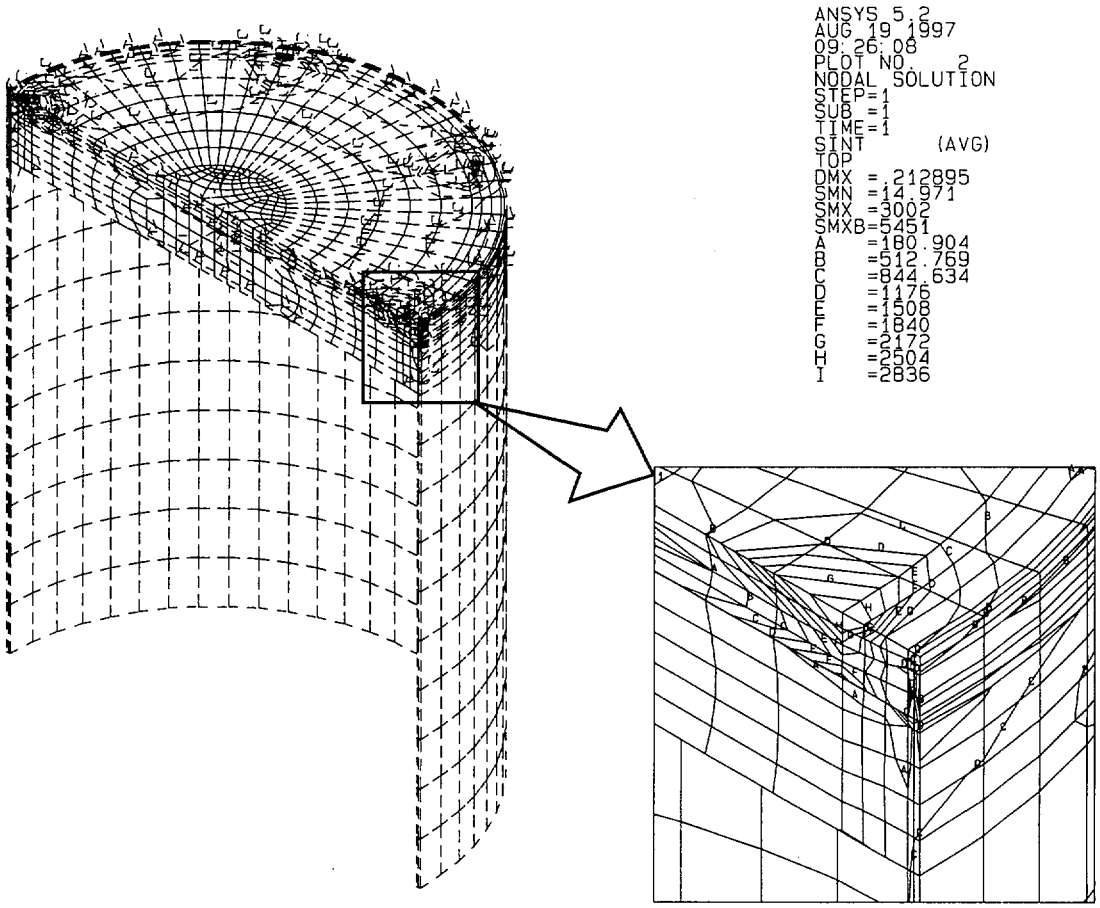

3.4.3.3 Transfer Cask Lift

The evaluation of the transfer cask presented here shows that the design meets NUREG-0612 [8] and ANSI N14.6 [9] requirements for nonredundant lift systems. The adequacy of the transfer cask is shown by evaluating the stress levels in all of the load-path components against the NUREG-0612 criteria.

3.4.3.3.1 Transfer Cask Shell and Trunnion

The adequacy of the trunnions and the cask shell in the region around the trunnions during lifting conditions is evaluated in this section in accordance with NUREG-0612 and ANSI N14.6.

A three-dimensional finite element model is used to evaluate the lifting of a fully loaded transfer cask. Because of symmetry, it was necessary to model only one-quarter of the transfer cask, including the trunnions and the shells at the trunnion region. The lead and the NS-4-FR between the inner and outer shells of the transfer cask are neglected since they are not structural components. SOLID95 (20 noded brick element) and SHELL93 (8 noded shell element) elements are used to model the trunnion and shells, respectively. Due to the absence of rotation degrees of freedom for the SOLID95 elements, BEAM4 elements perpendicular to the shells are used at the interface of the trunnion and the shells to transfer moments from the SOLID95 elements to SHELL93 elements. The finite element model is shown in Figure 3.4.3.3-1.

The total weight of the heaviest loaded transfer cask (Class 5 BWR) is calculated at approximately 208,000 lb. A conservative load of 210,000 lb., plus a 10% dynamic load factor, is used in the model. The load used in the quarter-symmetry model is (210,000 x 1.1)/4 = 57,750 lb. The load is applied upward at the trunnion as a "surface load" whose location is determined by the lifting yoke dimensions. The model is restrained along two planes of symmetry with symmetry boundary conditions. Vertical restraints are applied to the bottom of the model to resist the force applied to the trunnion.

The maximum temperature in the transfer cask shell/trunnion region is conservatively evaluated as 300°F. For the ASTM A-588 shell material, the yield strength, S_y, is 45.6 ksi, and the ultimate strength, S_u, is 70 ksi. The trunnions are constructed of ASTM A-350 carbon steel, Grade LF2, with a yield stress of 31.9 ksi and an ultimate stress of 70 ksi. The standard impact test temperature for ASTM A-350, Grade LF2 is -50°F. The NDT temperature range is -70°F to -10°F for ASTM A-588 with a thickness range of 0.625 in. to 3 in. [25]. Therefore, the minimum service

temperature for the trunnion and shells is conservatively established as 0°F (50°F higher than the NDT test temperature, in accordance with Section 4.2.6 of ANSI N14.6 [9].

Table 3.4.3.3-1 through Table 3.4.3.3-4 provide summaries of the top 30 maximum stresses for both surfaces of the outer shell and inner shell (see Figure 3.4.3.3-2 and Figure 3.4.3.3-3 for node locations for the outer sell and inner shell, respectively). Stress contour plots for the outer shell are shown in Figure 3.4.3.3- and Figure 3.4.3.3-5. Stress contours for the inner shell are shown in Figure 3.4.3.3-6 and Figure 3.4.3.3-. As shown in Table 3.4.3.3-1 through Table 3.4.3.3-4, all stresses, except local stresses, meet the NUREG-0612 and ANSI N14.6 criteria. That is, a factor of safety of 6 applies on material yield strength and 10 applies on material ultimate strength. The high local stresses, as defined in ASME Code Section III, Article NB-3213.10, which are relieved by slight local yielding, are not required to meet the 6 and 10 safety factor criteria [see Ref. 9, Section 4.2.1.2].

The localized stresses occur at the interfaces of the trunnion with the inner and outer shells. The size of the areas are less than 4.1 inches and 4.0 inches for the inner and outer shell, respectively. In accordance with ASME Code, Article NB-3213.10, the area of localized stresses cannot be larger than:

$$1.0\sqrt{Rt}$$

where:

R is the minimum midsurface radius

t is the minimum thickness in the region considered

Based on this formula, the size limitations for local stress regions are 5.1 inches (>4.06 inches) and 7.3 inches (>4.00 inches) for the inner and outer shells, respectively.

For the trunnion, the maximum tensile bending stress and average shear stresses occur at the interface with the outer shell. The linearized stresses through the trunnion are 3,377 psi in bending and 1,687 psi in shear. Comparing these stresses to the material allowable yield and ultimate strength (A350, Grade LF2), the factor of safety on yield strength is 9.4 (which is >6) and on ultimate strength is 20.7 (which is >10).

3.4.3.3.2 Retaining Ring and Bolts

The transfer cask uses a retaining ring bolted to the top flange to prevent inadvertent lifting of the canister out of the transfer cask, which could increase the radiation exposure to nearby workers. In the event that the loaded transfer cask is inadvertently lifted by attaching to the canister eyebolts instead of the transfer cask trunnions, the retaining ring and bolts have sufficient strength to support the weight of the heaviest transfer cask, plus a 10% dynamic load factor.

Retaining Ring

To qualify the retaining ring, the equations for annular rings are used (Roark [26], Table 24, Case 1e). The retaining ring is represented as shown in the sketch below. The following sketch assists in defining the variables used to calculate the stress in the retaining ring and bolts. The model assumes a uniform annular line load *w* applied at radius r_o.

The boundary conditions for the model are outer edge fixed, inner edge free with a uniform annular line load w at radius r_o.

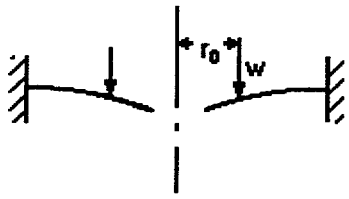

The material properties and parameters for the analysis are:

Plate dimensions:

thickness:
$t = 0.75$ in

outer radius (bolt circle):
$a = 37.28$ in

outer radius (outer edge)
$c = 38.52$ in

inner radius:
$b = 32.37$ in

Weight of bounding transfer cask:
$wt = 124{,}000 \text{ lb} \times 1.1$

Radial location of applied load:
$r_o = 33.53$ in

Material:
ASTM A588

Modulus of elasticity:
$E = 28.3 \times 10^6$ psi

Poisson's ratio:
$\nu = 0.31$

Number of bolts:
$Nb = 32$

Radial length of applied load:
$L_r = 2\pi r_o$
$L_r = 210.675$ in

Applied unit load:

$$w \equiv \frac{wt}{L_r}$$

$w = -647.44$ psi

The shear modulus is:

$$G = \frac{E}{2 \cdot (1 + v)}$$

$G = 1.08 \times 10^7$ psi

D is a plate constant used in determining boundary values; it is also used in the general equations for deflection, slope, moment and shear. K_{sb} and K_{sro} are tangential shear constants used in determining the deflection due to shear:

$$D = \frac{E \cdot t^3}{12 \cdot (1 - v^2)}$$

$D = 1.101 \times 10^6$ lb-in

Tangential shear constants, K_{sb} and K_{sro}, are used in determining the deflection due to shear:

$$K_{sb} = K_{sro} = -1.2 \cdot \frac{r_o}{a} \cdot \ln\left(\frac{a}{r_o}\right)$$

$$= -0.114$$

Radial moment M_{rb} and M_{ra} at points b and a (inner and outer radius, respectively) are:

M_{rb} (b,0) = 0 lb-in/in

M_{ra} (a,0) = 2207.86 lb-in/in

Transverse moment M_{tb} and M_{ta}, at points b and a (inner and outer radius, respectively) due to bending are:

M_{tb} (b,0) = -122.64 lb-in./in.

M_{ta} (a,0) = 684.44 lb-in./in.

The calculated shear stresses, τ_b and τ_a, at points b and a (inner and outer radius, respectively) are:

$\tau_b = 0$ psi

$$\tau_a = \frac{wt}{2\pi At}$$

τ_a = -776.42 psi

The calculated radial bending stresses, σ_{rb} and σ_{ra}, at points b and a (inner and outer radius) are:

$$\sigma_{r(i)} = \frac{6M_{r(i)}}{t^2}$$

σ_{rb} = 0 psi

σ_{ra} = 23,550 psi

The calculated transverse bending stresses, σ_{tb} and σ_{ta}, at points b and a (inner and outer radius) are:

$$\sigma_{t(i)} = \frac{6M_{t(i)}}{t^2}$$

σ_{tb} = -1308.2 psi

σ_{ta} = 7,300.7 psi

The principal stresses at the outer radius are:

σ_{1a} = 23,590 psi

σ_{2a} = 7,263.6 psi

σ_{3a} = 0 psi

The stress intensity, SI_a, at the outer radius ($P_m + P_b$) is:

$SI_a = \sigma_{1a} - \sigma_{3a}$

SI_a = 23,590 psi

The principal stresses at the inner radius are:

σ_{1b} = 0 psi

σ_{2b} = - 1308.2 psi

σ_{3b} = 0 psi

The stress intensity, SI_b, at the inner radius ($P_m + P_b$) is:

$$SI_b = \sigma_{1b} - \sigma_{2b}$$
$$SI_b = 1308.2 \text{ psi}$$

The maximum stress intensity occurs at the outer radius of the retaining ring. For the off-normal condition, the allowable stress intensity is equal to the lesser of 1.8 S_m and 1.5 S_y. For ASTM A588, the allowable stress intensity at 300°F is 1.8(23.3) = 41.94 ksi. The calculated stress of 23.59 ksi is less than the allowable stress intensity and the margin of safety is:

$$MS = \frac{41.94}{23.59} - 1 = 0.78$$

Retaining Ring / Canister Bearing

The bearing stress, S_{brg}, between the retaining ring and canister is calculated as:

Weight of Transfer Cask (TFR) = 124,000 x 1.1 = 136,400 lbs.
Area of contact between retaining ring and canister:

$$A = \pi\left(33.53^2 - 32.37^2\right) = 240 \text{ in}^2$$

$$S_{brg} = \frac{136{,}400}{240} = 568 \text{ psi}$$

Bearing stress allowable is S_y. For ASTM A588, the allowable stress at 300°F is 45.6 ksi. The calculated bearing stress is well below the allowable stress with a large margin of safety.

Shearing stress of Retaining Plate under the Bolt Heads

The shearing stress of the retaining plate under the bolt head is calculated as:

Outside diameter of bolt head d_b = 1.125 in.

Total shear area under bolt head $= \pi (1.125) \times 32 \times 0.75$

$= 84.82 \text{ in}^2$.

Shear stress of retaining plate, τ_p, under bolt head is:

$$\tau_p = \frac{136{,}400}{84.82} = 1608 \text{ psi}$$

Conservatively, the shear allowable for normal conditions is used.

$$\tau_{allowable} = (0.6)\ (S_m) = (0.6)\ (23.3 \text{ ksi}) = 13.98 \text{ ksi}$$

The Margin of Safety is: $\frac{13{,}980}{1{,}608} - 1 = +\text{large}$

Bolt Edge Distance

Using Table J3.5 "Minimum Edge Distance, in." of Section J3 from "Manual of Steel Construction Allowable Stress Design,"[23] the required saw-cut edge distance for a 0.75 inch bolt is 1.0 inch. As shown below, the edge distance for the bolts meets the criteria of the Steel Construction Manual.

$$\frac{77.04 - 74.56}{2} = 1.24 \text{ in} > 1.0 \text{ in}$$

Retaining Ring Bolts

The load on a single bolt, F_F, due to the reactive force caused by inadvertently lifting the canister, is:

$$F_F = \frac{wt}{N_b} = 4{,}262 \text{ lb}$$

where:

N_b = number of bolts, 32, and

wt = the weight of the cask, plus a 10% load factor, 124,000 lb × 1.1 = 136,400 lb.

The load on each bolt, F_M, due to the bending moment, is:

$$F_M = \left(\frac{2 \cdot \pi \cdot a}{N_b}\right) \cdot \left(\frac{\sigma \cdot t^2}{6 \cdot L}\right)$$

$F_M = 12{,}929$ lb

where:

a = the outer radius of the bolt circle, 37.28 in.,

t = the thickness of the ring, 0.75 in.,

σ = the radial bending stress at point *a*, σ_{ra} = 23,550 psi, and

L = the distance between the bolt center line and ring outer edge, c - a = 1.25 in.

The total tension, F, on each bolt is

$$F = F_F + F_M = 17{,}191 \text{ lb}$$

Knowing the bolt cross-sectional area, A_b, the bolt tensile stress is calculated as:

$$\sigma_t = \frac{F}{A_b} = 38{,}912 \text{ psi}$$

where:

$A_b = 0.4418 \text{ in}^2$

For off-normal conditions, the allowable primary membrane stress in a bolt is $2S_m$. The allowable stress for SA-193 Grade B6 bolts is 54 ksi at 120°F, the maximum temperature of the transfer cask top plate. The margin of safety for the bolts is

$$MS = \frac{54{,}000}{38{,}912} - 1 = +0.38$$

Since the SA-193 Grade B6 bolts have higher strength than the top plate, the shear stress in the threads of the top plate is evaluated. The yield and ultimate strengths for the top plate ASTM 588 material at a temperature of 120°F are:

S_y = 49.5 ksi
S_u = 70.0 ksi

From Reference 27, the shear area for the internal threads of the top plate, A_n , is calculated as:

$$A_n = 3.1416\, n\, L_e\, D_s min\left[\frac{1}{2n} + 0.57735\left(D_s min - E_n max\right)\right] = 1.525 \text{ in}^2$$

where:

D = 0.7482 in., basic major diameter of bolt threads,
n = 10, number of bolt threads per inch,
$D_s$min = 0.7353 in., minimum major diameter of bolt threads,
$E_n$max = 0.6927 in., maximum pitch diameter of lid threads, and
L_e = 1.625-0.74=0.885 in., minimum thread engagement.

The shear stress (τ_n) in the top plate is:

$$\tau_n = \frac{F}{A_n} = \frac{17{,}191 \text{ lb}}{1.525 \text{ in}^2} = 11{,}273 \text{ psi}$$

Where the total tension, F, on each bolt is

$$F = F_F + F_M = 17{,}191 \text{ lb}$$

The shear allowable for normal conditions is conservatively used:

$$\tau_{allowable} = (0.6)\ (S_m) = (0.6)\ (23.3 \text{ ksi}) = 13.98 \text{ ksi}$$

The Margin of Safety is: $\frac{13{,}980}{11{,}273} - 1 = +0.24$

Therefore, the threads of the top plate will not fail in shear.

Bottom Plate Weld Analysis

The bottom plate is connected to the outer and inner shell of the transfer cask by full penetration welds. The weight of a loaded canister along with the shield door rail structure is transmitted

from the bottom plate to the shell via the full penetration weld. For conservatism, only the length of the weld directly under the shell is considered effective in transmitting a load.

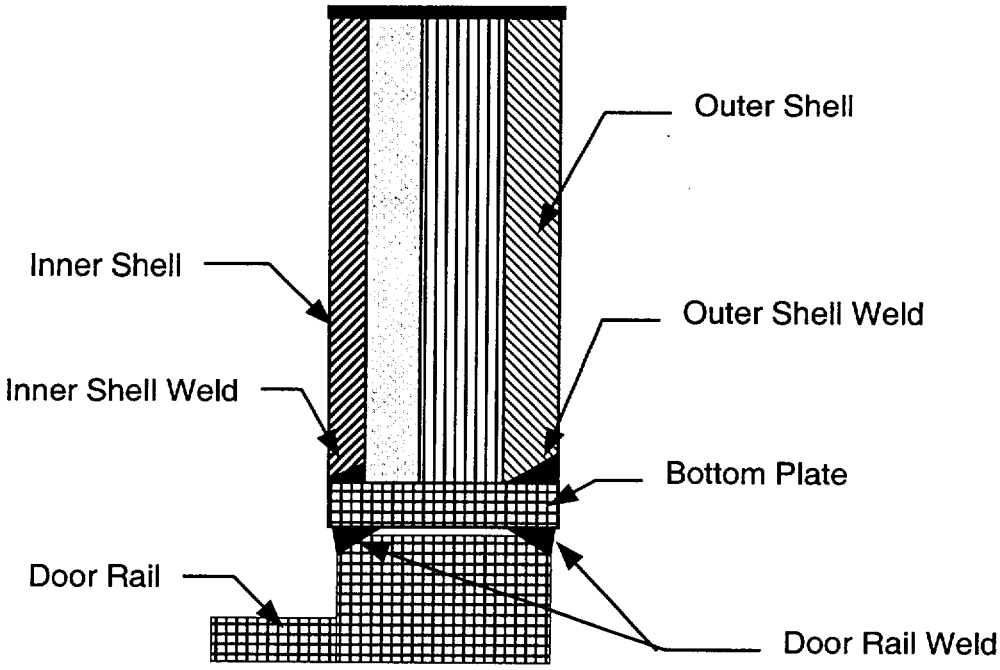

The weld connecting the outer and inner shell to the bottom plate has a length of approximately

l_w = (27.33 in. + 46.0 in.)/2 in. = 36.66 in.

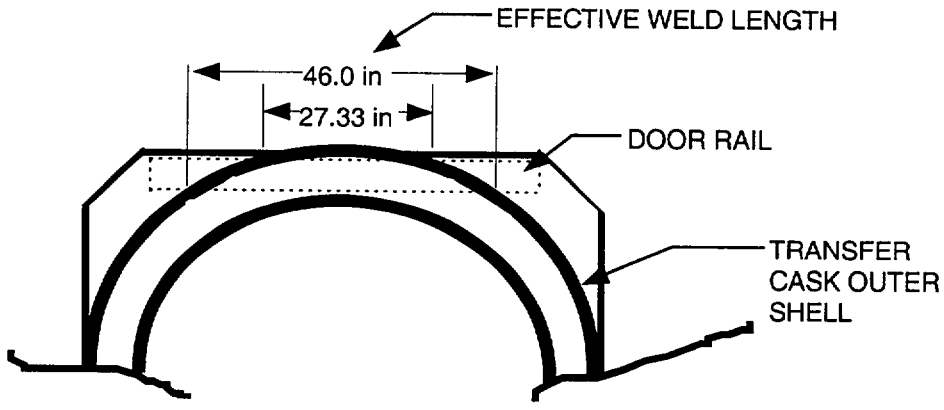

Stresses occurring in the outer shell to bottom plate weld are evaluated using a weight, W = 105,170 lb × 1.1 = 115,700 lb, which bounds the weight of the heaviest loaded canister, the weight of the water, and the weight of the shield doors and rails.

The door rail structure and canister load will be transmitted to both the inner and outer shell via full penetration welds. The thickness of the two shells and welds are different; however, for conservatism, this evaluation assumes both shell welds are 0.75 in. groove welds.

Weld effective area = (36.66 in.)(0.75 in. + 0.75 in.) = 54.99 in^2

$$\sigma_{axial} = \frac{P}{A} = \frac{(115{,}700 \text{ lb}) / (2)}{54.99 \text{ in}^2} = 1{,}052 \text{ psi}$$

For the bottom plate material (ASTM 588) at a bounding temperature of 400°F, the yield and ultimate stresses are:

S_y = 43.0 ksi

S_u = 70.0 ksi

$$FS_{yield} = \frac{43.0}{1.05} = +40.9 > 6$$

$$FS_{ultimate} = \frac{70.0}{1.05} = +66.5 > 10$$

Thus, the welds in the bottom plate meet the ANSI N14.6 and NUREG-0612 criteria for nonredundant systems.

3.4.3.3.3 Transfer Cask Shield Door Rails and Welds

This section demonstrates the adequacy of the transfer cask shield doors, door rails, and welds in accordance with NUREG-0612 and ANSI N14.6, which require safety factors of 6 and 10 on material yield strength and ultimate strength, respectively, for nonredundant lift systems.

The shield door rails support the weight of a wet, fully loaded canister and the weight of the shield doors themselves. The shield doors are 9.0-in. thick plates that slide on the door rails. The rails are 9.38 in. deep × 6.5 in. thick and are welded to the bottom plate of the transfer cask. The doors and the rails are constructed of A-350, Grade LF 2 low alloy steel.

The design weight used in this evaluation, W = 100,019 × 1.1 ≈ 110,000 lb, includes the weight of the heaviest loaded canister, the weight of the water in the canister and in the annulus between the canister and transfer cask, and the weight of the shield doors. A 10% dynamic load factor is included to ensure that the evaluation bounds all normal operating conditions. This evaluation shows that the door rail structures, and welds are adequate to support a wet, fully loaded canister.

Allowable stresses for the material are taken at 400°F, which bounds the maximum temperature at the bottom of the transfer cask under normal conditions. The material properties of A-350 Grade LF 2 low alloy steel are provided in Table 3.3-9. The standard impact test temperature for ASTM A-350, Grade LF2 is -50°F. The NDT temperature range is -70°F to -10°F for ASTM A-588 with a thickness range of 0.625 in. to 3 in. [28]. Therefore, the minimum service temperature for the trunnion and shells is conservatively established as 0°F (50°F higher than the NDT test temperature, in accordance with Section 4.2.6 of ANSI N14.6 [9].

Stress Evaluation for Door Rail

Each rail is assumed to carry a uniformly distributed load equal to 0.5W. The shear stress in each door rail bottom plate due to the applied load, W, is:

$$\tau = \frac{W}{A} = \frac{110{,}000 \text{ lb}}{281.25 \text{ in}^2} = 391 \text{ psi}$$

where:

A = 2.5 in. × 56.25 in. length/rail × 2 rails = 281.25 in^2.

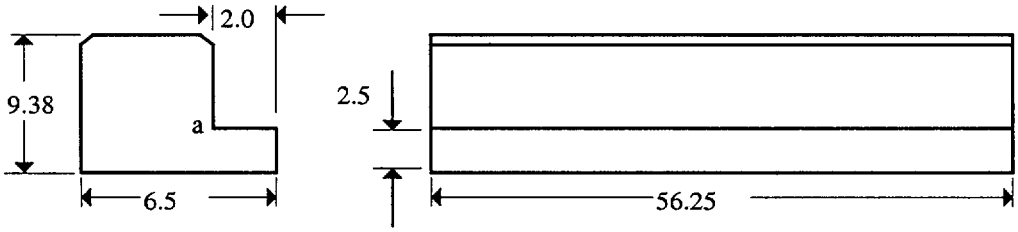

The bending stress in each rail bottom section due to the applied load of W is:

$$\sigma_b = \frac{M}{S} = \frac{65{,}450}{58.59} = 1{,}117 \text{ psi},$$

where:

M = moment at *a*,

$$= \frac{W}{2} \times \ell = \frac{110{,}000 \text{ lb.}}{2} \times 1.19 \text{ in.}$$

= 64,450 in-lb,

and,

$$\ell = 2 - \frac{2-(0.18+0.19)}{2}$$

ℓ = 1.19 in., applied load moment arm.

S, the section modulus = $\frac{56.25 \times 2.5^2}{6} = 58.59 \text{ in}^3$.

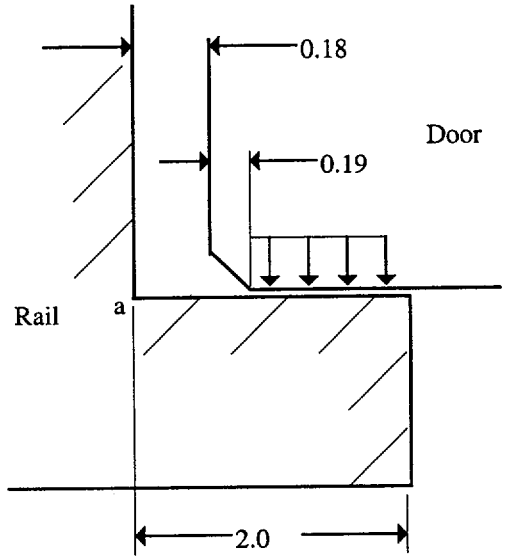

The maximum principal stress in the bottom section of the rail is:

$$\sigma = \left(\frac{\sigma_b}{2}\right) + \sqrt{\left(\frac{\sigma_b}{2}\right)^2 + \tau^2}$$

= 1,240 psi

The acceptability of the rail design is evaluated by comparing the allowable stresses to the maximum calculated stresses, considering the safety factors of NUREG-0612 and ANSI N14.6. For the yield strength criteria,

$$\frac{30{,}800 \text{ psi}}{1{,}240 \text{ psi}} = 24.8 > 6$$

For the ultimate strength criteria,

$$\frac{70{,}000 \text{ psi}}{1{,}240 \text{ psi}} = 56.5 > 10$$

The safety factors meet the criteria of NUREG-0612. Therefore, the rails are structurally adequate.

Stress Evaluation for the Shield Doors

The shield doors consist of a layer of NS-4-FR neutron shielding material sandwiched between low alloy steel plates (Note: steel bars are also welded on the edges of the doors so that the neutron shielding material is fully encapsulated). The door assemblies are 9 in. thick at the center and 6.75 in. thick at the edges, where they slide on the support rails. The stepped edges of the two door leaves are designed to interlock at the center and are, therefore, analyzed as a single plate that is simply supported on two sides.

The shear stress at the edge of the shield door where the door contacts the rail is:

$$\tau = \frac{W}{2 \times A_s} = \frac{110{,}000 \text{ lb}}{2 \times (49.2 \text{ in.} \times 4.75 \text{ in.})} = 235 \text{ psi}$$

where:

A = the total shear area, 4.75 in. thick × 49.2 in. long. Note that the effective thickness at the edge of the doors is taken as 4.75 in. because the neutron shield material and the cover plate are assumed to carry no shear load. The shear stress at the center of the doors approaches 0 psi.

The moment equation for the simply-supported beam with uniform loading is:

$$M = 55{,}000\, X - 1{,}541(X)(0.5\, X) = 55{,}000\, X - 771\, X^2$$

The maximum bending moment occurs at the center of the doors, X = 35.7 in. The bending moment at this point is:

$$M = 55{,}000 \text{ lb} \times (35.7 \text{ in.}) - 771 \text{ lb/in.} \times (35.7 \text{ in})^2$$
$$M = 9.81 \times 10^5 \text{ in.-lb.}$$

The maximum bending stress, σ_{max}, at the center of the doors, is

$$\sigma_{ax} = \frac{Mc}{I} = \frac{9.81 \times 10^5 \text{ in.–lb} \times 5.5 \text{ in.}}{2{,}378 \text{ in.}^4} = 2{,}269 \text{ psi.}$$

where:

$$c = \frac{h}{2} = \frac{7 \text{ in.}}{2} + 2 \text{ in.} = 5.5 \text{ in., and}$$

$$I = \frac{bh^3}{12} = \frac{83.2 \text{ in.} \times 7^3 \text{ in}}{12} = 2378 \text{ in}^4.$$

The acceptability of the door design is evaluated by comparing the allowable stresses to the maximum calculated stresses. As shown above, the maximum stress occurs for bending.

For the yield strength criteria,

$$\frac{30{,}800 \text{ psi}}{2{,}269 \text{ psi}} = 13.6 > 6$$

For the ultimate strength criteria,

$$\frac{70{,}000 \text{ psi}}{2{,}269 \text{ psi}} = 30.9 > 10$$

The safety factors satisfy the criteria of NUREG-0612. Therefore, the doors are structurally adequate.

Door Rail Weld Evaluation

The door rails are attached to the bottom of the transfer cask by 0.75-in. partial penetration bevel groove welds that extend the full length of the inside and outside of each rail. If the load is conservatively assumed to act at a point on the inside edge of the rail, the load, P, on each rail is,

$$P = \frac{W}{2} = \frac{110{,}000 \text{ lb}}{2} = 55{,}000 \text{ lb.}$$

Summing moments about the inner weld location:

$$0 = P \times a - F_o \times (b) = 55{,}000 \text{ lb} \times 1.19 \text{ in.} - F_o\,(4.5 \text{ in.}), \text{ or}$$

$$F_o = 14{,}544 \text{ lb}$$

Summing forces:

$$F_i = F_o + P = 14{,}544 \text{ lb} + 55{,}000 \text{ lb} = 69{,}544 \text{ lb}$$

The effective area of the inner weld is $0.75 \text{ in.} \times 56.25 \text{ in. long} = 42.19 \text{ in}^2$

The shear stress, τ, in the inner weld is

$$\tau = \frac{69{,}544 \text{ lb}}{42.19 \text{ in}^2} = 1{,}648 \text{ psi}$$

The factors of safety are

$$\frac{30{,}800 \text{ psi}}{1{,}648 \text{ psi}} = 18.7 > 6 \qquad \text{(For yield strength criteria)}$$

$$\frac{70{,}000 \text{ psi}}{1{,}648 \text{ psi}} = 42.4 > 10 \qquad \text{(For ultimate strength criteria)}$$

The safety factors meet the criteria of NUREG-0612. Thus, the rail attachment weld is adequate.

3.4.3.3.4 PWR Class 1 Transfer Cask with Transfer Cask Extension

The PWR Class 1 Transfer Cask, baseline weight of 110,821 lb. empty, can be equipped with a Transfer Cask extension to accommodate the loading of a PWR Class 2 canister. The purpose of the extended Transfer Cask configuration is to permit the loading of PWR Class 1 fuel assemblies with Control Element Assemblies inserted into a PWR Class 2 canister; the length of the control element assemblies requires the use of the longer PWR Class 2 canister. The weight

of the Transfer Cask extension is 5,421 pounds. Therefore the total weight of the PWR Class 1 Transfer Cask extension would be:

$$W_{TC} = 110{,}821 + 5{,}421 = 116{,}242 \text{ lbs.}$$

Transfer Cask Shell and Trunnion

From the analysis in Section 3.4.3.3.1 for the Transfer Cask Shell and Trunnion, the heaviest loaded transfer cask weight used in the analysis was 210,000 pounds (Class 5 BWR). The total weight of the loaded transfer cask is:

$$W_{TC\text{-}L} = 191{,}492 + 5{,}421 = 196{,}913 \text{ lbs}$$

where:

191,492 lbs = the weight of a PWR Class 1 Transfer Cask and Canister (with fuel, water, and shield lid)

The Class 5 BWR Transfer Cask configuration bounds the PWR Class 1 Transfer Cask with extension; therefore, no additional handling analysis is required for the transfer cask shell and trunnions.

Retaining Ring and Bolts

From Section 3.4.3.3.2, the bounding transfer cask weight used was 124,000 pounds. As stated above, the weight of the PWR Class 1 Transfer Cask with extension is 116,242 pounds; therefore, the existing analysis in Section 3.4.3.3.2 bounds the PWR Class 1 Transfer Cask with extension and no additional analysis is required.

Transfer Cask Extension Attachment Bolts

The transfer cask extension is attached to the transfer cask by 32 bolts that are identical to the Retaining Ring Bolts with the exception of bolt length. The retaining ring bolts are 2.25 inches long and the transfer cask extension attachment bolts are 9.0 inches long; the thread engagement lengths are identical. Since the transfer cask extension is 8.75 inches thick, the prying action is negligible for the transfer cask extension attachment bolts during an inadvertent lift of the transfer cask via the retaining ring during a canister handling operation. The PWR Class 1

Transfer Cask with extension weighs approximately 7,000 pound less than the bounding analysis weight; therefore, no additional analysis of the attachment bolts is required.

Figure 3.4.3.3-1 Finite Element Model for Transfer Cask Trunnion and Shells

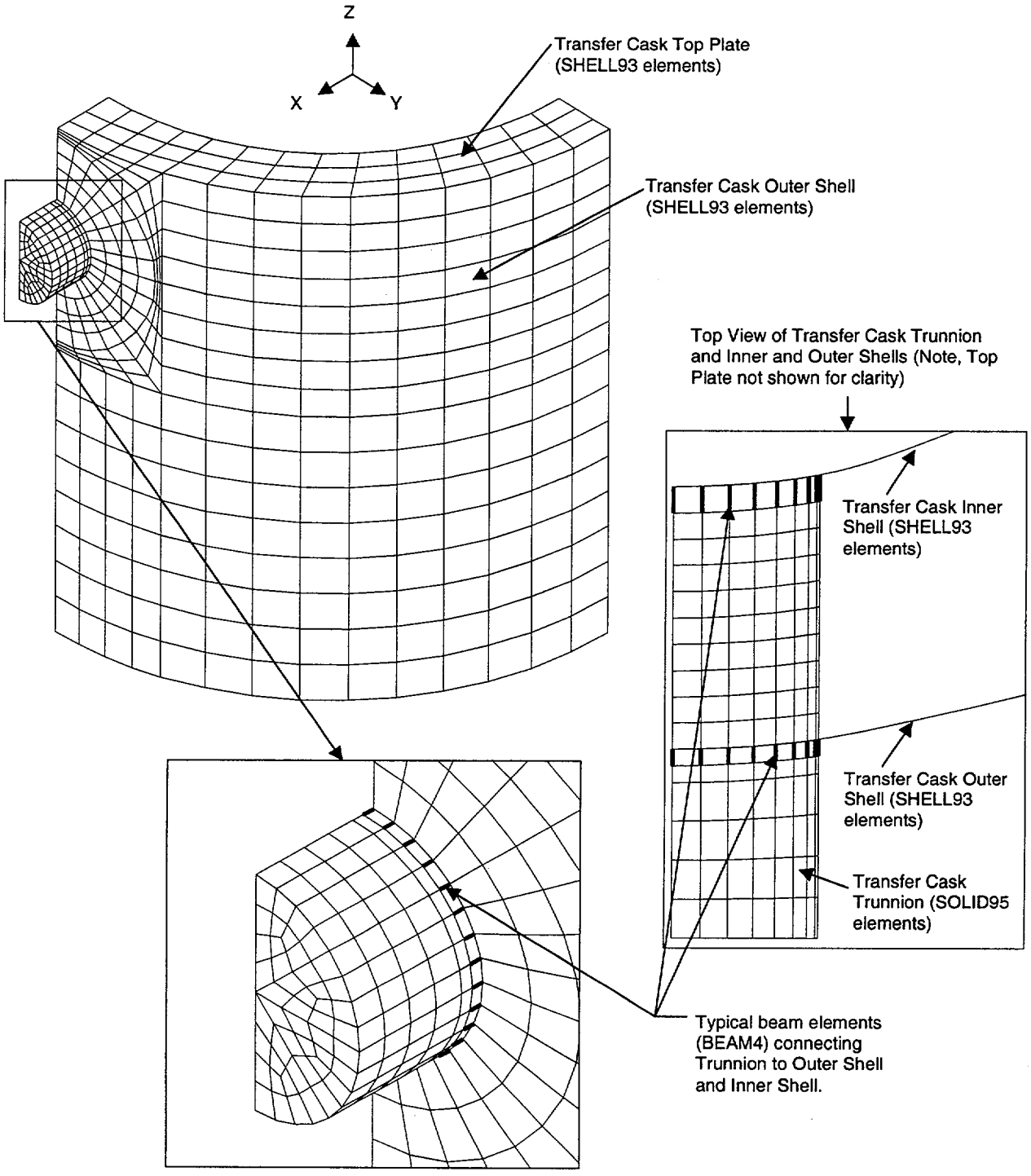

Figure 3.4.3.3-2 Node Locations for Transfer Cask Outer Shell Adjacent to Trunnion

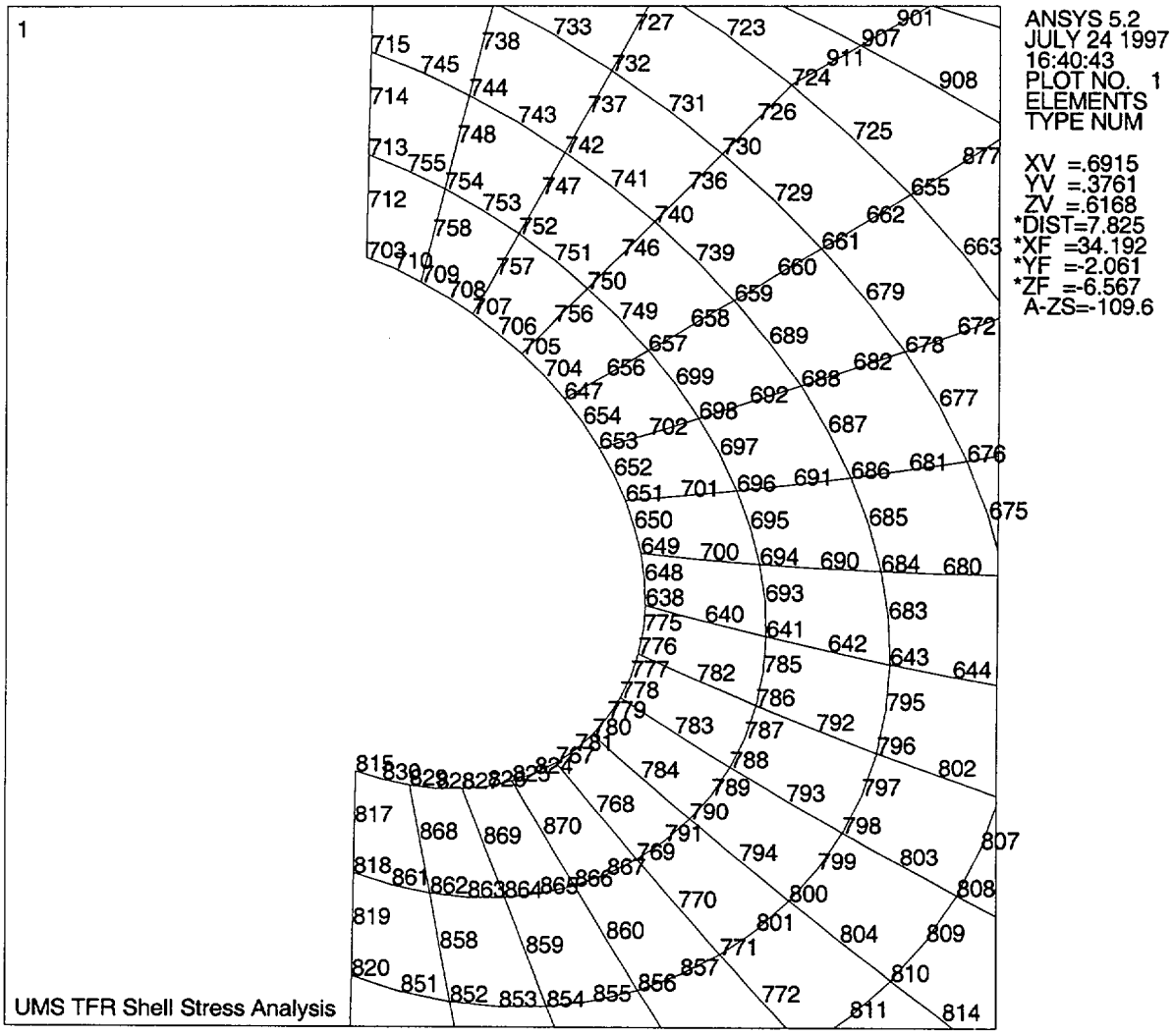

Figure 3.4.3.3-3 Node Locations for Transfer Cask Inner Shell Adjacent to Trunnion

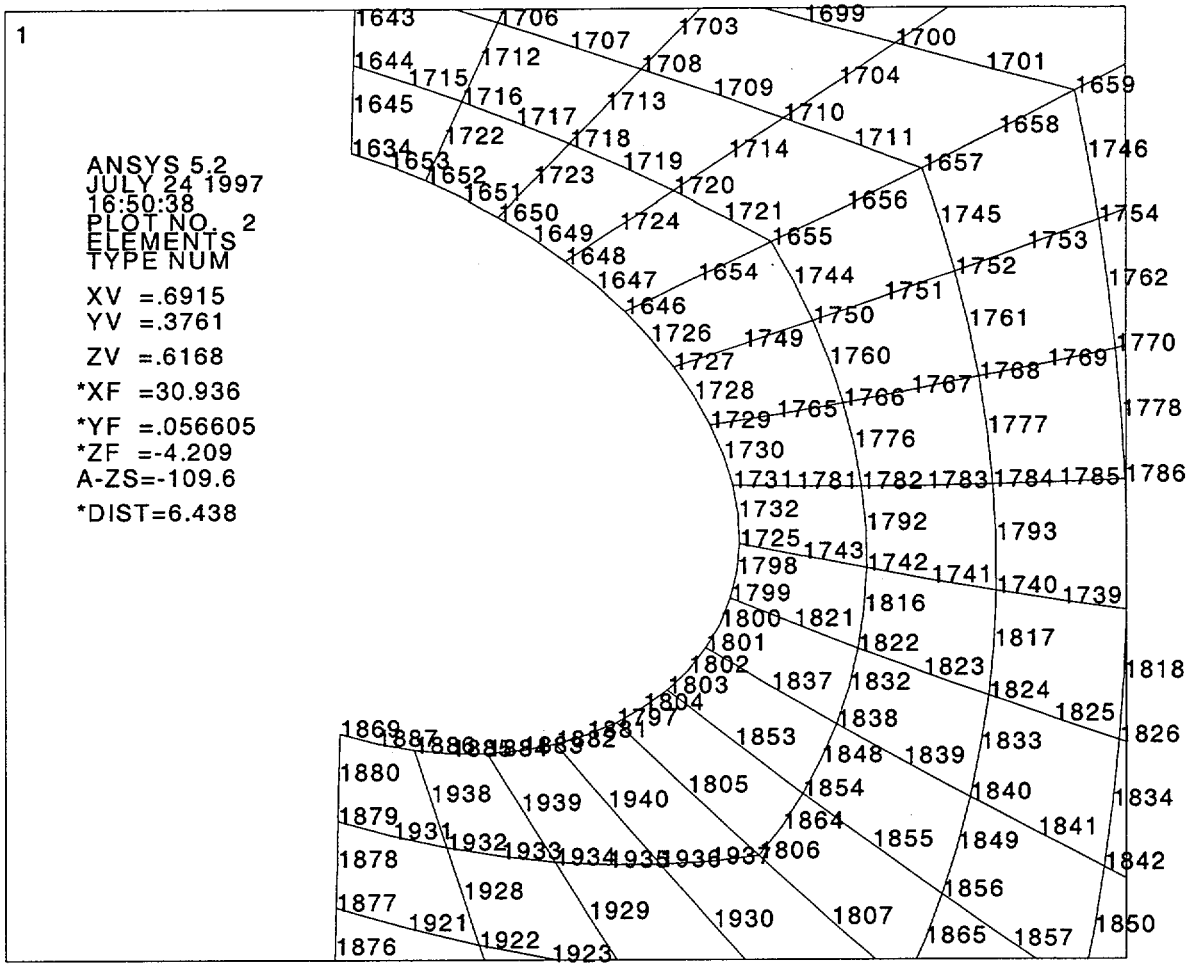

Figure 3.4.3.3-4 Stress Intensity Contours (psi) for Transfer Cask Outer Shell Element Top Surface

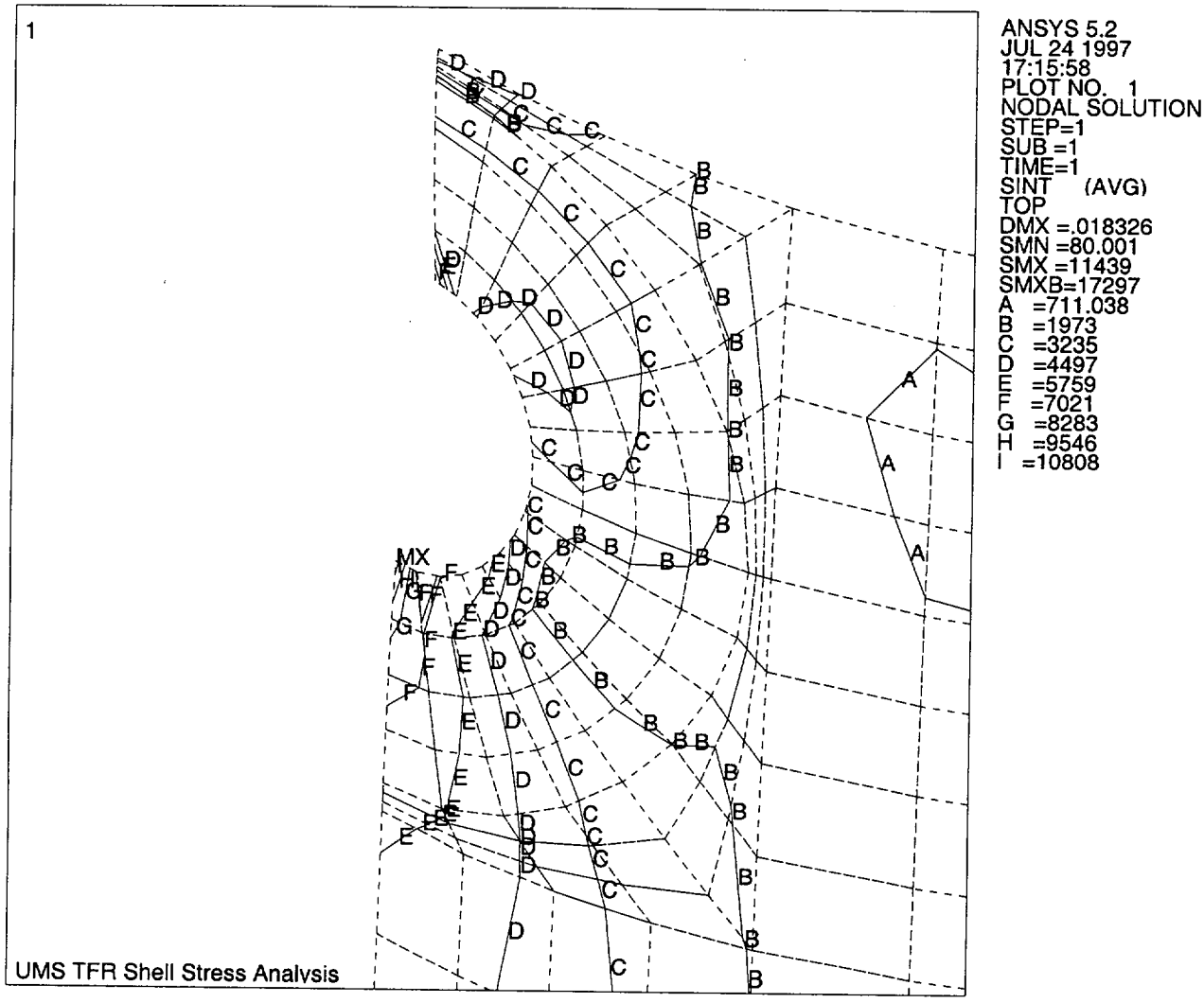

Figure 3.4.3.3-5 Stress Intensity Contours (psi) for Transfer Cask Outer Shell Element Bottom Surface

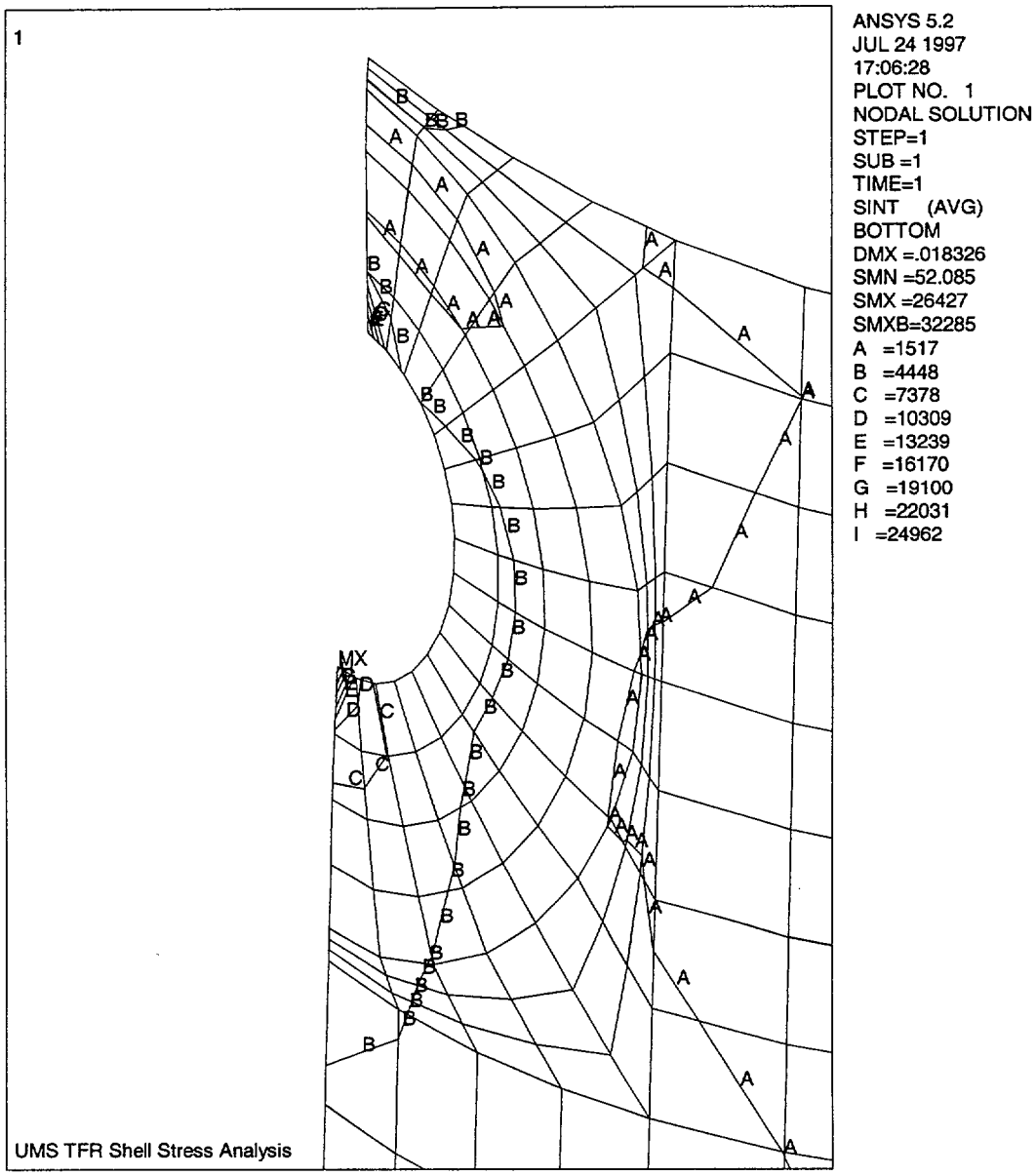

Figure 3.4.3.3-6 Stress Intensity Contours (psi) for Transfer Cask Inner Shell Element Top Surface

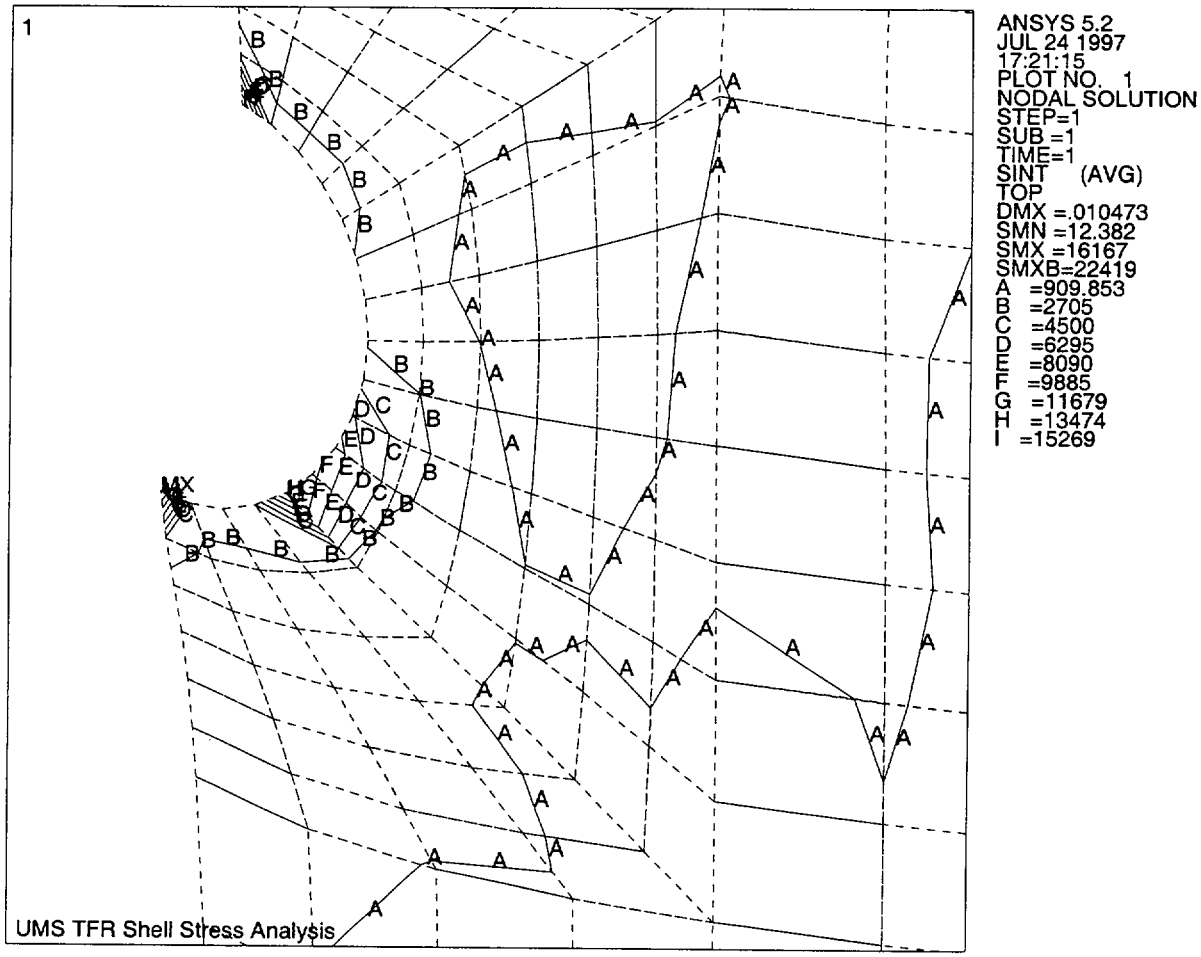

Figure 3.4.3.3-7 Stress Intensity Contours (psi) for Transfer Cask Inner Shell Element Bottom Surface

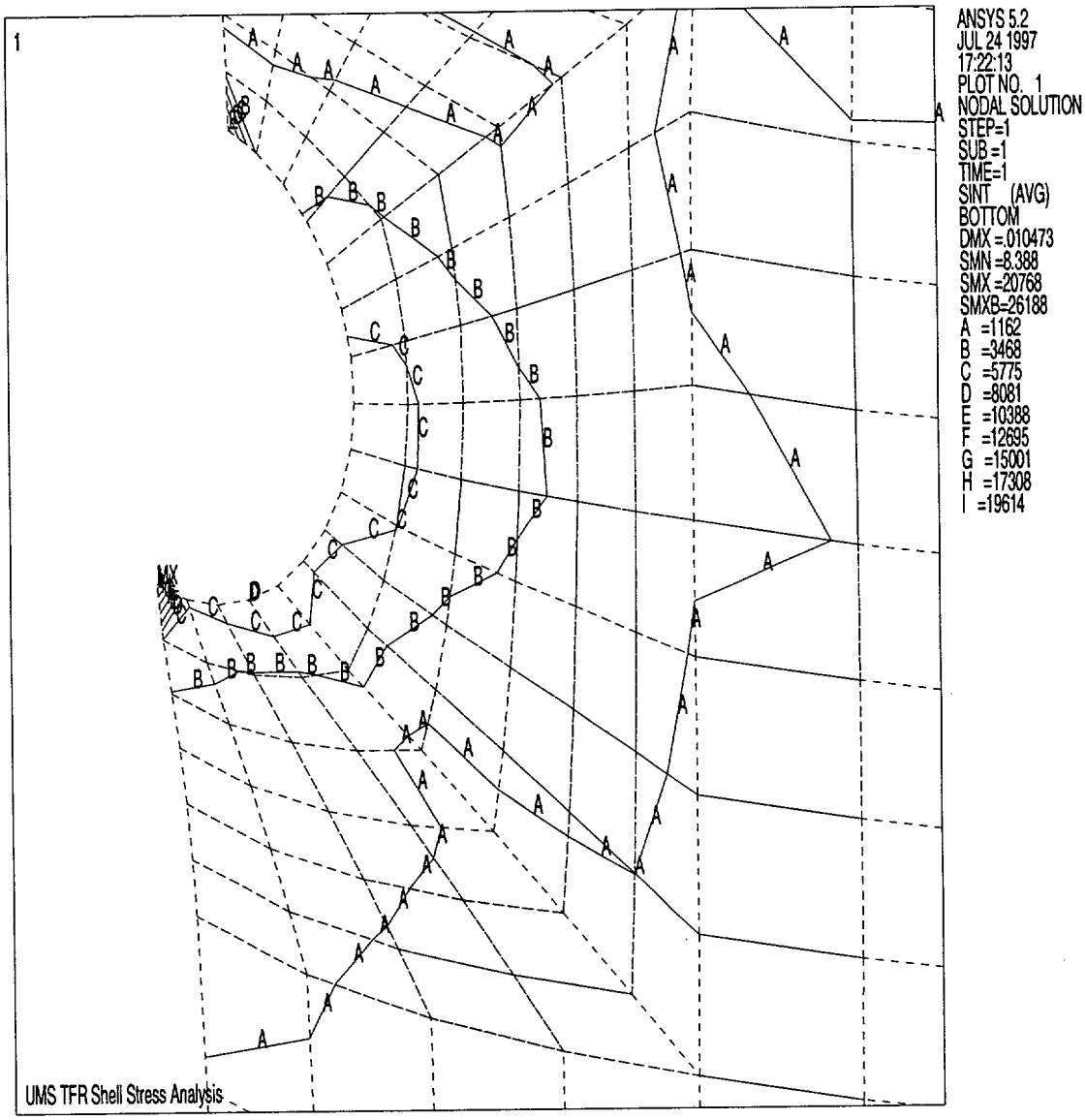

Table 3.4.3.3-1 Top 30 Stresses for Transfer Cask Outer Shell Element Top Surface

Node[1]	Principal Stresses(psi)			Nodal S.I. (psi)	F.S. on Yield S_y/S.I.[2]	F.S. on Ultimate (S_u/S.I.)[2]
	S1	S2	S3			
815	3521.5	-288.8	-7917.2	11439.0	N/A[3]	N/A[3]
818	5092.6	-4.7	-3640.3	8732.9	N/A	N/A
703	7056.8	719.0	-995.8	8052.5	N/A	N/A
820	4315.2	-2.5	-3128.0	7443.2	N/A	N/A
862	4091.0	3.8	-3005.9	7096.9	N/A	N/A
827	4908.7	8.5	-2161.6	7070.3	N/A	N/A
825	4727.4	39.0	-2214.8	6942.2	6.6	10.1
852	4134.8	0.7	-2756.8	6891.6	6.6	10.2
822	3927.3	-0.3	-2788.6	6716.0	6.8	10.4
829	3525.9	-15.5	-3132.6	6658.6	6.8	10.5
767	4010.9	111.0	-2445.3	6456.2	7.1	10.8
842	3806.4	0.2	-2475.5	6281.9	7.3	11.1
816	3607.1	-0.1	-2644.0	6251.1	7.3	11.2
943	3547.6	-0.1	-2638.2	6185.8	7.4	11.3
941	3495.7	-0.1	-2626.5	6122.2	7.4	11.4
2	3430.3	0.0	-2609.0	6039.3	7.6	11.6
832	3497.2	0.2	-2341.5	5838.7	7.8	12.0
964	3412.4	0.3	-2271.0	5683.3	8.0	12.3
864	3625.6	15.6	-2002.0	5627.7	8.1	12.4
854	3683.9	3.6	-1853.7	5537.7	8.2	12.6
954	3335.5	0.3	-2199.9	5535.4	8.2	12.6
8	3251.5	0.1	-2132.4	5383.9	8.5	13.0
780	2941.0	173.8	-2411.8	5352.8	8.5	13.1
871	5250.1	2907.8	-23.4	5273.6	8.6	13.3
47	2848.5	0.0	-2367.8	5216.3	8.7	13.4
844	3470.2	2.3	-1701.8	5172.0	8.8	13.5
657	2272.2	-18.5	-2625.5	4897.7	9.3	14.3
57	2781.3	-0.3	-2093.2	4874.5	9.4	14.4
705	3143.0	-323.9	-1675.6	4818.6	9.5	14.5
834	3227.7	1.9	-1578.1	4805.7	9.5	14.6

Notes:

1. See Figure 3.4.3.3-2 for node locations.
2. S_y = 45,600 psi, S_u = 70,000 psi.
3. Local stresses that are relieved by local material yielding. Therefore, stress design factors of 6 and 10 on material yield and ultimate strength are not applicable (ANSI N14.6, Section 4.2.1.2).

Table 3.4.3.3-2 Top 30 Stresses for Transfer Cask Outer Shell Element Bottom Surface

Node[1]	Principal Stresses(psi)			Nodal S.I. (psi)	F.S. on Yield S_y/S.I.[2]	F.S. on Ultimate (S_u/S.I.)[2]
	S1	S2	S3			
815	26042.0	1368.5	-385.3	26427.0	N/A[3]	N/A[3]
703	433.6	-1196.0	-16049.0	16482.0	N/A	N/A
829	11257.0	4762.2	-25.6	11283.0	N/A	N/A
818	9377.2	1335.4	-11.0	9388.2	N/A	N/A
862	8650.9	2600.4	-13.1	8663.9	N/A	N/A
638	3906.5	-37.6	-3390.4	7296.9	N/A	N/A
864	7245.0	2309.2	-13.3	7258.4	N/A	N/A
776	5054.5	156.6	-1993.6	7048.1	N/A	N/A
649	2372.4	-306.3	-4436.1	6808.5	6.7	10.3
827	6731.4	2737.4	-15.4	6746.9	6.8	10.4
820	6699.0	2463.6	-1.6	6700.6	6.8	10.4
778	5550.7	521.4	-837.7	6388.4	7.1	11.0
852	6375.9	2277.2	-3.5	6379.4	7.1	11.0
709	78.1	-4994.3	-6150.1	6228.2	7.3	11.2
825	6070.4	2367.2	-42.8	6113.2	7.5	11.5
651	1180.6	-998.2	-4879.3	6060.0	7.5	11.6
780	5703.3	1363.7	-312.2	6015.5	7.6	11.6
866	5998.4	1528.3	-1.7	6000.1	7.6	11.7
767	5772.1	2120.8	-131.9	5904.0	7.7	11.9
871	20.8	-416.7	-5855.7	5876.6	7.8	11.9
854	5737.9	1707.3	-4.5	5742.4	7.9	12.2
822	5656.1	1990.6	-0.3	5656.4	8.1	12.4
653	689.6	-2286.6	-4882.7	5572.3	8.2	12.6
842	5453.5	1832.8	-0.8	5454.3	8.4	12.8
873	20.0	-243.1	-5388.0	5408.0	8.4	12.9
769	5322.5	815.7	1.0	5321.5	8.6	13.2
641	3174.6	1.8	-1987.0	5161.6	8.8	13.6
786	3830.7	0.4	-1282.9	5113.5	8.9	13.7
694	2454.1	4.2	-2655.5	5109.6	8.9	13.7
816	5070.5	1851.7	-0.1	5070.6	9.0	13.8

Notes:

1. See Figure 3.4.3.3-2 for node locations.
2. S_y = 45,600 psi, S_u = 70,000 psi.
3. Local stresses that are relieved by local material yielding. Therefore, stress design factors of 6 and 10 on material yield and ultimate strength are not applicable (ANSI N14.6, Section 4.2.1.2).

Table 3.4.3.3-3 Top 30 Stresses for Transfer Cask Inner Shell Element Top Surface

Node[1]	Principal Stresses(psi)			Nodal S.I. (psi)	F.S. on Yield S_y/S.I.[2]	F.S. on Ultimate (S_u/S.I.)[2]
	S1	S2	S3			
1869	1765.2	-503.6	-14402.0	16167.0	N/A[3]	N/A[3]
1797	11044.0	-108.1	-2767.4	13811.0	N/A	N/A
1634	1615.7	-326.8	-12092.0	13708.0	N/A	N/A
1803	10114.0	3278.4	-293.2	10407.0	N/A	N/A
1801	8800.8	3432.8	-213.3	9014.1	N/A	N/A
1799	6238.1	3249.0	-161.2	6399.3	7.1	10.9
1882	728.3	-2351.9	-3701.0	4429.3	10.3	15.8
1633	4070.8	551.7	-1.6	4072.3	11.2	17.2
1879	350.0	-116.5	-3650.0	4000.0	11.4	17.5
1725	3690.7	2859.1	-166.8	3857.5	11.8	18.1
1648	485.8	-261.7	-3244.6	3730.5	12.2	18.8
1652	137.0	-1003.2	-3529.2	3666.2	12.4	19.1
1886	101.9	-2993.0	-3541.1	3643.1	12.5	19.2
1644	962.4	-24.8	-2674.1	3636.5	12.5	19.2
1650	433.9	11.7	-3137.7	3571.6	12.8	19.6
1884	416.6	-1841.5	-3125.6	3542.1	12.9	19.8
1666	3474.7	386.0	-0.3	3475.0	13.1	20.1
1822	3435.6	2108.1	-17.9	3453.6	13.2	20.3
1646	311.6	-945.1	-2960.5	3272.1	13.9	21.4
1838	3148.2	2452.5	-35.3	3183.5	14.3	22.0
1636	3157.0	750.3	-2.3	3159.3	14.4	22.2
1676	2879.2	707.8	-2.4	2881.6	15.8	24.3
1742	2725.1	1367.2	-8.9	2734.0	16.7	25.6
1727	308.8	-540.4	-2300.1	2608.9	17.5	26.8
1668	2486.6	121.0	-10.4	2496.9	18.3	28.0
1854	2393.3	2044.3	-55.4	2448.7	18.6	28.6
1731	2185.5	1530.9	-262.9	2448.4	18.6	28.6
1936	152.0	-126.5	-2235.5	2387.5	19.1	29.3
1638	2372.8	486.1	-2.7	2375.6	19.2	29.5
1120	4.2	-759.8	-2344.0	2348.2	19.4	29.8

Notes:

1. See Figure 3.4.3.3-3 for node locations.
2. S_y = 45,600 psi, S_u = 70,000 psi.
3. Local stresses that are relieved by local material yielding. Therefore, stress design factors of 6 and 10 on material yield and ultimate strength are not applicable (ANSI N14.6, Section 4.2.1.2).

Table 3.4.3.3-4 Top 30 Stresses for Transfer Cask Inner Shell Element Bottom Surface

Node[1]	Principal Stresses(psi)			Nodal S.I. (psi)	F.S. on Yield $S_y/S.I.$[2]	F.S. on Ultimate $(S_u/S.I.)$[2]
	S1	S2	S3			
1869	18955.0	554.4	-1812.1	20768.0	N/A[3]	N/A[3]
1634	10094.0	530.6	-887.6	10982.0	N/A	N/A
1882	7550.5	886.3	-631.4	8181.8	N/A	N/A
1797	1147.8	143.2	-5927.0	7074.8	N/A	N/A
1731	2320.8	-75.8	-4368.2	6689.0	6.8	10.5
1884	6149.9	517.9	-483.4	6633.3	6.9	10.6
1725	1242.9	-392.2	-5118.9	6361.8	7.2	11.0
1729	3117.2	52.5	-3023.5	6140.7	7.4	11.4
1803	474.7	-3926.6	-5631.6	6106.3	7.5	11.5
1886	5973.5	2440.1	-81.0	6054.5	7.5	11.6
1801	457.4	-3130.0	-5557.0	6014.4	7.6	11.6
1742	1965.5	-0.9	-4026.8	5992.3	7.6	11.7
1782	2451.4	-0.2	-3512.8	5964.2	7.6	11.7
1799	543.1	-1622.2	-5294.3	5837.4	7.8	12.0
1822	1595.1	4.2	-4233.9	5829.0	7.8	12.0
1766	2666.8	-1.0	-2994.6	5661.4	8.1	12.4
1879	5157.5	127.0	-284.2	5441.6	8.4	12.9
1727	3646.3	282.8	-1615.2	5261.4	8.7	13.3
1838	1426.6	25.3	-3770.7	5197.3	8.8	13.5
1740	2367.5	-2.5	-2661.6	5029.1	9.1	13.9
1784	2285.8	-0.7	-2712.6	4998.4	9.1	14.0
1750	2342.2	-6.7	-2516.2	4858.4	9.4	14.4
1646	3727.5	676.6	-1129.4	4856.9	9.4	14.4
1806	3417.2	95.3	-827.4	4244.6	10.7	16.5
1824	2109.9	-2.3	-2106.6	4216.5	10.8	16.6
1768	1813.3	-0.4	-2337.6	4150.9	11.0	16.9
1854	1304.9	49.1	-2746.8	4051.6	11.3	17.3
1738	2231.7	1.0	-1617.9	3849.6	11.8	18.2
1786	1897.7	0.5	-1860.4	3758.2	12.1	18.6
1932	3722.3	1449.3	-8.2	3730.5	12.2	18.8

Notes:

1. See Figure 3.4.3.3-3 for node locations.
2. S_y = 45,600 psi, S_u = 70,000 psi.
3. Local stresses that are relieved by local material yielding. Therefore, stress design factors of 6 and 10 on material yield and ultimate strength are not applicable (ANSI N14.6, Section 4.2.1.2).

THIS PAGE INTENTIONALLY LEFT BLANK

3.4.4 Normal Operating Conditions Analysis

The Universal Storage System is evaluated using individual finite element models for the fuel basket, canister, and vertical concrete cask. Because the individual components are free to expand without interference, the structural finite element models need not be connected.

3.4.4.1 Canister and Basket Analyses

The evaluations presented in this Section are based on consideration of the bounding conditions for each aspect of the analysis. Generally, the bounding condition is represented by the component, or combination of components, of each configuration that is the heaviest. The bounding thermal condition is established by the configuration having the largest thermal gradient in normal use. Some cases require the evaluation of both a PWR and a BWR configuration because of differences in the design of these systems. For reference, the bounding case used in each of the structural evaluations is:

Section	Aspect Evaluated	Bounding Condition	Configuration
3.4.4.1.1	Canister Thermal Stress	Largest temperature gradient	Temperature[a] distribution
3.4.4.1.2	Canister Dead Weight	Heaviest loaded canister	BWR Class 5
3.4.4.1.3	Canister Pressure	Bounding pressure 15 psig, smallest canister	PWR Class 1 BWR Class 4
3.4.4.1.4	Canister Handling	Shortest canister dimensions w/ heaviest canister load [b]	PWR Class 1 BWR Class 5
3.4.4.1.5	Canister Load Combinations	Bounding pressure 15 psig + shortest canister dimensions w/ heaviest loaded canister[b] (handling) + shortest canister dimensions w/ heaviest loaded canister [b] (dead load) largest temperature gradient (thermal)	PWR Class 3 PWR Class 1 BWR Class 5 PWR Class 1 BWR Class 5 Temperature[a] distribution
3.4.4.1.6	Canister Fatigue	Bounding thermal excursions (58°F)	Not Applicable
3.4.4.1.7	Canister Pressure Test	Loaded canister (smallest canister)	PWR Class 1
3.4.4.1.8	PWR Basket Support Disk	Loaded PWR Canister	PWR fuel basket
	BWR Basket Support Disk	Loaded BWR Canister	BWR fuel basket [c]
3.4.4.1.9	PWR Basket Weldment	Loaded PWR Canister	PWR Class 2
	BWR Basket Weldment	Loaded BWR Canister	BWR Class 5
3.4.4.1.10	PWR Fuel Tube	Loaded PWR Canister (Longest)	PWR Class 3
	BWR Fuel Tube	Loaded BWR Canister (Longest)	BWR Class 5
3.4.4.1.11	Canister Closure Weld	Same as 3.4.4.1.5	Same as 3.4.4.1.5

[a] See Section 3.4.4.1.1 for an explanation of the composite temperature distribution used in the analyses. The shortest canister, PWR Class 1, has the fewest number of fuel basket support disks.

[b] When combined with the heaviest fuel assembly/fuel basket weight (BWR Class 5), the load per support disk or weldment disk is maximized.

[c] The evaluation of the BWR basket uses the analysis presented in the UMS Transport SAR [2].

3.4.4.1.1 Canister Thermal Stress Analysis

A three-dimensional finite element model of the canister was constructed using ANSYS SOLID45 elements. By taking advantage of the symmetry of the canister, the model represents one-half (180° section) of the canister including the canister shell, bottom plate, structural lid, and shield lid. Contact between the structural and shield lids is modeled using COMBIN40 combination elements in the axial (UY) degree of freedom. Simulation of the backing ring is accomplished using a ring of COMBIN40 gap/spring elements connecting the shield lid and the canister in the axial direction at the lid lower outside radius. In addition, CONTAC52 elements are used to model the interaction between the structural lid and the canister shell and between the shield lid and canister shell, just below the respective lid weld joints as shown in Figure 3.4.4.1-2. The size of the CONTAC52 gaps is determined from nominal dimensions of contacting components. The gap size is defined by the "Real Constant" of the CONTAC52 element. Due to the relatively large gaps resulting from the nominal geometry, these gaps remain open during all loadings considered. The COMBIN40 elements used between the structural and shield lids and for the backing ring are assigned small gap sizes of 1×10^{-8} in. All gap/spring elements are assigned a stiffness of 1×10^{8} lb/in. The three-dimensional finite element model of the canister used in the thermal stress evaluation is shown in Figure 3.4.4.1-1 through Figure 3.4.4.1-3.

The model is constrained in the Z-direction for all nodes in the plane of symmetry. For the stability of the solution, one node at the center of the bottom plate is constrained in the Y-direction, and all nodes at the centerline of the canister are constrained in the X-direction. The directions of the coordinate system are shown in Figure 3.4.4.1-1.

This model represents a "bounding" combination of geometry and loading that envelopes the Universal Storage System PWR and BWR canisters. Specifically, the shortest canister (PWR Class 1) is modeled in conjunction with the heaviest fuel and fuel basket combination (BWR Class 5). By using the shortest canister (PWR Class 1), which has the fewest number of support disks, in combination with the weight of the heaviest loaded fuel basket, the load per support disk and weldment disk is maximized. Thus, the analysis yields very conservative results relative to the expected performance of the actual canister configurations.

The finite element thermal stress analysis is performed with canister temperatures that envelope the canister temperature gradients for off-normal storage (106°F and -40°F ambient temperatures) and transfer conditions for all canister configurations. Prior to performing the thermal stress analysis, the steady-state temperature distribution is determined using temperature data from the storage and transfer thermal analyses (Chapter 4.0). This is accomplished by converting the SOLID45 structural elements of the canister model to SOLID70 thermal elements and using the material properties from the thermal analyses. Nodal temperatures are applied at six key locations for the steady state heat transfer analysis — top-center of the structural lid, top-outer diameter of the structural lid, bottom-center of the shield lid, bottom-center of the bottom plate, bottom-outer diameter of the bottom plate, and mid-elevation of the canister shell.

The temperature distribution used in the structural analyses envelopes the temperatures and temperature gradients experienced by all PWR and BWR canister configurations under storage and transfer conditions. The temperatures at the key locations are:

Top center of the structural lid	=	180°F
Top outer diameter of the structural lid	=	170°F
Bottom center of the shield lid	=	195°F
Bottom center of the bottom plate	=	150°F
Bottom outer diameter of the bottom plate	=	200°F
Mid-elevation of the canister shell	=	500°F

Temperatures used for determining allowable stress values were selected to envelope the maximum temperatures experienced by the canister components during storage and transfer conditions. Allowable stress values for the structural/shield lid region were taken at 250°F, those for the center of the bottom plate were taken at 225°F, those for the outer radius of the bottom plate at 175°F, and those for the canister shell at 500°F.

The temperatures for all nodes in the canister model are obtained by the solution of the steady state thermal conduction problem. The key temperature differences, ΔT, of the of the worst-case

PWR and BWR canisters in the radial and axial directions and those used in the canister thermal stress analysis are:

Condition	Maximum ΔT (°F)							
	Top of Structural Lid (Radial)		Bottom Plate (Radial)		Shield and Structural Lid (Axial)		Canister Shell (Axial)	
	PWR	BWR	PWR	BWR	PWR	BWR	PWR	BWR
Storage, Normal 76°F ambient	4	1	5	3	9	8	246	282
Storage, Off-Normal 106°F ambient	3	1	6	3	9	9	246	281
Storage, Off-Normal, -40°F ambient	4	1	5	4	8	7	236	274
Storage, Off-Normal Half Inlets Blocked 76°F	3	1	6	3	9	8	244	279
Transfer, 76°F ambient	8	8	41	39	10	9	293	318
Parameters used for Canister Thermal Stress Analysis	10		50		15		330	

The resulting maximum (secondary) thermal stresses in the canister are summarized in Table 3.4.4.1-1. The sectional stresses at 16 axial locations are obtained for each angular division of the model (a total of 19 angular locations for each axial location). The locations of the stress sections are shown in Figure 3.4.4.1-4. After solving for the canister temperature distribution, the thermal stress analysis was performed by converting the SOLID70 elements back to SOLID45 structural elements.

3.4.4.1.2 Canister Dead Weight Load Analysis

The canister is structurally analyzed for dead weight load using the finite element model described in Section 3.4.4.1.1. The canister temperature distribution discussed in Section 3.4.4.1.1 is used in the dead load structural analysis to evaluate the material properties at temperature. The fuel and fuel basket assembly contained within the canister are not explicitly modeled but are included in the analysis by applying a uniform pressure load representing their combined weight to the top surface of the canister bottom plate. The nodes on the bottom surface of the bottom plate are restrained in the axial direction in conjunction with the constraints described in Section 3.4.4.1.1. The evaluation is based on the weight of the BWR Class 5 canister, which has the highest weight, and the length of the PWR Class 1 canister, which is the shortest configuration. An acceleration of 1g is applied to the model in the axial direction (Y) to simulate the dead load.

The resulting maximum canister dead load stresses are summarized in Table 3.4.4.1-2 and Table 3.4.4.1-3 for primary membrane and primary membrane plus bending stresses, respectively. The sectional stresses at 16 axial locations are obtained for each angular division of the model (a total of 19 angular locations for each axial location). The locations for the stress sections are shown in Figure 3.4.4.1-4.

The lid support ring is evaluated for the dead load condition using classical methods. The ring, which is made of ASTM A-479, Type 304 stainless steel, is welded to the inner surface of the canister shell to support the shield lid. For conservatism, a temperature of 400°F, which is higher than the anticipated temperature at this location, is used to determine the material allowable stress. The total weight, W, imposed on the lid support ring is conservatively considered to be the weight of the auxiliary shield, the shield lid, and the backing ring. A 10% load factor is also applied to ensure that the analysis bounds all normal operating loads. The stresses on the support ring are the bearing stresses and shear stresses at its weld to the canister shell.

The bearing stress $\sigma_{bearing}$ is:

$$\sigma_{bearing} = \frac{W}{area} = \frac{11{,}650 \text{ lb}}{103.4 \text{ in}^2} = 113 \text{ psi}$$

where:

W = (4,768 lb + 6,825 lb + 15 lb) × 1.1 = 11,608 lb, use 11,650 lb
A = π x D x t = 103.4 in^2
D = lid support ring diameter = 65.81 in.
t = radial thickness of support ring = 0.5 in.

The yield strength, S_y, for A-479, Type 304 stainless steel = 20,700 psi, and the ultimate allowable tensile stress, S_u = 64,400 psi at 400°F. The allowable bearing stress is 1.0 S_y per ASME Section III, Subsection NB. The acceptability of the support ring design is evaluated by comparing the allowable stresses to the maximum calculated stress:

$$MS = \frac{20{,}700 \text{ psi}}{113 \text{ psi}} - 1 = +\text{Large}$$

Therefore, the support ring is structurally adequate.

The attachment weld for the lid support ring is a 3/8 in. partial penetration groove weld. The total shear force on the weld is considered to be the weight of the shield lid, the auxiliary shield, the backing ring, and the lid support ring. The unit effective area of the weld, a_{eff} is equal to the depth of the chamfer, 0.375 minus 0.125, or 0.25 $in.^2/in.$ [Ref.23, Section J2]. The total effective area of each weld is $A_{eff} = a_{eff} \times \pi D$ = 0.25 $in.^2/in. \times \pi \times 65.81$ in. = 51.7 in^2. The average shear stress in the weld is:

$$\sigma_w = \frac{W}{A_{eff}} = \frac{11{,}650 \text{ lb}}{51.7 \text{ in}^2} = 225.3 \text{ psi}$$

The allowable stress on the weld is 0.30 × the nominal tensile strength of the weld material [Ref.23, Table J2.5]. The nominal tensile strength of E308-XX filler material is 80,000 psi [Ref.28, SFA-5.4, Table 5]. However, for conservatism, S_y and S_u for the base metal, are used. The acceptability of the support ring weld is evaluated by comparing the allowable stress to the maximum calculated stress:

$$MS = \frac{0.3 \times 20{,}700 \text{ psi}}{225.3 \text{ psi}} - 1 = +\text{Large}$$

Therefore, the support ring attachment weld is structurally adequate.

3.4.4.1.3 Canister Maximum Internal Pressure Analysis

The canister is structurally analyzed for a maximum internal pressure load using the finite element model and temperature distribution and restraints described in Section 3.4.4.1.1. A maximum internal pressure of 15 psig is applied as a surface load to the elements along the internal surface of the canister shell, bottom plate, and shield lid. This pressure bounds the calculated pressure of 5.8 psig that occurs in the smallest canister, PWR Class 1, under normal conditions. The PWR Class 1 canister internal pressure bounds the internal pressures of the other four canister configurations because it has the highest quantity of fission-gas-to-volume ratio.

The resulting maximum canister stresses for maximum internal pressure load are summarized in Table 3.4.4.1-9 and Table 3.4.4.1-10 for primary membrane and primary membrane plus primary bending stresses, respectively. The sectional stresses at 16 axial locations are obtained for each angular division of the model (a total of 19 angular locations for each axial location). The locations of the stress sections are shown in Figure 3.4.4.1-4.

3.4.4.1.4 Canister Handling Analysis

The canister is structurally analyzed for handling loads using the finite element model and conditions described in Section 3.4.4.1.1. Normal handling is simulated by restraining the model at nodes on the structural lid simulating three lift points and applying a 1.1g acceleration load, which includes a 10% dynamic load factor, to the model in the axial direction. The canister is lifted at six points; however, a three-point lifting configuration is conservatively used in the handling analysis. Since the model represents a one-half section of the canister, the three-point lift is simulated by restraining two nodes 120° apart (one node at the symmetry plane and a second node 120° from the first) along the bolt diameter at the top of the structural lid in the axial direction. Additionally, the nodes along the centerline of the lids and bottom plate are restrained in the radial direction, and the nodes along the symmetry face are restrained in the direction normal to the symmetry plane.

The maximum stresses occur for the BWR class 5 canister handling, which is the heaviest configuration. Thus, the BWR class 5 canister analysis is the bounding condition for handling loads.

The resulting maximum stresses in the canister are summarized in Table 3.4.4.1-4 and Table 3.4.4.1-5 for primary membrane and primary membrane plus primary bending stresses, respectively. The sectional stresses at 16 axial locations are obtained for each angular division of the model (a total of 19 angular locations for each axial location). The locations of the stress sections are shown in Figure 3.4.4.1-4.

3.4.4.1.5 Canister Load Combinations

The canister is structurally analyzed for combined thermal, dead, maximum internal pressure, and handling loads using the finite element model and the conditions described in Section 3.4.4.1.1. Loads are applied to the model as discussed in Sections 3.4.4.1.1 through 3.4.4.1.4. A maximum internal pressure of 15.0 psi is used in conjunction with a positive axial acceleration of 1.1g. Two nodes 120° apart (one node at the symmetry plane and a second node 120° from the first) are restrained along the bolt diameter at the top of the structural lid in the axial direction. Additionally, the nodes along the centerline of the lids and bottom plate are restrained in the radial direction, and the nodes along the symmetry face are restrained in the direction normal to the symmetry plane.

The resulting maximum stresses in the canister for combined loads are summarized in Table 3.4.4.1-6, Table 3.4.4.1-7, and Table 3.4.4.1-8, for primary membrane, primary membrane plus primary bending, and primary plus secondary stresses, respectively. The sectional stresses at 16 axial locations are obtained for each angular division of the model (a total of 19 angular locations for each axial location). The locations for the stress sections are shown in Figure 3.4.4.1-4.

As shown in Table 3.4.4.1-6 through Table 3.4.4.1-8, the canister maintains positive margins of safety for the combined load conditions.

3.4.4.1.6 Canister and Basket Fatigue Evaluation

The purpose of this section is to evaluate whether an analysis for cyclic service is required for the Universal Storage System components. The requirements for analysis for cyclic operation of components designed to ASME Code criteria are presented in ASME Section III, Subsection NB-3222.4 [5] for the canister and Subsection NG-3222.4 [6] for the fuel basket. Guidance for components designed to AISC standards is in the Manual of Steel Construction, Table A-K4.1 [23].

During storage conditions, the canister is housed in the vertical concrete cask. The concrete cask is a shielded, reinforced concrete overpack designed to hold a canister during long-term storage conditions. The cask is constructed of a thick inner steel shell surrounded by 28 in. of reinforced concrete. The cask inner shell is not subjected to cyclic mechanical loading. Thermal cycles are limited to changes in ambient air temperature. Because of the large thermal mass of the concrete cask and the relatively minor changes in ambient air temperature (when compared to the steady state heat load of the cask contents), fatigue as a result of cycles in ambient air is not significant, and no further fatigue evaluation of the inner shell is required.

ASME criteria for determining whether cyclic loading analysis is required are comprised of six conditions, which, if met, preclude the requirement for further analysis:

1. Atmospheric to Service Pressure Cycle
2. Normal Service Pressure Fluctuation
3. Temperature Difference — Startup and Shutdown
4. Temperature Difference — Normal Service
5. Temperature Difference — Dissimilar Materials
6. Mechanical Loads

Evaluation of these conditions follows.

Condition 1 — Atmospheric to Service Pressure Cycle

This condition is not applicable. The ASME Code defines a cycle as an excursion from atmospheric pressure to service pressure and back to atmospheric pressure. Once sealed, the canister remains closed throughout its operational life, and no atmospheric to service pressure cycles occur.

Condition 2 — Normal Service Pressure Fluctuation

This condition is not applicable. The condition establishes a maximum pressure fluctuation as a function of the number of significant pressure fluctuation cycles specified for the component, the design pressure, and the allowable stress intensity of the component material. Operation of the canister is not cyclic, and no significant cyclic pressure fluctuation are anticipated.

Condition 3 — Temperature Difference — Startup and Shutdown

This condition is not applicable. The Universal Storage System is a passive, long-term storage system that does not experience cyclic startups and shutdowns.

Condition 4 — Temperature Difference — Normal and Off-Normal Service

The ASME Code specifies that temperature excursions are not significant if the change in ΔT between two adjacent points does not experience a cyclic change of more than the quantity:

$$\Delta T = \frac{S_a}{2E\alpha} = 58°F,$$

where, for Type 304L stainless steel,

S_a = 28,200 psi, the value obtained from the fatigue curve for service cycles < 10^6,
E = 26.5×10^6 psi, modulus of elasticity at 400 °F,
α = 9.19×10^{-6} in./in.-°F.

Because of the large thermal mass of the canister and the concrete cask and the relatively constant heat load produced by the canister's contents, cyclic changes in ΔT greater than 58 °F will not occur.

Condition 5 — Temperature Difference Between Dissimilar Materials

The canister and its internal components contain several materials. However, the design of all components considers thermal expansion, thus precluding the development of unanalyzed thermal stress concentrations.

Condition 6 — Mechanical Loads

This condition does not apply. Cyclic mechanical loads are not applied to the vertical concrete cask and canister during storage conditions. Therefore, no further cyclic loading evaluation is required.

The criteria ASME Code Subsections NB-3222.4 and NG-3222.4 are met, and no fatigue analysis is required.

3.4.4.1.7 Canister Pressure Test

The canister is designed and fabricated to the requirements of ASME Code, Subsection NB, to the extent possible. A 20 psig pneumatic pressure test is performed in accordance with the requirements of ASME Code Subsection NB-6320 [5]. The pressure test is performed after the shield lid to canister shell weld is completed. After the pressure test, the weld is liquid penetrant examined. The test pressure slightly exceeds 1.2 × design pressure (1.2 × 15 psig = 18 psig).

The ASME Code requires that the pressure test loading comply with the following criteria from Subsection NB-3226:

(a) P_m shall not exceed $0.9S_y$ at test temperature. For convenience, the stress intensities developed in the analysis of the canister due to a normal internal pressure of 15 psig (Tables 3.4.4.1-9 and 3.4.4.1-10) are ratioed to demonstrate compliance with this requirement. From Table 3.4.4.1-9, the maximum primary stress intensity, P_m , is 2.51 ksi. The canister material is ASME SA-240, Type 304L stainless steel, and the test temperature is 100°F.

$(P_m)_{test} = (20/15)(2.51 \text{ ksi}) = 3.35 \text{ ksi}$, which is $< S_y = 24.2$ ksi.

Thus, criterion (a) is met.

(b) For $P_m < 0.67S_y$ (see criterion a), the primary membrane plus bending stress intensity, $P_m + P_b$, shall be $\leq 1.35S_y$. From Table 3.4.4.1-10, $P_m + P_b = 10.27$ ksi.

$(P_m + P_b)_{test} = (20/15) \times (10.27 \text{ ksi}) = 13.7 \text{ ksi}$, which is $\leq 1.35S_y = 32.7$ ksi (1.35×24.2 ksi).

Thus, criterion (b) is met.

(c) The external pressure shall not exceed 135% of the value determined by the rules of NB-3133. The exterior of the canister is at atmospheric pressure at the time the pressure test is conducted. Therefore, this criterion is met.

(d) For the 1.20 to 1.25 Design Pressure pneumatic test of NB-6321, the stresses shall be calculated and compared to the limits of criteria (a), (b), and (c). This calculation and the fatigue evaluation of (e) need not be revised unless the actual pneumatic test pressure exceeds 1.25 Design Pressure.

The test pressure slightly exceeds 1.25 × Design Pressure. However, the stresses used in this evaluation are ratioed to the test pressure. Thus, the stresses at the test pressure are calculated.

(e) Tests, with the exception of the first 10 pneumatic tests in accordance with NB-6320, shall be considered in the fatigue evaluation of the component.

The canisters are not reused, and the pneumatic test will be conducted only once. Thus, the pressure test is not required to be considered in the fatigue analysis.

The canister pneumatic pressure tests complies with all NB-3226 criteria.

3.4.4.1.8 Fuel Basket Support Disk Evaluation

The PWR and BWR fuel baskets are described in detail in Sections 1.2.1.2.1 and 1.2.1.2.2, respectively. The design of the basket is similar for the PWR and BWR configurations. The major components of the BWR basket are shown in Figure 3.4.4.1-5. The structural evaluation for the PWR and BWR support disks for the normal conditions of storage is presented in the following sections. During normal conditions, the support disk is subjected to its self-weight only (in canister axial direction) and is supported by the tie rods/spacers at 8 locations for PWR configuration and 6 locations for the BWR configuration. To account for the condition when the canister is handled, a handling load, defined as 10 percent of the dead load, is considered. Finite element analyses using the ANSYS program is performed for the support disk for PWR and BWR configurations, respectively. In addition to the dead load and handling load (10% of dead load), thermal stresses are also considered based on conservative temperatures that envelop those experienced by the support disk during normal, off-normal (106°F and –40°F ambient temperatures) and transfer conditions. The stress criteria is defined according to ASME Code, Section III, Subsection NG. For the normal condition of storage, the Level A allowable stresses from Subsection NG as shown below are used.

Stress Category	Normal (Level A) Allowable Stresses
P_m	S_m
P_m+P_b	$1.5\ S_m$
P+Q	$3.0\ S_m$

3.4.4.1.8.1 PWR Support Disk

As shown in Figure 3.4.4.1-6, a finite element model is generated to analyze the PWR fuel basket support disks. The model is constructed using the ANSYS three-dimensional SHELL63 elements and corresponds to a single support disk with a thickness of 0.5 inch. The only loading on the model is the inertial load (1.1g) that includes the dead load and handling load in the out-of-plane direction (Global Z) for normal conditions of storage. The model is constrained in eight locations in the out-of-plane direction to simulate the supports of the tie rods/spacers.

Note that a full model is generated because this model is also used for the evaluation of the support disk for the off-normal handling condition (Section 11.1.3) in which non-symmetric loading (side load) is present. In addition, this model is used for the evaluation of a support disk for the 24-inch end drop accident condition of the vertical concrete cask (Section 11.2.4).

The model accommodates thermal expansion effects by using the temperature data from the thermal analysis and the coefficient of thermal expansion. Prior to performing the structural analyses, the temperature distribution in the support disk is determined by executing a steady-state thermal conduction analysis. This is accomplished by converting the SHELL63 structural elements to SHELL57 thermal elements. A maximum temperature of 700°F is applied to the nodes at the center slot of the disk model and a minimum temperature 400°F is applied to the nodes around the outer circumferential edge of the disk. All other nodal temperatures are then obtained by the steady state conduction solution. Note that the applied temperatures (700°F and 400°F) are conservatively selected to envelope the maximum temperature, as well as the maximum radial temperature gradient (ΔT) of the disk for all normal and off-normal conditions of storage and transfer conditions.

To evaluate the most critical regions of the support disk, a series of cross sections are considered. The locations of these sections on a PWR support disk are shown in Figures 3.4.4.1-7 and 3.4.4.1-8. Table 3.4.4.1-11 lists the cross sections versus Point 1 and Point 2, which spans the cross section of the ligament in the plane of the support disk.

The stress evaluation for the support disk is performed according to ASME Code, Section III, Subsection NG. According to this subsection, linearized stresses of cross sections of the structure are to be compared against the allowable stresses. The stress evaluation results for the support disks for normal condition are presented in Tables 3.4.4.1-12 and 3.4.4.1-13. The tables

list the 40 highest P_m+P_b and P+Q stress intensities with large margins of safety. The Level A allowable stresses, $1.5S_m$ and $3S_m$ of the 17-4PH stainless steel at corresponding nodal temperatures, are used for the P_m+P_b and P+Q stresses respectively. Note that the P_m stresses for the support disk for normal conditions are essentially zero since there is no loads in the plane of the support disk.

3.4.4.1.8.2 BWR Support Disk

Similar to the evaluation for the PWR fuel basket support disk, a finite element model is generated to analyze the BWR fuel basket support disks, as shown in Figure 3.4.4.1-12. The model is constructed using the ANSYS three-dimensional SHELL63 elements and corresponds to a single support disk with a thickness of 5/8 inch. The only loading on the model is the inertial load (1.1g) that includes the dead load and handling load in the out-of-plane direction (Global Z) for normal conditions of storage. The model is constrained in six locations in the out-of-plane direction to simulate the supports of the tie rods/spacers.

The model accommodates thermal expansion effects by using the temperature data from the thermal analysis and the coefficient of thermal expansion. The temperature distribution in the BWR support disk is determined using the same method used in Section 3.4.4.1.8.1 for the PWR support disk. The boundary temperatures are selected as 700°F maximum (at disk center) and 400°F minimum (at disk outer edge) to bound the temperature distribution for all normal and off-normal conditions of storage and transfer conditions.

To evaluate the most critical regions of the support disk, a series of cross sections are considered. The locations of these sections on a BWR support disk are shown in Figures 3.4.4.1-13 through 3.4.4.1-16. Table 3.4.4.1-14 lists the cross sections versus Point 1 and Point 2, which spans the cross section of the ligament in the plane of the support disk.

The stress evaluation results for the BWR support disks for normal condition are presented in Tables 3.4.4.1-15 and 3.4.4.1-16. The tables list the 40 highest P_m+P_b and P+Q stress intensities with large margins of safety. The Level A allowable stresses from ASME Code, Section III, Subsection NG, $1.5S_m$ and $3.0S_m$ of the SA533 carbon steel at corresponding nodal temperatures, are used for the P_m+P_b and P+Q stresses, respectively. Note that the P_m stresses for the support disk for normal conditions are essentially zero, since there is no loads in the plane of the support disk.

3.4.4.1.9 Fuel Basket Weldments Evaluation

The PWR and BWR fuel basket weldments are evaluated for normal storage conditions using the finite element method. In addition to the dead load of the weldment, a 10% dynamic load factor is considered to account for handling loads. Therefore, a total acceleration of 1.1g is applied to the weldment model in the out of plane direction. Thermal stresses for the basket weldments are determined using the method presented in Sections 3.4.4.1.8.1 and 3.4.4.1.8.2 for the PWR and BWR support disks, respectively. The temperatures used in the model to establish the weldment temperature gradient are:

Basket Weldment	Temperature at Center of Weldment (°F)	Temperature at Edge of Weldment (°F)
PWR Top	500	275
PWR Bottom	250	170
BWR Top	450	250
BWR Bottom	350	175

These temperatures are conservatively selected to envelope the maximum temperature and the maximum radial temperature gradient of the weldments for all normal and off-normal conditions of storage. The results of the structural analyses for dead load, handling load, and thermal load are summarized in Table 3.4.4.1-17.

3.4.4.1.9.1 PWR Fuel Basket Weldments

The PWR top and bottom weldment plates are 1.25 and 1.0-in. thick Type 304 stainless steel plate, respectively. The weldments support their own weight plus the weight of up to 24 PWR fuel assembly tubes. An ANSYS finite element analysis was prepared for both plates because the support location for each weldment is different. Both models use the SHELL63 elements, which permits out-of-plane loading. The finite element models for the top and bottom weldments are shown in Figures 3.4.4.1-8 and 3.4.4.1-9, respectively. Note that the corner baffles are conservatively omitted in the top weldment model. The load from the fuel tube on the bottom weldment is represented as point forces applied to the nodes at the periphery of the fuel assembly slots. An average point force is applied. The application of the nodal loads at the slot periphery

is accurate because the tube weight is transmitted to the edge of the slot, which provides support to the fuel tubes while in the vertical position.

The maximum stress intensity and the margin of safety for the weldments are shown in Table 3.4.4.1-17. Note that the nodal stress intensity is conservatively used for the evaluation. The Pm stresses for the weldments for normal conditions are essentially zero since there are no loads in the plane of the weldments. The weldments satisfy the stress criteria in the ASME Code Section III, Subsection NG [6].

3.4.4.1.9.2 BWR Fuel Basket Weldments

In the BWR fuel basket transport analysis, the responses of the top and bottom weldment plates to normal storage conditions are evaluated in conjunction with the thermal expansion stress. The weldment plates are 1.0-in. thick Type 304 stainless steel. The weldments support their own weight and the weight of up to 56 BWR fuel assembly tubes. A finite element analysis was performed for the top and bottom plates because the support for each weldment differs depending upon the location of the welded ribs for each. Both models use SHELL63 elements, which permit out-of-plane loading. The finite element models for the top and bottom weldments are shown in Figure 3.4.4.1-18 and Figure 3.4.4.1-19, respectively. The load from the fuel tube on the bottom weldment is represented as average point forces applied to the nodes at the periphery of the fuel assembly slots because the tube weight is transmitted to the edge of the slot in the end-impact condition.

The maximum stress intensity and the margin of safety for the weldments are shown in Table 3.4.4.1-17. Note that the nodal stress intensity is conservatively used for the evaluation. The P_m stresses for the weldments for normal conditions are essentially zero since there are no loads in the plane of the weldments. The weldments satisfy the stress criteria in the ASME Code Section III, Subsection NG [6].

3.4.4.1.10 Fuel Tube Analysis

Under normal storage conditions, the fuel tubes, Figure 3.4.4.1-9 (PWR) and Figure 3.4.4.1-17 (BWR), support only their own weight. The fuel assemblies are supported by the canister bottom plate, not by the fuel tubes. Thermal stresses are considered to be negligible since the tubes are free to expand axially and radially. The handling load is taken as 10% of the dead load.

The weight of the fuel tube, with a load of 1.1g (to account for both the dead load and handling load) is carried by the tube cross-section. The cross sectional area of a PWR fuel tube is:

$$\text{Area} = (8.9 \text{ in})^2 - (8.9 \text{ in.} - 2 \times 0.048 \text{ in.})^2 = 1.7 \text{ in}^2$$

The weight of the heaviest (longest) PWR fuel tube, including the 0.075 in. thick BORAL plates, is about 153 lb. Considering a g-load of 1.1, the maximum compressive and bearing stress in the fuel tube is about 99 psi (153 lb × 1.1 / 1.7 in.^{2}). Limiting the compressive stress level in the tube to the material yield strength ensures the tube remains in position in storage conditions. The yield strength of Type 304 stainless steel is 17,300 psi at a conservatively high temperature of 750°F.

$$\text{MS} = 17{,}300/99 - 1 = +\text{Large}$$

The cross sectional area of a BWR fuel tube is:

$$\text{Area} = (5.996 \text{ in})^2 - (5.9969 \text{ in.} - 2 \times 0.048 \text{ in.})^2 = 1.14 \text{ in}^2$$

The weight of the heaviest (longest) BWR fuel tube, including 0.135 in. thick BORAL plates on two sides, is about 83 lb. Considering a g-load of 1.1, the maximum compressive and bearing stress in the fuel tube is about 80 psi (83 lb × 1.1 / 1.14 in.^{2}). Limiting the compressive stress level in the tube to the material yield strength ensures the tube remains in position in storage conditions. The yield strength of Type 304 stainless steel is 17,300 psi at a conservatively high temperature of 750°F.

$$\text{Margin of Safety} = 17{,}300/80 - 1 = +\text{Large}$$

Thus, the tubes are structurally adequate under normal storage and handing conditions.

3.4.4.1.11 Canister Closure Weld Evaluation

The closure weld for the canister is a 0.9-inch groove weld between the structural lid and the canister shell. The evaluation of this weld incorporates a 0.8 stress reduction factor in accordance with NRC Interim Staff Guidance (ISG) No. 4, Revision 1. The use of this factor is in accordance with ISG No. 4, since the strength of the weld material (E308) is greater than that of the base material (Type 304 or 304L stainless steel).

The stresses for the canister closure weld are evaluated using sectional stresses as permitted by Subsection NB of the ASME Code. The location of the section for the canister closure weld evaluation is shown in Figure 3.4.4.1-4 and corresponds to Section 13. The governing P_m, $P_m + P_b$, and P + Q stress intensities for Section 13, and the associated allowables, are listed in Table 3.4.4.1-6, Table 3.4.4.1-7, and Table 3.4.4.1-8, respectively. The factored allowables, incorporating the 0.8 stress reduction factor, and the resulting controlling Margins of Safety are shown below.

This evaluation confirms that the canister closure weld is acceptable for normal operation conditions.

Stress Category	Analysis Stress Intensity (ksi)	0.8 x Allowable Stress (ksi)	Margin of Safety
P_m	1.78	13.36	6.51
$P_m + P_b$	2.46	20.04	7.15
P + Q	4.13	40.08	8.70

Critical Flaw Size for the Canister Closure Weld

The closure weld for the canister is comprised of multiple weld beads using a compatible weld material for Type 304L stainless steel. An allowable (critical) flaw evaluation has been performed to determine the critical flaw size in the weld region. The result of the flaw evaluation is used to define the minimum flaw size, which must be identifiable in the nondestructive examination of the weld. Due to the inherent toughness associated with Type 304L stainless steel, a limit load analysis is used in conjunction with a J-integral/tearing modulus approach.

The safety factor used in this evaluation is that defined in Section XI of the ASME Code.

The stress component used in the evaluation for the critical flaw size is the radial stress component in the weld region of the structural lid. For the normal operation condition, in accordance with ASME Code Section XI, a safety factor of 3 is required. For the purpose of identifying the stress for the flaw evaluation, the weld region corresponding to Section 13 in Figure 3.4.4.1-4 is considered. The radial stress corresponds to SX in Tables 3.4.4.1-1 through 3.4.4.1-10. The maximum reported radial tensile stress is 0.9 ksi.

To perform the flaw evaluation, a 10 ksi stress is conservatively used, resulting in a significantly larger actual safety factor than the required safety factor of 3. Using a 10 ksi stress as the basis for the evaluation of the structural lid weld, the critical flaw size is 0.52 inch for a flaw that extends 360 degrees around the circumference of the structural lid weld. Stress components for the circumferential (Z) and axial (Y) directions are also reported in Tables 3.4.4.1-1 through 3.4.4.1-10, which would be associated with flaws oriented in the radial or horizontal directions, respectively. As shown in Table 3.4.4.1-7 at Section No. 13 (the structural lid weld), the maximum tensile stress reported for these components (SY and SZ) is 1.8 ksi, which is also enveloped by the value of 10 ksi used in the critical flaw evaluation for stresses in the radial direction.

The 360-degree flaw employed for the circumferential direction is considered to be bounding with respect to any partial flaw in the weld, which could occur in the radial and horizontal directions. Therefore, using a minimum detectable flaw size of 0.375 inch is acceptable, since it is less than the very conservatively determined 0.52-inch critical flaw size.

The Type 304L stainless steel structural lid may be forged (SA-182 material), or fabricated from plate (SA-240 material). Since the forged material is required to have ultimate and yield strengths that are equal to, or greater than, the plate material, the critical flaw size determination is applicable to both materials.

Figure 3.4.4.1-1 Canister Composite Finite Element Model

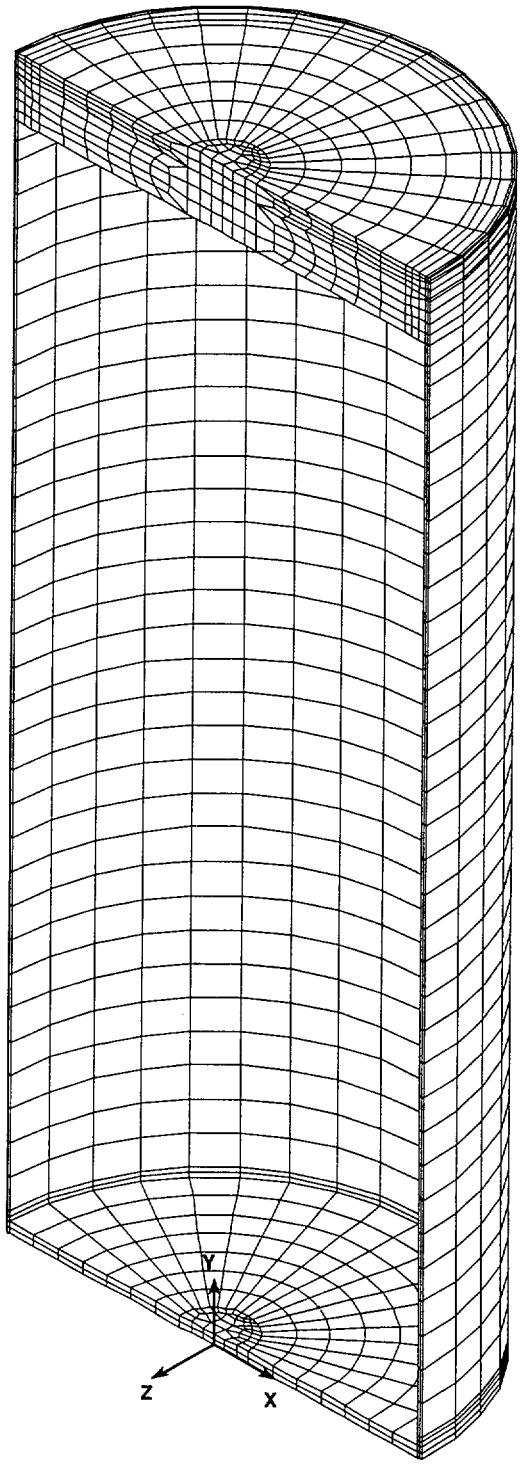

Figure 3.4.4.1-2 Weld Regions of Canister Composite Finite Element Model at Structural and Shield Lids

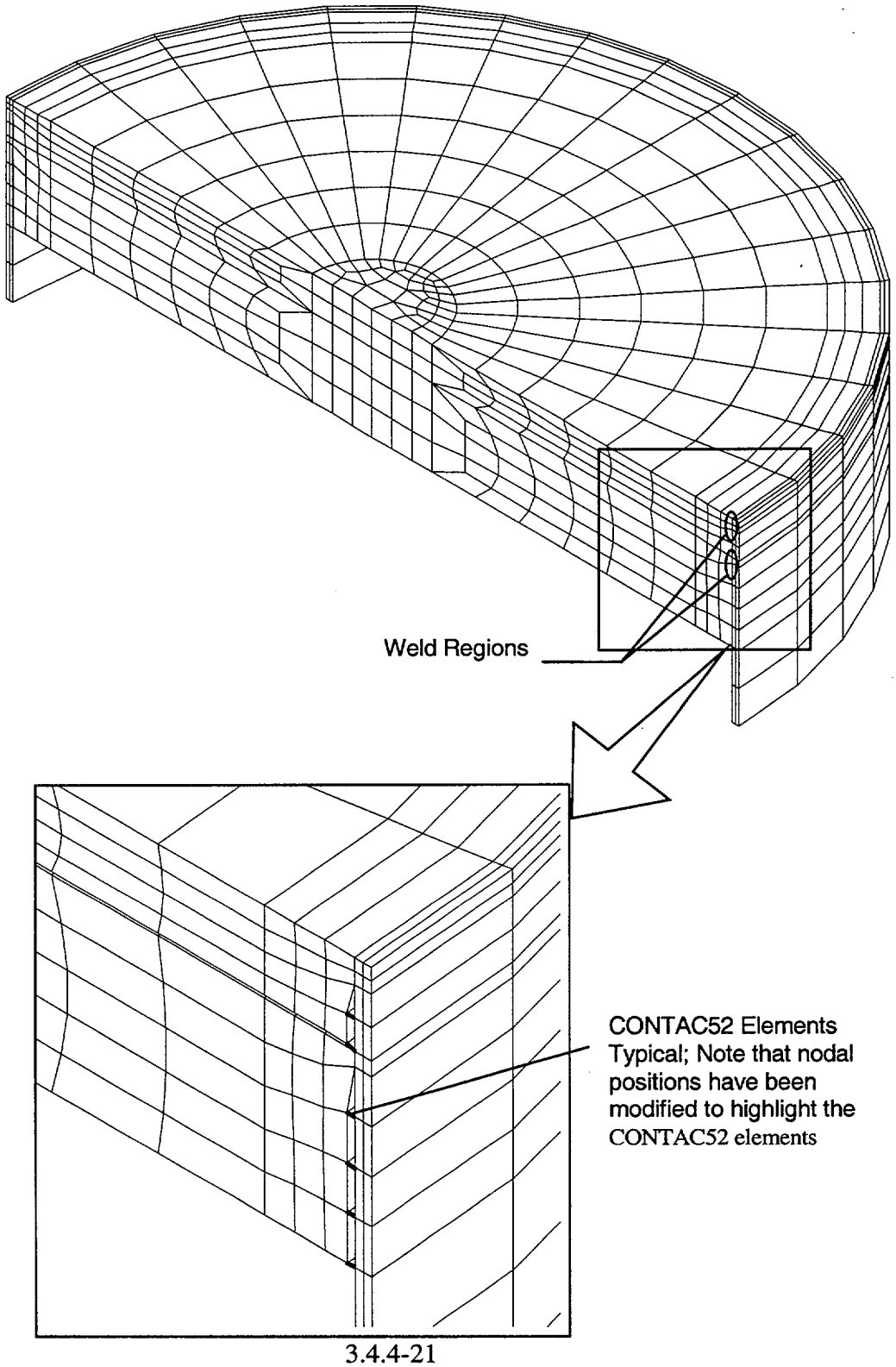

Figure 3.4.4.1-3 Bottom Plate of the Canister Composite Finite Element Model

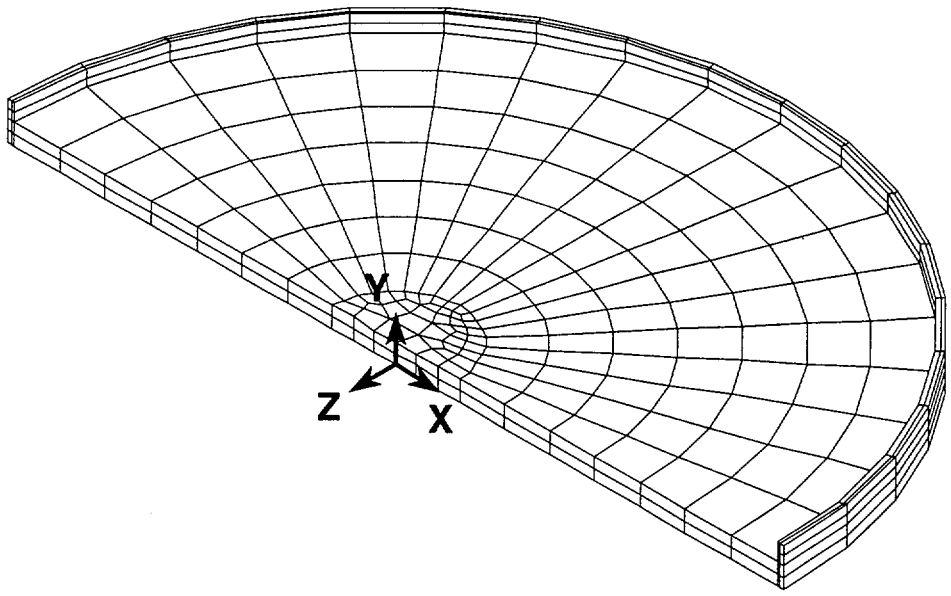

Figure 3.4.4.1-4 Locations for Section Stresses in the Canister Composite Finite Element Model

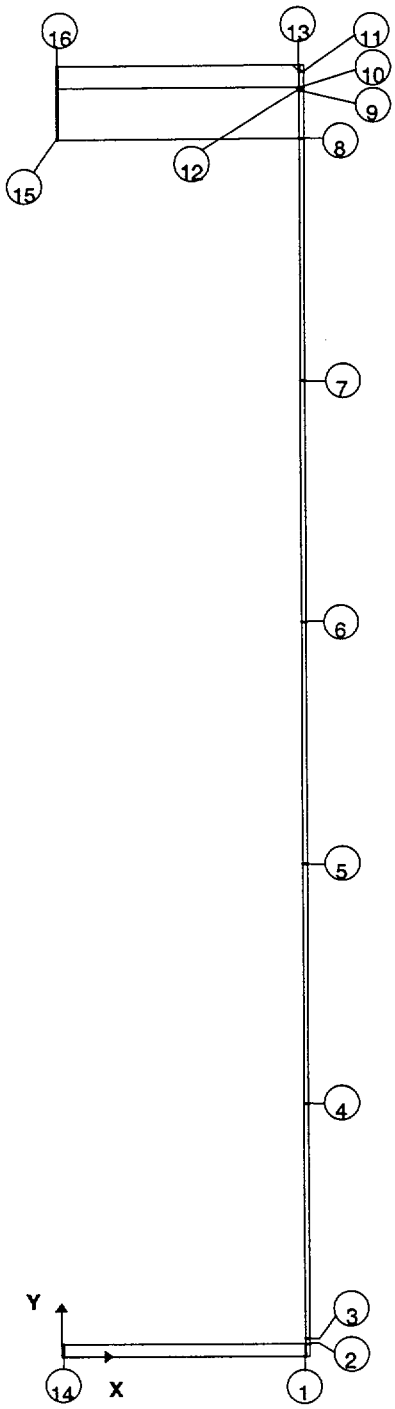

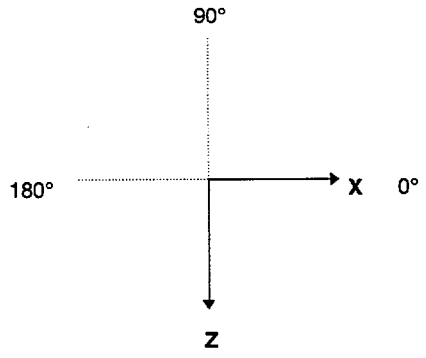

Top View of Axis

Section Coordinates at Z=0 and X>0

Axial Section	Node 1		Node 2	
	X	Y	X	Y
1	32.905	0.0	32.905	1.75
2	32.905	1.75	33.53	1.75
3	32.905	2.50	33.53	2.50
4	32.905	34.45	33.53	34.45
5	32.905	67.15	33.53	67.15
6	32.905	99.85	33.53	99.85
7	32.905	132.55	33.53	132.55
8	32.905	165.25	33.53	165.25
9	32.905	171.75	33.53	171.75
10	32.905	172.25	33.53	172.25
11	32.905	174.37	33.53	174.37
12	32.905	171.75	32.905	172.25
13	32.905	174.37	32.905	175.25
14	0.1	0.0	0.1	1.75
15	0.1	165.25	0.1	172.25
16	0.1	172.25	0.1	175.25

Figure 3.4.4.1-5 BWR Fuel Assembly Basket Showing Typical Fuel Basket Components

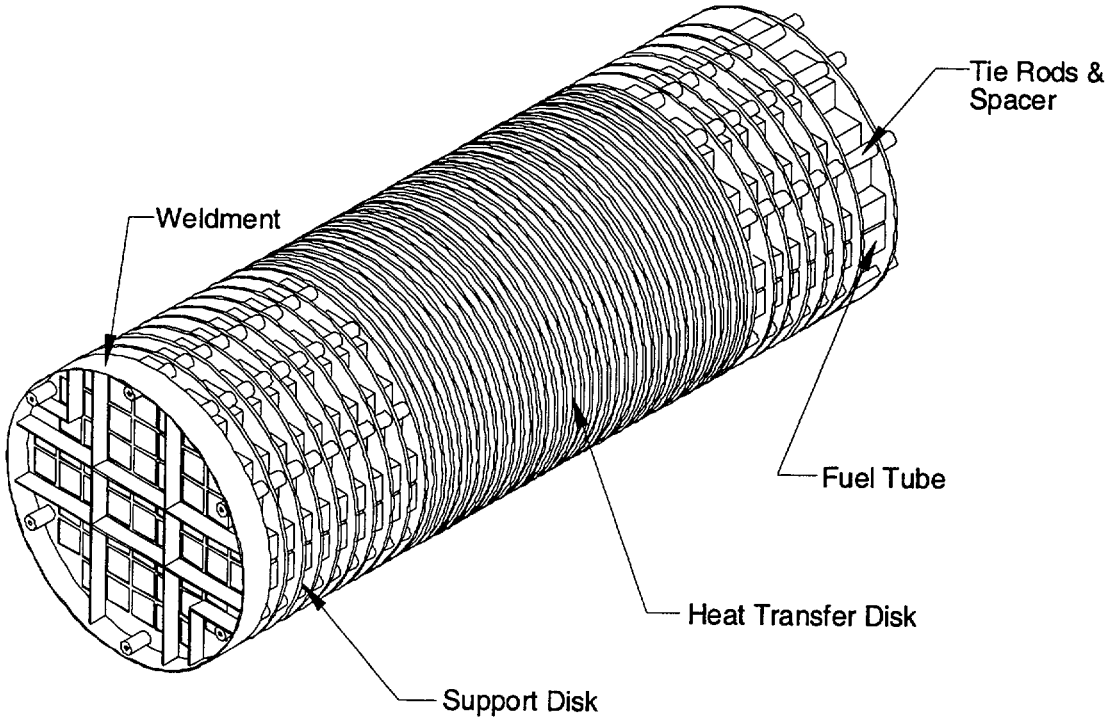

Figure 3.4.4.1-6 PWR Fuel Basket Support Disk Finite Element Model

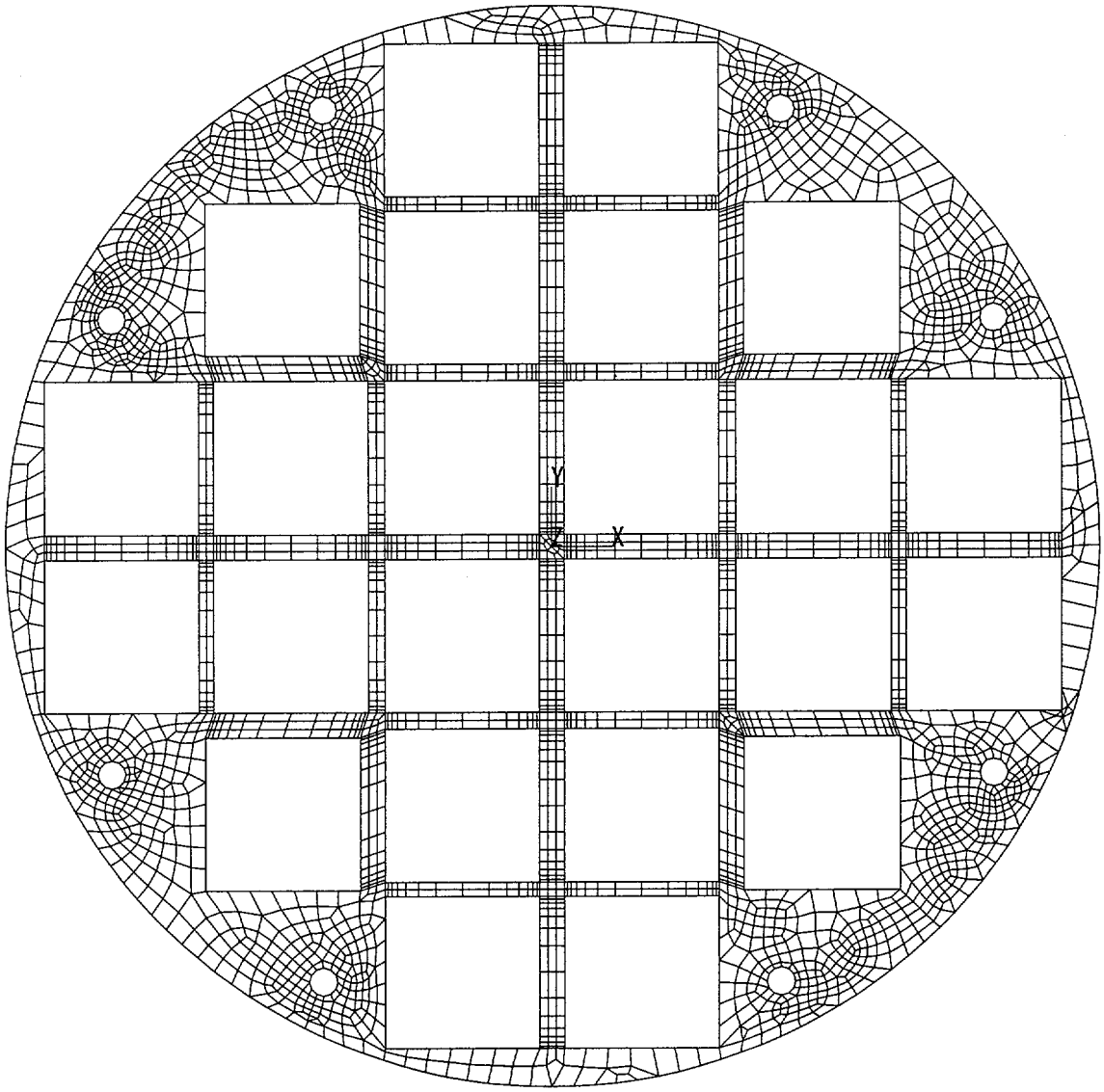

Figure 3.4.4.1-7 PWR Fuel Basket Support Disk Sections for Stress Evaluation (Left-Half)

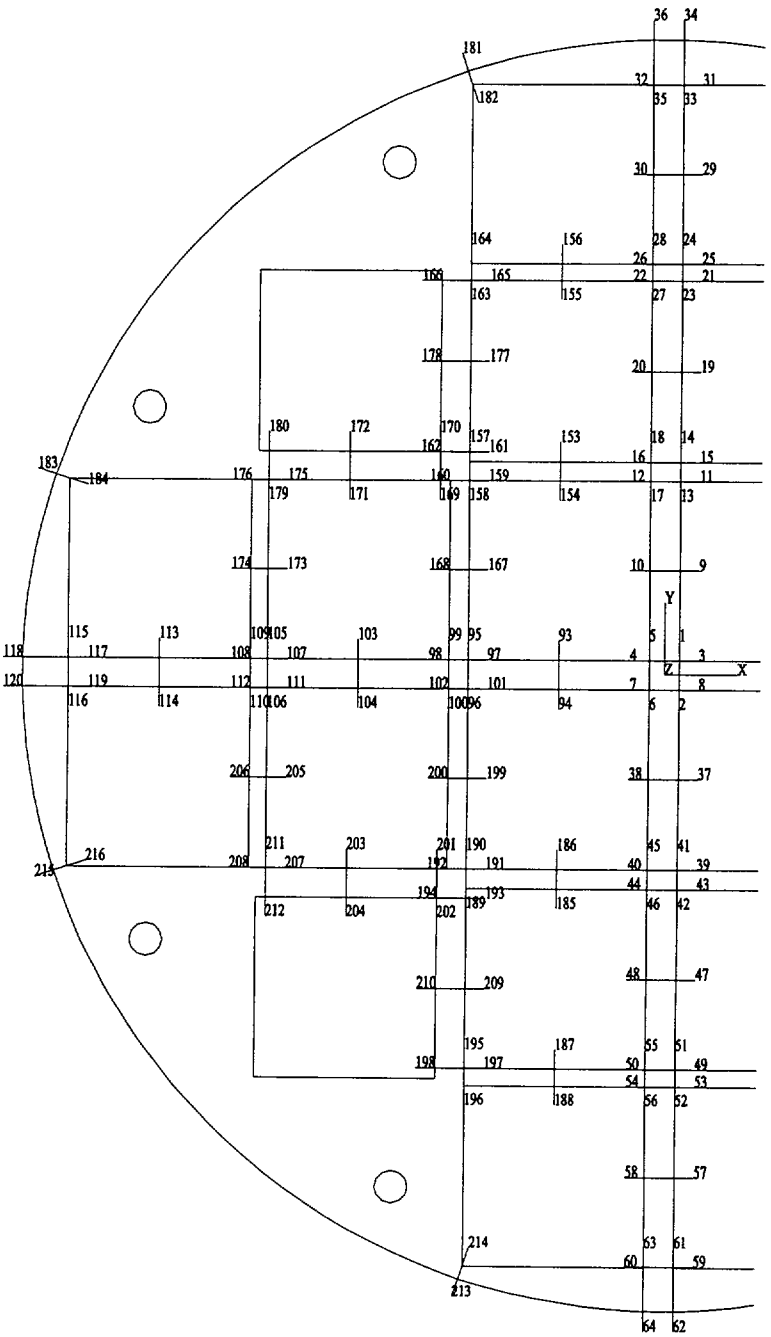

Figure 3.4.4.1-8 PWR Fuel Basket Support Disk Sections for Stress Evaluation (Right-Half)

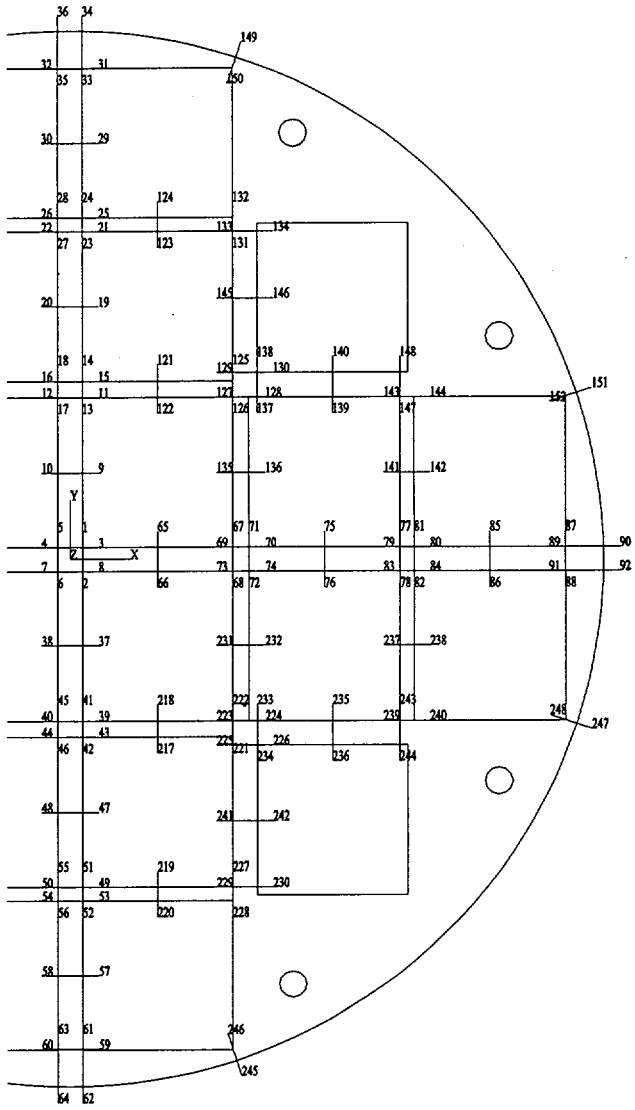

Figure 3.4.4.1-9 PWR Class 3 Fuel Tube Configuration

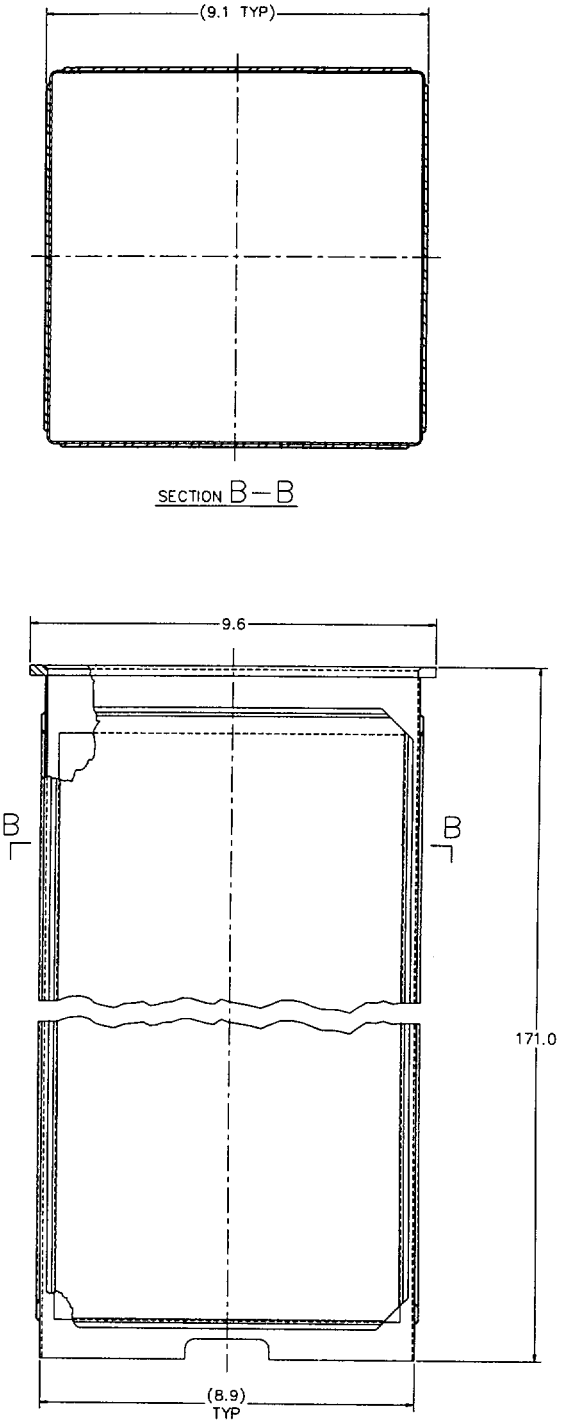

Figure 3.4.4.1-10 PWR Top Weldment Plate Finite Element Model

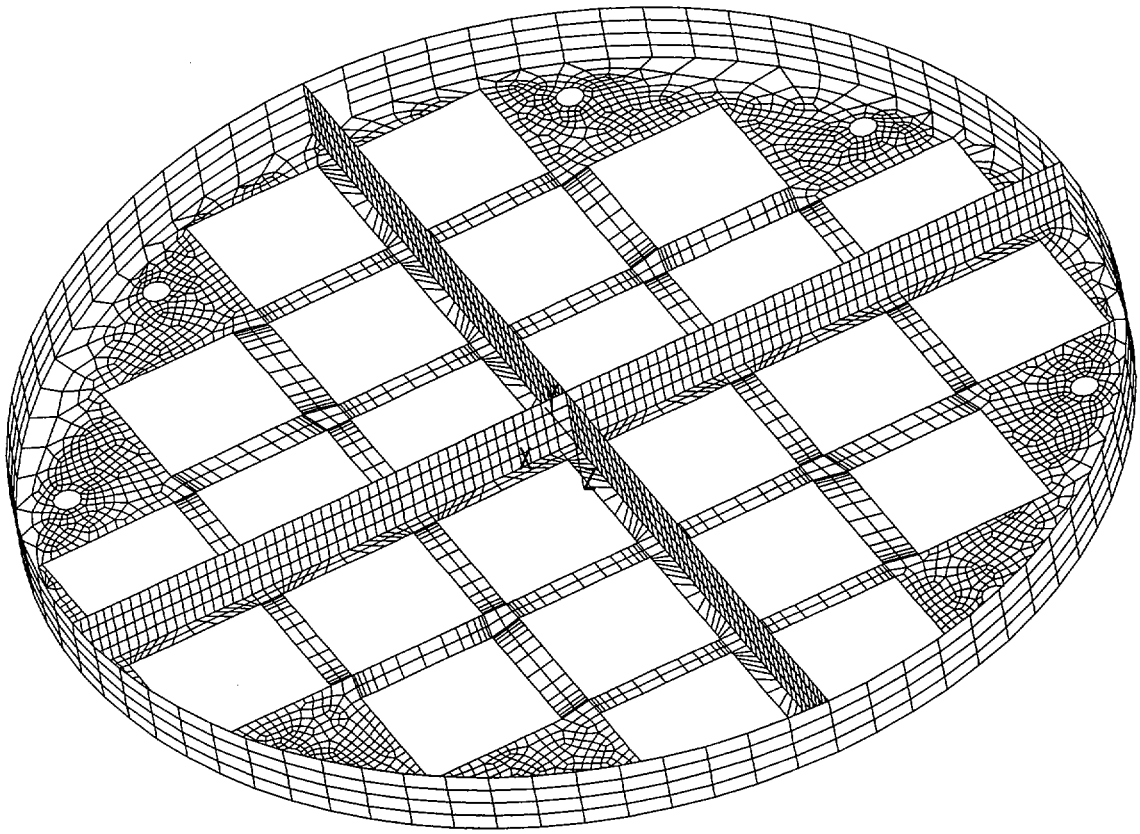

Figure 3.4.4.1-11 PWR Bottom Weldment Plate Finite Element Model

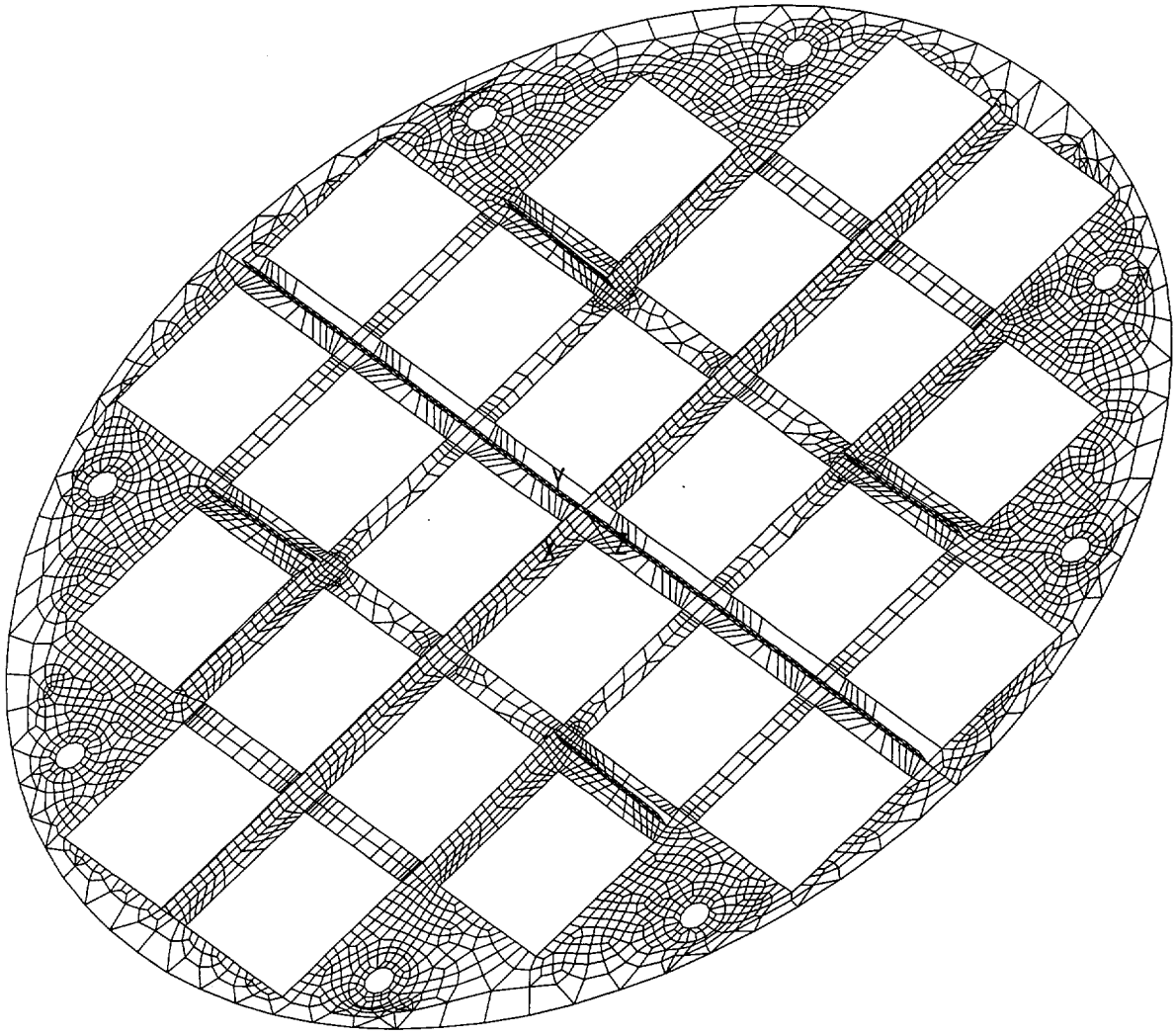

(Figure Inverted to Show Weldment Stiffeners)

Figure 3.4.4.1-12 BWR Fuel Basket Support Disk Finite Element Model

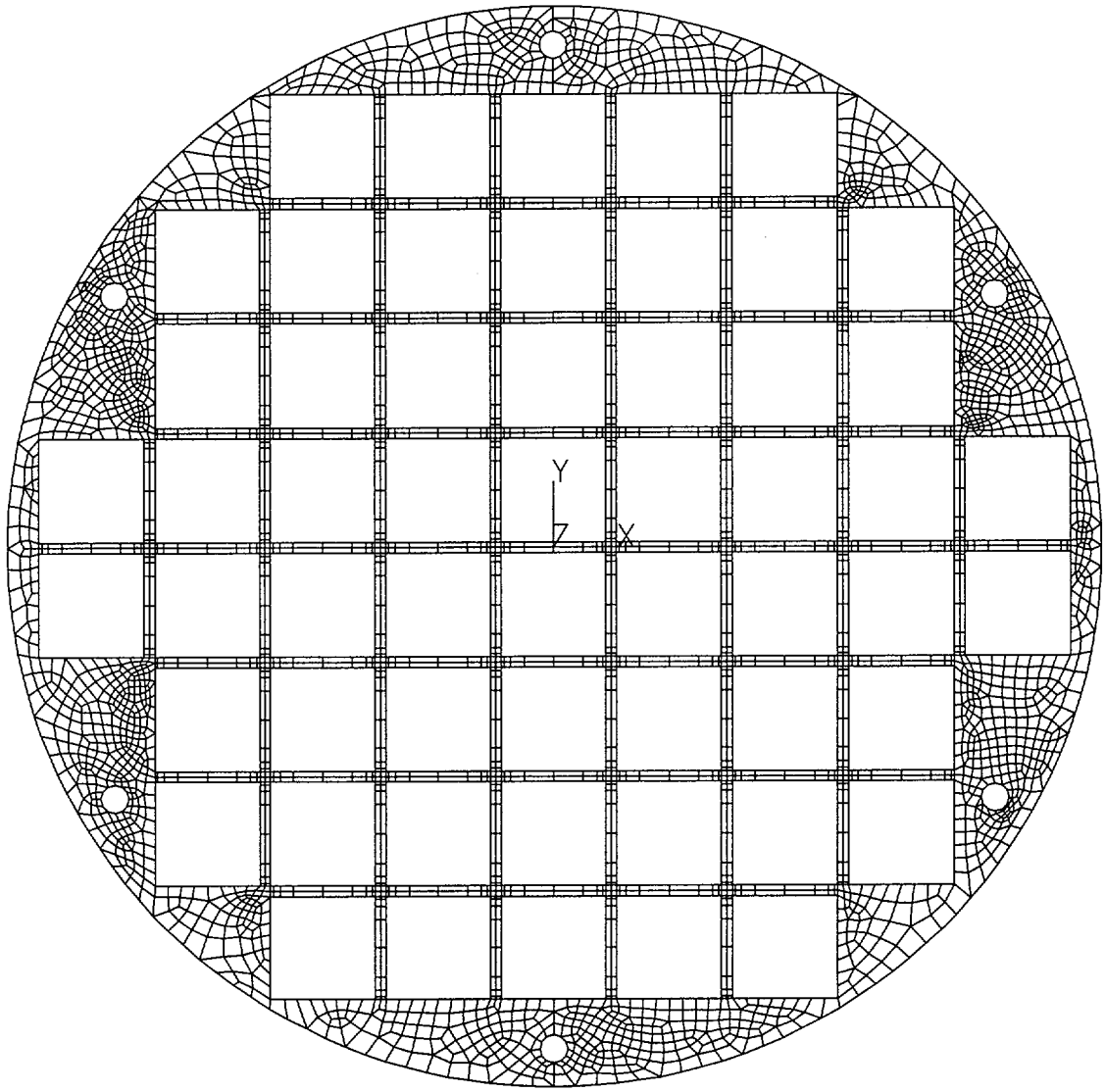

Figure 3.4.4.1-13 BWR Fuel Basket Support Disk Sections for Stress Evaluation (Quadrant I)

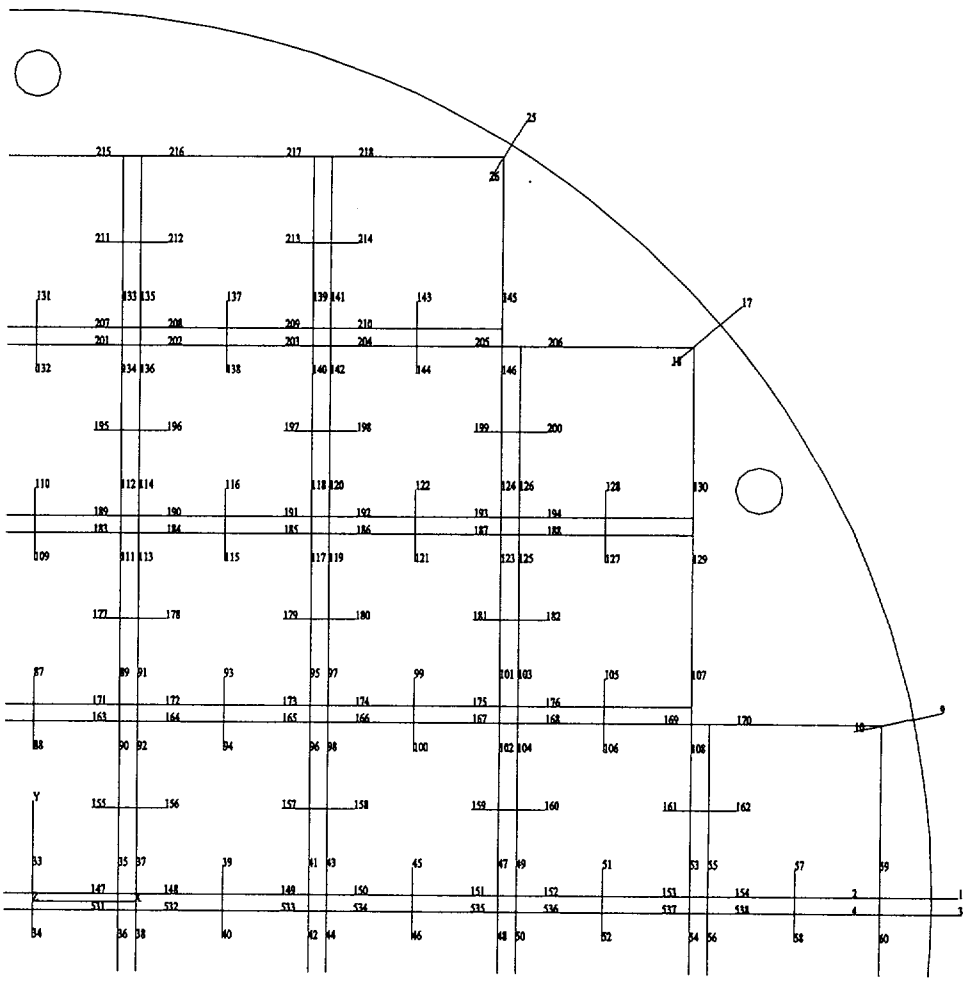

Figure 3.4.4.1-14 BWR Fuel Basket Support Disk Sections for Stress Evaluation (Quadrant II)

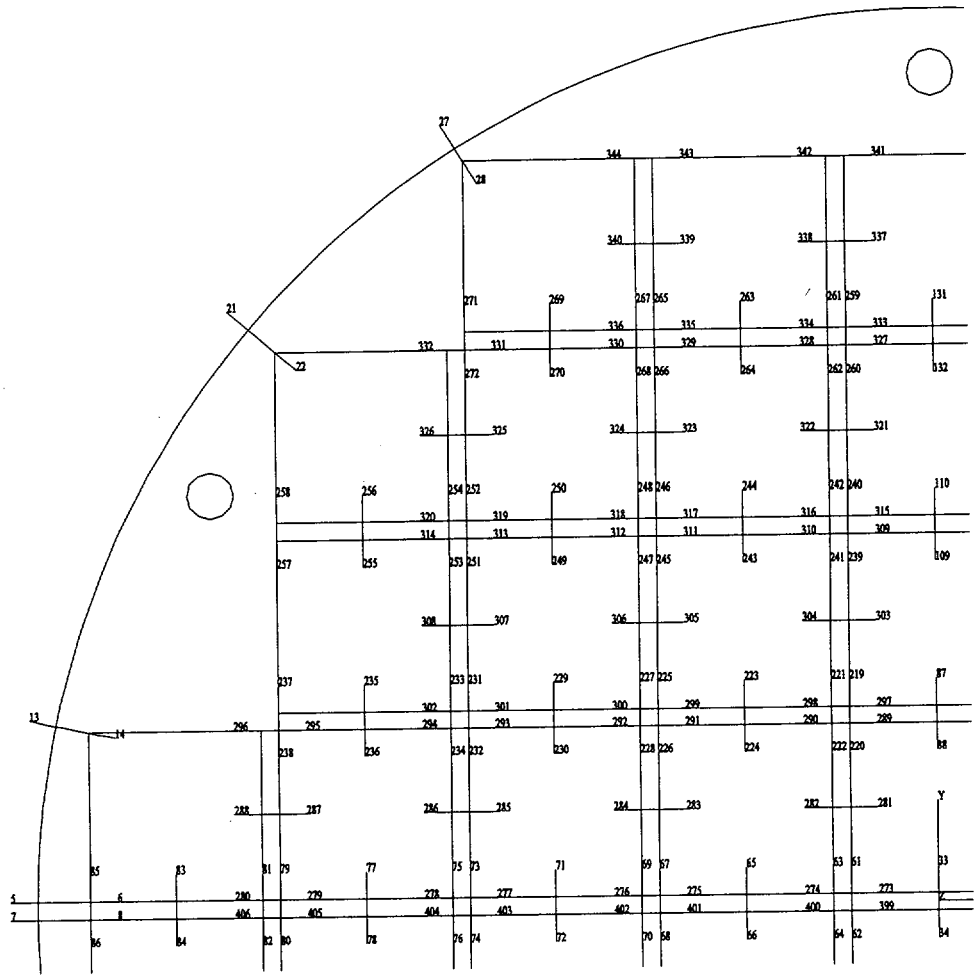

Figure 3.4.4.1-15 BWR Fuel Basket Support Disk Sections for Stress Evaluation (Quadrant III)

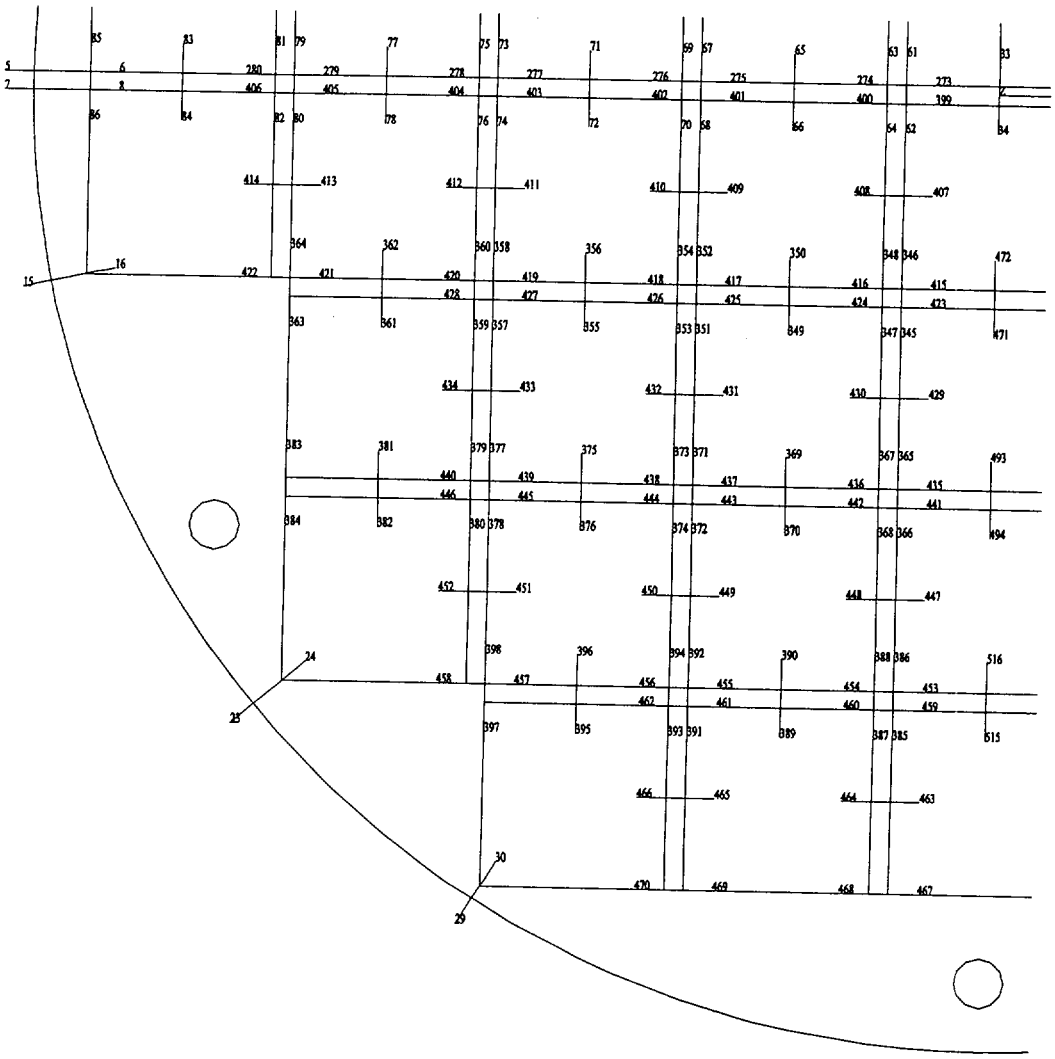

Figure 3.4.4.1-16 BWR Fuel Basket Support Disk Sections for Stress Evaluation (Quadrant IV)

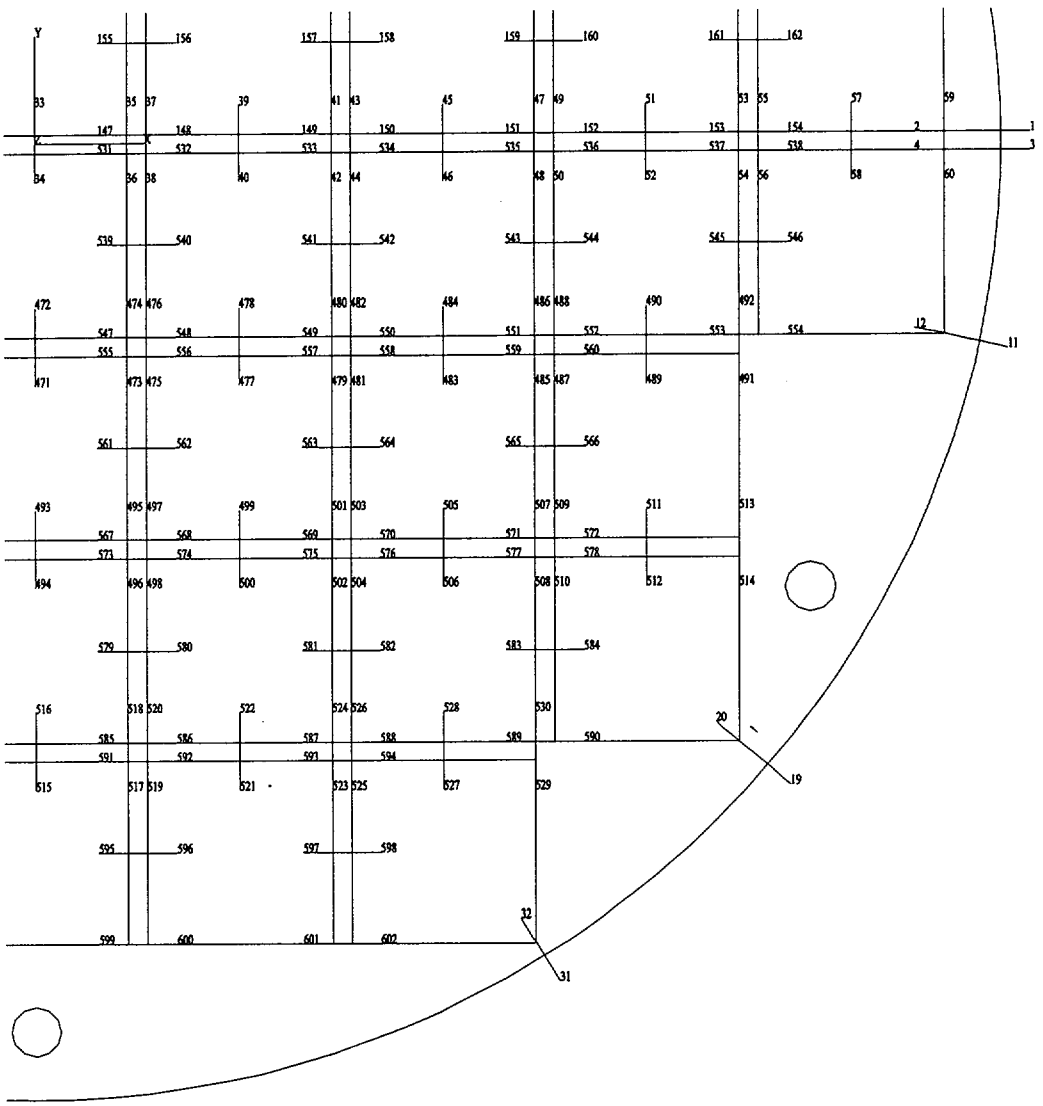

Figure 3.4.4.1-17 BWR Class 5 Fuel Tube Configuration

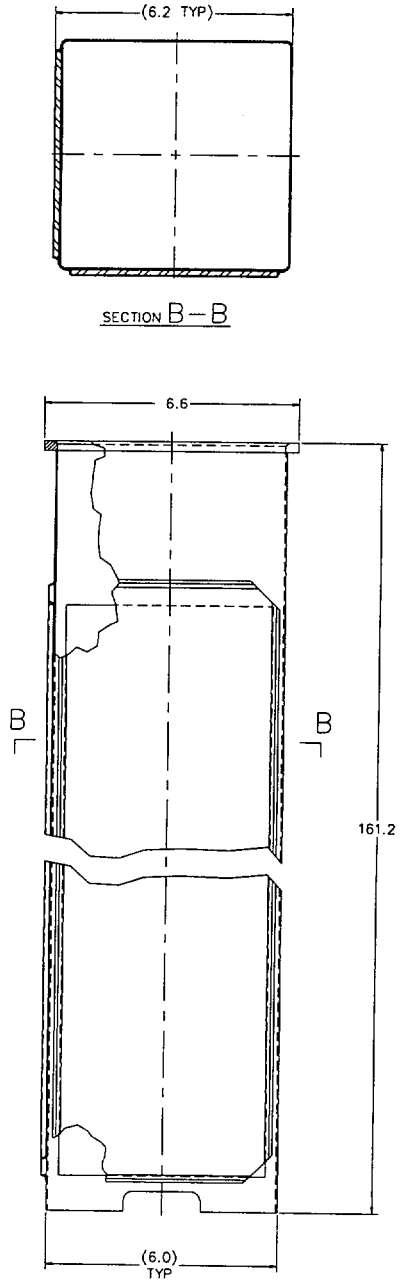

Figure 3.4.4.1-18 BWR Top Weldment Plate Finite Element Model

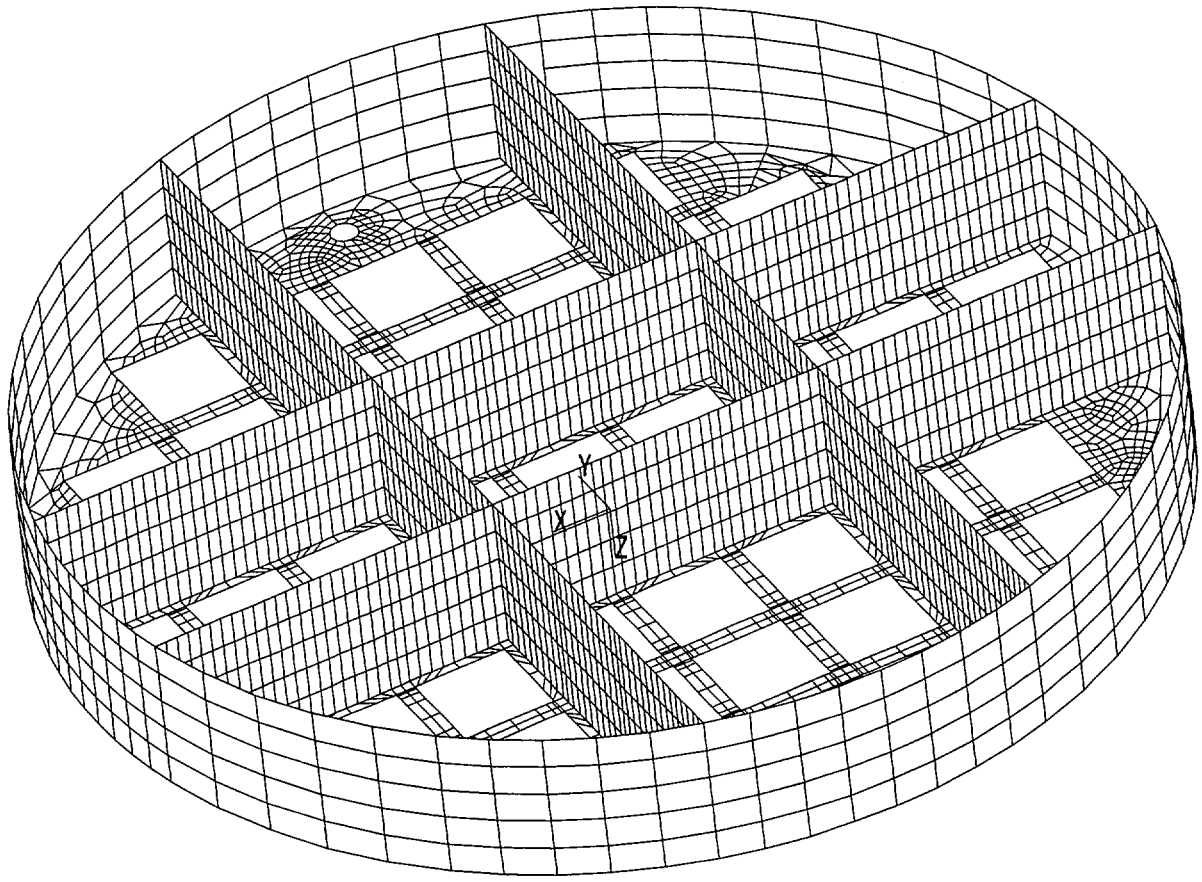

Figure 3.4.4.1-19 BWR Bottom Weldment Plate Finite Element Model

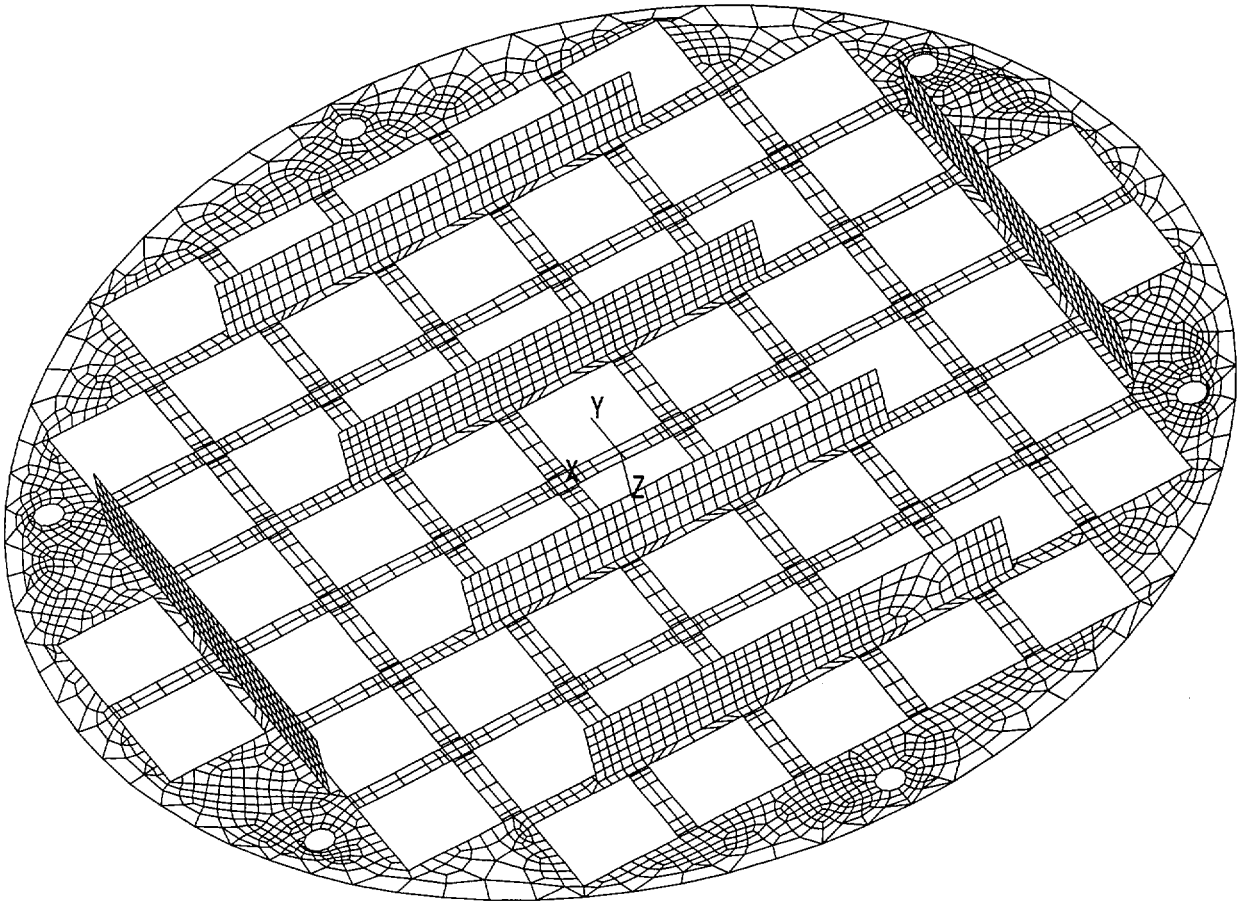

(Figure Inverted to Show Weldment Stiffeners)

Table 3.4.4.1-1 Canister Secondary (Thermal) Stresses (ksi)

Section No.[1]	SX	SY	SZ	SXY	SYZ	SXZ	Stress Intensity
1	0.6	1.3	0.1	0	0	0	1.21
2	0.2	-2.3	-1.3	-0.1	0	-0.1	2.47
3	-0.3	2.7	-0.1	0.2	0	0	3.05
4	0	0	0	0	0	0	0.02
5	0	0.1	0	0	0	0	0.14
6	0	0.1	0	0	0	0	0.16
7	0	0	0	0	0	0	0.02
8	0	0.1	-0.1	0	0	0	0.25
9	2.3	1.2	0.9	0.7	-0.1	0	1.87
10	-1.4	2.4	0.2	0.6	-0.1	0.1	3.95
11	1.3	-5.7	-1.3	0.4	-0.1	-0.2	7.02
12	-4.2	-0.8	-1.7	-0.5	0	0.1	3.52
13	-2.2	0.9	-0.3	0.4	0	0.2	3.21
14	11.4	7.3	11.2	-0.1	0.8	-0.1	4.35
15	-0.4	0.1	-0.5	0	0	0	0.50
16	-1.2	-0.9	-1.2	0	0.1	0	0.33

1. See Figure 3.4.4.1-4 for definition of locations of stress sections.

Table 3.4.4.1-2 Canister Dead Weight Primary Membrane (P_m) Stresses (ksi), $P_{internal}$ = 0 psig

Section No.[1]	SX	SY	SZ	SXY	SYZ	SXZ	Stress Intensity
1	0	-0.1	0	0	0	0	0.05
2	0	-0.1	0	0	0	0	0.12
3	0	-0.1	0	0	0	0	0.12
4	0	-0.1	0	0	0	0	0.12
5	0	-0.1	0	0	0	0	0.11
6	0	-0.1	0	0	0	0	0.10
7	0	-0.1	0	0	0	0	0.09
8	0	-0.1	0	0	0	0	0.06
9	0	0	0	0	0	0	0.03
10	0	0	0	0	0	0	0.05
11	0	0	0	0	0	0	0.04
12	0	0	0	0	0	0	0.04
13	0	0	0	0	0	0	0.04
14	0	0	0	0	0	0	0.02
15	0	0	0	0	0	0	0.00
16	0	0	0	0	0	0	0.00

1. See Figure 3.4.4.1-4 for definition of locations of stress sections.

Table 3.4.4.1-3 Canister Dead Weight Primary Membrane plus Bending ($P_m + P_b$) Stresses (ksi), $P_{internal} = 0$ psig

Section No.[1]	SX	SY	SZ	SXY	SYZ	SXZ	Stress Intensity
1	0	-0.1	0	0	0	0	0.07
2	0	-0.1	0	0	0	0	0.15
3	0	-0.1	0	0	0	0	0.13
4	0	-0.1	0	0	0	0	0.12
5	0	-0.1	0	0	0	0	0.11
6	0	-0.1	0	0	0	0	0.10
7	0	-0.1	0	0	0	0	0.09
8	0	-0.1	0	0	0	0	0.07
9	0	-0.1	0	0	0	0	0.08
10	0	-0.1	0	0	0	0	0.12
11	0	0.1	0	0	0	0	0.11
12	0	0.1	0	0	0	0	0.06
13	0	0	0	0	0	0	0.06
14	0	0	0	0	0	0	0.02
15	0.1	0	0.1	0	0	0	0.07
16	0	0	0	0	0	0	0.03

1. See Figure 3.4.4.1-4 for definition of locations of stress sections.

Table 3.4.4.1-4 Canister Normal Handling With No Internal Pressure Primary Membrane (P_m) Stresses, (ksi)

Section No.[1]	SX	SY	SZ	SXY	SYZ	SXZ	Stress Intensity
1	0.1	1.8	0.7	-0.3	0	0	1.76
2	1.2	-1.2	-1.7	-0.3	0	-0.2	2.92
3	-0.2	0.5	-2.6	0.5	0	-0.2	3.42
4	0	0.5	0	0	0	0	0.51
5	0	0.6	0	0	0	0	0.56
6	0	0.6	0	0	0	0	0.63
7	0	0.7	0	0	0	0	0.75
8	0	1.1	0	0	0.1	0	1.17
9	0.1	1.5	0.4	0.1	0.1	0	1.51
10	-0.3	1.9	0.4	0.1	0.2	0.1	2.26
11	-0.6	1.1	0.7	-0.5	0.1	0.1	2.06
12	-0.1	2	0.5	0.2	0.1	0.1	2.18
13	0.3	-0.3	1	-0.6	0.1	0.2	1.66
14	0.2	0	0.2	0.2	-0.2	0	0.64
15	0	0	0	0	0	0	0.01
16	0	0	0	0	0	0	0.06

1. See Figure 3.4.4.1-4 for definition of locations of stress sections.

Table 3.4.4.1-5 Canister Normal Handling With No Internal Pressure Primary Membrane plus Bending ($P_m + P_b$) Stresses (ksi)

Section No.[1]	SX	SY	SZ	SXY	SYZ	SXZ	Stress Intensity
1	1.3	4.4	-0.1	0	0	-0.1	4.41
2	0.6	-8.4	-4.0	-0.6	0	-0.4	9.03
3	-0.8	11.9	0.5	0.6	0	0.1	12.80
4	0	0.5	0	0	0	0	0.55
5	0	0.5	-0.1	0	0	0	0.65
6	0	0.6	-0.2	0	0	0	0.75
7	0	0.7	-0.2	0	0	0	0.88
8	0	1.1	-0.1	0	0.1	0	1.25
9	-0.1	1.7	0.3	0	0.2	0	1.75
10	0.4	2.9	-0.1	-0.1	-0.2	-0.5	3.36
11	-0.9	1.1	0.6	-1.0	0.2	0.1	2.86
12	0.3	2.7	-0.2	-0.1	-0.2	-0.5	3.16
13	1.3	-0.7	1.5	-0.3	0	0.3	2.36
14	6.3	0	6.3	0.2	-0.2	0	6.30
15	0.1	-0.1	0.1	0	0	0	0.15
16	0.2	-0.1	0.2	0	0	0	0.32

1. See Figure 3.4.4.1-4 for definition of locations of stress sections.

Table 3.4.4.1-6 Summary of Canister Normal Handling plus Normal Internal Pressure Primary Membrane (P_m) Stresses (ksi)

Section No.[1]	SX	SY	SZ	SXY	SYZ	SXZ	Stress Intensity	Stress Allowable[2]	Margin of Safety
1	0.2	3.3	1.3	-0.5	0	0.1	3.19	16.7	4.24
2	2.1	-2.1	-2.9	-0.5	0	-0.4	5.15	16.7	2.24
3	-0.4	1	-4.5	0.9	-0.1	-0.4	5.93	16.7	1.82
4	0	0.9	0.8	0	0	0.1	0.91	16.57	17.18
5	0	0.9	0.8	0	0	0.1	0.94	15.41	15.33
6	0	1	0.8	0	0	0.1	1.01	15.22	14.07
7	0	1.1	0.8	0	0	0.1	1.13	16.06	13.28
8	0	1.5	0.4	0	0.1	0	1.51	16.7	10.07
9	0	1.8	0.5	0.1	0.1	0	1.78	16.7	8.39
10	-0.3	2.1	0.5	0	0.2	0.1	2.48	16.7	5.72
11	-0.4	1	0.9	-0.5	0.1	0.1	1.71	16.7	8.78
12	-0.2	2.1	0.6	0.1	0.1	0.1	2.25	16.7	6.41
13	0.2	0.1	1.3	-0.6	0	0.2	1.78	16.7	8.39
14	0.4	0	0.4	0.4	-0.3	0	1.14	16.7	13.64
15	0	0	0	0	0	0	0.02	16.7	929.36
16	0	0	0	0	0	0	0.07	16.7	242.51

1. See Figure 3.4.4.1-4 for definition of locations of stress sections.
2. ASME Code Service Level A is used for material allowable stresses.

Table 3.4.4.1-7 Summary of Canister Normal Handling, Plus Normal Pressure Primary Membrane plus Bending ($P_m + P_b$) Stresses (ksi)

Section No.[1]	SX	SY	SZ	SXY	SYZ	SXZ	Stress Intensity	Stress Allowable[2]	Margin of Safety
1	2.4	7.9	0.1	0	0	-0.1	7.82	25.05	2.20
2	1.0	-15.2	-7.1	-1.1	0.1	-0.7	16.39	25.05	0.53
3	-1.6	21.4	1.2	1.1	-0.1	0.2	23.08	25.05	0.09
4	0	1.0	0.9	0	0	0.1	0.96	24.85	24.92
5	0	1.0	0.9	0	0	0.1	0.98	23.11	22.57
6	0	1.1	1.0	0	0	0.1	1.07	22.83	20.39
7	0	1.2	1.0	0	0	0.1	1.20	24.09	19.15
8	0	1.5	0.3	0	0.1	0	1.51	25.05	15.57
9	-0.1	2.1	0.5	0	0.2	0	2.18	25.05	10.50
10	-0.5	3.0	0.7	0.1	0.1	0.1	3.47	25.05	6.22
11	-0.6	2.0	1.2	-1.0	0.2	0.1	3.22	25.05	6.77
12	-0.5	2.7	0.6	0.1	0.1	0.1	3.23	25.05	6.74
13	0.9	-0.5	1.8	-0.2	-0.1	0.3	2.46	25.05	9.20
14	11.1	0.1	11.2	0.4	-0.4	0	11.16	25.05	1.24
15	-0.3	0	-0.3	0	0	0	0.30	25.05	82.67
16	0.8	0	0.8	0	0	0	0.83	25.05	29.09

1. See Figure 3.4.4.1-4 for definition of locations of stress sections.
2. ASME Code Service Level A is used for material allowable stresses.

Table 3.4.4.1-8 Summary of Maximum Canister Normal Handling, plus Normal Pressure, plus Secondary (P + Q) Stresses (ksi)

Section No.[1]	SX	SY	SZ	SXY	SYZ	SXZ	Stress Intensity	Stress Allowable[2]	Margin of Safety
1	3.9	11.3	1.1	0.2	0	-0.1	10.23	50.10	3.90
2	1.3	-18.4	-8.6	-1.2	0.1	-0.8	19.84	50.10	1.53
3	-1.8	24.8	1.3	1.3	-0.1	0.2	26.74	50.10	0.87
4	0	1.0	0.9	0	0	0.1	0.97	49.70	50.14
5	0	1.0	0.9	0	0	-0.1	1.04	46.23	43.58
6	0	1.1	0.6	0	0	0.1	1.07	45.65	41.59
7	0	1.2	1.0	0	0	0.1	1.21	48.19	38.99
8	0	1.6	0.4	0	0.1	0	1.64	50.10	29.64
9	0.9	2.5	0.7	0.9	0.1	0	2.48	50.10	19.19
10	-4.7	1.9	-1.1	-0.4	0.1	0.3	6.65	50.10	6.53
11	1.7	-7.4	-1.6	-0.5	-0.1	0.2	9.10	50.10	4.50
12	-4.7	1.9	-1.1	-0.4	0.1	0.3	6.65	50.10	6.53
13	-2.8	1.2	-0.2	-0.5	-0.1	-0.2	4.13	50.10	11.14
14	22.3	7.4	22.2	0.3	0.5	-0.1	14.98	50.10	2.34
15	-2.8	-2.3	-2.8	0	-0.2	0	0.64	50.10	76.90
16	-0.5	-0.9	-0.5	0	0.1	0	0.50	50.10	99.40

1. See Figure 3.4.4.1-4 for definition of locations of stress sections.
2. ASME Code Service Level A is used for material allowable stresses.

Table 3.4.4.1-9 Canister Normal Internal Pressure Primary Membrane (P_m) Stresses (ksi)

Section No.[1]	SX	SY	SZ	SXY	SYZ	SXZ	Stress Intensity
1	0.1	1.5	0.6	-0.2	0	0	1.43
2	1	-0.9	-1.2	-0.2	0	-0.2	2.24
3	-0.2	0.4	-1.9	0.4	0	-0.2	2.51
4	0	0.4	0.8	0	0	0.1	0.80
5	0	0.4	0.8	0	0	0.1	0.80
6	0	0.4	0.8	0	0	0.1	0.80
7	0	0.4	0.8	0	0	0.1	0.80
8	0	0.4	0.4	0	0	0	0.41
9	0	0.3	0.2	0	0	0	0.26
10	-0.1	0.2	0.1	0	0	0	0.34
11	0.1	0	0.1	0	0	0	0.21
12	0	-0.2	-0.1	0	0.1	0	0.25
13	0	0.2	0.1	0	0	0	0.22
14	0.2	0	0.2	0.2	-0.1	0	0.50
15	0	0	0	0	0	0	0.01
16	0	0	0	0	0	0	0.03

1. See Figure 3.4.4.1-4 for definition of locations of stress sections.

Table 3.4.4.1-10 Canister Normal Internal Pressure Primary Membrane plus Bending ($P_m + P_b$) Stresses (ksi)

Section No.[1]	SX	SY	SZ	SXY	SYZ	SXZ	Stress Intensity
1	1.1	3.5	0.1	0	0	-0.1	3.41
2	0.5	-6.8	-3.1	-0.5	0	-0.3	7.35
3	-0.7	9.5	0.7	0.5	0	0.1	10.27
4	0	0.4	0.8	0	0	0.1	0.81
5	0	0.4	0.8	0	0	0.1	0.81
6	0	0.4	0.8	0	0	0.1	0.81
7	0	0.4	0.8	0	0	0.1	0.81
8	0	0.4	0.4	0	0	0	0.44
9	0	0.6	0.3	0.1	0	0	0.58
10	-0.1	0.7	0.3	0	0	0	0.85
11	0	-0.5	0.1	0	0	0	0.60
12	-0.1	-0.4	-0.2	0	0.1	0	0.36
13	-0.2	0.1	0	0	0	0	0.30
14	4.8	0	4.9	0.2	-0.2	0	4.85
15	-0.4	0	-0.4	0	0	0	0.34
16	0.2	0	0.2	0	0	0	0.17

1. See Figure 3.4.4.1-4 for definition of locations of stress sections.

Table 3.4.4.1-11 Listing of Sections for Stress Evaluation of PWR Support Disk

Section Number[1]	Point 1	Point 2	Point 1		Point 2	
			X	Y	X	Y
1	1	2	0.75	0.75	0.75	-0.75
2	3	4	0.75	0.75	-0.75	0.75
3	5	6	-0.75	0.75	-0.75	-0.75
4	7	8	-0.75	-0.75	0.75	-0.75
5	9	10	0.75	5.39	-0.75	5.39
6	11	12	0.75	10.02	-0.75	10.02
7	13	14	0.75	10.02	0.75	11.02
8	15	16	0.75	11.02	-0.75	11.02
9	17	18	-0.75	10.02	-0.75	11.02
10	19	20	0.75	15.66	-0.75	15.66
11	21	22	0.75	20.29	-0.75	20.29
12	23	24	0.75	20.29	0.75	21.17
13	25	26	0.75	21.17	-0.75	21.17
14	27	28	-0.75	20.29	-0.75	21.17
15	29	30	0.75	25.81	-0.75	25.81
16	31	32	0.75	30.44	-0.75	30.44
17	33	34	0.75	30.44	0.75	32.74
18	35	36	-0.75	30.44	-0.75	32.74
19	37	38	0.75	-5.39	-0.75	-5.39
20	39	40	0.75	-10.02	-0.75	-10.02
21	41	42	0.75	-10.02	0.75	-11.02
22	43	44	0.75	-11.02	-0.75	-11.02
23	45	46	-0.75	-10.02	-0.75	-11.02
24	47	48	0.75	-15.66	-0.75	-15.66
25	49	50	0.75	-20.29	-0.75	-20.29
26	51	52	0.75	-20.29	0.75	-21.17
27	53	54	0.75	-21.17	-0.75	-21.17
28	55	56	-0.75	-20.29	-0.75	-21.17
29	57	58	0.75	-25.81	-0.75	-25.81
30	59	60	0.75	-30.44	-0.75	-30.44
31	61	62	0.75	-30.44	0.75	-32.74
32	63	64	-0.75	-30.44	-0.75	-32.74
33	65	66	5.39	0.75	5.39	-0.75
34	67	68	10.02	0.75	10.02	-0.75
35	69	70	10.02	0.75	11.02	0.75
36	71	72	11.02	0.75	11.02	-0.75
37	73	74	10.02	-0.75	11.02	-0.75
38	75	76	15.66	0.75	15.66	-0.75
39	77	78	20.29	0.75	20.29	-0.75
40	79	80	20.29	0.75	21.17	0.75
41	81	82	21.17	0.75	21.17	-0.75
42	83	84	20.29	-0.75	21.17	-0.75
43	85	86	25.81	0.75	25.81	-0.75
44	87	88	30.44	0.75	30.44	-0.75
45	89	90	30.44	0.75	32.74	0.75

1. Section locations are shown in Figures 3.4.4.1-7 and 3.4.4.1-8.

Table 3.4.4.1-11 Listing of Sections for Stress Evaluation of PWR Support Disk (Continued)

Section Number[1]	Point 1	Point 2	Point 1		Point 2	
			X	Y	X	Y
46	91	92	30.44	-0.75	32.74	-0.75
47	93	94	-5.39	0.75	-5.39	-0.75
48	95	96	-10.02	0.75	-10.02	-0.75
49	97	98	-10.02	0.75	-11.02	0.75
50	99	100	-11.02	0.75	-11.02	-0.75
51	101	102	-10.02	-0.75	-11.02	-0.75
52	103	104	-15.66	0.75	-15.66	-0.75
53	105	106	-20.29	0.75	-20.29	-0.75
54	107	108	-20.29	0.75	-21.17	0.75
55	109	110	-21.17	0.75	-21.17	-0.75
56	111	112	-20.29	-0.75	-21.17	-0.75
57	113	114	-25.81	0.75	-25.81	-0.75
58	115	116	-30.44	0.75	-30.44	-0.75
59	117	118	-30.44	0.75	-32.74	0.75
60	119	120	-30.44	-0.75	-32.74	-0.75
61	121	122	5.39	11.02	5.39	10.02
62	123	124	5.39	20.29	5.39	21.17
63	125	126	10.02	11.02	10.02	10.02
64	127	128	10.02	10.02	11.02	10.02
65	129	130	10.02	11.52	11.52	11.52
66	131	132	10.02	20.29	10.02	21.17
67	133	134	10.02	20.29	11.52	20.29
68	135	136	10.02	5.39	11.02	5.39
69	137	138	11.52	10.02	11.52	11.52
70	139	140	16.16	10.02	16.16	11.52
71	141	142	20.29	5.39	21.17	5.39
72	143	144	20.29	10.02	21.17	10.02
73	145	146	10.02	16.16	11.52	16.16
74	147	148	20.29	10.02	20.29	11.52
75	149	150	10.24	31.11	10.02	30.44
76	151	152	31.11	10.24	30.44	10.02
77	153	154	-5.39	11.02	-5.39	10.02
78	155	156	-5.39	20.29	-5.39	21.17
79	157	158	-10.02	11.02	-10.02	10.02
80	159	160	-10.02	10.02	-11.02	10.02
81	161	162	-10.02	11.52	-11.52	11.52
82	163	164	-10.02	20.29	-10.02	21.17
83	165	166	-10.02	20.29	-11.52	20.29
84	167	168	-10.02	5.39	-11.02	5.39
85	169	170	-11.52	10.02	-11.52	11.52
86	171	172	-16.16	10.02	-16.16	11.52
87	173	174	-20.29	5.39	-21.17	5.39
88	175	176	-20.29	10.02	-21.17	10.02
89	177	178	-10.02	16.16	-11.52	16.16
90	179	180	-20.29	10.02	-20.29	11.52

1. Section locations are shown in Figures 3.4.4.1-7 and 3.4.4.1-8.

Table 3.4.4.1-11 Listing of Sections for Stress Evaluation of PWR Support Disk (Continued)

Section Number[1]	Point 1	Point 2	Point 1		Point 2	
			X	Y	X	Y
91	181	182	-10.24	31.11	-10.02	30.44
92	183	184	-31.11	10.24	-30.44	10.02
93	185	186	-5.39	-11.02	-5.39	-10.02
94	187	188	-5.39	-20.29	-5.39	-21.17
95	189	190	-10.02	-11.02	-10.02	-10.02
96	191	192	-10.02	-10.02	-11.02	-10.02
97	193	194	-10.02	-11.52	-11.52	-11.52
98	195	196	-10.02	-20.29	-10.02	-21.17
99	197	198	-10.02	-20.29	-11.52	-20.29
100	199	200	-10.02	-5.39	-11.02	-5.39
101	201	202	-11.52	-10.02	-11.52	-11.52
102	203	204	-16.16	-10.02	-16.16	-11.52
103	205	206	-20.29	-5.39	-21.17	-5.39
104	207	208	-20.29	-10.02	-21.17	-10.02
105	209	210	-10.02	-16.16	-11.52	-16.16
106	211	212	-20.29	-10.02	-20.29	-11.52
107	213	214	-10.24	-31.11	-10.02	-30.44
108	215	216	-31.11	-10.24	-30.44	-10.02
109	217	218	5.39	-11.02	5.39	-10.02
110	219	220	5.39	-20.29	5.39	-21.17
111	221	222	10.02	-11.02	10.02	-10.02
112	223	224	10.02	-10.02	11.02	-10.02
113	225	226	10.02	-11.52	11.52	-11.52
114	227	228	10.02	-20.29	10.02	-21.17
115	229	230	10.02	-20.29	11.52	-20.29
116	231	232	10.02	-5.39	11.02	-5.39
117	233	234	11.52	-10.02	11.52	-11.52
118	235	236	16.16	-10.02	16.16	-11.52
119	237	238	20.29	-5.39	21.17	-5.39
120	239	240	20.29	-10.02	21.17	-10.02
121	241	242	10.02	-16.16	11.52	-16.16
122	243	244	20.29	-10.02	20.29	-11.52
123	245	246	10.24	-31.11	10.02	-30.44
124	247	248	31.11	-10.24	30.44	-10.02

1. Section locations are shown in Figures 3.4.4.1-7 and 3.4.4.1-8.

Table 3.4.4.1-12 $P_m + P_b$ Stresses for PWR Support Disk - Normal Conditions (ksi)

Section[1]	Sx	Sy	Sxy	Stress Intensity	Allow. Stress	Margin of Safety
66	0.7	0.3	0.3	0.8	65.4	76
120	0.3	0.7	-0.3	0.8	65.4	77
82	0.7	0.3	-0.3	0.8	65.4	77
72	0.3	0.7	0.3	0.8	65.4	77
42	0.2	-0.4	0	0.6	65	106
40	0.2	-0.4	0	0.6	65	106
12	-0.4	0.2	0	0.6	65	106
56	0.2	-0.4	0	0.6	65	106
28	-0.4	0.2	0	0.6	65	106
54	0.2	-0.4	0	0.6	65	106
14	-0.4	0.2	0	0.6	65	106
26	-0.4	0.2	0	0.6	65	107
122	0.4	0.1	-0.2	0.5	65.4	120
90	0.4	0.1	-0.2	0.5	65.4	120
106	0.4	0.1	0.2	0.5	65.4	121
74	0.4	0.1	0.2	0.5	65.4	121
99	0.1	0.4	0.2	0.5	65.4	122
115	0.1	0.4	-0.2	0.5	65.4	124
83	0.1	0.4	-0.2	0.5	65.4	124
67	0.1	0.4	0.2	0.5	65.4	124
114	0.2	0.2	-0.3	0.5	65.4	124
88	0.2	0.2	-0.3	0.5	65.4	125
104	0.2	0.2	0.2	0.5	65.4	132
98	0.2	0.2	0.2	0.5	65.4	133
3	-0.4	-0.2	-0.1	0.4	62.1	138
4	-0.2	-0.4	-0.1	0.4	62.1	138
1	-0.4	-0.2	-0.1	0.4	62.1	138
2	-0.2	-0.4	-0.1	0.4	62.1	138
51	-0.1	-0.4	-0.1	0.4	64	148
9	-0.4	-0.1	0.1	0.4	64	148
23	-0.4	-0.1	-0.1	0.4	64	148
49	-0.1	-0.4	0.1	0.4	64	148
7	-0.4	-0.1	-0.1	0.4	64	148
21	-0.4	-0.1	0.1	0.4	64	148
35	-0.1	-0.4	-0.1	0.4	64	148
37	-0.1	-0.4	0.1	0.4	64	148
39	0.2	-0.2	0.1	0.4	65	151
11	-0.2	0.2	-0.1	0.4	65	151
25	-0.2	0.2	-0.1	0.4	65	151
53	0.2	-0.2	-0.1	0.4	65	151

1. Section locations are shown in Figures 3.4.4.1-7 and 3.4.4.1-8.

Table 3.4.4.1-13 $P_m + P_b + Q$ Stresses for the PWR Support Disk - Normal Conditions (ksi)

Section[1]	Sx	Sy	Sxy	Stress Intensity	Allow. Stress	Margin of Safety
92	1.6	14.5	4	15.6	131.4	7.4
91	14.6	1.1	3.4	15.4	131.4	7.6
9	-14.5	-4.9	1.7	14.8	128	7.7
51	-4.8	-14.5	-1.6	14.8	128	7.7
60	-0.1	15	-0.8	15.1	131.3	7.7
49	-4.9	-14.4	1.7	14.7	128	7.7
18	15	0	0.9	15.1	131.3	7.7
59	-0.2	14.6	1	14.9	131.3	7.8
32	14.4	-0.3	-0.9	14.8	131.3	7.9
23	-14.2	-4.9	-1.7	14.5	128	7.9
31	14.5	-0.2	0.8	14.8	131.3	7.9
21	-14.1	-4.6	1.6	14.3	128	7.9
17	14.5	-0.1	-0.9	14.6	131.3	8.0
35	-4.7	-14	-1.6	14.3	128	8.0
45	-0.4	14.1	-0.8	14.6	131.3	8.0
37	-4.8	-13.9	1.7	14.2	128	8.0
7	-13.9	-4.6	-1.6	14.2	128	8.0
108	1.9	13.7	-3.3	14.6	131.4	8.0
75	13.4	1.8	-3.3	14.3	131.4	8.2
46	-0.6	12.5	2.7	14.2	131.3	8.2
96	-5.3	-13.6	-1.5	13.8	129.5	8.4
76	1.8	13.2	-3.2	14	131.4	8.4
79	-13.4	-5.8	1.5	13.7	129.5	8.5
80	-5.8	-13.3	1.5	13.5	129.5	8.6
111	-13.1	-5.9	1.5	13.5	129.5	8.6
107	12.6	2	-3.4	13.6	131.4	8.7
64	-5.2	-13.1	-1.5	13.4	129.5	8.7
95	-13	-5.1	-1.4	13.3	129.5	8.8
63	-13	-5.1	-1.5	13.3	129.5	8.8
112	-5.5	-12.8	1.4	13	129.5	8.9
124	2.6	11	3.7	12.4	131.4	9.6
123	11.3	1	3.1	12.1	131.4	9.9
30	-7.6	-8.2	3.2	11.1	131.3	10.8
44	-7.9	-7.4	3.2	10.9	131.3	11.1
6	-8	-6.9	2.9	10.5	128	11.3
48	-6.9	-8	3	10.4	128	11.3
20	-7.8	-7	-2.9	10.3	128	11.4
16	-6.7	-8.1	2.9	10.5	131.3	11.6
34	-6.8	-7.7	2.9	10.2	128	11.6
58	-8.1	-6.7	-2.8	10.4	131.3	11.7

1. Section locations are shown in Figures 3.4.4.1-7 and 3.4.4.1-8.

Table 3.4.4.1-14 Listing of Sections for Stress Evaluation of BWR Support Disk

Section Number[1]	Point 1	Point 2	Point 1		Point 2	
			X	Y	X	Y
1	1	2	32.74	0.33	30.85	0.33
2	3	4	32.74	-0.33	30.85	-0.33
3	5	6	-32.74	0.33	-30.85	0.33
4	7	8	-32.74	-0.33	-30.85	-0.33
5	9	10	32.03	6.85	30.85	6.6
6	11	12	32.03	-6.85	30.85	-6.6
7	13	14	-32.03	6.85	-30.85	6.6
8	15	16	-32.03	-6.85	-30.85	-6.6
9	17	18	24.87	21.30	23.89	20.46
10	19	20	24.87	-21.30	23.89	-20.46
11	21	22	-24.87	21.30	-23.89	20.46
12	23	24	-24.87	-21.30	-23.89	-20.46
13	25	26	17.27	27.83	17.00	27.39
14	27	28	-17.27	27.83	-17.00	27.39
15	29	30	-17.27	-27.83	-17.00	-27.39
16	31	32	17.27	-27.83	17.00	-27.39
17	33	34	0	0.33	0	-0.33
18	35	36	3.14	0.33	3.14	-0.33
19	37	38	3.79	0.33	3.79	-0.33
20	39	40	6.93	0.33	6.93	-0.33
21	41	42	10.07	0.33	10.07	-0.33
22	43	44	10.72	0.33	10.72	-0.33
23	45	46	13.86	0.33	13.86	-0.33
24	47	48	17	0.33	17	-0.33
25	49	50	17.65	0.33	17.65	-0.33
26	51	52	20.78	0.33	20.78	-0.33
27	53	54	23.92	0.33	23.92	-0.33
28	55	56	24.57	0.33	24.57	-0.33
29	57	58	27.71	0.33	27.71	-0.33
30	59	60	30.85	0.33	30.85	-0.33
31	61	62	-3.14	0.33	-3.14	-0.33
32	63	64	-3.79	0.33	-3.79	-0.33
33	65	66	-6.93	0.33	-6.93	-0.33
34	67	68	-10.07	0.33	-10.07	-0.33
35	69	70	-10.72	0.33	-10.72	-0.33
36	71	72	-13.86	0.33	-13.86	-0.33
37	73	74	-17	0.33	-17	-0.33
38	75	76	-17.65	0.33	-17.65	-0.33
39	77	78	-20.78	0.33	-20.78	-0.33
40	79	80	-23.92	0.33	-23.92	-0.33
41	81	82	-24.57	0.33	-24.57	-0.33
42	83	84	-27.71	0.33	-27.71	-0.33
43	85	86	-30.85	0.33	-30.85	-0.33
44	87	88	0	7.25	0	6.6
45	89	90	3.14	7.25	3.14	6.6
46	91	92	3.79	7.25	3.79	6.6
47	93	94	6.93	7.25	6.93	6.6
48	95	96	10.07	7.25	10.07	6.6
49	97	98	10.72	7.25	10.72	6.6
50	99	100	13.86	7.25	13.86	6.6

1. Section locations are shown in Figures 3.4.4.1-13 and 3.4.4.1-16.

Table 3.4.4.1-14 Listing of Sections for Stress Evaluation of BWR Support Disk (Continued)

Section Number[1]	Point 1	Point 2	Point 1		Point 2	
			X	Y	X	Y
51	101	102	17	7.25	17	6.6
52	103	104	17.65	7.25	17.65	6.6
53	105	106	20.78	7.25	20.78	6.6
54	107	108	23.92	7.25	23.92	6.6
55	109	110	0	13.53	0	14.18
56	111	112	3.14	13.53	3.14	14.18
57	113	114	3.79	13.53	3.79	14.18
58	115	116	6.93	13.53	6.93	14.18
59	117	118	10.07	13.53	10.07	14.18
60	119	120	10.72	13.53	10.72	14.18
61	121	122	13.86	13.53	13.86	14.18
62	123	124	17	13.53	17	14.18
63	125	126	17.65	13.53	17.65	14.18
64	127	128	20.78	13.53	20.78	14.18
65	129	130	23.92	13.53	23.92	14.18
66	131	132	0	21.11	0	20.46
67	133	134	3.14	21.11	3.14	20.46
68	135	136	3.79	21.11	3.79	20.46
69	137	138	6.93	21.11	6.93	20.46
70	139	140	10.07	21.11	10.07	20.46
71	141	142	10.72	21.11	10.72	20.46
72	143	144	13.86	21.11	13.86	20.46
73	145	146	17	21.11	17	20.46
74	147	148	3.14	0.33	3.79	0.33
75	149	150	10.07	0.33	10.72	0.33
76	151	152	17	0.33	17.65	0.33
77	153	154	23.92	0.33	24.57	0.33
78	155	156	3.14	3.46	3.79	3.46
79	157	158	10.07	3.46	10.72	3.46
80	159	160	17	3.46	17.65	3.46
81	161	162	23.92	3.46	24.57	3.46
82	163	164	3.14	6.6	3.79	6.6
83	165	166	10.07	6.6	10.72	6.6
84	167	168	17	6.6	17.65	6.6
85	169	170	23.92	6.6	24.57	6.6
86	171	172	3.14	7.25	3.79	7.25
87	173	174	10.07	7.25	10.72	7.25
88	175	176	17	7.25	17.65	7.25
89	177	178	3.14	10.39	3.79	10.39
90	179	180	10.07	10.39	10.72	10.39
91	181	182	17	10.39	17.65	10.39
92	183	184	3.14	13.53	3.79	13.53
93	185	186	10.07	13.53	10.72	13.53
94	187	188	17	13.53	17.65	13.53
95	189	190	3.14	14.18	3.79	14.18
96	191	192	10.07	14.18	10.72	14.18
97	193	194	17	14.18	17.65	14.18
98	195	196	3.14	17.32	3.79	17.32
99	197	198	10.07	17.32	10.72	17.32
100	199	200	17	17.32	17.65	17.32

1. Section locations are shown in Figures 3.4.4.1-13 and 3.4.4.1-16.

Table 3.4.4.1-14 Listing of Sections for Stress Evaluation of BWR Support Disk (Continued)

Section Number[1]	Point 1	Point 2	Point 1		Point 2	
			X	Y	X	Y
101	201	202	3.14	20.46	3.79	20.46
102	203	204	10.07	20.46	10.72	20.46
103	205	206	17	20.46	17.65	20.46
104	207	208	3.14	21.11	3.79	21.11
105	209	210	10.07	21.11	10.72	21.11
106	211	212	3.14	24.25	3.79	24.25
107	213	214	10.07	24.25	10.72	24.25
108	215	216	3.14	27.39	3.79	27.39
109	217	218	10.07	27.39	10.72	27.39
110	219	220	-3.14	7.25	-3.14	6.6
111	221	222	-3.79	7.25	-3.79	6.6
112	223	224	-6.93	7.25	-6.93	6.6
113	225	226	-10.07	7.25	-10.07	6.6
114	227	228	-10.72	7.25	-10.72	6.6
115	229	230	-13.86	7.25	-13.86	6.6
116	231	232	-17	7.25	-17	6.6
117	233	234	-17.65	7.25	-17.65	6.6
118	235	236	-20.78	7.25	-20.78	6.6
119	237	238	-23.92	7.25	-23.92	6.6
120	239	240	-3.14	13.53	-3.14	14.18
121	241	242	-3.79	13.53	-3.79	14.18
122	243	244	-6.93	13.53	-6.93	14.18
123	245	246	-10.07	13.53	-10.07	14.18
124	247	248	-10.72	13.53	-10.72	14.18
125	249	250	-13.86	13.53	-13.86	14.18
126	251	252	-17	13.53	-17	14.18
127	253	254	-17.65	13.53	-17.65	14.18
128	255	256	-20.78	13.53	-20.78	14.18
129	257	258	-23.92	13.53	-23.92	14.18
130	259	260	-3.14	21.11	-3.14	20.46
131	261	262	-3.79	21.11	-3.79	20.46
132	263	264	-6.93	21.11	-6.93	20.46
133	265	266	-10.07	21.11	-10.07	20.46
134	267	268	-10.72	21.11	-10.72	20.46
135	269	270	-13.86	21.11	-13.86	20.46
136	271	272	-17	21.11	-17	20.46
137	273	274	-3.14	0.33	-3.79	0.33
138	275	276	-10.07	0.33	-10.72	0.33
139	277	278	-17	0.33	-17.65	0.33
140	279	280	-23.92	0.33	-24.57	0.33
141	281	282	-3.14	3.46	-3.79	3.46
142	283	284	-10.07	3.46	-10.72	3.46
143	285	286	-17	3.46	-17.65	3.46
144	287	288	-23.92	3.46	-24.57	3.46
145	289	290	-3.14	6.6	-3.79	6.6
146	291	292	-10.07	6.6	-10.72	6.6
147	293	294	-17	6.6	-17.65	6.6
148	295	296	-23.92	6.6	-24.57	6.6
149	297	298	-3.14	7.25	-3.79	7.25
150	299	300	-10.07	7.25	-10.72	7.25

1. Section locations are shown in Figures 3.4.4.1-13 and 3.4.4.1-16.

Table 3.4.4.1-14 Listing of Sections for Stress Evaluation of BWR Support Disk (Continued)

Section Number[1]	Point 1	Point 2	Point 1		Point 2	
			X	Y	X	Y
151	301	302	-17	7.25	-17.65	7.25
152	303	304	-3.14	10.39	-3.79	10.39
153	305	306	-10.07	10.39	-10.72	10.39
154	307	308	-17	10.39	-17.65	10.39
155	309	310	-3.14	13.53	-3.79	13.53
156	311	312	-10.07	13.53	-10.72	13.53
157	313	314	-17	13.53	-17.65	13.53
158	315	316	-3.14	14.18	-3.79	14.18
159	317	318	-10.07	14.18	-10.72	14.18
160	319	320	-17	14.18	-17.65	14.18
161	321	322	-3.14	17.32	-3.79	17.32
162	323	324	-10.07	17.32	-10.72	17.32
163	325	326	-17	17.32	-17.65	17.32
164	327	328	-3.14	20.46	-3.79	20.46
165	329	330	-10.07	20.46	-10.72	20.46
166	331	332	-17	20.46	-17.65	20.46
167	333	334	-3.14	21.11	-3.79	21.11
168	335	336	-10.07	21.11	-10.72	21.11
169	337	338	-3.14	24.25	-3.79	24.25
170	339	340	-10.07	24.25	-10.72	24.25
171	341	342	-3.14	27.39	-3.79	27.39
172	343	344	-10.07	27.39	-10.72	27.39
173	345	346	-3.14	-7.25	-3.14	-6.6
174	347	348	-3.79	-7.25	-3.79	-6.6
175	349	350	-6.93	-7.25	-6.93	-6.6
176	351	352	-10.07	-7.25	-10.07	-6.6
177	353	354	-10.72	-7.25	-10.72	-6.6
178	355	356	-13.86	-7.25	-13.86	-6.6
179	357	358	-17	-7.25	-17	-6.6
180	359	360	-17.65	-7.25	-17.65	-6.6
181	361	362	-20.78	-7.25	-20.78	-6.6
182	363	364	-23.92	-7.25	-23.92	-6.6
183	365	366	-3.14	-13.53	-3.14	-14.18
184	367	368	-3.79	-13.53	-3.79	-14.18
185	369	370	-6.93	-13.53	-6.93	-14.18
186	371	372	-10.07	-13.53	-10.07	-14.18
187	373	374	-10.72	-13.53	-10.72	-14.18
188	375	376	-13.86	-13.53	-13.86	-14.18
189	377	378	-17	-13.53	-17	-14.18
190	379	380	-17.65	-13.53	-17.65	-14.18
191	381	382	-20.78	-13.53	-20.78	-14.18
192	383	384	-23.92	-13.53	-23.92	-14.18
193	385	386	-3.14	-21.11	-3.14	-20.46
194	387	388	-3.79	-21.11	-3.79	-20.46
195	389	390	-6.93	-21.11	-6.93	-20.46
196	391	392	-10.07	-21.11	-10.07	-20.46
197	393	394	-10.72	-21.11	-10.72	-20.46
198	395	396	-13.86	-21.11	-13.86	-20.46
199	397	398	-17	-21.11	-17	-20.46
200	399	400	-3.14	-0.33	-3.79	-0.33

1. Section locations ar shown in Figures 3.4.4.1-13 and 3.4.4.1-16.

Table 3.4.4.1-14 Listing of Sections for Stress Evaluation of BWR Support Disk (Continued)

Section Number[1]	Point 1	Point 2	Point 1		Point 2	
			X	Y	X	Y
201	401	402	-10.07	-0.33	-10.72	-0.33
202	403	404	-17	-0.33	-17.65	-0.33
203	405	406	-23.92	-0.33	-24.57	-0.33
204	407	408	-3.14	-3.46	-3.79	-3.46
205	409	410	-10.07	-3.46	-10.72	-3.46
206	411	412	-17	-3.46	-17.65	-3.46
207	413	414	-23.92	-3.46	-24.57	-3.46
208	415	416	-3.14	-6.6	-3.79	-6.6
209	417	418	-10.07	-6.6	-10.72	-6.6
210	419	420	-17	-6.6	-17.65	-6.6
211	421	422	-23.92	-6.6	-24.57	-6.6
212	423	424	-3.14	-7.25	-3.79	-7.25
213	425	426	-10.07	-7.25	-10.72	-7.25
214	427	428	-17	-7.25	-17.65	-7.25
215	429	430	-3.14	-10.39	-3.79	-10.39
216	431	432	-10.07	-10.39	-10.72	-10.39
217	433	434	-17	-10.39	-17.65	-10.39
218	435	436	-3.14	-13.53	-3.79	-13.53
219	437	438	-10.07	-13.53	-10.72	-13.53
220	439	440	-17	-13.53	-17.65	-13.53
221	441	442	-3.14	-14.18	-3.79	-14.18
222	443	444	-10.07	-14.18	-10.72	-14.18
223	445	446	-17	-14.18	-17.65	-14.18
224	447	448	-3.14	-17.32	-3.79	-17.32
225	449	450	-10.07	-17.32	-10.72	-17.32
226	451	452	-17	-17.32	-17.65	-17.32
227	453	454	-3.14	-20.46	-3.79	-20.46
228	455	456	-10.07	-20.46	-10.72	-20.46
229	457	458	-17	-20.46	-17.65	-20.46
230	459	460	-3.14	-21.11	-3.79	-21.11
231	461	462	-10.07	-21.11	-10.72	-21.11
232	463	464	-3.14	-24.25	-3.79	-24.25
233	465	466	-10.07	-24.25	-10.72	-24.25
234	467	468	-3.14	-27.39	-3.79	-27.39
235	469	470	-10.07	-27.39	-10.72	-27.39
236	471	472	0	-7.25	0	-6.6
237	473	474	3.14	-7.25	3.14	-6.6
238	475	476	3.79	-7.25	3.79	-6.6
239	477	478	6.93	-7.25	6.93	-6.6
240	479	480	10.07	-7.25	10.07	-6.6
241	481	482	10.72	-7.25	10.72	-6.6
242	483	484	13.86	-7.25	13.86	-6.6
243	485	486	17	-7.25	17	-6.6
244	487	488	17.65	-7.25	17.65	-6.6
245	489	490	20.78	-7.25	20.78	-6.6
246	491	492	23.92	-7.25	23.92	-6.6
247	493	494	0	-13.53	0	-14.18
248	495	496	3.14	-13.53	3.14	-14.18
249	497	498	3.79	-13.53	3.79	-14.18
250	499	500	6.93	-13.53	6.93	-14.18

1. Section locations are shown in Figures 3.4.4.1-13 and 3.4.4.1-16.

Table 3.4.4.1-14 Listing of Sections for Stress Evaluation of BWR Support Disk (Continued)

Section Number[1]	Point 1	Point 2	Point 1		Point 2	
			X	Y	X	Y
251	501	502	10.07	-13.53	10.07	-14.18
252	503	504	10.72	-13.53	10.72	-14.18
253	505	506	13.86	-13.53	13.86	-14.18
254	507	508	17	-13.53	17	-14.18
255	509	510	17.65	-13.53	17.65	-14.18
256	511	512	20.78	-13.53	20.78	-14.18
257	513	514	23.92	-13.53	23.92	-14.18
258	515	516	0	-21.11	0	-20.46
259	517	518	3.14	-21.11	3.14	-20.46
260	519	520	3.79	-21.11	3.79	-20.46
261	521	522	6.93	-21.11	6.93	-20.46
262	523	524	10.07	-21.11	10.07	-20.46
263	525	526	10.72	-21.11	10.72	-20.46
264	527	528	13.86	-21.11	13.86	-20.46
265	529	530	17	-21.11	17	-20.46
266	531	532	3.14	-0.33	3.79	-0.33
267	533	534	10.07	-0.33	10.72	-0.33
268	535	536	17	-0.33	17.65	-0.33
269	537	538	23.92	-0.33	24.57	-0.33
270	539	540	3.14	-3.46	3.79	-3.46
271	541	542	10.07	-3.46	10.72	-3.46
272	543	544	17	-3.46	17.65	-3.46
273	545	546	23.92	-3.46	24.57	-3.46
274	547	548	3.14	-6.6	3.79	-6.6
275	549	550	10.07	-6.6	10.72	-6.6
276	551	552	17	-6.6	17.65	-6.6
277	553	554	23.92	-6.6	24.57	-6.6
278	555	556	3.14	-7.25	3.79	-7.25
279	557	558	10.07	-7.25	10.72	-7.25
280	559	560	17	-7.25	17.65	-7.25
281	561	562	3.14	-10.39	3.79	-10.39
282	563	564	10.07	-10.39	10.72	-10.39
283	565	566	17	-10.39	17.65	-10.39
284	567	568	3.14	-13.53	3.79	-13.53
285	569	570	10.07	-13.53	10.72	-13.53
286	571	572	17	-13.53	17.65	-13.53
287	573	574	3.14	-14.18	3.79	-14.18
288	575	576	10.07	-14.18	10.72	-14.18
289	577	578	17	-14.18	17.65	-14.18
290	579	580	3.14	-17.32	3.79	-17.32
291	581	582	10.07	-17.32	10.72	-17.32
292	583	584	17	-17.32	17.65	-17.32
293	585	586	3.14	-20.46	3.79	-20.46
294	587	588	10.07	-20.46	10.72	-20.46
295	589	590	17	-20.46	17.65	-20.46
296	591	592	3.14	-21.11	3.79	-21.11
297	593	594	10.07	-21.11	10.72	-21.11
298	595	596	3.14	-24.25	3.79	-24.25
299	597	598	10.07	-24.25	10.72	-24.25
300	599	600	3.14	-27.39	3.79	-27.39
301	601	602	10.07	-27.39	10.72	-27.39

1. Section locations are shown in Figures 3.4.4.1-13 and 3.4.4.1-16.

Table 3.4.4.1-15 $P_m + P_b$ Stresses for BWR Support Disk - Normal Conditions (ksi)

Section[1]	Sx	Sy	Sxy	Stress Intensity	Allow. Stress	Margin of Safety
257	1	0.4	0.2	1.1	45	42
171	0.2	1	0.1	1	45	44
108	0.2	1	-0.1	1	45	44
234	0.2	1	-0.1	1	45	45
129	0.9	0.3	0.2	1	45	45
65	0.9	0.3	-0.2	1	45	45
182	0.9	0.2	0.2	1	45	46
192	0.9	0.3	-0.2	1	45	46
300	0.1	0.9	0.1	0.9	45	47
119	0.9	0.2	-0.2	0.9	45	48
54	0.9	0.2	0.2	0.9	45	48
246	0.9	0.2	-0.2	0.9	45	48
103	0.3	0.3	0.2	0.5	45	91
235	-0.1	0.4	0	0.5	45	93
229	0.2	0.3	0.2	0.5	45	94
77	0.2	-0.3	0.1	0.5	45	93
140	0.2	-0.3	-0.1	0.5	45	94
269	0.2	-0.3	-0.1	0.5	45	94
203	0.2	-0.3	0.1	0.5	45	94
295	0.2	0.3	-0.2	0.5	45	95
301	-0.1	0.4	0	0.5	45	95
134	0	0.2	-0.2	0.5	45	96
197	0	0.2	0.2	0.5	45	96
71	0	0.2	0.2	0.5	45	96
263	0	0.2	-0.2	0.5	45	96
172	-0.1	0.4	0	0.5	45	97
166	0.2	0.3	-0.2	0.5	45	97
40	0.3	-0.2	0.1	0.5	45	97
27	0.3	-0.2	-0.1	0.5	45	97
228	-0.2	-0.1	0.2	0.5	45	97
165	-0.2	-0.1	-0.2	0.5	45	98
102	-0.2	-0.1	0.2	0.5	45	98
294	-0.2	-0.1	-0.2	0.5	45	98
252	-0.4	-0.1	-0.2	0.5	45	99
124	-0.4	-0.1	-0.2	0.5	45	99
60	-0.4	-0.1	0.2	0.5	45	99
187	-0.4	-0.1	0.2	0.5	45	99
109	0	0.4	0	0.5	45	99
73	0.1	0.3	0.2	0.4	45	99
199	0.1	0.3	0.2	0.4	45	100

1. Section locations are shown in Figures 3.4.4.1-13 and 3.4.4.1-16.

Table 3.4.4.1-16 $P_m + P_b + Q$ Stresses for BWR Support Disk - Normal Conditions (ksi)

Section[1]	Sx	Sy	Sxy	Stress Intensity	Allow. Stress	Margin of Safety
3	-0.1	13.5	-0.2	13.6	90	5.6
4	-0.1	13.5	-0.2	13.6	90	5.6
1	-0.4	13	-0.1	13.4	90	5.7
2	-0.4	13	-0.1	13.4	90	5.7
16	10.5	4.3	4.9	13.3	90	5.8
15	11.5	3.4	-3.8	13	90	5.9
13	10.5	3.1	-4	12.3	90	6.3
268	-5.6	-11.7	1.4	12	90	6.5
76	-5.6	-11.6	-1.4	12	90	6.5
202	-5.7	-11.6	-1.4	11.9	90	6.5
139	-5.6	-11.5	1.4	11.9	90	6.6
14	10.4	1.6	3.5	11.6	90	6.8
295	-0.9	-11.5	0.8	11.6	90	6.8
166	-1.3	-11.4	0.8	11.5	90	6.9
103	-1.2	-11.3	-0.8	11.4	90	6.9
229	-0.9	-11.2	-0.7	11.3	90	7.0
289	-3.4	-11	1	11.1	90	7.1
97	-3.3	-10.8	-1	11	90	7.2
160	-3.3	-10.8	0.9	10.9	90	7.2
223	-3.4	-10.7	-1	10.9	90	7.3
276	-4.2	-10.6	1	10.8	90	7.4
84	-4.2	-10.6	-1	10.7	90	7.4
147	-4.2	-10.5	1	10.7	90	7.4
210	-4.1	-10.5	-0.9	10.7	90	7.4
200	-6.3	-9.9	-1.6	10.5	90	7.6
77	-5	-10.2	-1.2	10.5	90	7.6
269	-5	-10.2	1.2	10.5	90	7.6
74	-6.3	-9.9	-1.6	10.5	90	7.6
203	-4.9	-10.2	-1.2	10.5	90	7.6
140	-5.1	-10.2	1.2	10.5	90	7.6
137	-6.3	-9.9	1.6	10.4	90	7.6
266	-6.3	-9.8	1.6	10.4	90	7.6
31	-9.6	-5.6	-1.9	10.4	90	7.7
18	-9.6	-5.6	-1.9	10.4	90	7.7
21	-9.5	-4.8	-1.7	10	90	8.0
34	-9.5	-4.8	-1.7	10	90	8.0
37	-8.8	-6.5	-2	10	90	8.0
24	-8.7	-6.6	2	9.9	90	8.1
211	-3.4	-9.6	-1.2	9.9	90	8.1
85	-3.2	-9.6	-1.1	9.8	90	8.2

1. Section locations are shown in Figures 3.4.4.1-13 and 3.4.4.1-16.

Table 3.4.4.1-17 Summary of Maximum Stresses for PWR and BWR Fuel Basket Weldments - Normal Conditions (ksi)

Component	Stress Catagory	Maximum Stress Intensity[1]	Stress Allowable[2]	Margin of Safety
PWR Top Weldment	$P_m + P_b$	0.5	26.3	+Large
	$P_m + P_b + Q$	35.7	52.5	0.47
PWR Bottom Weldment	$P_m + P_b$	0.3	30.0	+Large
	$P_m + P_b + Q$	11.1	60.0	+Large
BWR Top Weldment	$P_m + P_b$	0.6	27.2	+Large
	$P_m + P_b + Q$	9.5	54.3	+Large
BWR Bottom Weldment	$P_m + P_b$	1.0	29.0	+Large
	$P_m + P_b + Q$	34.1	58.1	0.70

1. Nodal stresses are from the finite element analysis.
2. Allowable stresses are conservatively determined using the maximum temperature of the weldment.

3.4.4.2 Vertical Concrete Cask Analyses

The stresses in the concrete cask are evaluated in this section for normal conditions of storage. The evaluation for the steel base plate at the bottom of the cask is presented in Section 3.4.3.1. The stresses in the concrete due to dead load, live load, and thermal load are calculated in this section. The evaluations for off-normal and accident loading conditions are presented in Chapter 11.0. The radial dimensions of the concrete cask are the same for all cask configurations, only the height of the cask varies. Thus, the temperature differences through the concrete for all cask configurations vary only as a function of the heat source. Using the model described in this section, thermal analyses were run for both the maximum BWR and PWR heat loads for normal, off-normal, and accident conditions. The results of these analyses showed that the maximum temperature differences across the concrete cask wall occurred under normal operating conditions (76°F, with a 1.275 load factor) for the BWR casks and under accident conditions (133°F, with a load factor of 1.0) for the PWR casks. Thus, the structural analyses in this chapter use the temperature gradients from the BWR cask at 76°F and the analyses in Chapter 11 use the temperature differences for the PWR cask at 133°F. A summary of calculated stresses for the load combinations defined in Table 2.2-1 is presented in Figure 3.4.4.2-2 Concrete Cask Thermal Stress Model - Vertical and Horizontal Rebar Detail. As shown in Table 3.4.4.2-2, the concrete cask meets the structural requirements of ACI-349-85 [4].

The structural evaluation of the Universal Storage System is based on consideration of the bounding conditions for each aspect of the analysis. Generally, the bounding condition is represented by the component, or combination of components, of each configuration that is the heaviest. For reference, the bounding case used in each of the structural evaluations is presented below.

Section	Aspect Evaluated	Bounding Condition	Configuration
3.4.4.2.1	Dead Load	Heaviest concrete cask	PWR Class 3
3.4.4.2.2	Live Load	Heaviest loaded transfer cask	BWR Class 5
	Snow Load	Same for all configurations	Not Applicable
3.4.4.2.3	Thermal Load	Highest temperature gradient under normal conditions	BWR Class 4

3.4.4.2.1 Dead Load

The concrete cask dead load evaluation is based on the PWR Class 3 concrete cask, which is the heaviest concrete cask. The weight used in this analysis bounds the calculated weight of the PWR Class 3 concrete cask, as shown in Tables 3.2-1 and 3.2-2. The dead load of the cask concrete is resisted by the lower concrete surface only. The concrete compression stress due to the weight of the concrete cask is:

$$\sigma_v = -W/A = -25.6 \text{ psi (compression)}$$

where:

W = 245,000 lb concrete cask dead weight
OD = 136 in. concrete exterior diameter
ID = 79.5 in. concrete interior diameter
A = $\pi (OD^2 - ID^{2)} / 4 = 9{,}563 \text{ in.}^2$

This evaluation of stress at the base of the concrete conservatively considers the weight of the empty concrete cask, rather than the concrete alone. The weight of the canister is not supported by the concrete.

3.4.4.2.2 Live Load

The concrete cask is subjected to two live loads: the snow load and the weight of the fully loaded transfer cask resting atop the concrete cask. These loads are conservatively assumed to be applied to the concrete portion of the cask. No loads are assumed to be taken by the concrete cask's steel liner. The loads from the canister and its contents are transferred to the steel support inside the concrete cask and are not applied to the concrete. The stress in the steel support is evaluated in Section 3.4.3.1. Under these conditions, the only stress component is the vertical compression stress.

Snow Load

The calculated snow load and the resulting stresses are the same for all five of the concrete cask configurations because the top surface areas are the same for all configurations. The snow load on the concrete cask is determined in accordance with ANSI/ASCE 7-93 [30].

The uniformly distributed snow load on the top of the concrete cask, P_f, is

$$P_f = 0.70\, C_e\, C_t\, I\, P_g = 101 \text{ lbf/ft}^2$$

The concrete cask top area,

$$A_{top} = \pi\,(D/2)^2 = 14{,}527 \text{ in.}^2 = 101 \text{ ft}^2$$

The maximum snow load, F_s, is,

$$F_s = P_f \times A_{top} = 101 \text{ lbf/ft}^2 \times (101 \text{ ft}^2) = 10{,}201 \text{ lbf.}$$

The snow load is uniformly distributed over the top surface of the concrete cask. This load is negligible.

Transfer Cask Load

The live load of the heaviest loaded transfer cask is bounded by the weight used in this analysis, which is much greater than the weight of the maximum postulated snow load. Consequently, the stress due to the snow load is bounded by the stress due to the weight of the heaviest transfer

cask. As with the snow load, the calculated transfer cask load, and the resulting stresses, are the same for all five of the concrete cask configurations because the top surface areas are the same for all configurations.

W = 196,000 lb-transfer cask weight (fully loaded)
D = 136 in.-concrete exterior diameter
ID = 79.5 in.-concrete interior diameter
$A = \pi (D^2 - ID^2)/4 = 9563 \text{ in.}^2$

Compression stress at the base of the concrete is:

$\sigma_v = W/A = -20.5$ psi (compressive)

3.4.4.2.3 Thermal Load

A three dimensional finite element model, shown in Figure 3.4.4.2-1, comprised of SOLID45, LINK8 (elements which support uniaxial loads only—no bending), and CONTAC52 elements was used to determine the stresses in the concrete cask due to thermal expansion. The SOLID45 elements represented the concrete while the LINK8 elements were used to represent the hoop and the vertical reinforcement bars. The model of the reinforcement bars is shown in Figure 3.4.4.2-2. The concrete cask has two sets of vertical reinforcement. At the inner radius of the concrete cask, there are 36 sets of vertical reinforcement, while at the outer radius, 56 sets of vertical reinforcement are used. The finite element model is a 1/56th circumferential model (or 360/56 = 6.42°), and the vertical reinforcement is modeled at the angular center of the model. To compensate for the smaller number of reinforcement elements at the inner radial location, the cross sectional area of the LINK8 elements were factored by 36/56. The cross sectional area of the LINK8s at the outer radial location corresponds to a Number 6 reinforcement bar, which has a 0.75-in. diameter and a cross sectional area of 0.44 in^2. LINK8s are also employed for the hoop reinforcements. The hoop reinforcements at the inner radial location are modeled 8-in. on center, while the outer hoop reinforcements are modeled on 4-in. centers. The nodal locations of the SOLID45 elements also correspond to the reinforcement locations to allow for the correct placement of the LINK8 elements in the model.

To allow the reinforcement to contain the tension stiffness of the concrete, the SOLID45 elements having nodes at a specified horizontal plane were separated by a small vertical distance

(0.1 in.) and were connected by CONTAC52 elements. The model contains three horizontal planes located at points ¼ , ½, and ¾ of the axial length of the model. The CONTAC52 elements transmit compression across the horizontal planes, which allows the concrete elements to be subjected to compression. The LINK8 elements maintain a continuous connection from top to bottom. The structural boundary conditions are shown in Figure 3.4.4.2-3. The side of the model at 0° is restrained from translation in the circumferential direction. At 6.4°, the circumferential reinforcing bar (LINK8) elements extend beyond the model boundary and are also restrained at their ends from circumferential translation. The remaining nodes at 6.4° are attached to the CONTAC52 elements that only support compressive loading. The steel inner liner is radially coupled to the concrete, since for the thermal conditions analyzed, the steel will expand more than the concrete. The boundary conditions used simulate a complete fracture of the concrete at the 6.4° plane and between each of the axial sections of the model.

Analysis of the thermal loads and conditions for all cask configurations showed that maximum temperature gradient across the concrete wall of the cask under normal conditions, 62.42°F, occurs for the BWR configuration. Thus, the steady-state, three-dimensional thermal conduction analysis used the surface temperature boundary conditions for the 76°F normal operating condition to determine the temperature field throughout the model. These temperatures were applied with a load factor of 1.275 along the steel liner interior and concrete shell.

After the thermal solution was obtained, the thermal model was converted to a structural model. The nodal temperatures developed from the heat transfer analysis became the thermal load boundary conditions for the structural model.

The membrane stresses occurring in each individual circumferential reinforcement bar (rebar) varied on the basis of the rebar location along the longitudinal axis of the cask. The maximum circumferential tensile stress, 5,839 psi, occurred in the outer rebar, 56.4 in. from the base of the concrete cask.

The membrane stresses occurring in the vertical rebar varied on the basis of the radial location within the concrete shell. The maximum vertical tensile stress, 4,853.0 psi, occurred in the outer rebar 140.3 in. from the base of the cask.

The maximum allowable stress in the ASTM A615 rebar material is:

$F_c = 60{,}000$ psi

The maximum allowable stress for the rebar assembly in the concrete cask shell is:

$$\sigma_{rebar} = \phi F_c = (0.9)(60{,}000 \text{ psi}) = 54{,}000 \text{ psi}$$

where:

F_c = 60,000 psi, the allowable stress on the rebar, and

ϕ = 0.90, a load reduction factor based on the rebar configuration.

Thus, the margin of safety of the rebar in the BWR cask under normal operating conditions is

$$MS = \frac{54{,}000\,\text{psi}}{5{,}389\,\text{psi}} - 1 = +9.0$$

The concrete component of the shell carries the compressive loads in both the circumferential and the vertical direction. The maximum calculated compressive stress, which occurs 144 in. from base of cask, is 105 psi in the circumferential direction. The maximum compressive concrete stress in the vertical direction is 594 psi, which occurs 136.34 in. from base of the cask.

Tensile stresses were examined in both the axial and circumferential directions. Two vertical planes (at 0° and at 6.4° for circumferential stress) and three horizontal planes (bottom, middle and top, for axial stress) were examined at each of the four concrete sections modeled. The locations of the planes where the stress evaluations are performed are shown in Figures 3.4.4.2-4 and 3.4.4.2-5. The appropriate element stress is examined at each plane to determine if the stress is tensile or compressive. If the stress is tensile, the component stress and face area of that element are used to calculate an average concrete stress on the plane. If compressive, the element results are excluded from the calculation. Experimental studies show that the tensile strength of concrete is 8% to 15% of the concrete compressive strength [35]. Using a compressive strength of 4,000 psi and an 8% factor, an allowable tensile strength of 320 psi is used in the evaluation.

The results of the evaluation, presented in Tables 3.4.4.2-3 and 3.4.4.2-4, show that maximum tensile stress in the concrete is 129.8 psi and 222.1 psi, for the normal and accident conditions, respectively. These maximum stresses are less than the allowable stress (320 psi). Consequently, no cracking of the concrete will occur.

Applying the ACI 349-85 load reduction factor, the allowable bearing stress on the concrete shell is,

$$\sigma_{bearing} = \phi f_c' = (0.70)\,(4{,}000) = 2{,}800 \text{ psi}$$

where:

ϕ, the strength reduction factor for the concrete shell = 0.70

f_c', the nominal concrete compressive strength = 4,000 psi

The maximum 76°F normal operating thermally induced stress of 594 psi represents a margin of safety of

$$MS = \frac{2{,}800\,\text{psi}}{594\,\text{psi}} - 1 = +3.7$$

Figure 3.4.4.2-1 Concrete Cask Thermal Stress Model

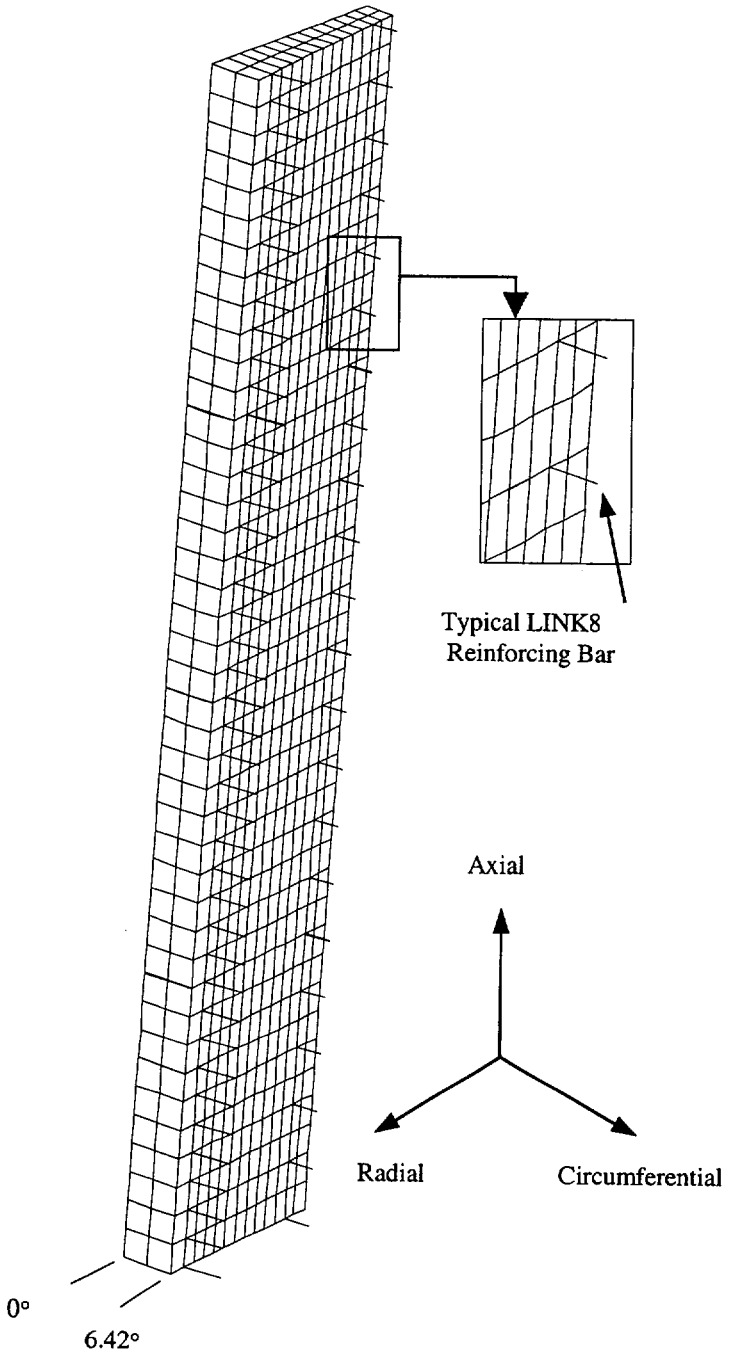

Figure 3.4.4.2-2 Concrete Cask Thermal Stress Model - Vertical and Horizontal Rebar Detail

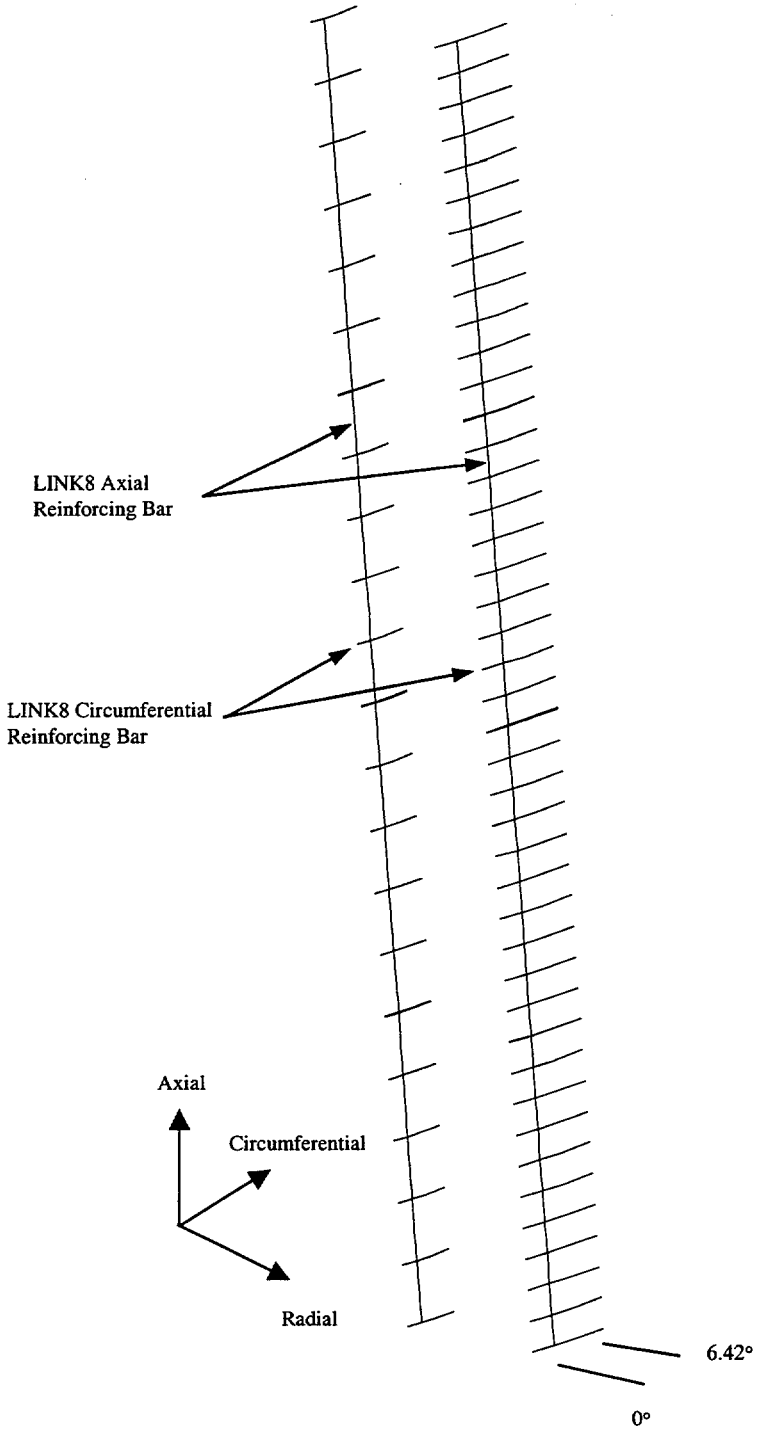

Figure 3.4.4.2-3 Concrete Cask Thermal Model Boundary Conditions

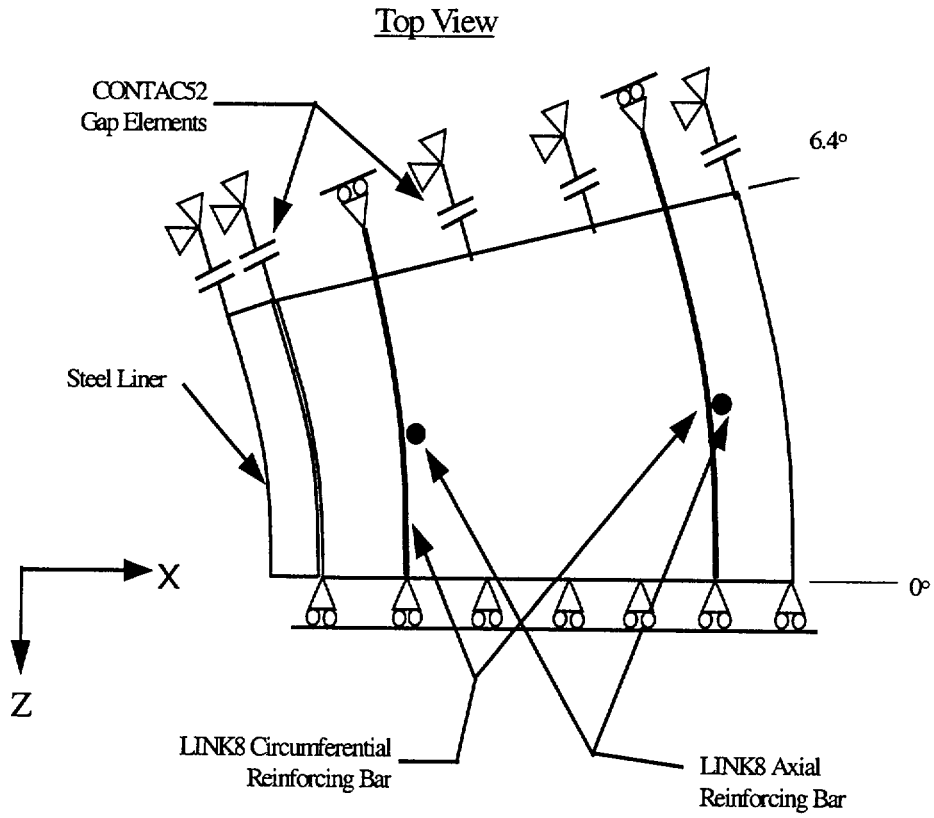

Note: CONTAC52 GAP Elements allow radial translation but don't transmit tensile loading

Figure 3.4.4.2-4 Concrete Cask Thermal Model Axial Stress Evaluation Locations

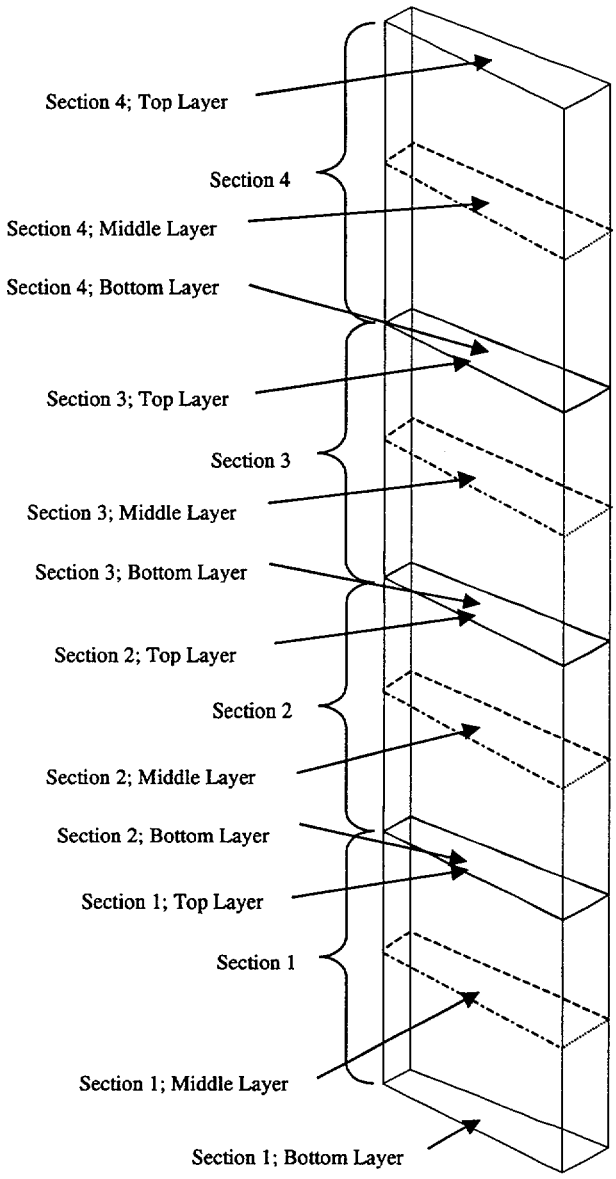

Figure 3.4.4.2-5 Concrete Cask Thermal Model Circumferential Stress Evaluation Locations

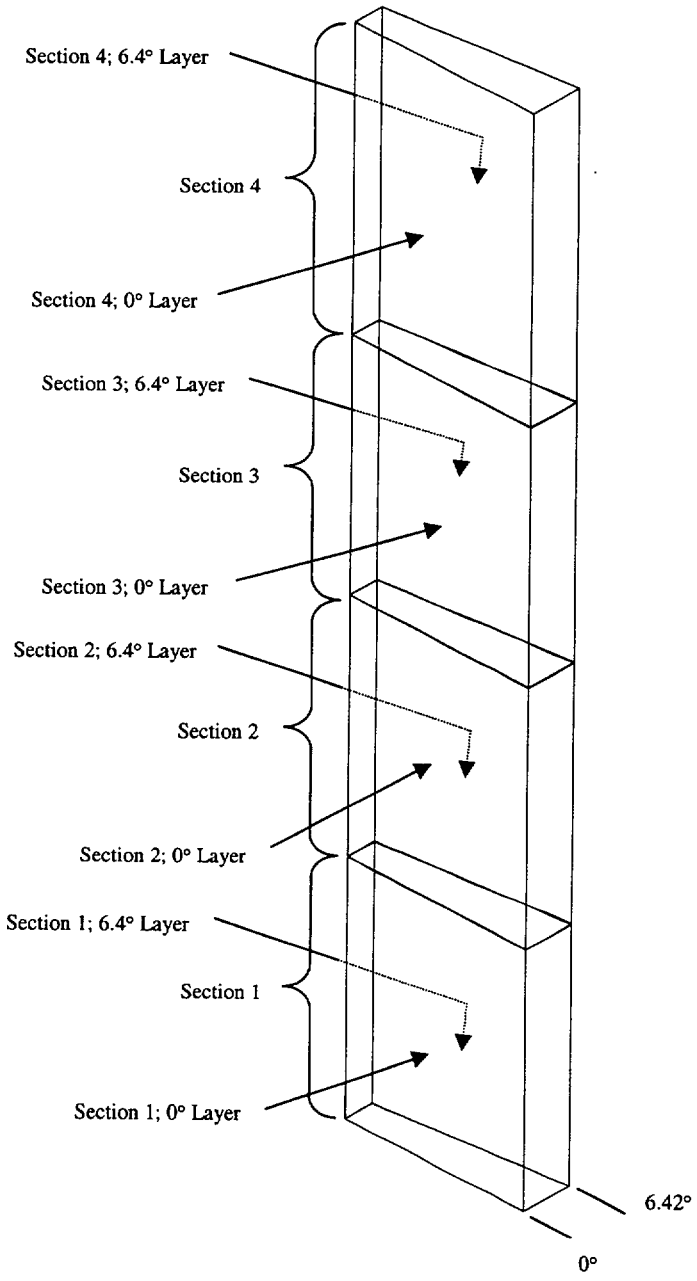

Table 3.4.4.2-1 Summary of Maximum Stresses for Vertical Concrete Cask Load Combinations

Load Comb[a]	Stress Direction	Stress [b] (psi)							
		Dead	Live	Wind [c]	Thermal [d]	Seismic [e]	Tornado [f]	Flood [g]	Total
Concrete Outside Surface:									
1	Vertical	-36.0	-36.0	—	—	—	—	—	-72.0
2	Vertical	-27.0	-27.0	—	—	—	—	—	-54.0
3	Vertical	-27.0	-27.0	-24.0	—	—	—	—	-78.0
4	Vertical	-26.0	-21.0	—	—	—	—	—	-47.0
5	Vertical	-26.0	-21.0	—	—	-116.0	—	—	-163.0
7	Vertical	-26.0	-21.0	—	—	—	—	-17.0	-64.0
8	Vertical	-26.0	-21.0	—	—	—	-20.0	—	-67.0
Concrete Inside Surface:									
1	Vertical	-36.0	-36.0	—	---	—	—	—	-72.0
	Circumferential	0.0	0.0	—	---	—	—	—	0.0
2	Vertical	-27.0	-27.0	—	-757.0	—	—	—	-811.0
	Circumferential	0.0	0.0	—	-134.0	—	—	—	-134.0
3	Vertical	-27.0	-27.0	-24.0	-757.0	—	—	—	-835.0
	Circumferential	0.0	0.0	0.0	-134.0	—	—	—	-134.0
4	Vertical	-26.0	-21.0	—	-655.0	—	—	—	-702.0
	Circumferential	0.0	0.0	—	-94.0	—	—	—	-94.0
5	Vertical	-26.0	-21.0	—	-594.0	-86.0	—	—	-727.0
	Circumferential	0.0	0.0	—	-105.0	—	—	—	-105.0
7	Vertical	-26.0	-21.0	—	-594.0	—	—	-17.0	-658.0
	Circumferential	0.0	0.0	—	-105.0	—	—	—	-105.0
8	Vertical	-26.0	-21.0	—	-594.0	—	-20.0	—	-661.0
	Circumferential	0.0	0.0	—	-105.0	—	—	—	-105.0

[a] Load combinations are defined in Table 2.2-1. See Section 11.2.4 and 11.2.12 for evaluations of drop/impact and tipover conditions for load combination No. 6.

[b] Positive stress values indicate tensile stresses and negative values indicate compressive stresses.

[c] Stress results from Section 11.2.11 (tornado) are conservatively used with a load factor of 1.275.

[d] Tensile stresses (at concrete outside surface) are taken by the steel reinforcing bars and therefore are not shown in this Table. Stress Results for T_a (load combination #4) are obtained from Section 11.2.7.

[e] Stress results are obtained from Section 11.2.8.

[f] Stress results are obtained from Section 11.2.11 (tornado wind).

[g] Stress results are obtained from Section 11.2.9.

Table 3.4.4.2-2 Maximum Concrete and Reinforcing Bar Stresses

	Calculated (psi)	**Allowable[1] (psi)**	**Margin of Safety**
Concrete	835	2,800	+2.4
Reinforcing Bar			
Normal - vertical	4,853	54,000	+10
- hoop	5,389	54,000	+9
Accident[2] - vertical	6,017	54,000	+8
- hoop	7,154	54,000	+6.5

1 Allowable compressive stress for concrete is (0.7)(4,000 psi)=2,800 psi, where 0.7 is the strength reduction factor per ACI 349-85, Section 9.3; 4,000 psi is the nominal concrete strength. Allowable stress for reinforcing bar is determined in the calculation in this Section.

2 Results are obtained from Section 11.2.11.

Table 3.4.4.2-3 Concrete Cask Average Concrete Axial Tensile Stresses

	Normal Conditions			Accident Conditions		
Stress Location	Calculated Stress (psi)	Allowable Stress (psi)	M.S.	Calculated Stress (psi)	Allowable Stress (psi)	M.S.
Section 1; Bottom Layer	34.8	320	8.2	135.5	320	1.36
Section 1; Middle Layer	24.1	320	12.3	41.9	320	6.6
Section 1; Top Layer	9.0	320	+Large	5.3	320	+Large
Section 2; Bottom Layer	77.5	320	3.1	121.3	320	1.6
Section 2; Middle Layer	38.3	320	7.3	81.6	320	2.9
Section 2; Top Layer	17.5	320	17.3	40.0	320	7.0
Section 3; Bottom Layer	69.9	320	3.6	109.0	320	1.9
Section 3; Middle Layer	60.3	320	4.3	123.3	320	1.6
Section 3; Top Layer	65.4	320	3.9	108.0	320	1.9
Section 4; Bottom Layer	33.2	320	8.6	59.3	320	4.4
Section 4; Middle Layer	53.4	320	5.0	105.9	320	2.0
Section 4; Top Layer	129.8	320	1.4	222.1	320	0.44

Table 3.4.4.2-4 Concrete Cask Average Concrete Hoop Tensile Stresses

	Normal Conditions			Accident Conditions		
Stress Location	Calculated Stress (psi)	Allowable Stress (psi)	M.S.	Calculated Stress (psi)	Allowable Stress (psi)	M.S.
Section 1; 0° Layer	26.1	320	11.3	45.2	320	6.1
Section 1; 6.42° Layer	25.2	320	11.7	39.3	320	7.1
Section 2; 0° Layer	51.5	320	5.2	81.3	320	2.9
Section 2; 6.42° Layer	53.7	320	4.9	77.6	320	3.1
Section 3; 0° Layer	78.7	320	3.1	103.5	320	2.1
Section 3; 6.42° Layer	77.6	320	3.1	98.6	320	2.2
Section 4; 0° Layer	55.9	320	4.7	72.6	320	3.4
Section 4; 6.42° Layer	52.3	320	5.1	67.2	320	3.76

THIS PAGE INTENTIONALLY LEFT BLANK

3.4.5 Cold

Severe cold environments are evaluated in Section 11.1.1. Stress intensities corresponding to thermal loads in the canister are evaluated by using a finite element model as described in Section 3.4.4.1. The thermal stresses that occur in the canister as a result of the maximum off-normal temperature gradients in the canister are bounded by the analysis of extreme cold in Section 11.1.1.

The PWR canister and basket are fabricated from stainless steel and aluminum, which are not subject to a ductile-to-brittle transition in the temperature range of interest. The BWR canister and basket are fabricated from stainless steel, aluminum, with carbon steel support disks. The carbon steel support disk thickness, 5/8 in., is selected to preclude brittle fracture at the design basis low temperature (-40°F). However, low temperature handling limits do apply to the transfer cask (See Section 12.2.2.9).

THIS PAGE INTENTIONALLY LEFT BLANK

3.5 Fuel Rods

The Universal Storage System is designed to limit fuel cladding temperatures to levels below those where Zircaloy degradation is expected to lead to fuel clad failure. As shown in Chapter 4, fuel cladding temperature limits for PWR and BWR fuel have been established at 380°C based on 5-year cooled fuel for normal conditions of storage and 570°C for short term off-normal and accident conditions.

As shown in Table 4.1-4 and 4.1-5, the calculated maximum fuel cladding temperatures are well below the temperature limits for all design conditions of storage.

THIS PAGE INTENTIONALLY LEFT BLANK

3.6 Structural Evaluation of Site Specific Spent Fuel

This section presents the structural evaluation of fuel assemblies or configurations, which are unique to specific reactor sites or which differ from the UMS® Storage System design basis fuel. These site specific configurations result from conditions that occurred during reactor operations, participation in research and development programs, and from testing programs intended to improve reactor operations. Site specific fuel includes fuel assemblies that are uniquely designed to accommodate reactor physics, such as axial fuel blanket and variable enrichment assemblies, and fuel that is classified as damaged. Damaged fuel includes fuel rods with cladding that exhibit defects greater than pinhole leaks or hairline cracks.

Site specific fuel assembly configurations are either shown to be bounded by the analysis of the standard design basis fuel assembly configuration of the same type (PWR or BWR), or are shown to be acceptable contents by specific evaluation.

3.6.1 Structural Evaluation of Maine Yankee Site Specific Spent Fuel for Normal Operating Conditions

This section describes the structural evaluation for site specific spent fuel configurations. As described in Sections 1.3.2.1 and 2.1.3.1, the inventory of site specific spent fuel configurations includes fuel classified as intact, intact with additional fuel and non fuel-bearing hardware, consolidated fuel and fuel classified as damaged. Damaged fuel is separately containerized in the Maine Yankee fuel can to reduce the potential for release of gross particulates from damaged fuel cladding. These configurations are evaluated in this section to ensure that they are bounded by the design basis fuel assembly analysis.

3.6.1.1 Maine Yankee Intact Spent Fuel

The description for Maine Yankee site specific fuel is in Section 1.3.2.1. The standard spent fuel assembly for the Maine Yankee site is the Combustion Engineering (CE) 14x 14fuel assembly. Fuel of the same design has also been supplied by Westinghouse and by Exxon. The standard 14x14 fuel assemblies are included in the population of the design basis PWR fuel assemblies for the UMS® Storage System (see Table 2.1.1-1). The structural evaluation for the UMS®

transport system loaded with the standard Maine Yankee fuels is bounded by the structural evaluations in Chapter 3 for normal conditions of storage and Chapter 11 for off-normal and accident conditions of storage.

With the Control Element Assembly (CEA) inserted, the weight of a standard CE 14x14 fuel assembly is 1,360 pounds. This weight is bounded by the weight of the design basis PWR fuel assembly (37,608/24 = 1,567 lbs) used in the structural evaluations (Table 3.2-1). The fuel configurations with removed fuel rods, with fuel rods replaced by solid stainless steel or Zircaloy rods, or with poison rods replaced by hollow Zircaloy rods, all weigh less than the standard CE 14x14 fuel assembly. The configuration with instrument thimbles installed in the center guide tube position weighs less than the standard assembly with the installed control element assembly. Consequently, this configuration is also bounded by the weight of the design basis fuel assembly. Since the weight of any of these fuel assembly configurations is bounded by the design basis fuel assembly weight, no additional analysis of these configurations is required.

The two consolidated fuel lattices are each constructed of 17x17 stainless steel fuel grids and stainless steel end fittings, which are connected by 4 stainless steel support rods. One of the consolidated fuel lattices has 283 fuel rods with 2 empty positions. The other has 172 fuel rods, with the remaining positions either empty or holding stainless steel rods. The calculated weight for the heaviest of the two consolidated fuel lattices is 2,100 pounds. Only one consolidated fuel lattice can be loaded into any one canister. The weight of the site specific 14x14 fuel assembly plus the CEA is approximately 1,360 lbs. Twenty-three (23) assemblies (at 1,360 lbs each) in addition to the consolidated fuel assembly (at approximately 2,100 lbs) would result in a total weight of 33,380 pounds.

Therefore, the design basis UMS® PWR fuel weight of 37,608 lbs bounds the site specific fuel and consolidated fuel by 12%. The evaluations for the Margin of Safety for the dead weight load of the fuel and the lifting evaluations in Section 3.4.4 bound the Margins of Safety for the Maine Yankee site specific fuel.

3.6.1.2 Maine Yankee Damaged Spent Fuel

The Maine Yankee fuel can, shown in Drawings 412-501 and 412-502, is provided to accommodate Maine Yankee damaged fuel. The fuel can fits within a standard PWR basket fuel tube. The primary function of the Maine Yankee fuel can is to confine the fuel material within

the can to minimize the potential for dispersal of the fuel material into the canister cavity volume.

The Maine Yankee fuel can is designed to hold an intact fuel assembly, a damaged fuel assembly, a fuel assembly with a burnup between 45,000 and 50,000 MWD/MTU and having a cladding oxidation layer thickness greater than 80 microns, or consolidated fuel in the Maine Yankee fuel inventory.

The fuel can is a square cross-section tube made of Type 304 stainless steel with a total length of 162.8 inches. The can walls are 0.048-inch thick sheet (18 gauge). The minimum internal width of the can is 8.52 inches. The bottom of the can is a 0.63-inch thick plate. Four holes in the plates, screened with a Type 304 stainless steel wire screen (250 openings/inch x 250 openings/inch mesh), permit water to be drained from the can during loading operations. Since the bottom surface of the fuel can rests on the canister bottom plate, additional slots are machined in the fuel can (extending from the holes to the side of the bottom assembly) to allow the water to be drained from the can. At the top of the can, the wall thickness is increased to 0.15-inches to permit the can to be handled. Slots in the top assembly side plates allow the use of a handling tool to lift the can and contents. To confine the contents within the can, the top assembly consists of a 0.88-inch thick plate with screened drain holes identical to those in the bottom plate. Once the can is loaded, the can and contents are inserted into the basket, where the can may be supported by the sides of the fuel assembly tube, which are backed by the structural support disks. Alternately, the empty fuel can may be placed in the basket prior to having the designated contents inserted in the fuel can.

In normal operation, the can is in a vertical position. The weight of the fuel can contents is transferred through the bottom plate of the can to the canister bottom plate, which is the identical load path for intact fuel. The only loading in the vertical direction is the weight of the can and the top assembly. The lifting of the can with its contents is also in the vertical direction.

Classical hand calculations are used to qualify the stresses in the Maine Yankee fuel can.

A conservative bounding temperature of 600°F is used for the evaluation of the fuel can for normal conditions of storage. A temperature of 300°F is used for the lifting components at the top of the fuel can and for the lifting tool.

Calculated stresses are compared to allowable stresses in accordance with ASME Code, Section III, Subsection NG. The ASME Code, Section III, Subsection NG allowable stresses used for stress analysis are:

Property	600°F	300°F
S_u	63.3 ksi	66.0 ksi
S_y	18.6 ksi	22.5 ksi
S_m	16.7 ksi	20.0 ksi
E	25.2×10^3 ksi	27.0×10^3 ksi

The Maine Yankee fuel can is evaluated for dead weight and handling loads for normal conditions of storage. Since the can is not restrained, it is free to expand. Therefore, the thermal stress is considered to be negligible.

The Maine Yankee fuel can lifting components and handling tools are designed with a safety factor of 3.0 on material yield strength.

3.6.1.2.1 Dead Weight and Handling Loading Evaluation

The weight of the Maine Yankee fuel can is 130 pounds. The maximum compressive stress acting in the tube of the fuel can is due to its own weight in addition to that of the top assembly. A 10% dynamic load factor is applied to the fuel can weight for an applied load of 143 pounds to account for loads due to handling. Based on the minimum cross sectional area of $(8.62)^2 - (8.52)^2 = 1.714$ in^2, the margin of safety at 300°F is:

$$\text{M.S.} = 20{,}000/(143/1.714) - 1$$
$$\text{M.S.} = +\text{LARGE}$$

3.6.1.2.2 Lifting Evaluation

Based on the loaded weight of the fuel can, the lift evaluation does not require the use of the design criteria of ANSI N14.6 or NUREG-0612. However, for purposes of conservatism and good engineering practice, a factor of safety of three on material yield strength is used for the stress evaluations for the lift condition. Since a combined stress state results from the loading

and the calculated stresses are compared to material yield strength, the Von Mises stress is computed.

Side Plates

The side plates will be subjected to bending, shear, and bearing stresses because of interaction with the lifting tool during handling operations. The lifting tool engages the 1.875-inch × 0.38-inch lifting slots with lugs that are 1-inch wide and lock into the four lifting slots. For this evaluation, the handling load is the weight of the consolidated fuel assembly (2,100 lbs design weight) plus the Maine Yankee fuel can weight (130 lbs), amplified by a dynamic load factor of 10%. Although the four slots are used to lift the can, the analysis assumes that the entire design load is shared by only two lift slots.

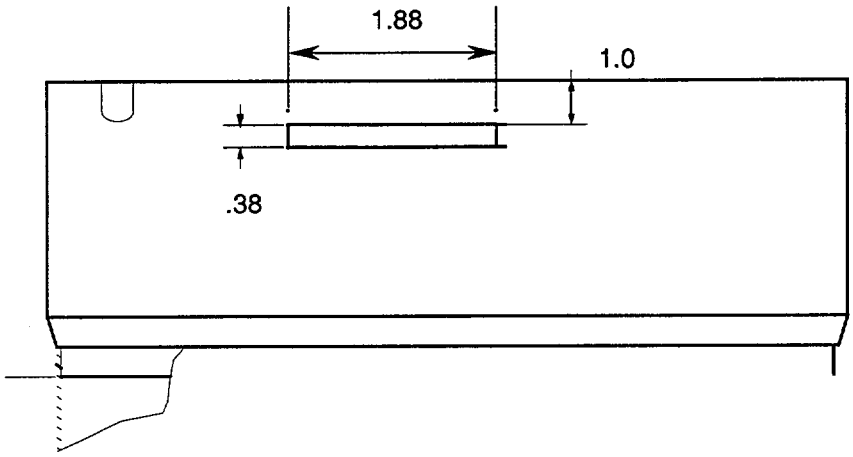

The stress in the side plate above the slot is determined by analyzing the section above the slot as a 0.15-inch wide × 1.875-inch long × 1.125-inch deep beam that is fixed at both ends. The lifting tool lug is 1 inch wide and engages the last 1 inch of the slot. The following figure represents the configuration to be evaluated:

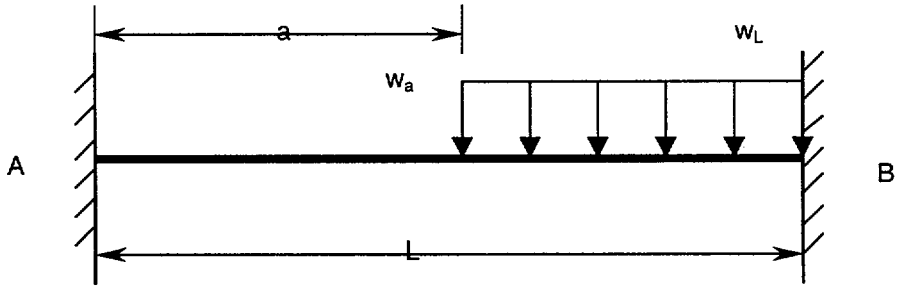

where:

$a = 0.875$ in.
$L = 1.875$ in.
$w_a = w_L = (2{,}230 \text{ lbs}/2)(1.10)/1.0 \text{ in.} = 613.3 \text{ lbs/in, use } 620 \text{ lbs/in.}$

Reactions and moments at the fixed ends of the beam are calculated per Roark's Formula, Table 3, Case 2d.

The reaction at the left end of the beam (R_A) is:

$$R_A = \frac{w_a}{2L^3}(L-a)^3(L+a)$$

$$= \frac{620}{2(1.875)^3}(1.875-0.875)^3(1.875+0.875) = 129.3 \text{ lbs}$$

The moment at the left end of the beam (M_A) is:

$$M_A = \frac{-w_a}{12L^2}(L-a)^3(L+3a)$$

$$= \frac{-620}{12(1.875)^2}(1.875-0.875)^3(1.875+3(0.875)) = -66.1 \text{ lbs} \cdot \text{in.}$$

The reaction at the right end of the beam (R_B) is:

$$R_B = w_a(L-a) - R_A = 620(1.875-0.875) - 164.2 = 490.7 \text{ lbs}$$

The moment at the right end of the beam (M_B) is:

$$M_B = R_A L + M_A - \frac{w_a}{2}(L-a)^2$$

$$= 129.3(1.875) + (-66.1) - \frac{620}{2}(1.875-0.875)^2 = -133.7 \text{ lbs} \cdot \text{in.}$$

The maximum bending stress (σ_b) in the side plate is:

$$\sigma_b = \frac{Mc}{I} = \frac{133.7(0.50)}{0.017} = 4{,}224 \text{ psi}$$

The maximum shear stress (τ) occurs at the right end of the slot:

$$\tau = \frac{R_B}{A} = \frac{490.7}{1.125(0.15)} = 2{,}908 \text{ psi}$$

The Von Mises stress (σ_{max}) is:

$$\sigma_{max} = \sqrt{\sigma_b^2 + 3\tau^2} = \sqrt{4{,}224^2 + 3(2{,}908)^2} = 6{,}573 \text{ psi}$$

The yield strength (S_y) for Type 304 stainless steel is 22,500 psi at 300°F. The factor of safety is calculated as:

$$FS = \frac{22{,}500}{6{,}573} = 3.4 > 3$$

The design condition requiring a safety factor of 3 on material yield strength is satisfied.

Tensile Stress

The tube body will be subjected to tensile loads during lifting operations. The load (P) includes the can contents (2,100 lbs design weight), the tube body weight (78.77 lbs), and the bottom assembly weight (12.98 lbs) for a total of 2,191.8 pounds. A load of 2,200 lbs with a 10% dynamic load factor is used for the analysis.

The tensile stress (σ_t) is then:

$$\sigma_t = \frac{1.1P}{A} = \frac{1.1(2{,}200 \text{ lb})}{1.714 \text{ in.}^2} = 1{,}412 \text{ psi}$$

where:

A = tube cross-section area = $8.62^2 - 8.52^2 = 1.714$ in^2

The factor of safety (FS) based on the yield strength at 600°F (18,000 psi) is:

$$FS = \frac{18{,}600 \text{ psi}}{1{,}412} = 13.2 > 3$$

Weld Evaluation

The welds joining the tube body to the bottom weldment and to the side plates are full penetration welds (Type III, paragraph NG-3352.3). In accordance with NG-3352-1, the weld quality factor (n) for a Type III weld with visual surface inspection is 0.5.

The weld stress (σ_w) is:

$$\sigma_w = \frac{1.1(P)}{A} = \frac{1.1(2{,}200)}{1.714} = 1{,}412 \text{ psi}$$

where:

P = the combined weight of the tube body, bottom weldment, and can contents
A = cross sectional area of thinner member joined

The factor of safety (FS) is:

$$FS = \frac{n \cdot S_y}{\sigma_w} = \frac{0.5(18{,}600 \text{ psi})}{1{,}412 \text{ psi}} = +6.6 > 3$$

3.7 References

1. 10 CFR 72, Code of Federal Regulations, "Licensing Requirements for the Independent Storage of Spent Fuel and High Level Radioactive Waste," January 1996.

2. "Safety Analysis Report for the UMS® Safety Analysis Report for the UMS® Universal Transport Cask," EA790-SAR-001, Docket No. 71-9270, NAC International, Atlanta, GA, April 1997.

3. ANSI/ANS 57.9-1992, "Design Criteria for an Independent Spent Fuel Storage Installation (Dry Type)," American National Standards Institute, May 1992.

4. American Concrete Institute, "Code Requirements for Nuclear Safety Related Concrete Structures (ACI-349-95) and Commentary (ACI 349R-85)," March 1986.

5. ASME Boiler and Pressure Vessel Code, Section III, Division I, Subsection NB, "Class 1 Components," 1995 Edition with 1995 Addenda.

6. ASME Boiler and Pressure Vessel Code, Section III, Division I, Subsection NG, "Core Support Structures," 1995 Edition with 1995 Addenda.

7. NUREG/CR 6322, "Buckling Analysis of Spent Fuel Baskets," U.S. Nuclear Regulatory Commission, May 1995.

8. NUREG-0612, "Control of Heavy Loads at Nuclear Power Plants," U.S. Nuclear Regulatory Commission, July 1980.

9. American National Standards Institute, "Radioactive Materials - Special Lifting Devices for Shipping Containers Weighing 10,000 Pounds (4,500 kg) or More," ANSI N14.6-1993, 1993.

10. ASME Boiler and Pressure Vessel Code, Section II, Part D, "Material Properties," 1995 Edition, with 1995 Addenda.

11. ASME Boiler and Pressure Vessel Code, Division I, Section III, Appendices, 1995 Edition, with 1995 Addenda.

12. "Metallic Materials Specification Handbook," 4th Edition, R. B. Ross, London, Chapman and Hall, 1992.

13. ASME Boiler and Pressure Vessel Code, Code Cases-Nuclear Components, 1995 Edition, American Society of Mechanical Engineers, New York, July 1995.

14. ASTM A 615- 95b, Standard Specification for Deformed and Plain Billet-Steel Bars for Concrete Reinforcement, Annual Book of ASTM Standards, Vol. 01.04, American Society for Testing and Materials, Conshohocken, PA, 1996.

15. Metallic Materials and Elements for Aerospace Vehicle Structures, Military Handbook MIL-HDBK-5G, U.S. Department of Defense, November 1994.

16. Handbook of Concrete Engineering, 2nd Edition, M. Fintel, Van Nosttrand Reinhold Co., New York.

17. "NS-4-FR Fire Resistant Neutron and/or Gamma Shielding Material," GESC Product Data, Genden Engineering Services & Construction Co., Tokyo, Japan.

18. NRC Bulletin 96-04, "Chemical, Galvanic, or Other Reactions in Spent Fuel Storage and Transportation Casks," U.S. Nuclear Regulatory Commission, July 5, 1996.

19. ASM Handbook, Corrosion, Vol. 13, ASM International, 1987.

20. "Guidelines for the use of Aluminum with Food and Chemicals (Compatibility Data on Aluminum in the Food and Chemical Process Industries," Aluminum Association, Inc., Washington, DC, April 1984.

21. TRW, Nelson Division, "Embedment Properties of Headed Studs," Design Data 10, 1975.

22. "Design of Weldments, Omer Blodgett, The Lincoln Arc Welding Foundation, Cleveland, OH, August 1976.

23. "Manual of Steel Construction, Allowable Stress Design," American Institute of Steel Construction, Inc., Ninth Edition, Chicago, Illinois, 1991.

24. "Machinery's Handbook," 22nd Edition, Erik Oberg, et. al, First Printing, Industrial Press, Inc., New York, 1984.

25. NUREG/CR-1815, "Recommendations for Protecting Against Failure by Brittle Fracture in Ferritic Steel Shipping Containers Up to Four Inches Thick," U.S. Nuclear Regulatory Commission, Washington, DC, 1981.

26. "Roark's Formulas for Stress and Strain," Sixth Edition, Warren C. Young, McGraw-Hill, Inc., New York, 1989.

27. "Machinery's Handbook," 23rd Edition, Erik Oberg, Fourth Printing, Industrial Press, Inc., New York, 1990.

28. NUREG/CR-1815, "Recommendations for Protecting Against Failure by Brittle Fracture in Ferritic Steel Shipping Containers Up to Four Inches Thick," U. S. Nuclear Regulatory Commission, Washington, DC, 1981.

29. ASME Boiler and Pressure Vessel Code, Section II, Part C, "Specifications for Welding Rods, Electrodes, and Filler Metals," 1995 Edition, American Society of Mechanical Engineers, New York, July 1995.

30. American Society of Civil Engineers, "Minimum Design Loads for Buildings and Other Structures," ANSI/ASCE 7-93, May 1994.

31. ASME Boiler and Pressure Vessel Code, Section III-A, "Appendices," 1995 Edition, American Society of Mechanical Engineers, New York, July 1995.

32. Maddux, Gene E., "Stress Analysis Manual," AFFDL-TR-69-42, Air Force Flight Dynamics Laboratory, August 1969.

33. Avallone, Eugene A. and Baumeister III, Theodore, "Marks' Standard Handbook for Mechanical Engineers," Ninth Edition, McGraw-Hill Book Company, New York, New York, 1987.

34. "Code Requirements for Nuclear Safety Related Concrete Structures," ACI-349-90, American Concrete Institute, 1990.

35. Leet, Kenneth, "Reinforced Concrete Design," 2nd Edition, McGraw-Hill, 1991.

36. "Coating Handbook for Nuclear Power Plants," EPRI TR 106160, Electric Power Research Institute, June 1996.

37. ASTM B733-97, "Standard Specification for Autocatalytic (Electroless) Nickel-Phosphorus Coatings on Metal," Annual Book of ASTM Standards, Vol. 02.05, American Society for Testing and Materials, Conshohocken, PA, 1996.

38. American Society for Metals, "Metals Handbook," 1985.

39. Duncan, R.N., "Corrosion Resistance of High-Phosphorus Electroless Nickel Coatings," Plating and Surface Finishing, July 1986, pages 52-56.

THIS PAGE INTENTIONALLY LEFT BLANK

3.8 Carbon Steel Coatings Technical Data

This Section presents the technical data sheets for Carboline 890 and Keeler & Long E-Series Epoxy Enamel. These coatings are applied to protect exposed carbon steel surfaces of the transfer cask and the vertical concrete cask. Also provided is a description of the electroless nickel coating that is applied to the BWR support disks. Each coating meets the service and performance requirements that are established for the coating by the design and service environment of the component to be covered.

The service and performance requirements for the coatings of the carbon steel components of the transfer cask, the vertical concrete cask, and the BWR support disks are similar and require that the coating:

- be applied to carbon steel
- be submersible for up to a week in clean water
- is rated Service Level 1 or 2 (EPRI TR-106160 for paints)
- does not contain Zinc
- have a service temperature of at least 200°F in water and 600°F in a dry environment
- generate no hydrogen, or minimal hydrogen, when submersed in water
- have no, or limited, special processes required for proper application or curing
- have a service environment in a high radiation field.

Either Carboline 890 or Keeler & Long E-Series Epoxy Enamel may be used on the exposed carbon steel surfaces of the transfer cask, transfer cask extension and the vertical concrete cask, including the concrete cask lifting lugs, if present. These coatings are listed in EPRI TR 106160, "Coating Handbook for Nuclear Power Plants," June 1996 [36], as meeting the requirements for Service Level 1 or 2.

Electroless nickel coating is used on the carbon steel BWR support disks to provide a submersible, passive protective finish. This coating has a history of acceptance and sucessful performance in similar service conditions.

No coating characteristics that may enhance the performance of the coated components (such as better emissivity) are considered in the analyses of these components. Therefore, no adverse affect on system performance results from incidental scratching or flaking of the coating, and no touchup of the coating on the BWR support disks or the storage cask liner is required.

3.8.1 Carboline 890

product data sheet

carboline®

CARBOLINE® 890

VOC

SELECTION DATA

GENERIC TYPE: Two component, cross-linked epoxy.

GENERAL PROPERTIES: CARBOLINE 890 is a high solids, high gloss, high build epoxy topcoat that can be applied by spray, brush, or roller. The cured film provides a tough, cleanable and esthetically pleasing surface. Available in a wide variety of clean, bright colors. Features include:

- Good flexibility and lower stress upon curing than most epoxy coatings.
- Very good weathering resistance for a high gloss epoxy.
- Very good abrasion resistance.
- Excellent performance in wet exposures.
- Meets the most stringent VOC (Volatile Organic Content) regulations.

RECOMMENDED USES: Recommended where a high performance, attractive, chemically resistant epoxy topcoat is desired. Offers outstanding protection for interior floors, walls, piping, equipment and structural steel or as an exterior coating for tank farms, railcars, structural steel and equipment in various corrosive environments. Recommended industrial environments include Chemical Processing, Offshore Oil and Gas, Food Processing and Pharmaceutical, Water and Waste Water Treatment, Pulp and Paper, Power Generation among others. May be used as a two coat system direct to metal or concrete for Water and Municipal Waste Water immersion. CARBOLINE 890 has been accepted for use in areas controlled by USDA regulations for incidental food contact. Consult Carboline Technical Service Department for other specific uses.

NOT RECOMMENDED FOR: Strong acid or solvent exposures, or immersion service other than recommended.

TYPICAL CHEMICAL RESISTANCE:

Exposure	Immersion	Splash and Spillage	Fumes
Acids	NR	Very Good	Very Good
Alkalies	NR	Excellent	Excellent
Solvents	NR	Very Good	Excellent
Salt Solutions	Excellent	Excellent	Excellent
Water	Excellent	Excellent	Excellent

*NR = Not recommended

TEMPERATURE RESISTANCE:
Continuous: 200° F (93° C)
Non-continuous: 250° F (121° C)

At 300° F, coating discoloration and loss of gloss is observed, without loss of film integrity.

SUBSTRATES: Apply over suitably prepared metal, concrete, or other surfaces as recommended.

COMPATIBLE COATINGS: May be applied directly over inorganic zincs, weathered galvanizing, catalyzed epoxies, phenolics or other coatings as instructed. A test patch is recommended before use over existing coatings. May be used as a tiecoat over inorganic zincs. A mist coat of CARBOLINE 890 is required when applied over inorganic zincs to minimize bubbling. May be topcoated to upgrade weathering resistance. Not recommended over chlorinated rubber or latex coatings. Consult Carboline Technical Service Department for specific recommendations.

April 91 Replaces Oct. 90

SPECIFICATION DATA

9960

THEORETICAL SOLIDS CONTENT OF MIXED MATERIAL:*

	By Volume
CARBOLINE 890	75%±2%

VOLATILE ORGANIC CONTENT:*
As Supplied: 1.78 lbs./gal.(214 gm/liter)
Thinned: The following are nominal values utilizing:
CARBOLINE Thinner # 2 (spray application)

% Thinned	Fluid Ounces/Gal.	Pounds/ Gallon	Grams/ Liter
10%	12.8	2.26	271

CARBOLINE Thinner #33 (brush & roller application)

12%	16	2.38	285

*Varies with color

RECOMMENDED DRY FILM THICKNESS PER COAT:
4-6 mils(100-150 microns).
5-7 mils (125-175 microns) DFT for a more uniform gloss over inorganic zincs.
Dry film thicknesses in excess of 10 mils(250 microns) per coat are not recommended. Excessive film thickness over inorganic zinc may increase damage during shipping or erection.

THEORETICAL COVERAGE PER MIXED GALLON:
1203 mil sq. ft. (30 sq. m/l at 25 microns)
241 sq. ft. at 5 mils(6.0 sq. m/l at 125 microns)
Mixing and application losses will vary and must be taken into consideration when estimating job requirements.

STORAGE CONDITIONS: Store Indoors
Temperature: 40-110° F (4-43° C)
Humidity: 0-100%

SHELF LIFE: Twenty-four months minimum when stored at 75° F (24° C).

COLORS: Available in Carboline Color Chart colors. Some colors may require two coats for adequate hiding. Colors containing lead or chrome pigments are not USDA acceptable. Consult your local Carboline representative or Carboline Customer Service for availability.

* See notice under DRYING TIMES.

GLOSS: High gloss (Epoxies lose gloss and eventually chalk in sunlight exposure).

ORDERING INFORMATION

Prices may be obtained from your local Carboline Sales Representative or Carboline Customer Service Department.

APPROXIMATE SHIPPING WEIGHT:

	2 Gal. Kit	10 Gal. Kit
CARBOLINE 890	29 lbs. (13 kg)	145 lbs. (66 kg)
THINNER #2	8 lbs. in 1's (4 kg)	39 lbs. in 5's (18 kg)
THINNER #33	9 lbs. in 1's (4 kg)	45 lbs. in 5's (20 kg)

FLASHPOINT: (Pensky-Martens Closed Cup)

CARBOLINE 890 Part A	73° F (23° C)
CARBOLINE 890 Part B	71° F (22° C)
THINNER #2	24° F (– 5° C)
THINNER #33	98° F (37° C)

APPLICATION INSTRUCTIONS
CARBOLINE® 890

These instructions are not intended to show product recommendations for specific service. They are issued as an aid in determining correct surface preparation, mixing instructions and application procedure. It is assumed that the proper product recommendations have been made. These instructions should be followed closely to obtain the maximum service from the materials.

0986

SURFACE PREPARATION: Remove oil or grease from surface to be coated with clean rags soaked in CARBOLINE Thinner #2 or Surface Cleaner #3 (refer to Surface Cleaner #3 instructions) in accordance with SSPC-SP 1.

Steel: Normally applied over clean, dry recommended primers. May be applied directly to metal. For immersion service, abrasive blast to a minimum Near White Metal Finish in accordance with SSPC-SP10, to a degree of cleanliness in accordance with NACE #2 to obtain a 1.5-3 mil (40-75 micron) blast profile. For non-immersion, abrasive blast to a Commercial Grade Finish in accordance with SSPC-SP6, to a degree of cleanliness in accordance with NACE #3 to obtain a 1.5-3 mil (40-75 micron) blast profile.

Concrete: Apply over clean, dry recommended surfacer or primer. Can be applied directly to damp(not visibly wet) or dry concrete where an uneven surface can be tolerated. Remove laitance by abrasive blasting or other means.

Do not coat concrete treated with hardening solutions unless test patches indicate satisfactory adhesion. Do not apply coating unless concrete has cured at least 28 days at 70° F (21° C) and 50% RH or equivalent time.

MIXING: Mix separately, then combine and mix in the following proportions:

	2 Gal. Kit	10 Gal. Kit
CARBOLINE 890 Part A	1 gallon	5 gallons
CARBOLINE 890 Part B	1 gallon	5 gallons

THINNING: For spray applications, may be thinned up to 10% (12.8 fl. oz./gal.) by volume with CARBOLINE Thinner #2.

For brush and roller application may be thinned up to 12 % (16 fl. oz./gal.) by volume with CARBOLINE Thinner #33.

Refer to Specification Data for VOC information.

Use of thinners other than those supplied or approved by Carboline may adversely affect product performance and void product warranty, whether express or implied.

POT LIFE: Three hours at 75° F (24° C) and less at higher temperatures. Pot life ends when material loses film build.

APPLICATION CONDITIONS:

	Material	Surfaces	Ambient	Humidity
Normal	60-85° F (16-29° C)	60-85° F (16-29° C)	60-90° F (16-32° C)	0-80%
Minimum	50° F (10° C)	50° F (10° C)	50° F (10° C)	0%
Maximum	90° F (32° C)	125° F (52° C)	110° F (43° C)	80%

Do not apply when the surface temperature is less than 5° F (or 3° C) above the dew point.

Special thinning and application techniques may be required above or below normal conditions.

SPRAY: This is a high solids coating and may require slight adjustments in spray techniques. Wet film thicknesses are easily and quickly achieved. The following spray equipment has been found suitable and is available from manufacturers such as Binks, DeVilbiss and Graco.

Conventional: Pressure pot equipped with dual regulators, 3/8" I.D. minimum material hose, .070" I.D. fluid tip and appropriate air cap.

Airless:
Pump Ratio: 30:1 (min.)*
GPM Output: 3.0 (min.)
Material Hose: 3/8"I.D.(min.)
Tip Size: .017-.021"
Output psi: 2100-2300
Filter Size: 60 mesh

*Teflon packings are recommended and are available from the pump manufacturer.

BRUSH OR ROLLER: Use medium bristle brush, or good quality short nap roller, avoid excessive rebrushing and rerolling. Two coats may be required to obtain desired appearance, hiding and recommended DFT. For best results, tie-in within 10 minutes at 75° F (24° C).

DRYING TIMES: These times are at 5 mils (125 microns) dry film thickness. Higher film thicknesses will lengthen cure times.

Dry to Touch 2 1/2 hours at 75° F (24° C)
Dry to Handle 6 1/2 hours at 75° F (24° C)

Temperature	Dry to Topcoat**	Final Cure
50° F (10° C)	24 hours	3 days
60° F (16° C)	16 hours	2 days
75° F (24° C)	8 hours	1 day
90° F (32° C)	4 hours	16 hours

**When recoating with CARBOLINE 890, recoat times will be drastically reduced. Contact Carboline Technical Service for specific recommendation.

Recommended minimum cure before immersion service is 5 days at 75° F (24° C).

EXCESSIVE HUMIDITY OR CONDENSATION ON THE SURFACE DURING CURING MAY RESULT IN SURFACE HAZE OR BLUSH; ANY HAZE OR BLUSH MUST BE REMOVED BY WATER WASHING BEFORE RECOATING.

CLEANUP: Use CARBOLINE Thinner #2.

CAUTION: READ AND FOLLOW ALL CAUTION STATEMENTS ON THIS PRODUCT DATA SHEET AND ON THE MATERIAL SAFETY DATA SHEET FOR THIS PRODUCT.

CAUTION: CONTAINS FLAMMABLE SOLVENTS. KEEP AWAY FROM SPARKS AND OPEN FLAMES. IN CONFINED AREAS WORKMEN MUST WEAR FRESH AIRLINE RESPIRATORS. HYPERSENSITIVE PERSONS SHOULD WEAR GLOVES OR USE PROTECTIVE CREAM. ALL ELECTRIC EQUIPMENT AND INSTALLATIONS SHOULD BE MADE AND GROUNDED IN ACCORDANCE WITH THE NATIONAL ELECTRICAL CODE. IN AREAS WHERE EXPLOSION HAZARDS EXIST, WORKMEN SHOULD BE REQUIRED TO USE NONFERROUS TOOLS AND TO WEAR CONDUCTIVE AND NONSPARKING SHOES.

carboline
350 Hanley Industrial Ct • St. Louis, MO 63144-1599
an RPM company • 314-644-1000

3.8.2 Keeler & Long E-Series Epoxy Enamel

March, 1995 SSU-1

HEADQUARTERS:
P. O. Box 460
856 Echo Lake Road
Watertown, CT 06795
Tel (860) 274-6701
Fax (860) 274-5857

PROTECTIVE COATING SYSTEMS FOR NUCLEAR POWER PLANTS

INTRODUCTION

In the 1960's Keeler & Long made the commitment to develop Protective Coating Systems for Nuclear Power Plants. Coating Systems were developed and qualified in accordance with accepted standards, with emphasis upon their usage and specification for NEW construction projects. These systems were applied directly to either concrete or carbon steel substrates utilizing ideal surface preparation.

Presently, there is a necessity to apply these same coating systems or newly formulated systems over the original systems or over substrates which cannot be ideally prepared. Several years ago, Keeler & Long initiated a test program in order to test and qualify systems in conjunction with competitors products and/or with methods of preparation which are considered less than ideal. This test program provides OPERATING Nuclear Plants with qualified methods of preparation and a variety of qualified mixed coating systems.

HISTORY

In 1967, we embarked upon a testing program in order to comply with standards being prepared by the experts in the field and under the jurisdiction of The American National Standards Institute (ANSI). Earlier testing had involved research in order to determine the radiation tolerance and the decontamination properties of a variety of generic coating types including zinc rich, alkyds, chlorinated rubbers, vinyls, latex emulsions, and epoxies. This testing was conducted by various independent laboratories, such as Oak Ridge National Laboratory, Idaho Nuclear, and The Western New York Nuclear Research Center. It was concluded from these tests that almost any generic coating type would produce satisfactory radiation resistance and decontaminability.

Upon completion of the first ANSI Standards, however, it became evident that only Epoxy Coatings would meet the specific minimum acceptance criteria set forth in these standards. The single most important change from the earlier testing was the inclusion of a test which simulates the operation of the emergency core cooling system. This test is referred to as the Loss of Coolant Accident (LOCA) or the Design Basis Accident Condition (DBA). The test involves a high pressure, high temperature, alkaline, immersion environment.

Simultaneous with the preparation of these standards, we prepared to test Epoxy Systems in order to comply with the requirements. First hand knowledge of these standards was available since our personnel assisted in the development of these documents. Equipment was designed and built by our laboratory in order to conduct in-house DBA tests. The required physical and chemical tests were either conducted by us or by universities through research grants.

In 1972, the testing program was taken a step further in order to establish more credibility. The Franklin Institute of Philadelphia constructed an apparatus in order to simulate various Design Basis Accident Conditions and we prepared blocks and panels for an independent evaluation. The test results were among the "First" from an independent source, and these tests substantiated more than two years of in-house testing.

The Franklin Institute tests, along with our in-house testing program, were used as a basis for qualification until 1976. During this period also the following ANSI standards were revised and/or developed:

ANSI N5.9-1967 "Protective Coatings (Paints) for the Nuclear Industry" (Rev. ANSI N512-1974)

ANSI N101.2-1972 "Protective Coatings (Paints) for Light Water Nuclear Reactor Containment Facilities"

ANSI N101.4-1972 "Quality Assurance for Protective Coatings Applied to Nuclear Facilities"

Simultaneously, we developed a written Quality Assurance Program in compliance with ANSI N101.4 - 1972, Appendix B 10CFR50 of the Federal Register, and ANSI N45.2-1971 "Quality Assurance Program Requirements For Nuclear Power Plants".

In 1976, Oak Ridge national Laboratory (ORNL) established a testing program in order to conduct Radiation, Decontamination, and DBA tests under one roof. Keeler & Long, under contract with ORNL, conducted a series of tests in compliance with the parameters established by a major engineering firm and the ANSI standards. These tests, and similar series of tests conducted two years later in 1978, became the basis for the qualification of several of our concrete and carbon steel coating systems. From 1978 to the present day we have continued to qualify through ORNL and several other independent testing agencies any modifications to existing formulas and any changes in surface preparation or application requirements. We have also maintained an in-house testing program used to screen new products as well as modifications of existing systems. Furthermore, progress has continued in the revision of the ANSI standards during this time frame. Revision of these documents is presently under the jurisdiction of the American Society for Testing and Materials (ASTM) as outlined in D3842-80 "Standard Guide for Selection of Test Methods for Coatings Used in Light-Water Nuclear Power Plants".

The future dictates significantly less construction of new Nuclear Plants and much more emphasis upon the repair and maintenance of existing facilities. Our commitment remains the same as it was in 1965; that is, to meet the coating requirements of Nuclear Power Plants.

NUCLEAR COATINGS

SSU-1

Level One Coating Systems

The following Coating Systems are qualified for Coating Service Level One of a Nuclear Power Plant. "Coating Service Level One pertains to those systems applied to structures, systems and other safety related components which are essential to the prevention of, or the mitigation of the consequences of postulated accidents that could cause undue risk to the health and safety of the public."

SYSTEM IDENTIFICATION	COATING SYSTEMS	DRY FILM THICKNESS RANGE
CARBON STEEL COATING SYSTEMS		
System S-1		
Primer	No. 6548/7107 EPOXY WHITE PRIMER	3.0 - 14.0 mils DFT
Finish	No. E-1 SERIES EPOXY ENAMEL	2.5 - 6.0 mils DFT
System S-10		
Primer	No. 6548/7107 EPOXY WHITE PRIMER	5.0 - 12.0 mils DFT
Finish	No. D-1 SERIES EPOXY HI-BUILD ENAMEL	3.0 - 6.0 mils DFT
System S-11		
Primer/Finish	No. 6548/7107 EPOXY WHITE PRIMER	8.0 - 18.0 mils DFT
System S-12		
Primer/Finish	No. 4500 EPOXY SELF-PRIMING SURFACING ENAMEL	5.0 - 18.0 mils DFT
System S-14 (FLOORS ONLY)		
Finish	No. 5000 EPOXY SELF-LEVELING FLOOR COATING	10.0 - 25.0 mils DFT
System S-15		
Primer	No. 6548/7107 EPOXY WHITE PRIMER	2.5 - 6.0 mils DFT
Finish	No. 9600 N KEELOCK	5.0 - 8.0 mils DFT
CONCRETE COATING SYSTEMS		
System KL-2		
Curing Compound/Sealer	No. 4129 EPOXY CLEAR CURING COMPOUND	0.5 - 1.75 mils DFT
Surfacer	No. 6548-S EPOXY SURFACER	Flush - 50.0 mils DFT
Finish	No. E-1 SERIES EPOXY ENAMEL	2.5 - 6.0 mils DFT
System KL-8		
Curing Compound/Sealer	No. 4129 EPOXY CLEAR CURING COMPOUND	0.5 - 1.75 mils DFT
Surfacer	No. 6548-S EPOXY SURFACER	Flush - 50.0 mils DFT
Finish	No. D-1 SERIES EPOXY HI-BUILD ENAMEL	4.0 - 8.0 mils DFT
System KL-9		
Curing Compound/Sealer	No. 4129 EPOXY CLEAR CURING COMPOUND	0.5 - 1.75 mils DFT
Surfacer	No. 6548/7107 EPOXY WHITE PRIMER	5.0 - 10.0 mils DFT
Finish	No. D-1 SERIES EPOXY HI-BUILD ENAMEL	3.0 - 8.0 mils DFT
System KL-10		
Curing Compound/Sealer	No. 4129 EPOXY CLEAR CURING COMPOUND	0.5 - 1.75 mils DFT
Surfacer	No. 4000 EPOXY SURFACER	Flush - 50.0 mils DFT
Finish	No. D-1 SERIES EPOXY HI-BUILD ENAMEL	3.0 - 6.0 mils DFT
System KL-12		
Curing Compound/Sealer	No. 4129 EPOXY CLEAR CURING COMPOUND	0.5 - 1.75 mils DFT
Surfacer/Finish	No. 4500 EPOXY SELF-PRIMING SURFACING ENAMEL	10.0 - 50.0 mils DFT
System KL-14 (FLOORS ONLY)		
Primer/Sealer	No. 6129 EPOXY CLEAR PRIMER/SEALER	1.5 - 2.5 mils DFT
Finish	No. 5000 EPOXY SELF-LEVELING FLOOR COATING	35.0 - 50.0 mils DFT

SUMMARY OF QUALIFICATION TEST RESULTS

KEELER & LONG maintains a complete file of Nuclear Test Reports which substantiate the specification of the carbon steel and concrete coating systems listed in this bulletin. This file was initiated in the early 1970's and provides complete qualification in accordance with ANSI Standards N512 and N101.2. Results for radiation tolerance, decontamination, and the Design Basis Accident Condition are reported as performed by independent Laboratories. Also reported are the chemical and physical tests which were conducted by the Keeler & Long Laboratory in compliance with the ANSI Standards.

TEST REPORT REFERENCE

K&L COATING SYSTEM	SUBSTRATE	KEELER & LONG TEST REPORT NO. 78-0728-1	78-0810-1	85-0404	85-0524	90-0227	93-0818	93-0601
S-1	Steel	•	•					
S-10	Steel		•					
S-11	Steel		•					
S-12	Steel			•				
S-14	Steel					•		
S-15	Steel						•	
KL-2	Concrete	•	•					
KL-8	Concrete	•						
KL-9	Concrete	•	•					
KL-10	Concrete		•					
KL-12	Concrete				•			
KL-14	Concrete					•		•

This information is presented as accurate and correct, in good faith, to assist the user in application. No warranty is expressed or implied. No liability is assumed.

KOLOR KEELER & LONG INC.

SSPC SUSTAINING MEMBER

E.340

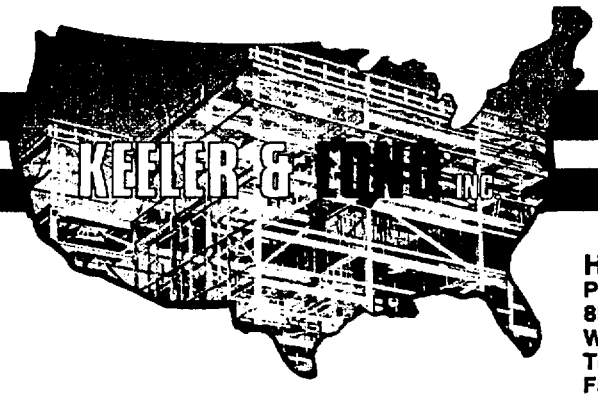

HEADQUARTERS:
P. O. Box 460
856 Echo Lake Road
Watertown, CT 06795
Tel (860) 274-6701
Fax (860) 274-5857

EPOXY ENAMEL
E-SERIES

GENERIC TYPE: POLYAMIDE EPOXY

PRODUCT DESCRIPTION: A two component, polyamide epoxy enamel formulated to provide excellent chemical resistance, as well as being extremely resistant to abrasion and direct impact, for interior exposures.

RECOMMENDED USES: As a topcoat for concrete and steel surfaces subject to radiation, decontamination, and loss-of-coolant accidents in Coating Service Level I Areas of nuclear power plants.

NOT RECOMMENDED FOR: Areas other than the above, as the J-SERIES can be utilized in Coating Service Level II and III Areas, as well as Balance of Plant, of nuclear power plants, with attendant cost savings.

COMPATIBLE UNDERCOATS: Epoxy White Primer
Epoxy Surfacer

PRODUCT CHARACTERISTICS:

Solids by Volume:	53% ± 3%
Solids by Weight:	66% ± 3%
Recommended Dry Film Thickness:	2.0 - 2.5 mils
Theoretical Coverage:	425 Sq. Ft./Gallon @ 2.0 mils DFT
Finish:	Full Gloss (E-1), Semi-Gloss (E-2)
Available Colors:	White, light tints, and dark red
Drying Time @ 72°F	
To Touch:	4 Hours
To Handle:	8 Hours
To Recoat:	48 Hours
VOC Content:	3.4 Pounds/Gallon 407 Grams/Liter

June, 1994

TECHNICAL BULLETIN

E-SERIES E 340

TECHNICAL DATA

PHYSICAL DATA:	Weight per gallon:	10.2 ± 0.5 (pounds)
	Flash Point (Pensky-Martens):	85°F± 2°
	Shelf Life:	1 Year
	Pot Life @ 72°F:	8 Hours
	Temperature Resistance:	350°F
	Viscosity @ 77°F:	85 ± 5 (Krebs Units)
	Gloss (60° meter):	95 ± 5 (E-1)
	Storage Temperature:	55 - 95°F
	Mixing Ratio (Approx. by Volume):	4:1
APPLICATION DATA:	Application Procedure Guide:	APG-2
	Wet Film Thickness Range:	4.0 - 5.0 mils
	Dry Film Thickness Range:	2.0 - 2.5 mils
	Temperature Range:	55 - 120°F
	Relative Humidity:	80% Maximum
	Substrate Temperature:	Dew Point + 5°F
	Minimum Surface Preparation:	Primed
	Induction Time @ 72°F:	1 Hour
	Recommended Solvent	
	@ 50 - 85°F:	No. 4093
	@ 86 - 120°F:	No. 2200

Application Methods

Air Spray		
	Tip Size:	.055"
	Pressure:	30 - 60 PSIG
	Thin:	1.0 - 2.0 Pts/Gal
Airless Spray		
	Tip Size:	.011" - .017"
	Pressure:	2500 - 3000 PSIG
	Thin:	0.5 - 1.5 Pts/Gal
Brush or Roller		
	Thin:	1.0 - 2.0 Pts/Gal

KEELER & LONG INC.

KOLORS

P. O. Box 460, 856 Echo Lake Road
Watertown, CT 06795
Tel: (860) 274-6701 Fax: (860) 274-5857

SSPC SUSTAINING MEMBER

This information is presented as accurate and correct, in good faith, to assist the user in specification and application. No warranty is expressed or implied. No liability is assumed. Product specifications are subject to change without notice. Data listed above is for white or base color of the product. Data for other colors may differ.

3.8.3 Description of Electroless Nickel Coating

This section provides a description of the electroless Nickel coating process as prepared by the ASM Committee on Nickel Plating. The electroless Nickel coating is used to provide corrosion protection of the BWR carbon steel support disks during the short time period from placement of the BWR canister in the spent fuel pool to the time of completion of vacuum drying and inerting with helium. The coating is applied in accordance with ASTM B733-SC3, Type V, Class 1 [37].

Electroless nickel is a nickel/phosphorus alloy that is produced by the use of a chemical reducing agent a hot aqueous solution to deposit nickel on a catalytic surface without the use of an electric current. The chemical reduction process produces a uniform, predicable coating thickness. Adhesion of the nickel coating to properly cleaned carbon steel is excellent with reported bond strength in the range of 40 to 60 ksi [38].

Electroless nickel coating is highly corrosion resistant because of its non-porous structure that seals off the coated surface from the environment. During the time following completion of the coating of the UMS BWR support disk until actual use, the nickel surface bonds with oxygen atoms in the air to create a passive nickel oxide layer on the surfaces of the support disk. Thus, very few free electrons are available on the surface to cathodically react with water and produce hydrogen gas. Test data for electroless nickel coated steel have been reported to show corrosion rates from 1 to 2 μm per year in water [39].

The coating classification of SC3 provides a minimum thickness of 25 μm (0.001 inch).

Nonelectrolytic Nickel Plating

*By the ASM Committee on Nickel Plating**

THREE METHODS may be employed for depositing nickel coatings without the use of electric current:

1 Immersion plating
2 Chemical reduction of nickelous oxide at 1600 to 2000 F
3 Autocatalytic chemical reduction of nickel salts by hypophosphite anions in an aqueous bath at 190 to 205 F ("electroless" nickel plating).

All three methods are, under certain limited conditions, useful substitutes for nickel electroplating; they are particularly useful in applications in which electroplating is impracticable or impossible because of cost or technical difficulties. Of the three methods, electroless nickel plating is in widest use, and is the method to which the most attention is devoted in this article.

Immersion Plating

The composition and operating conditions of an aqueous immersion plating bath are as follows:

Nickel chloride ($NiCl_2 \cdot 6H_2O$)	80 oz per gal
Boric acid (H_3BO_3)	4 oz per gal
pH	3.5 to 4.5
Temperature	160 F

When using this bath, it is desirable, but not mandatory, to move the work at a rate of about 16 ft per min.

This solution is capable of depositing a very thin (about 0.025 mil) and uniform coating of nickel on steel in periods of up to 30 min. The coating is porous and possesses only moderate adhesion, but these conditions can be improved by heating the coated part at 1200 F for 45 min in a nonoxidizing atmosphere. (Higher temperatures will promote diffusion of the coating.)

High-Temperature Chemical-Reduction Coating

By the reduction of a mixture of nickelous oxide and dibasic ammonium phosphate in hydrogen or other reducing atmosphere at 1600 to 2000 F, a nickel coating can be deposited without the use of electric current. This method (U. S. Patent 2,633,631) consists of applying a slurry of the two chemicals to all or selected surfaces of the workpiece, drying the slurry in air, and performing the chemical reduction at elevated temperature. No special tanks or other plating facilities are required. Some diffusion of nickel and phosphorus into the basis metal occurs at elevated temperature; when the coating is applied to steel, it will consist of nickel, iron, and about 3% phosphorus. The slurry may be used for brazing.

* See page 422 for committee list.

Electroless Nickel Plating

The electroless nickel plating process employs a chemical reducing agent (sodium hypophosphite) to reduce a nickel salt (such as nickel chloride) in hot aqueous solution and to deposit nickel on a catalytic surface. The deposit obtained from an electroless nickel solution is an alloy containing from 4 to 12% phosphorus and is quite hard. (As indicated later in this article, the hardness of the as-plated deposit can be increased by heat treatment.) Because the deposit is not dependent on current distribution, it is uniform in thickness, regardless of the shape or size of the plated surface.

Electroless nickel deposits may be applied to provide the basis metal with resistance to corrosion or wear, or for the buildup of worn areas. Typical applications of electroless nickel for these purposes are given in Table 1, which also indicates plate thicknesses and postplating heat treatments.

Surface Cleaning. In general, the methods employed for cleaning and preparing metal surfaces for electroless nickel plating are the same as those used for conventional electroplating. Heavy oxides are removed mechanically, and oils and grease are removed by vapor degreasing. A typical precleaning cycle might consist of alkaline cleaning (either agitated soak or anodic) and acid pickling, both followed by water rinsing.

Prior to electroless plating, the surfaces of all stainless steel parts must be chemically activated in order to obtain satisfactory adhesion of the plate. One activating treatment consists of immersing the work for about 3 min in a hot (200 F) solution containing equal volumes of water and concentrated sulfuric acid. Another treatment consists of immersing the work for 2 to 3 min in the following solution at 160 F:

Sulfuric acid (66° Bé)	25% by volume
Hydrochloric acid (18° Bé)	5% by volume
Ferric chloride hexahydrate	0.83 oz per gal

Pretreatments that are unique to electroless nickel plating include:

1 A strike copper plate must be applied to parts made of or containing lead, tin, cadmium or zinc, to insure adequate coverage and to prevent contamination of the electroless solution.
2 Massive parts are preheated to bath temperature to avoid delay in the deposition of nickel from the hot electroless bath.

Bath Characteristics. A simplified equation that describes the formation of electroless nickel deposits is:

$$NiSO_4 + NaH_2PO_2 + H_2O \xrightarrow[\text{catalyst}]{\text{heat}} Ni + NaH_2PO_3 + H_2SO_4$$

The essential requirements for any electroless nickel solution are:

1 A salt to supply the nickel
2 A hypophosphite salt to provide chemical reduction
3 Water
4 A complexing agent
5 A buffer to control pH
6 Heat
7 A catalytic surface to be plated.

Detailed discussions of the chemical characteristics of electroless baths, and of the critical concentration limits of the various reactants, can be found in several of the references listed at the end of this article.

Both alkaline (pH, 7.5 to 10) and acid (pH, 4.5 to 6) electroless nickel baths are used in industrial production. Although the acid baths are easier to maintain and are more widely used, the alkaline baths are reported to have greater compatibility with sensitive substrates (such as magnesium, silicon and aluminum).

Catalysis. Nickel and hypophosphite ions can exist together in a dilute solution without interaction, but will react on a catalytic surface to form a deposit. Furthermore, the surface of the deposit is also catalytic to the reaction, so that the catalytic process continues until any reasonable plate thickness is applied. This autocatalytic effect is the principle upon which all electroless nickel solutions are based.

Metals that catalyze the plating reaction are members of group VIII in the periodic table, which group includes nickel, cobalt and palladium. A deposit will begin to form on surfaces of these metals by simple contact with the solution. Other metals, such as aluminum or low-alloy steel, first form an

Table 1. Typical Applications of Electroless Nickel Plating

Part and basis metal	Typical plate thickness, mils	Postplating heat treatment(a)
Plate Applied for Corrosion Resistance		
Valve body, cast iron	5.0	None
Printing rolls, cast iron	1.0	None
Electronic chassis, 1010 steel	1.0	None
Railroad tank cars, 1020 steel	3.5	1 hr at 1150 F
Reactor vessels, 1020 steel	4.0	1 hr at 1150 F
Pressure vessel, 4130 steel	1.5	3 hr at 350 F
Tubular shaft, 4340 steel	1.5	3 hr at 375 F
Plate Applied for Wear Resistance		
Centrifugal pump, steel	1.0	2 hr at 400 F
Plastic extrusion dies, steel	2.0	2 hr at 375 F
Printing-press bed, steel	1.0	None
Valve inserts, steel	0.5	2 hr at 1150 F
Hydraulic pistons, 4340 steel	1.0	1 hr at 750 F
Screws, 410 stainless	0.2	None
Stator and rotor blades, 410 stainless	0.8 to 1.0	1 hr at 750 F
Spray nozzles, brass	0.5	None
Plate Applied for Buildup of Worn Areas		
Carburized gear (bearing journal)	0.8 to 1.0	5 hr at 275 F
Splined shaft (ID spline), 16-28-6 stainless	0.5	1 hr at 750 F
Connecting arm (dowel-pin holes), type 410	5.0	1 hr at 750 F

(a) Heat treatments above 450 F should be carried out in an inert or reducing atmosphere.

immersion deposit of nickel on their surfaces, which then catalyzes the reaction; still others, such as copper, require a galvanic nickel deposit in order to be plated. Such a galvanic nickel deposit can be formed by the plating solution itself, if the copper is in contact with steel or aluminum.

Plastics, glass, ceramics and other nonmetallics also can be plated, if their surfaces can be made catalytic. This usually is done by the application of traces of a strongly catalytic metal to the nonmetallic surface by chemical or mechanical means.

There is, however, a group of metals that not only do not display any catalytic action, but also interfere with all plating activity. The salts of these metals, if dissolved in a solution even in comparatively small amounts, are poisons and stop the plating reaction on all metals, thus necessitating the discarding of the solution and the formulation of a new one. Examples of these anticatalysts are Pb, Sn, Zn, Cd, Sb, As and Mo.

Paradoxically, the deliberate introduction of extremely minute traces of poisons has been practiced by a number of users of electroless nickel, with the intent of stabilizing the solution. Being an inherently metastable mixture, electroless nickel solutions are likely to decompose spontaneously, with the nickel and hypophosphite reacting on trace amounts of solid impurities present in any plating bath. In order to minimize this problem, a poisoning element is added in trace concentrations of parts per million (or per trillion) to the original make-up of the solution. The poison is adsorbed on the solid impurities in quantities large enough to destroy their catalytic nature. This selective adsorption on catalytic centers decreases the concentration of the catalytic poison to a level below the critical threshold, so that normal deposition of nickel is not impeded, although the rate of deposition is somewhat reduced. The deliberate introduction of catalytic poisons for the purpose of stabilization is covered by several patents, including U. S. Patents 2,762,723 and 2,847,327.

Table 2. Alkaline Electroless Nickel Baths

Constituent or condition	Bath 1	Bath 2	Bath 3
Composition, Grams per Liter			
Nickel chloride	30	45	30
Sodium hypophosphite	10	11	10
Ammonium chloride	50	50	50
Sodium citrate	..	100	..
Ammonium citrate	..	..	65
Ammonium hydroxide	to pH	to pH	to pH
Operating Conditions			
pH	8 to 10	8.5 to 10	8 to 10
Temperature, F	195 to 205	195 to 205	195 to 205
Plating rate (approx), mil per hr	0.3	0.4	0.3

Table 3. Acid Electroless Nickel Plating Baths(a)

Constituent or condition	Bath 4	Bath 5	Bath 6	Bath 7	Bath 8	Bath 9
Composition, Grams per Liter						
Nickel chloride	30	..	..	30	..	30
Nickel sulfate	..	21	20	..	15	..
Sodium hypophosphite	10	24	27	10	14	12
Sodium acetate	..	..	..	..	13	..
Sodium hydroxyacetate	50	..	..	10	..	..
Sodium succinate	..	..	16	..	..	..
Lactic acid (80%)	..	34 ml	..	..	..	..
Propionic acid (100%)	..	2.2 ml	..	..	..	10
Operating Conditions						
pH	4 to 6	4.3 to 4.8	4.5 to 5.5	4 to 6	5 to 6	4.5 to 5.5
Temperature, F	190 to 210	203	200 to 210	190 to 210	190 to 210	190 to 210
Plating rate (approx), mil per hr	0.6	1.0	1.0	0.4	0.7	0.6

(a) Baths 4 and 7 are covered by U. S. Patent 2,532,283 (a public patent assigned to the National Bureau of Standards); bath 5, by U. S. Patents 2,822,293 and 2,821,294, and bath 6 by U. S. Patents 2,658,841 and 2,658,842.

Alkaline Baths. Most alkaline baths in commercial use today are based on the original formulations developed by Brenner and Riddell. They contain a nickel salt, sodium hypophosphite, ammonium hydroxide, and an ammonium salt; they may also contain sodium citrate or ammonium citrate. The ammonium salt serves to complex the nickel and buffer the solution. Ammonium hydroxide is used to maintain the pH between 7.5 and 10. Table 2 gives the compositions and operating conditions of three alkaline electroless baths.

At the operating temperatures of these baths (about 200 F), ammonia losses are considerable. Thorough ventilation and frequent adjustment of pH are required. The alkaline solutions are inherently unstable and are particularly sensitive to the poisoning effects of anticatalysts such as lead, tin, zinc, cadmium, antimony, arsenic and molybdenum — even when these elements are present in only trace quantities. However, when depletion occurs, these solutions undergo a definite color change from blue to green, indicating the need for addition of ammonium hydroxide.

Acid baths are more widely used in commercial installations than alkaline baths. Essentially, acid baths contain a nickel salt, a hypophosphite salt, and a buffer; some solutions also contain a chelating agent. Frequently, wetting agents and stabilizers also are added.

These baths are more stable than alkaline solutions, are easier to control, and usually provide a higher plating rate. Except for the evaporation of water, there is no loss of chemicals when acid baths are heated to their operating range. Table 3 gives the compositions and operating conditions of several acid electroless baths.

Solution Control. In order to assure optimum results and consistent plating rates, the composition of the plating solution should be kept relatively constant; this requires periodic analyses for the determination of pH, nickel content, and phosphite and hypophosphite concentrations. The rate at which these analyses should be made depends on the quantity of work being plated and the volume and type of solution being used. The following methods have been employed:

pH — Standard electrometric method

Nickel — Any one of the colorimetric, gravimetric or volumetric methods is satisfactory; the cyanide method is probably the most popular.

Phosphite — A 10-ml sample of the plating solution is combined with 20 ml of a 5% solution of sodium bicarbonate and cooled in an ice bath. Next, 50 ml of 0.1*N* iodine solution is added and the flask containing this mixture is stoppered and permitted to stand for 2 hr at room temperature. Then the flask is cooled for 15 min in ice water, after which it is unstoppered, the mixture is acidified with acetic acid, and the excess iodine is titrated with 0.1*N* sodium thiosulfate, with starch as an indicator. Determination is then made as follows:

$$\text{NaH}_2\text{PO}_2 \text{ per liter} = \frac{\text{net ml of 0.1N iodine} \times 6.3}{\text{ml of plating solution}}$$

Hypophosphite (U. S. Patent 2,697,651) — A 25-ml sample of the plating solution is diluted to 1 liter. A 5-ml aliquot of the

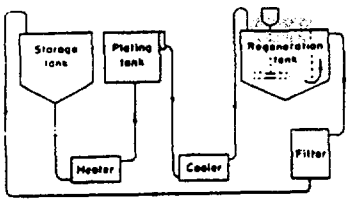

Fig. 1. Schematic of continuous-type system for electroless nickel plating. See text.

dilution is combined with 10 ml of a 10% solution of ammonium molybdate and 10 ml of fresh 6% sulfurous acid. The sample is covered and heated to boiling, and a deep blue color develops. The sample is cooled and diluted to 100 ml, and transmittance at a wave length of 440 microns is determined. The calibration curve on semilog paper is linear.

Hypophosphite (alternative method) — A 5-ml sample of the plating solution is mixed in a beaker with 5 ml of methyl orange solution made up of 1 gram of methyl orange in 1 liter of water. In another beaker is placed 15 ml of an acid solution made up by (a) dissolving 40 grams of sodium metabisulfate in 200 ml of water, (b) slowly adding the sodium metabisulfate solution to a cold solution of 82 ml of sulfuric acid in 650 ml of water, and then (c) diluting this mixture with water to 1 liter. When the acid solution and the solution containing the sample and methyl orange reach a temperature of 77 F in a thermostat, the two solutions are mixed. The time between mixing and the disappearance of the red color is recorded. The hypophosphite concentration is a function of this time and is read from a concentration-time curve made from known standards.

Equipment Requirements. The precleaning and post-treating equipment for an electroless nickel line is comparable to that employed in conventional electrodeposition. The plating tank itself, however, is unique.

The preferred plating tank for batch operations is constructed of stainless steel or aluminum and is lined with a coating of an inert material, such as tetrafluoroethylene or a phenolic-base organic. The size and shape of the tank are usually dictated by the parts to be plated, but the surface area of the plating solution should not be so large that excessive heat loss occurs as a result of evaporation.

A large heat-transfer area and a low temperature gradient are necessary between the heating medium and the plating solution. This combination provides for a reasonable heat-up time without local hot spots that could decompose the solution. It is accepted practice to surround the plating tank with a hot-water jacket or to immerse it in a tank containing hot water. Heating jackets using low-pressure steam also have been used successfully. The use of immersed steam coils is not favored, however, because it entails the sacrifice of a large amount of working area in the tank.

Accessory equipment required or recommended for the tank includes:

1 An accurate temperature controller
2 A filter to remove any suspended solids
3 A pH meter
4 An agitator to prevent gas streaking
5 On small tanks, a cover, to minimize heat loss and exclude foreign particles.
6 On large tanks, a separate small tank to dissolve and filter additives before they are put into the plating tank.

Considerably more equipment is required for a continuous-type system, such as that shown in Fig. 1. The bath is prepared and stored in a separate tank and flows through a heater (which raises its temperature to 205 F) into the plating tank. From the plating tank, the solution is pumped through a cooler, which decreases its temperature to 175 F or below, and then to an agitated regeneration tank, where reagents are added in controlled amounts to restore the solution to its original composition. The solution is then directed past a vertical underflow baffle and out of the regeneration tank to a filter, and then returned to storage.

In externally heated continuous-type systems such as the one shown in Fig. 1, the plating tank and other components of the system that come in contact with the plating solution are constructed of type 304 stainless steel and are not lined or coated; these components are periodically deactivated by chemical treatment. Details of this type of system are covered by several patents, including U. S. Patents 2,941,902; 2,658,839 and 2,874,073.

Properties of the Deposit. Electroless nickel is a hard, lamellar, brittle, uniform deposit. As plated, the hardness

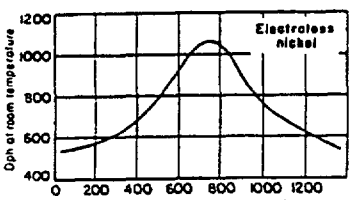

Effect of temperature of 1-hr precipitation heat treatment on room-temperature hardness of a typical electroless nickel deposit (Eberbach tester, 100-gram load). Above 450 F, heat treatment was in an inert atmosphere.

Fig. 2. Heat treatment of coating

varies over a considerable range (425 to 575 dph), depending primarily on phosphorus content, which ranges from 4 to 12%. This hardness can be increased by a precipitation heat treatment. As indicated in Fig. 2, which shows temperature-hardness relationships for a typical deposit, by heating at 750 F for ½ to 1 hr, hardness can be increased to about 1000 dph.

The corrosion resistance of electroless nickel deposits is superior to that of electrodeposited nickel of comparable thickness, but this superiority varies with exposure conditions. Outdoor exposure and salt spray corrosion data indicate that about 25% more resistance is given a steel panel by electroless nickel than by electrolytic.

Table 4. Physical Properties of Electroless Nickel Deposits

Property	Value
Specific gravity	7.8 to 8.5
Melting point	1635 to 1850 F
Electrical resistivity	60 microhm-cm
Thermal expansion	13 X 10^{-6} per °C
Thermal conductivity	0.0108 to 0.0135 cal/cm sec/°C

Table 5. Costs for Electroless Nickel Plating (Example 2) (a)

Cost factor	Cost per year(b)
Original investment	$18,000
Fixed costs:	
Depreciation (10 years)	$ 1,800
Insurance	450
Floor space (200 sq ft)	192
Repairs and maintenance	450
Variable costs:	
Raw material	6,100
Utilities	760
Labor costs:	
Direct	10,400
Indirect	2,630
Total	$22,782
Total cost per hr	$9.48
Total cost per sq ft coated to 1 mil	$1.00

(a) Exclusive of costs for: overhead and administration; racking, cleaning and unracking; and preplating and postplating processes. (b) Based on deposition of 1 mil on 0.1-sq-ft parts at rate of 0.8 mil per hr (capacity: 117 pieces, or 9.4 sq-ft/mil, per hr), on a schedule of 10 hr per day, 20 days per month, 2400 hr per year.

Some of the physical properties of electroless nickel are listed in Table 4.

Advantages and Limitations. Some advantages of electroless nickel are:

1 Good resistance to corrosion and wear
2 Excellent uniformity
3 Solderability and brazability
4 Good oxidation resistance.

Limitations of electroless nickel are:

1 High cost
2 Brittleness
3 Poor welding characteristics
4 Lead, tin, cadmium and zinc must be copper strike plated before electroless nickel can be applied
5 Slower plating rate (in general), as compared to electrolytic methods
6 Full brightness in deposit cannot be obtained without extreme brittleness.

Cost. Electroless nickel is considerably more expensive than electrodeposited nickel. Actual costs for electroless nickel plating, as reported by two users, are given in the following examples.

Example 1. Based on the experience of one manufacturing plant, it costs $1.20 to deposit an electroless nickel coating 1 mil thick on a square foot of surface area: 37¢ for chemicals, 59¢ for labor, and 24¢ for equipment and maintenance.

Example 2. Another manufacturing plant reports that it costs $1 per sq ft to plate a 1-mil thickness of electroless nickel on specific parts with a surface area of 0.1 sq ft, on the basis of data obtained over a one-year period (2400 working hours). An analysis of their costs is given in Table 5.

Selected References

A. Brenner, Electroless Plating Comes of Age, *Metal Finishing*, November 1954, p 68-76; December 1954, p 81-88

A. Brenner and G. Riddell, Nickel Plating on Steel by Chemical Reduction, *J Res Nat Bur Stds*, July 1946, p 31-34, and *Proc Am Electroplaters' Soc*, 1946, p 23-29; Deposition of Nickel and Cobalt by Chemical Reduction, *J Res Nat Bur Stds*, Nov 1947, p 385-395, and *Proc Am Electroplaters' Soc*, 1948, p 156-169

G. Gutzeit, Industrial Nickel Coating by Chemical Catalytic Reduction, *Trans Inst Metal Finishing*, 33, 383-423 (1955-1956), and *Corrosion Technol*, 3, 208 (1956)

G. Gutzeit, An Outline of the Chemistry Involved in the Process of Catalytic Nickel Deposition from Aqueous Solution, *Plating*, Oct 1959, p 1158-1164; Nov 1959, p 1275-1278; Dec 1959, p 1377-1378; Jan 1960, p 63-70

C. H. de Minjer and A. Brenner, Studies on Electroless Nickel Plating, *Plating*, December 1957, p 1297-1305

Symposium on Electroless Nickel Plating (Catalytic Deposition of Nickel-Phosphorus Alloys by Chemical Reduction in Aqueous Solution), ASTM STP No. 265 (1959)

THIS PAGE INTENTIONALLY LEFT BLANK